

Structure/Performance Relationships in Surfactants

ACS SYMPOSIUM SERIES 253

Structure/Performance Relationships in Surfactants

Milton J. Rosen, EDITOR

*Brooklyn College of the
City University of New York*

Based on a symposium sponsored by
the Division of Colloid and Surface Chemistry
at the 186th Meeting
of the American Chemical Society,
Washington, D.C.,
August 28–September 2, 1983



American Chemical Society, Washington, D.C. 1984



Library of Congress Cataloging in Publication Data

Structure/performance relationships in surfactants.
(ACS symposium series, ISSN 0097-6156; 253)

"Based on a symposium sponsored by the Division of Colloid and Surface Chemistry at the 186th Meeting of the American Chemical Society, Washington, D.C., August 28-September 2, 1983."

Includes bibliographies and indexes.

1. Surface active agents—Congresses. 2. Surface chemistry—Congresses.

I. Rosen, Milton J. II. American Chemical Society. Division of Colloid and Surface Chemistry. III. American Chemical Society. Meeting (186th: 1983: Washington, D.C.) IV. Title. V. Series.

TP994.S77 1984 668'.1 84-6384
ISBN 0-8412-0839-5

Copyright © 1984

American Chemical Society

All Rights Reserved. The appearance of the code at the bottom of the first page of each chapter in this volume indicates the copyright owner's consent that reprographic copies of the chapter may be made for personal or internal use or for the personal or internal use of specific clients. This consent is given on the condition, however, that the copier pay the stated per copy fee through the Copyright Clearance Center, Inc., 21 Congress Street, Salem, MA 01970, for copying beyond that permitted by Sections 107 or 108 of the U.S. Copyright Law. This consent does not extend to copying or transmission by any means—graphic or electronic—for any other purpose, such as for general distribution, for advertising or promotional purposes, for creating a new collective work, for resale, or for information storage and retrieval systems. The copying fee for each chapter is indicated in the code at the bottom of the first page of the chapter.

The citation of trade names and/or names of manufacturers in this publication is not to be construed as an endorsement or as approval by ACS of the commercial products or services referenced herein; nor should the mere reference herein to any drawing, specification, chemical process, or other data be regarded as a license or as a conveyance of any right or permission, to the holder, reader, or any other person or corporation, to manufacture, reproduce, use, or sell any patented invention or copyrighted work that may in any way be related thereto. Registered names, trademarks, etc., used in this publication, even without specific indication thereof, are not to be considered unprotected by law.

PRINTED IN THE UNITED STATES OF AMERICA

American Chemical
Society Library

1155 16th St. N. W.

Washington, D. C. 20038
In Structure/Performance Relationships in Surfactants; Rosen, M.;
ACS Symposium Series; American Chemical Society: Washington, DC, 1984.

ACS Symposium Series

M. Joan Comstock, *Series Editor*

Advisory Board

Robert Baker
U.S. Geological Survey

Martin L. Gorbaty
Exxon Research and Engineering Co.

Herbert D. Kaesz
University of California—Los Angeles

Rudolph J. Marcus
Office of Naval Research

Marvin Margoshes
Technicon Instruments Corporation

Donald E. Moreland
USDA, Agricultural Research Service

W. H. Norton
J. T. Baker Chemical Company

Robert Ory
USDA, Southern Regional
Research Center

Geoffrey D. Parfitt
Carnegie Mellon University

Theodore Provder
Glidden Coatings and Resins

James C. Randall
Phillips Petroleum Company

Charles N. Satterfield
Massachusetts Institute of Technology

Dennis Schuetzle
Ford Motor Company
Research Laboratory

Davis L. Temple, Jr.
Mead Johnson

Charles S. Tuesday
General Motors Research Laboratory

C. Grant Willson
IBM Research Department

FOREWORD

The ACS SYMPOSIUM SERIES was founded in 1974 to provide a medium for publishing symposia quickly in book form. The format of the Series parallels that of the continuing ADVANCES IN CHEMISTRY SERIES except that in order to save time the papers are not typeset but are reproduced as they are submitted by the authors in camera-ready form. Papers are reviewed under the supervision of the Editors with the assistance of the Series Advisory Board and are selected to maintain the integrity of the symposia; however, verbatim reproductions of previously published papers are not accepted. Both reviews and reports of research are acceptable since symposia may embrace both types of presentation.

PREFACE

WORLDWIDE CONSUMPTION OF SURFACTANTS, even excluding soaps, is now measured in billions of pounds. In the United States alone, surfactants are a multibillion dollar industry, with hundreds of different types used in industrial and consumer products for a multitude of different purposes.

Although a vast literature exists on the properties of surfactants, the amount of data from which reliable chemical structure/property relationships can be drawn is surprisingly meagre. A major reason for this paucity of data is the marked effect that very small quantities of highly surface-active impurities can have on the properties of surfactants in solution, coupled with the difficulty of removing some of these impurities when they are present. Moreover, many investigations into the properties of surfactants have dealt with commercial materials that are mixtures of surface-active compounds, and structure/property correlations so based are often of questionable validity because of insufficient characterization of the materials investigated. On the other hand, the effect of surface-active impurities has been known for about 40 years now, and careful investigators have compiled a body of data that, although limited in scope, has made available some information on chemical structure/property relationships.

Recent years have seen a revival of interest in the study of surfactants and their properties, in part due to their potentialities for use in enhanced oil recovery. In addition, greater awareness of the effects of impurities, the availability of a variety of high-purity surfactants from a number of commercial sources, and improved methods for characterizing and purifying materials have resulted in an increased number of investigations containing data on surfactant properties from which reliable conclusions can be drawn.

The symposium on which this book is based assembled the results of worldwide research on surfactant structure/performance relationships by most of the active groups throughout the world. Most of the papers included here embody recent research results; a few are invited overview papers.

The use of the facilities of the Department of Chemistry of Brooklyn College, City University of New York, greatly expedited the editing of the manuscripts and is gratefully acknowledged. I should like to thank Theresa Rudd and Barbara Fudge of the secretarial staff of the department for typing revised portions of the manuscripts and the necessary correspondence. My thanks also to the unnamed referees for their conscientious examination of

the manuscripts, and to the authors for their interest in the symposium and their cooperation in making this volume possible.

MILTON J. ROSEN
Great Neck, New York

February 1984

Interfacial and Performance Properties of Sulfated Polyoxyethylenated Alcohols

M. J. SCHWUGER

Henkel KGaA, (4000) Düsseldorf, Box 1100, Germany

Alkyl ether sulfates are, after alkyl benzene sulfonates (LAS), the group of technically important anionic surfactants with the largest production volume and product value. They have in comparison with other anionic surfactants special properties which are based on the particular structure of the molecule. These are expressed, for example, in the general adsorption properties at different interfaces, and in the Krafft-Point. Alkyl ether sulfates may be used under conditions, at which the utilization of other surfactant classes is very limited. They possess particularly favorable interfacial and application properties in mixtures with other surfactants. The paper gives a review of all important mechanisms of action and properties of interest for application.

Alkyl ether sulfates with chain lengths ranging from C_{12} to C_{14} are quantitatively the most important products currently based on fatty alcohols. It is estimated, that about 20 % of all surfactant alcohols - about 40 % of all fatty alcohols in the coconut range (C_{12} - C_{14}) - are used in the form of alkyl ether sulfates (1). Alkyl ether sulfates are the most important group of anionic surfactants after linear alkylbenzenesulfonate (LAS) (2).

In 1980, the total consumption of alkyl ether sulfates in Western Europe equaled that of all other anionic surfactants with the exception of alkylbenzenesulfonates (Fig. 1). Since alkyl ether sulfates are the most expensive group of anionic surfactants, which are produced in larger quantities, their importance on a

0097-6156/84/0253-0003\$06.00/0
© 1984 American Chemical Society

value basis is even more pronounced. The main areas of application of fatty ether sulfates in Europe are cosmetic rinse-off preparations (shampoos, bubble baths, shower baths) and manual liquid dishwashing detergents.

In addition, in the USA ether sulfates are used on a large scale in laundry detergents. For that reason, their market share in the USA is even larger than in Europe (3). At present, alkyl ether sulfates are primarily used in the form of their Na salts. In the past, however, cosmetic preparations containing ammonium and Mg salts have also been quite common (4).

The great technical and economic importance of this product group was reached despite its higher price only because of its special properties. Due to the ionic sulfate group and the adjacent ether groups, ether sulfates combine the classical elements of ionic and nonionic surfactants in one molecule. This provides a number of properties, one of which, the Krafft-Point, is of special importance for the technical application of these compounds.

Krafft Points

The Krafft Point may be defined as the temperature above which the solubility of a surfactant increases steeply. At this temperature, the solubility of the surfactant becomes equal to the critical micelle concentration (c_M) of the surfactant. Therefore, surfactant micelles only exist at temperatures above the Krafft Point. This point is a triple point at which the surfactant coexists in the monomeric, the micellar, and the hydrated solid state (5, 6).

The temperature dependence of the solubility is demonstrated in Fig. 2 for Na dodecyl sulfate (7). Below the Krafft Point, the surfactant dissolves in a molecularly dispersed manner until the saturation concentration is reached. At higher concentrations, a hydrated solid is in equilibrium with individual molecules. Above the Krafft Point, the hydrated solid is in equilibrium with micelles and individual molecules.

Therefore, the physical meaning of the solubility curve of a surfactant is different from that of ordinary substances. Above the critical micelle concentration the thermodynamic functions, for example, the partial molar free energy, the activity, the enthalpy, remain more or less constant. For that reason, micelle formation can be considered as the formation of a new phase. Therefore, the Krafft Point depends on a complicated three phase equilibrium.

With increasing length of the n-alkyl chain an

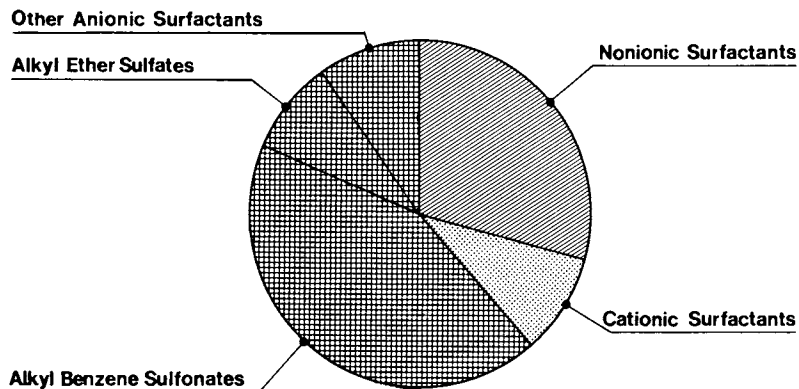


Fig. 1 Use of synthetic surfactants in Western Europe (1980)

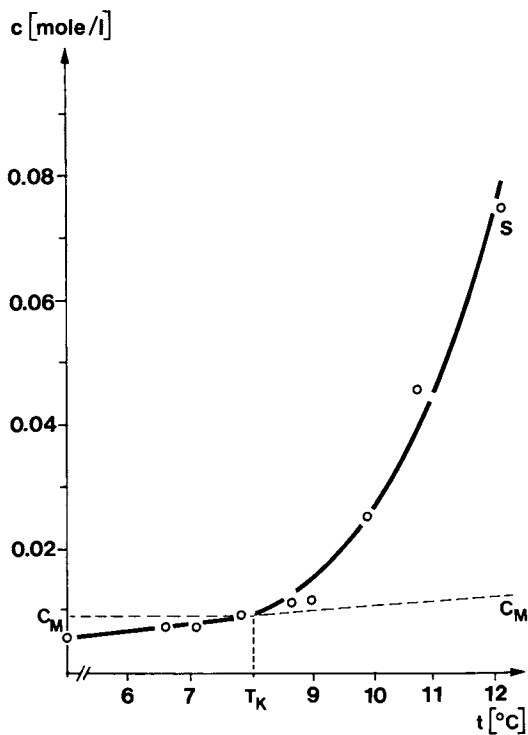


Fig. 2 Solubility of sodium dodecyl sulfate (purity 99.8%)

increase of the Krafft Point is observed. The Krafft Points of many common surfactants, such as alkyl sulfates, alkane sulfonates, p-n-alkyl benzene sulfonates, lie above room temperature (7, 8). Since the solubility of the surfactants depends both on the aqueous and on the crystalline phase, the heat of formation of crystals must be increased in order to effect a depression of the Krafft Point. This can be achieved by branching in the hydrophobic portion of the surfactant or by using surfactant mixtures of different chain length. With Na salts, these measures lead to a sufficiently large depression of the Krafft Point. An application of the respective surfactants in Ca salt form is not possible, because the Krafft Point is mostly too high. For example, for Na-tetradecyl sulfate, the Krafft Point is 21 °C, whereas the Ca salt has a value of 67 °C (9). Therefore, in a number of large fields of application, such as detergents, many surfactants may only be used in combination with complexing agents and/or ion exchangers.

An especially effective reduction of the Krafft Point results from the insertion of ether groups into the molecule of the anionic surfactant. In table I this is exemplified with Na dodecyl sulfate and Na-tetradecyl sulfate in comparison to various n-alkyl ether sulfates of the same chain length (10). As a measure of the Krafft Point, a temperature is defined at which a 1 % solution dissolves clearly. By the incorporation of oxyalkylene groups into the molecule, the Krafft Point and the melting point are greatly depressed. This depression is especially effective if there is branching in the oxyalkylene groups.

The depression of Krafft Points of Ca salts (11) is of special importance from an application point of view. As shown in table II, Ca dodecyl sulfate has a Krafft Point of 50 °C. The introduction of one oxyethylene group into the molecule results in a 35 °C reduction. The reduction is more strongly pronounced than with the corresponding Na salts. These peculiarities of alkyl ether sulfates are of great importance for the selection of these surfactants in a number of fields of application. The Krafft Points are shifted to higher temperatures with increasing length of the hydrocarbon chain and, within a particular group of the Periodic System, with increasing atomic weight of the cation, as well as, within a period of the Periodic System, with increasing valency (12).

TABLE I

Temperature for the Solubility of 1 % Solutions
and Melting Points of R (OCH₂CHR')_mOSO₃Na

R	(OCH ₂ CHR') _m	Melting Point (°C)	Temperature (°C)
C ₁₂ H ₂₅	None	190 - 95	16
C ₁₂ H ₂₅	OC ₂ H ₄	143 - 146	11
C ₁₂ H ₂₅	(OC ₂ H ₄) ₂	126 - 136	< 0
C ₁₂ H ₂₅	OCH ₂ CH(CH ₃)	137 - 142	< 0
C ₁₂ H ₂₅	[OCH ₂ CH(CH ₃)] ₂	87 - 93	< 0
C ₁₂ H ₂₅	OCH ₂ CH(C ₂ H ₅)	77 - 82	< 0
C ₁₂ H ₂₅	[OCH ₂ CH(C ₂ H ₅)] ₂	< 25	< 0
C ₁₄ H ₂₉	None	182 - 183	30
C ₁₄ H ₂₉	OC ₂ H ₄	146 - 150	25
C ₁₄ H ₂₉	(OC ₂ H ₄) ₂	130 - 134	< 0
C ₁₄ H ₂₉	OCH ₂ CH(CH ₃)	139 - 140	14
C ₁₄ H ₂₉	[OCH ₂ CH(CH ₃)] ₂	82 - 87	< 0
C ₁₄ H ₂₉	OCH ₂ CH(C ₂ H ₅)	74 - 76	13
C ₁₄ H ₂₉	[OCH ₂ CH(C ₂ H ₅)] ₂	< 25	< 0

TABLE II

Krafft Points (°C) of n-Dodecyl Ether Sulfates

Surfactant anion	Na salt	Ca salt	Sr salt	Ba salt
C ₁₂ H ₂₅ OSO ₃ ⁻	9	50	64	105
C ₁₂ H ₂₅ OCH ₂ CH ₂ OSO ₃ ⁻	5	15	32	62
C ₁₂ H ₂₅ (OCH ₂ CH ₂) ₂ OSO ₃ ⁻	- 1	< 0	--	35
C ₁₂ H ₂₅ (OCH ₂ CH ₂) ₃ OSO ₃ ⁻	< 0	< 0	< 0	12

The Special Character of Oxyethylene Groups in Alkyl Ether Sulfates

The lower Krafft Points resulting from the incorporation of oxyethylene groups into the surfactant molecule is an essential, but not sufficient, property for the utilization of alkyl ether sulfates.

Several variations in chemical constitution, which lead to a depression of the Krafft-Point (for example, branching of the hydrophobic part of the molecule), frequently result in diminished hydrophobicity of the molecule. At constant molecular weight, the critical micelle concentration (c_M) is shifted with increased branching to higher concentrations, the surface activity diminishes, the tendency to adsorb at hydrophobic interfaces decreases, etc. (13, 14, 15). Therefore, the nature of the oxyethylene groups in alkyl ether sulfates is of major importance.

From a physical chemical viewpoint, oxyethylene groups located adjacent to the ionic sulfate group may be considered at the first glance as additional hydrophilic groups, in analogy to nonionic ethylene oxide (EO) adducts.

For pure nonionic EO adducts, increase in the number of oxyethylene groups in the molecule results in a decrease in the tendency to form micelles and an increase in the surface tension of the solution at the critical micelle concentration (16) (17). This change in surface activity is due to the greater surface area of the molecules in the adsorption layer and at the micellar surface as a result of the presence there of the highly hydrated polyoxyethylene chain. The reduction in the tendency to form micelles is due to the increase in the free energy of micelle formation as a result of partial dehydration of the polyoxyethylene chain during incorporation into the micelle (16) (17).

In the case of alkyl ether sulfates, an increase in the number of oxyethylene groups produces an opposite result (19 - 22). Fig. 3 shows a decrease of the critical micelle concentration (c_M) and the concentration for a given surface tension (for example, 50 mN/m). Only the same increase in the surface tension for solutions at the critical micelle concentration is observed. Therefore, EO incorporation into the surfactant molecule seems to increase the hydrophobic nature of the molecule. This is apparently in contradiction to known correlations between solubility and hydrophobicity.

Nonionic EO adducts always have much smaller c_M values than ionic surfactants with the same hydro-

phobic group. For this reason it was proposed that the introduction of oxyethylene groups into an alkyl sulfate ion weakened its ionic character. This should result in an increased approximation of the properties to those of nonionic surfactants (19, 23, 24). This conception was, however, always very questionable because the sulfate group remain ionic.

The dissociation of the counter-ions of micelles is a characteristic feature of ionic surfactants. For alkyl ether sulfates the degree of dissociation α of the counter-ions of the micelles has been determined by several authors by various methods (21, 25, 26). With increasing number of oxyethylene groups in the molecule the degree of dissociation increases. These data are summarized in Fig. 4. Although the agreement of the absolute values between individual authors is not quite satisfying, they all show an increase of dissociation. This is just contrary to what should be expected with a decrease in ionic character.

Moreover, it is characteristic of ionic surfactants that c_M is greatly reduced by electrolyte addition and that, simultaneously, the surface tension curves in the nonmicellar region are shifted significantly to smaller concentrations (Fig. 3). With nonionic EO adducts the influence of electrolyte is barely present. The curves of alkyl ether sulfates are shifted in the same way as simple alkyl sulfate by the addition of salt. This shift is even larger than with Na dodecyl sulfate. An additional indication of the ionic nature of alkyl ether sulfates is derived from static light scattering. The micelle aggregation numbers are presented in Table III. As can be expected for ionic surfactants (27), they increase in the presence of NaCl.

Therefore, the hypothesis of an increasing non-ionic character of alkyl ether sulfates with increasing number of oxyethylene groups is not tenable. Some time ago (30), it was suggested that a certain hydrophobic nature can be attributed to the polyoxyethylene chain of alkyl ether sulfates. At first, this appears to be in contradiction to the decidedly hydrophilic character of the polyoxyethylene chain for nonionic surfactants. However, the possibility of EO group hydration impairment by the sulfate group cannot be excluded.

Table III shows some data regarding the possible hydrophobic nature of ether sulfates. From several investigations, it is known that, for nonionic surfactants with identical hydrophobic groups, an increase in the hydrophilic part of the molecule causes a decrease in the aggregation number (28). This is caused by the

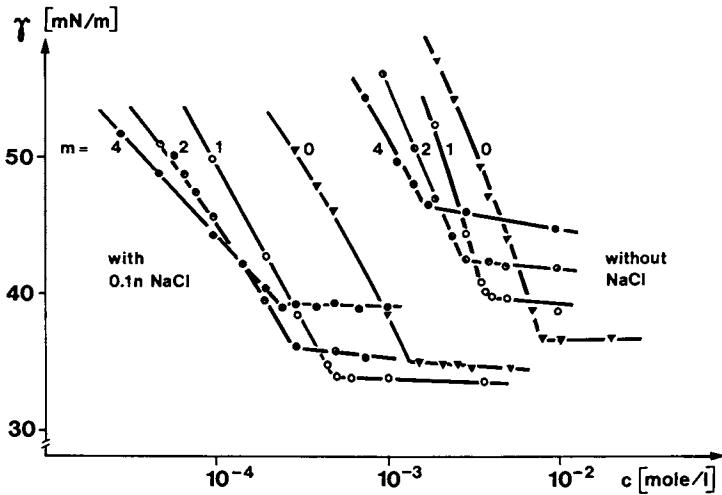


Fig. 3 Surface tension of aqueous solutions of $C_{12}H_{25}(-O-CH_2-CH_2-)_mOSO_3Na$ at $25^\circ C$ (purity 98-99.5%)

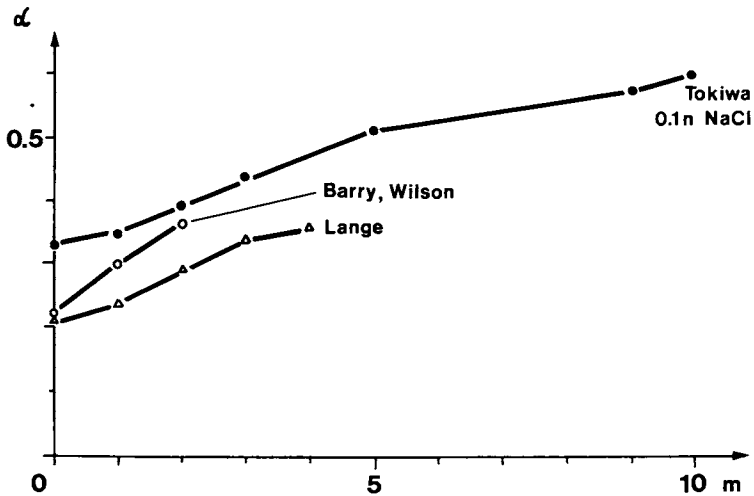


Fig. 4 Degree of dissociation (α) of dodecyl ether sulfate micelles
 m = number of oxyethylene groups in the molecule

increased affinity of the polyethylene chain for water. Comparing the change of the micelle aggregation number at the transition from dodecyl sulfate to dodecyl monoglycol ether sulfate, an increase can be observed with and without salt. This corresponds to the known increase of the micelle aggregation number with increasing length of the n-alkyl chain (29). However, this increase is less pronounced in comparison with dodecyl and tetradecyl sulfate.

TABLE III

Micelle Aggregation Numbers at 25 °C

Substance	without salt	with 0.1 n NaCl
$C_{12}H_{25}OSO_3Na$	60	91
$C_{12}H_{25}OCH_2CH_2OSO_3Na$	72	96
$C_{14}H_{29}OSO_3Na$	80	--

In addition, there may be still another possible reason for the observed effects. The hydration of the polyglycol portion of the micelle increases with increasing number of oxyethylene groups (31). The area demand of a molecule adsorbed at the surface, and, therefore, also the distances between the charged groups will become larger. Since, in addition, the chains are more or less stretched because of the electrical repulsion of the terminal sulfate groups, the distance between sulfate groups also increases. For this reason, the work to overcome the electrical repulsion is diminished, the c_M reduced, and the aggregation number increased. This model was checked experimentally with the adsorption at the water/air interface (21, 22).

Fig. 5, curve 1, shows - for dodecyl ether sulfates - the areas occupied by a molecule at c_M as a function of the number, m , of EO groups. The values were calculated by the Gibbs' equation from the surface tension measurements. For $0 \leq m \leq 2$ there is an area increase with increasing m , however, considerably

weaker than for $m > 2$. For comparison the area values for dodecyl polyglycol ethers are also given. The two different curves were taken from different sources (16, 18). With alkyl ether sulfates the increase of area per molecule and, therefore, also of the distance between the terminal groups in the adsorption layer is smaller, at $m = 0$ to $m = 2$, and larger, at $m > 2$, than for the corresponding nonionic compounds.

Parallel results were found with micelles (31). It was concluded from measurements of sedimentation, diffusion, and viscosity, that the hydration of the micelles of the dodecyl ether sulfates at $m = 0 - 2$ shows only a little increase, whereas a strong one was observed at $m > 2$. A similar trend should also exist with the distance of the terminal groups on the surface of the micelles.

For compounds with one and two oxyethylene groups in their molecule, the increase of the micelle formation tendency can be explained by a contribution of these groups to the hydrophobic part of the molecule. With a longer polyoxyethylene chain in the molecule, however, the increased tendency to form micelles is primarily caused by the increased distance between the charged groups due to increased hydration of the ether groups.

Fig. 3 shows that increase in the number of oxyethylene units in the dodecyl ether sulfate molecule results in increased adsorption at the aqueous solution/air interface at concentrations below c_M . It was interesting to determine whether an analogous effect is shown for adsorption onto solid surfaces. Measurements of the adsorption of Na dodecyl sulfate and dodecyl ether sulfates onto activated carbon at the constant and very low surfactant concentration of $1 \cdot 10^{-4}$ mol/l, which is well below c_M (22, 23), show that the incorporation of oxyethylene groups leads to an increase of adsorption (Table IV). The effect, however of one group is far weaker than the influence of an extension of the hydrocarbon chain by two CH_2 groups. Contrary to this (Fig. 6), the saturation values of adsorption onto graphon above the critical micelle concentration decrease with increasing length of the polyoxyethylene chain, as the surface area per adsorbed molecule increases. This observation corresponds with the result of studies on adsorption at the aqueous solution/air interface.

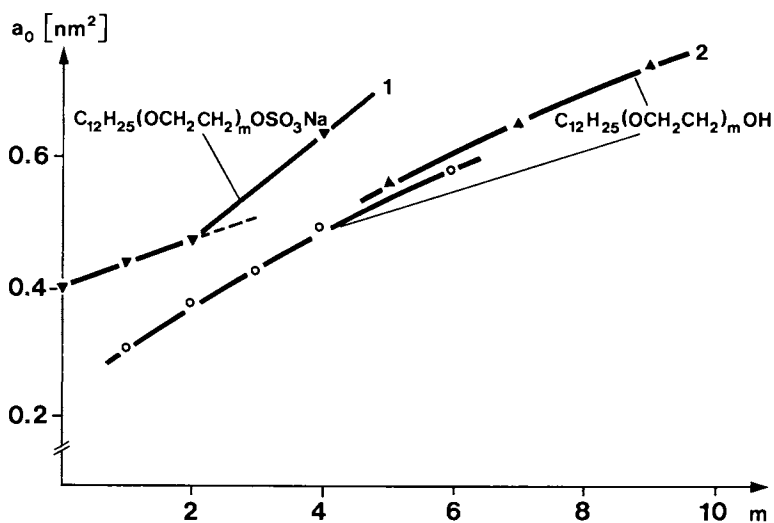


Fig. 5 Areas per molecule at the aqueous solution/air interface as a function of the number of oxyethylene groups

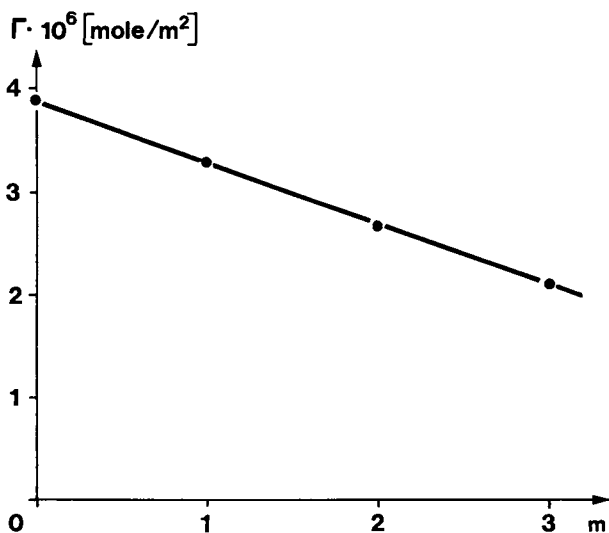


Fig. 6 Adsorption of alkyl ether sulfates on graphon (plateau values) at 25°C (product purity 98-99.5%)

TABLE IV

Adsorption of Surfactants on Active Charcoal

Substance	$Q \cdot 10^5$ (mole/g)
$C_{12}H_{25}OSO_3Na$	5.40
$C_{12}H_{25}(OCH_2CH_2)_1OSO_3Na$	7.29
$C_{14}H_{29}OSO_3Na$	8.12
$C_{12}H_{25}(OCH_2CH_2)_2OSO_3Na$	8.82
$C_{16}H_{33}OSO_3Na$	12.67

Practical Results

Washing and Cleaning Action. The properties of alkyl ether sulfates, due to the good solubility and the special hydrophilic/hydrophobic properties of the molecule, are of particular practical interest. From the investigations described in sections 2 and 3, it can be concluded that, in addition to the decrease in the Krafft Point, favorable properties for practical applications can be expected as a result of the inclusion of the oxyethylene groups into the hydrophobic part of the molecule. As is true for other anionic surfactants, the electrical double layer will be compressed by the addition of multivalent cations. By this means, the adsorption at the interface is increased, the surface activity is raised, and, furthermore, the critical micelle concentration decreased. In the case of the alkyl ether sulfates, however these effects can be obtained without encountering undesirable salting out effects.

In Fig. 7, this is exemplified with surface tension concentration curves for Na n-tetradecyl diethyleneglycol ether sulfates (33). Less soluble surfactants would produce with increasing water hardness increased formation of sparingly soluble Ca salts. Therefore, the critical micelle concentration would be shifted toward much larger concentrations.

However, in the case of Na tetradecyl dioxyethylene sulfate, the surface tension and the critical micelle concentration will be reduced in the presence of water hardness. If a complexing agent is added, the effect is weakened because of the complexing of the

multivalent alkaline earth ions. Thus alkyl ether sulfates have special advantages in hard water and in products containing no complexing agents.

In Fig. 8, the soil removal from woollens by various technically important surfactants are presented as a function of the water hardness (34). The favorable properties of alkyl ether sulfates in comparison to other anionic surfactants at higher water hardnesses are clearly evident.

If sufficient amounts of complexing agents or of ion exchangers are added, the soil removal of water hardness-sensitive surfactants, for example LAS, becomes independent of the Ca ion concentration. However, in the case of alkyl ether sulfates an increase in the washing effect can still be observed with increasing water hardness (33). In this case, the stronger influence of Ca and Mg ions than that of Na ions can be attributed to their stronger compression of the electrical double layer at the interface. Only in the lower range of hardness does the addition of sodium sulfate bring a certain advantage. In analogy to the surface tension measurements, there is even a small deterioration of the soil removal as consequence of complexing by Na triphosphate present in solution (Fig. 9).

The results indicate that in detergent formulations without complexing agents or ionic exchangers, alkyl ether sulfates may have definite advantages. Detailed investigations of washing conditions in the United States showed best results with tetradecyl 3 EO sulfate (35). It may be used preferably in liquid heavy duty detergents without phosphate (36).

TABLE V

Foam Volume in cm³ Determined with the Beating Method Using a Perforated Disk after 30 sec. at 40°C, 1 g/l

Substances (techn.)	Water hardness		Foam Decrease %
	10 °d	17 °d	
C ₁₂ Sulfate (Na salt)	780	170	78
C ₁₂₋₁₈ Sulfate (Na salt)	870	145	83
C ₁₂₋₁₆ 4EO Sulfate (Na Mg salt)	840	560	33
C ₁₂ 2EO Sulfate (Na salt)	830	675	19

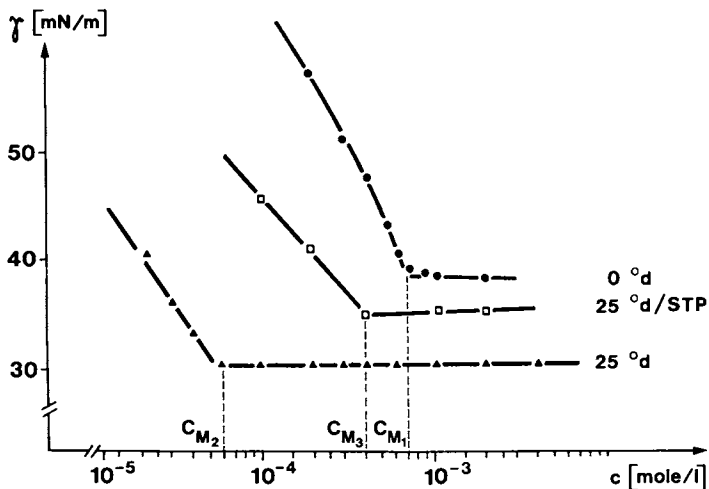
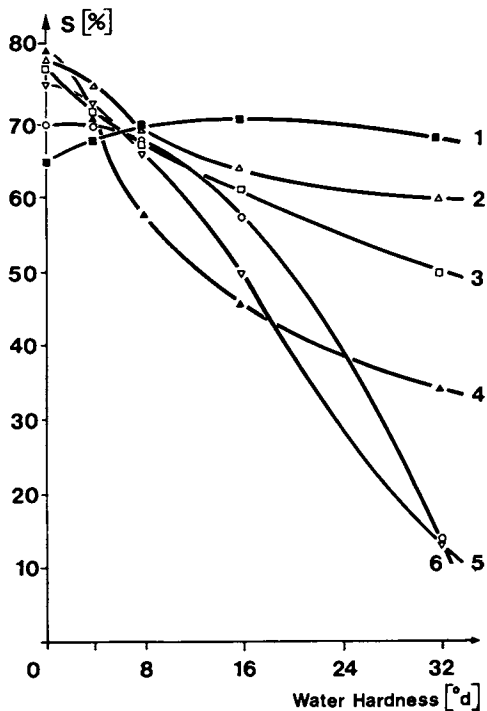


Fig. 7 Surface tension of aqueous solutions of sodium tetradecyl diglycol ether sulfate at 25°C (technical product)

Fig. 8 Soil removal from wool by different anionic surfactants. Test conditions: temperature, 30°C ; time, 15 min; concentration, surfactant 0.15 g/L + Na_2SO_4 1.5 g/L; soil, sebum/pigment mixture; surfactant (1) C_{12-14} alcohol 2EO sulfate, (2) C_{15-18} olefinic sulfonate, (3) C_{16-18} sulfo fatty ester, (4) C_{12-18} fatty alcohol sulfate, (5) C_{13-18} alkyl sulfonate, (6) C_{10-13} alkyl benzene sulfonate.



Cosmetic Rinse off Preparations. In certain cosmetic products, for example hair shampoos, it is not possible to use complexing agents because of the irritation of mucous membranes. Here a low sensitivity of surfactants to water hardness is a precondition for their application. Foam formation is generally considered to be a measure of shampoo quality (Table V). With increase in water hardness the foam volume of alkyl sulfates decreases very much, whereas with the corresponding alkyl ether sulfates this decrease is relatively small. For cosmetic applications, the good skin compatibility and low irritation to mucous membranes of alkyl ether sulfates is of high importance (37).

Bulk Properties. Because of viscosity and stability requirements for product manufacture and processing, the appearance of mesomorphous phases in mixtures with water is very important. In the case of dodecyl monoglycol ether sulfate and dodecyl sulfate, a highly viscous middle phase is observed up to a concentration of 80 %. For the corresponding diglycol ether compound, however, the middle phase is present only in a concentration range up to about 65 % (38). Above this concentration, a lamellar neat phase exists.

The middle phase is much more viscous than the neat phase, though the concentration of the latter is higher. If a concentrated system of an alkyl ether sulfate and water existing initially as a neat phase is stepwise diluted, the range of the middle phase will be reached. This is accompanied by a steep increase in viscosity. The formation of the neat phase allows the manufacture and handling of highly concentrated fluid preparations. This property, however, can lead to processing problems upon dilution.

Table VI shows the results of polarized light microscopic observations. Sometimes isotropic regions and the middle phase exist simultaneously. The region of the middle phase is marked by heavy lines. The range of the especially viscous middle phase narrows with transition from two to three oxyethylene groups in the surfactant molecule. Up to 27 %, the system appears optically isotropic. In this concentration range the viscosity can be increased strongly by addition of NaCl, as shown in table VII.

In the case of sodium dodecyl sulfate, there is no corresponding effect. This thickening is at any rate not associated with the formation of the middle phase since the products remain isotropic. However, x-ray diffraction measurements indicate the presence of a crystalline, randomly oriented phase (39). It is still

unsettled, whether or not thickening is caused by the formation of a gel system, as described in the literature (40). Various salt additions (Hoffmeister Series) have little effect on the range of existence of the middle phase. The possibility to change the viscosity by means of surfactant concentration or by electrolyte addition has advantages for the manufacture of fluid and gel products containing alkyl ether sulfates.

TABLE VI

Phases of Concentrated Solutions of n-Dodecyl Ether Sulfates

Weight %	Number of EO-Groups			
	0	1	2	3
25		-	-	
30	-	- (M)	- (M)	-
35	M	M	M (-)	-
40	M	M	M	M
50	M	M	M	M
60	M	M	M	M
65			M (N)	N
70	M	M	N (M)	N
80		M		N

- optically isotropic, M middle phase, N neat phase

TABLE VII

Influence of Sodium Chloride on the Viscosity (mPa·s) of Surfactants

Substance (techn.)	Sodium chloride addition %		
	3	5	7
C ₁₂₋₁₄ Sulfate	< 100	< 100	< 100
C ₁₂₋₁₄ 2EO Sulfate	< 100	2,500	20,500

Alkyl Ether Sulfates in Mixtures

In most products, alkyl ether sulfates are used in form of mixtures with other surfactants. Alkyl benzene sulfonate (LAS) is the most important anionic surfactant used in combination with alkyl ether sulfates. As a result, the properties of mixtures of alkyl ether sulfates and LAS are of special practical interest.

General Remarks. In the use of products containing alkyl ether sulfates, oily soil removal as well as dispersion plays an important role. The driving force responsible for the separation of oily soil from a substrate (Fig. 10) is the wetting tension j defined by equation (1):

$$j = \gamma_{so} - \gamma_{sw} = -\gamma_{ow} \cos\theta_0 \quad (1)$$

The sketch in Fig. 10 shows the equilibrium of forces with an obtuse contact angle in the oil phase (θ_0). In this case the wetting tension, j , of the aqueous phase is positive, which means that the adhering oil droplet is pushed together by the aqueous phase. With the increase in j the tendency of an oil droplet to be cut off and removed from a solid substrate increases. Because of this, the impeding force for the removal of oil is the interfacial tension oil/water (γ_{ow}), which should be minimized. By minimization of the interfacial tension, moreover, the requirements for emulsification and stabilization of soil in the washing and cleaning liquid will be improved.

In general, at hydrophobic surfaces the final stage of the spontaneous complete oil removal will not be achieved, since a wetting equilibrium will be reached. The necessary additional work for complete removal of an oil droplet from the system must be added to the system in the form of mechanical energy.

In application-related problems the question may also be formulated in terms of minimizing the necessary additional work. From knowledge of the interfacial properties of surfactant mixtures the surface activity, tendency to form micelles, adsorption, etc., can be increased. The following effects may pertain:

a) The charged ionic groups of a surfactant in a mixed film may be shielded by the incorporation of a nonionic surfactant. The repulsion of the similarly charged groups is diminished and the impeding electrostatic forces of repulsion reduced.

b) If the hydrophilic head group of one surfactant of the mixture has a weak or strong charge opposite to

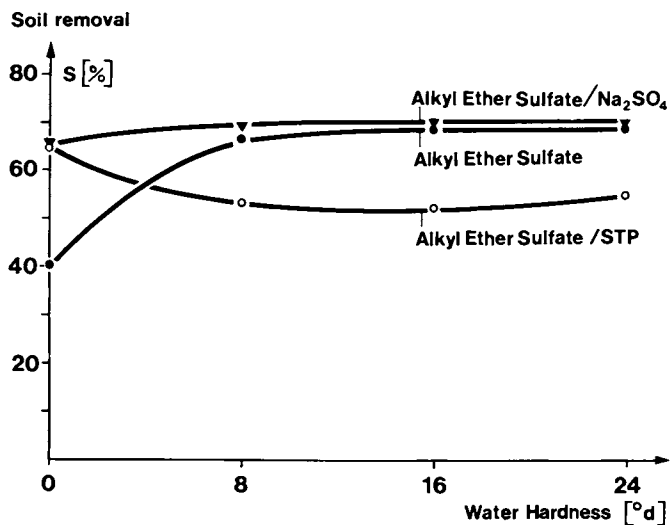


Fig. 9 Soil removal from wool by C₁₂₋₁₄ 2EO sulfate

Test condition:
 temperature: 30°C
 electrolyte conc.: 1.5 g/l
 surfactant conc.: 0.5 g/l
 soil: sebum/pigment mixture

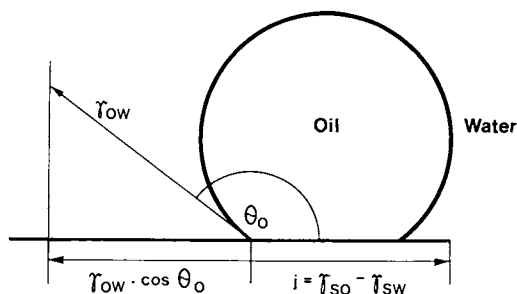


Fig. 10 Oil droplet on substrate in water

that of the other, not only shielding effects but also forces of attraction should be considered. (For example in mixtures of anionic and cationic surfactants, or anionic surfactants and amine oxides).

c) Inhibition of incorporation into an interfacial layer may be also reduced by an enlargement of the distances between the hydrophilic groups of the individual surfactants.

d) In addition to reduction of electrostatic repulsion, intensification of electrostatic attraction or van der Waal's forces of attraction may also be accomplished. This occurs by means of special interaction between the hydrophobic parts of the surfactant molecule. Such a special case was already discussed.

Selected Results. No mutual intensification of interfacial effects is observed between Na dodecyl sulfate as the first member of the homologous series of dodecyl ether sulfates and LAS. In Fig. 11, the oil/water interfacial tensions are shown. Neither the electrostatic nor the van der Waal's interactions of the mixtures are intensified.

However, this situation is changed significantly by the incorporation of a single oxyethylene group into the molecule of the alkyl sulfate. This is shown in Fig. 12 for various dodecyl ether sulfates. In contrast to the mixtures with dodecyl sulfate, a significant decrease of the interfacial tension with well defined minima at certain LAS/alkyl ether sulfate ratios are observed. With increasing number, m , of oxyethylene groups, this effect becomes more pronounced, and the minima of interfacial tension are shifted strongly in favour of LAS-rich solutions. Small additions of alkyl ether sulfates to LAS improve the interfacial properties to a significant extent. Intensification of other interfacial properties in LAS/alkyl ether sulfate mixtures is also to be expected. This is shown in Fig. 13 by means of two substrate specific and two substrate-nonspecific criteria of importance for the washing process. In the series of mixtures investigated, properties such as wetting tension on polyester, contact angle on polyester, olive oil/water, interfacial tension, and emulsification of olive oil all show a definite extreme point. This corresponds to the optimum surfactant mixture and should be also observed under application conditions.

In Fig. 14, the results of a dishwashing test close to practice are presented (41, 42). Plates soiled with fat are cleaned in a detergent solution at 45 °C and the decay of previously generated foam as well as

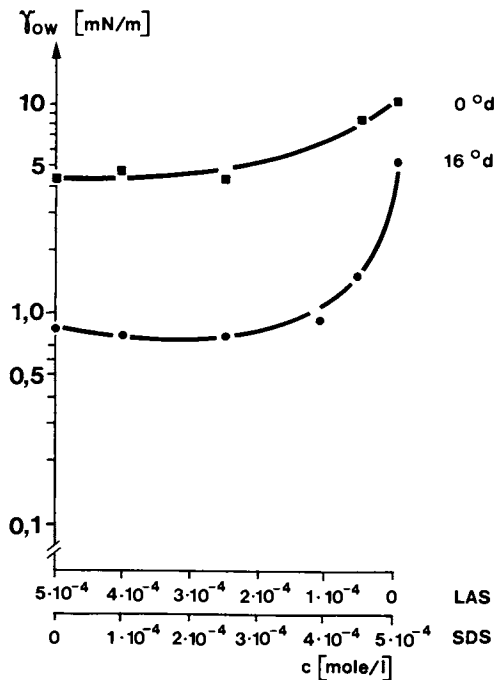


Fig. 11 Olive oil/water interfacial tension for LAS/SDS-mixtures

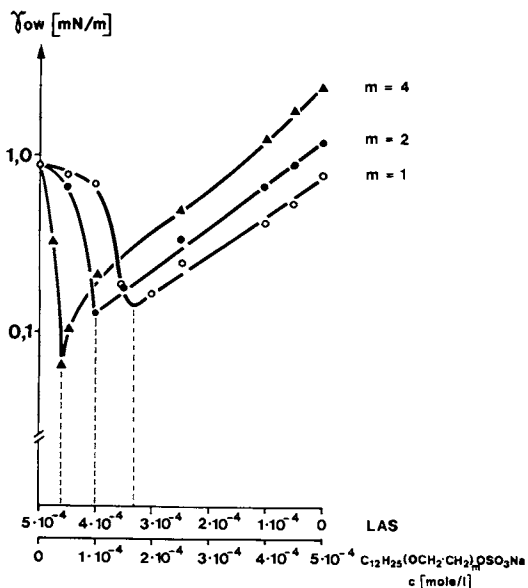


Fig. 12 Olive oil/water interfacial tension for LAS/Alkyl ether sulfate mixtures (purity: LAS- technical product, ether sulfates 98.0-99.5%)

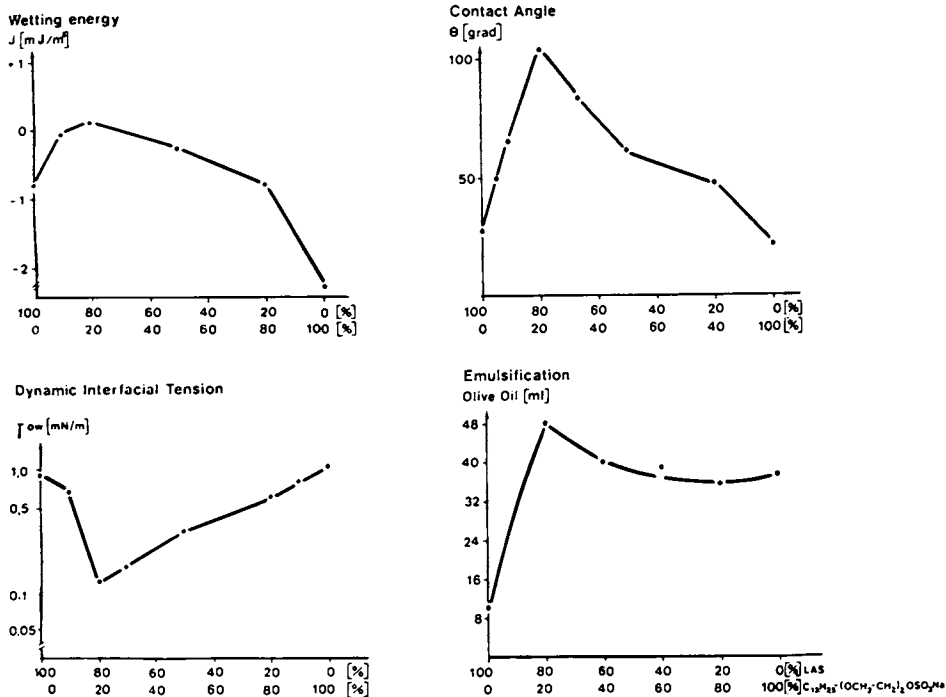


Fig. 13 Interfacial properties of LAS/ $C_{12}H_{25}(-O-CH_2-CH_2-)_2OSO_3Na$ mixtures

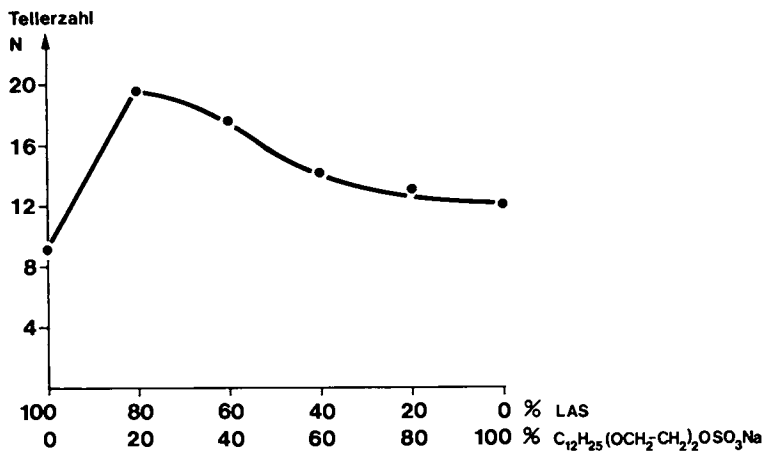


Fig. 14 Dishwashing by LAS/dodecyl 2EO sulfate mixtures
N: number of plates washed at 45°C (technical products)

possible deposition of fat are evaluated. As a measure for the quality of a detergent the number, N , of plates washed until the foam decays was used. The largest number of perfectly clean dishes is obtained in the case of an equal ratio of LAS and dodecyl ether sulfate, as could be predicated from the measurement of interfacial properties. In addition, similar results were obtained in washing experiments, where the maximum of soil removal was found to be at the same ratio of surfactants (Fig. 15).

Physicochemical and application results show that mixtures of LAS and alkyl ether sulfates have especially positive properties. This makes it understandable why products containing both types of substances are so widely used.

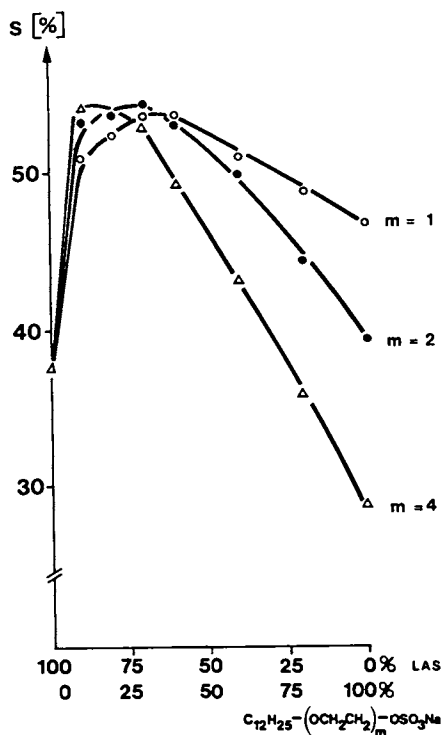


Fig. 15 Soil removal from wool by LAS/alkyl ether sulfate mixtures (technical products)
 Test condition:
 temperature: 30°C
 concentration: 5×10^{-3} mole/l
 soil: sebum/pigment mixture

Literature Cited

1. Glasl, J.; in: "Fettalkohole", Ed. by Henkel KGaA, Düsseldorf, 1981, p. 125
2. Grün, R. von der; Scholz-Weigel, S., Seifen, Öle, Fette, Wachse, 1982, 108, 121
3. Cox, M.F.; Matson, T.P., Soap Cosm. Chem. Spec., 1982, 58, 46
4. Felleitschin, G.; J. Soc. Cosm. Chem., 1964, 15, 245
5. Shinoda, K.; Nakagawa, T.; Tamamushi, B.; Isemura, T., in: "Colloidal Surfactants" Academic Press, New York, 1963
6. Shinoda, K.; Becher, P., "Principles of Solution and Solubility", Marcel Dekker Inc. New York, 1978, p. 159
7. Lange, H.; Schwuger, M.J., Kolloid-Z. Z.-Polymere, 1968, 223, 145
8. Tartar, H.V.; Wright, K.A., J. Amer. Chem. Soc., 1938, 61, 539
9. Schwuger, M.J.; Kolloid-Z. Z.-Polymere, 1969, 233, 979
10. Weil, J.K.; Stirton, A.J.; Wrigley, A.N., in: Proc. 5th Int. Congr. on Surface Active Agents, Ediciones Unidas Sa, Barcelona 1969, Vol. I, p. 45
11. Shinoda, K.; Pure and Appl. Chem., 1980, 52, 1195
12. Hato, M.; Tahara, M.; Suda, Y., J. Coll. Interface Sci., 1979, 72, 458
13. Asinger, F.; Berger, W.; Fanhänel, E.; Müller, K.R. J. Prakt. Chem., 1965, 27, 82
14. Götte, E.; Schwuger, M.J., Tenside, 1969, 6, 131
15. Schwuger, M.J.; Chem. Ing. Techn., 1970, 42, 433
16. Lange, H.; in: Proc. 3rd Int. Congr. Surface Active Agents, Cologne 1960, Vol. I, p. 279
17. Rosen, M.J.; Cohen, A.W.; Dahanayake, M.; Hua, X.Y., J. Phys. Chem., 1982, 86, 541
18. Lange, H.; Kolloid-Z., 1965, 201, 131
19. Weil, J.K.; Bristline, R.G.; Stirton, A.J., J. Phys. Chem., 1958, 67, 1796
20. Götte, E.; in: Proc. 3rd Int. Congr. Surface Active Agents, Cologne 1960, Vol. I, p. 45
21. Lange, H.; Tenside, 1975, 12, 27
22. Lange, H.; Schwuger, M.J., Colloid Polymer Sci., 1980, 258, 1264
23. Schick, M.J.; J. Phys. Chem., 1963, 67, 1796
24. Schick, M.J.; J. Amer. Oil Chemist's Soc., 1963, 40, 680
25. Tokiwa, F.; J. Phys. Chem., 1968, 72, 4331
26. Barry, B.W.; Wilson, R., Colloid Polymer Sci., 1978, 256, 251

27. Kratochvil, J.P.; J. Colloid Interface Sci., 1980, 75, 271
28. Tanford, C.; Nozaki, Y.; Rohde, M.F., J. Phys. Chem., 1977, 81, 1555
29. Herrmann, K.W.; J. Phys. Chem., 1962, 66, 295
30. Tokiwa, F.; J. Phys. Chem., 1968, 72, 1214
31. Tokiwa, F.; Ohki, K., J. Phys. Chem., 1967, 71, 1343
32. Schwuger, M.J.; Fette, Seifen, Anstrichmittel, 1970, 72, 25
33. Jakobi, G.; Schwuger, M.J., Chemiker-Z., 1975, 99, 182
34. Andree, H.; Krings, P., Chemiker-Z., 1975, 99, 168
35. Stüpel, H.; Scharer, D.H., in: Proc. 7th Int. Congr. Surface Active Agents, Moscow 1978, Vol. III, p. 202
36. Kravetz, L.; Scharer, D.H.; Stüpel, H., in: Proc. 7th Int. Congr. on Surface Active Agents, Moscow 1978, Vol. III, p. 192
37. Kästner, W.; Frosch, P.J., Fette, Seifen, Anstrichmittel, 1981, 83, 33
38. Lange, H.; unpublished data
39. Weiß, A.; unpublished data
40. Ekwall, P.; in: "Advances in Liquid Crystals" Ed. by G.H. Brown, Acad. Press, New York, 1975, Vol. I, p. 1
41. Lehmann, H.J.; Fette, Seifen, Anstrichmittel, 1972, 74, 163
42. Jakobi, G.; in: "Tensid-Taschenbuch", Ed. by H. Stache, Carl-Hanser-Verlag, München, 1981, p. 302

RECEIVED January 10, 1984

Effects of Structure on the Properties of Polyoxyethylenated Nonionic Surfactants

TSUNEHICO KUWAMURA

Department of Synthetic Chemistry, Gunma University, Kiryu, 376 Japan

Data on the relationship of chemical structure to fundamental properties of polyoxyethylene(POE) nonionics in aqueous solution are reviewed. These include : 1) the adsorption, micelle formation and thermodynamics of a series of highly purified POE n-alkyl monoethers, varying systematically in chain length of both alkyl and POE groups, 2) the effects on the aqueous properties of multi-chain and alicyclic structure in hydrophobe, 3) the evaluation of hydrophilicity and surface properties for a new class of nonionics, alkyl crown ethers, 4) the adsorption and dissolution behavior of long N-acyl α -amino acid POE monoesters having a short chain of homogeneous POE, $R^1CONR^2CHR^3COO(C_2H_4O)_mH$, with special reference to the structural effects of the α -amino acid residue.

The correct understanding of the relationships between chemical structure and properties in surfactants is most important to both their effective use in many applications and to molecular designing of new surfactants. Some reliable information is available on various structural effects in ionic surfactants. On the other hand, only a limited amount of reliable information is available for nonionics with much of the data in the literature being insufficient both in reliability and in the variety of structures dealt with, mainly because of the difficulty in obtaining well-characterized compounds.

This paper will discuss data from the recent literatures and from our laboratory on structural effects for the usual and novel types of polyoxyethylene(POE) nonionics listed in Table I. These will be described for each type of nonionic in the order listed in Table I.

0097-6156/84/0253-0027\$06.00/0
© 1984 American Chemical Society

Table I. Scope of Chemical Structure of the Nonionics mentioned in this Paper

No of series	General formula ^{a)}	Structural feature	POE ^{b)} grade
1	$\text{H}(\text{CH}_2)_{\text{N}-1}\text{O}(\text{EO})_{\text{m}}\text{H}$	Straight chain	Homogeneous
2	$\left\{ \text{H}(\text{CH}_2)_{\text{N}/2} \right\}_2 \text{CH}_2\text{O}(\text{EO})_{\text{m}}\text{H}$ $\left\{ \text{H}(\text{CH}_2)_{\text{N}/3} \right\}_3 \text{C}(\text{O})\text{O}(\text{EO})_{\text{m}}\text{H}$	Multi-chain in hydrophobe	Heterogeneous (Poisson distribution)
3	$(\text{CH}_2)_{\text{N}-1} \text{CH}_2\text{O}(\text{EO})_{\text{m}}\text{H}$	Alicyclic hydrophobe	
4	$\text{H}(\text{CH}_2)_{\text{N}-1} \text{O}(\text{EO})_{\text{m}-2}$	Cyclic POE ^{b)}	
5	$\text{H}(\text{CH}_2)_{\text{N}-1} \text{CO} \begin{matrix} \text{O} \\ \\ \text{N} \\ \\ \text{R}' \end{matrix} \text{CHR}'' \text{CO} \begin{matrix} \text{O} \\ \\ \text{O}(\text{EO})_{\text{m}}\text{H} \end{matrix}$	Amido ester inserted between alkyl and POE	

a) EO : $-\text{CH}_2\text{CH}_2\text{O}-$

b) POE : polyoxyethylene

n-Alkyl POE Monoethers (No 1 series)

Although a considerable number of reports have been published on the surface and micellar properties of nonionics of this fundamental structure, there are only a few investigations using highly purified compounds in which chain length of either alkyl or POE group was varied systematically.

Meguro and coworkers recently reported the effect of variation in alkyl chain length(N) on the properties of homogeneous materials of structure $\text{H}(\text{CH}_2)_{\text{N}}\text{O}(\text{EO})_{\text{m}}\text{H}$, where N was varied from 10 to 15, including both even and odd chain lengths (1, 2). They found that most of the plots of surface tension at the critical micelle concentration(cmc) vs. N at various temperature(15 - 40°C) gave a zig-zag line, decreasing with increase in N and having a convex break point at each odd number of N. They have observed a similar tendency also for the plots of surface area per molecule vs. N. From these results, they suggest that the packing of the adsorbed film of the surfactant molecule with an odd number of carbons is looser than that with even number of carbons. On the other hand, plots of the log of the cmc vs. N gave a linear relationship, indicating no difference between even and odd carbon number compounds in micellar properties.

They have studied also the N dependence of the thermodynamic parameters of micellization, calculated from the cmc values and their temperature dependence, as shown in Figure 1, where ΔG_m is

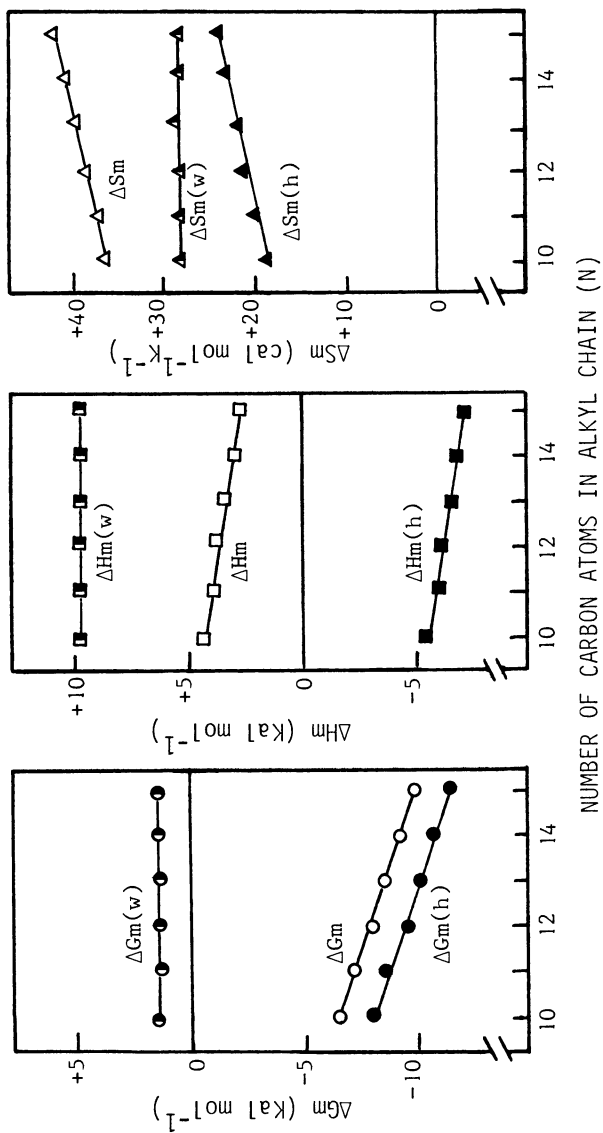


Figure 1. Thermodynamic parameters of micellization at 25°C as a function of alkyl chain length for $H(CH_2)_N O(EO)_8 H$ (from Meguro et al., Ref. 2. 1981)

the free energy, ΔH_m the enthalpy and ΔS_m the entropy of micellization. These parameters were separated into contributions from the hydrophobe and from the hydrophile, such as $\Delta G(h)$ and $\Delta G(w)$. Their conclusions are as follows: The hydrocarbon chain is an important factor in micellization. The hydrophobic part of the enthalpy, $\Delta H(h)$, is negative and $\Delta S(h)$ is positive, therefore both terms jointly contribute to the negative value of ΔG_m . This contribution increases linearly with increasing N . On the other hand, the POE group opposes micellization, due to a large positive value of $\Delta H(w)$, suggesting dehydration of the hydrated monomeric POE chains on micellization.

Rosen and coworkers have also investigated similar properties for a homogeneous series of POE dodecyl monoethers, varying in the number of oxyethylene(OE) units from 2 to 8 (3). Table II shows a part of their data on the thermodynamics of micellization. Their results indicate that a steady increase in ΔG_m , (or cmc) with lengthening POE chain is predominantly due to the change in the ΔH_m term, and suggest that desolvation of POE chain oxygens in micelle formation increases progressively with increasing OE unit number. They also determined the thermodynamic parameters of surface adsorption from cmc and surface tension data and discussed the value of $(\Delta G_m - \Delta G_{ad})$, which is the work involved in transferring the nonionic molecule from a monolayer at zero surface pressure to the micelle. As shown in Table III, the positive value for the work of transfer increases with increasing OE unit number, mainly due to the enthalpy factor. Based on the results, they suggest that the motion of the alkyl chain in the surface film is not as restricted as in the interior of the micelle, and that dehydration of the POE chain required for micellization is greater than that for adsorption.

Rosen's group reported also the effect of POE chain length on wetting properties (4).

Table II. Thermodynamic Parameters of Micellization for Nonionic of $n\text{-C}_{12}\text{H}_{25}\text{O}(\text{EO})_m\text{H}$ at 25°C , data from Rosen et al.(3)

m	$\Delta G^{\circ}_{mic}/$ (kJ mol^{-1})	$\Delta H^{\circ}_{mic}/$ (kJ mol^{-1})	$\Delta S^{\circ}_{mic}/$ ($\text{kJ mol}^{-1}\text{K}^{-1}$)
2	-25.6	+4.2	+0.10 ₀
3	-24.4	+5.9	+0.10 ₂
4	-23.9	+8.8	+0.11 ₀
5	-23.9	+9.9	+0.11 ₃
7	-23.3	+12.5	+0.12 ₀
8	-22.6	+13.2	+0.12 ₀

Table III. Effects of POE Chain Length on Micellization and Adsorption for Nonionics of $n\text{-C}_{12}\text{H}_{25}\text{O}(\text{EO})_m\text{H}$, data from Rosen et al. (3)

m	$\Delta G^{\circ}_{\text{mic}} - \Delta G^{\circ}_{\text{ad}}/$ (kJ mol ⁻¹)	$\Delta H^{\circ}_{\text{mic}} - \Delta H^{\circ}_{\text{ad}}/$ (kJ mol ⁻¹)	$T(\Delta S^{\circ}_{\text{mic}} - \Delta S^{\circ}_{\text{ad}})/$ (kJ mol ⁻¹)
2	+9.6	+5.6	-3.9
3	+11.1	+6.2	-4.8
4	+12.0	+8.4	-3.6
5	+12.4	+9.3	-3.0
7	+13.6	+10.1	-3.6
8	+14.8	+9.9	-5.0

Multi-chain and Alicyclic Hydrophobe (No 2 and 3 series)


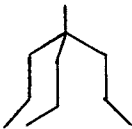


There have been few studies of the properties of pure compounds in these series of nonionics (5, 6). In our laboratory, the nonionics shown in Table IV and V have been synthesized by the addition of ethylene oxide under the same conditions to pure ethylene glycol monoethers, rather than to secondary or tertiary alcohols. This method has been found to give the same Poisson distribution of OE units and to be suitable for evaluating quantitatively the structural effects of the hydrophobe (7).

Table IV shows a comparison of some aqueous solution properties of nonionics having the same total number (ten) of carbon atoms in the hydrophobe and a comparable POE chain length, but different hydrophobe structure. It can be seen that multi-chain hydrophobes bring about a striking decrease in the cloud point and in the surface tension at the cmc, and an increase in the cmc, while cyclic fixation of the alkyl chain causes a large increase in the cloud point, the cmc and in the surface tension at the cmc.

Table V shows the same structural effects for the higher homologues of these series. Here, molecular area and cmc of the highest members do not depend so much on the hydrophobe structure.

The effect characteristic of a multi-chain hydrophobe, that is, increase in the cmc and simultaneous decrease in the cloud point, appears to be inconsistent with the well-known HLB concept in surfactants. Tanford has pointed out that based on geometric considerations of micellar shape and size, amphiphilic molecules having a double-chain hydrophobe tend to form a bilayer micelle more highly packed rather than those of single-chain types (8). In fact, a higher homologue of α, α' -dialkylglyceryl polyoxyethylene monoether has been found to form a stable vesicle or lamellar micelle (9). Probably, the multi-chain type nonionics listed in

Table IV. Effects of Multi-chain and Alicyclic Structures of Hydrocarbon Group in $R-O(EO)_mH$

Properties	R-						
	m		7.0	7.0	5.5	7.2	4.1
Cp^a ($^{\circ}C$)		75	22	17	58	80	>100
γ_{cmc}^b (mNm^{-1})		36.0	28.3	---	33.9	47.3	48.0
$cmc \times 10^3$ ($mol\ l^{-1}$)		0.85	6.0	4.8	6.0	20.5	27.0

a) Cp : cloud point b) γ_{cmc} : surface tension at cmc

Table V. Effects of Multi-chain and Alicyclic Structures of Hydrocarbon Group in the Higher Member of $R-O(EO)_mH$

R-	m	Cp ($^{\circ}C$)	$cmc \times 10^4$ ($mol\ l^{-1}$)	γ_{cmc-1} (mNm^{-1})	$A \times 10^2$ a) (nm^2)
$n-C_{13}H_{27}-$	8.9	79	0.35	32.6	61
$(n-C_6H_{13})_2CH-$	9.2	35	1.3	27.9	60
$(n-C_4H_9)_3C-$	9.2	34	5.8	27.5	71
$n-C_{12}H_{25}-$	9.4	84	0.94	32.5	62
$(CH_2)_{11}CH-$	9.2	75	15.0	36.9	86
$n-C_{16}H_{33}-$	12.2	97	0.15	34.3	58
$(n-C_8H_{17})_2CH-$	11.6	36	0.11	28.8	63
$(n-C_5H_{11})_3C-$	12.0	48	0.72	27.3	68
$(CH_2)_{15}CH-$	11.9	80	0.32	36.7	65

a) A : molecular area on the adsorption film

these Tables also form lamellar micelles above their cmc's, despite their high cmc values due to less hydrophobic character of

the hydrocarbon part. Such micellization should be accompanied by closer packing of the POE moiety and greater dehydration of POE chain than in micelle formation by the usual type of nonionic. This seems to be related to the unexpectedly low cloud point of the multi-chain type of nonionics.

Higher Alkyl Crown Ethers (No 4 series)

During the past ten years, there have been numerous reports on the synthesis and the application of crown ethers of specific character to various fields. There have been also a few studies of the surface and micellar properties of crown ethers with hydrophobic groups (10 - 17). The author has called them surface active crown ethers as a new class of surfactant possessing a promising function (11).

Okahara and coworkers have developed a one-step cyclization of oligoethylene glycol (18, 19) and applied it to the convenient synthesis of crown ethers with higher alkyl chains (20, 21). They have prepared many series of n-alkyl crown ethers and N-alkyl monoazacrown ethers varying in both alkyl chain length and OE unit number, and compared their properties with those of the corresponding open chain compounds (14, 15).

Figure 2 shows the plots of cloud point vs. alkyl chain length for these compounds having the same number (six) of OE units. It can be seen that cyclization of the POE chain lowers the cloud point, indicating that the cyclic POE without the hydroxyl group has a lower hydrophilicity, and that replacing the oxygen atom in the ring with a nitrogen atom considerably raises the cloud point, implying stronger hydration of the amino group. The same conclusions are also reached from the results of the relation of cloud point to OE unit number and from structural effects on the cmc.

Table VI shows a comparison of the surface properties of the crown and the corresponding open chain compound. The former has a lower aqueous surface tension and a larger molecular area than the latter, reflecting the lower hydrophilicity and the greater rigidity of cyclic POE.

Thus, an estimation can be made of the hydrophilicity of the crown ring. The acetal-type crown ring obtained from hexaethylene glycol and a higher aliphatic aldehyde is estimated to be equivalent to about four OE units in an alkyl POE monoether, from our study of the cloud point (11). Moroi et al. concluded, from a comparison of the cmc, that a diaza-18-crown-6 is equivalent to 20 OE units in the usual type of nonionic (12). Okahara's group evaluated the effective HLB based on the cloud point, phenol index and phase-inversion-temperature in emulsion of oil/water system and they concluded that 18-crown-6 and monoaza-18-crown-6 rings with dodecyl group are approximately equivalent to 4.0 and 4.5 units, respectively, of OE chains with the same alkyl chain (17).

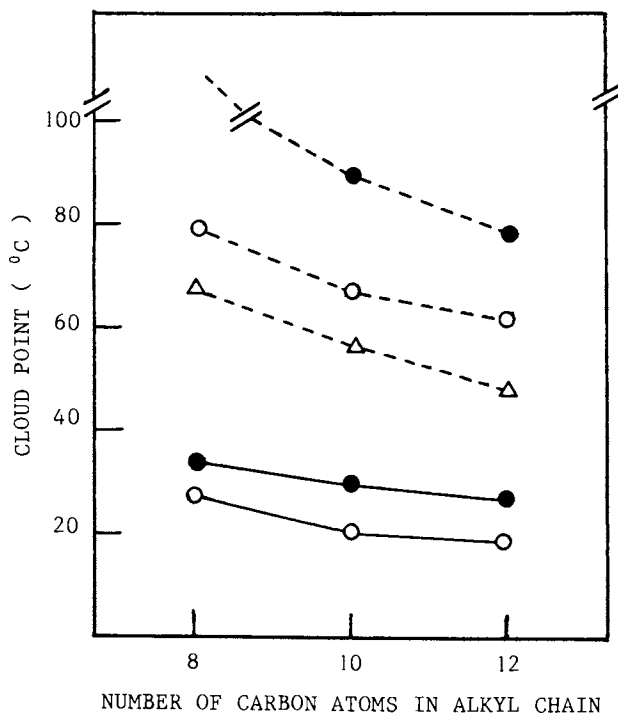
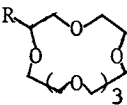
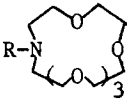


Figure 2. Effect of hydrophile-structure on cloud point (the data points from Kuo, Ikeda and Okahara, Ref. 14. and 15. 1982).

—●—: N-alkyl monoaza 18-crown-6, ---●---: RN(EO)₃H₂, —○—: alkyl 18-crown-6, ---○---: HOCHRCH₂O(EO)₅H, ---△---: RO(EO)₆H

Table VI. Effect of the Hydrophile-Structure on the Surface Properties at 20°C, data from Okahara et al. (14,15)^{a)}

Structure	R-	Surface tension at cmc (mNm^{-1})	Area/molecule ($\text{nm}^2 \times 10^2$)
	C ₈	32.9 (-)	55 (-)
	C ₁₀	33.0 (36.5)	56 (45)
	C ₁₂	34.7 (-) ^{b)}	56 (-) ^{b)}
	C ₈	34.0 (36.5)	53 (47)
	C ₁₀	34.0 (36.5)	53 (45)
	C ₁₂	33.0 (35.5)	54 (47)

a) The data for the corresponding precursor of the crown ether are shown in parentheses b) Measured at 10°C

Surface-active crown ethers are distinctly differ from usual type of nonionics in salt effect on the aqueous properties, due to the selective complexing ability with cations depending on the ring size of the crown. As shown in Figure 3 (22), the cloud point of the crowns is selectively raised by the added salts. This indicates that the degree of cloud point increase is a measure of the crown-complex stability in water (23).

Long N-Acyl α -Amino Acid POE Monoesters (No 5 series)

The salts of long N-acyl amino acids have been gaining more interest and commercial use in the fields of detergents, cosmetics and toiletries, due to good surface properties, mildness to skin and high biodegradability. In order to develop a new type of nonionics possessing noteworthy character from these materials, we have recently investigated the synthesis and the aqueous properties of homogeneous series of oligoethylene glycol esters of various N-acyl α -amino acids (25).

The results show the effect of inserting typical α -amino acid residues between a long alkyl group and a POE chain, based on a comparison of properties with those of the usual type of nonionic.

Table VII shows that glycine(G), and particularly glycyglycine(G₂), residues raise the melting, Krafft and cloud points. On the other hand, the melting and Krafft points of nonionics having a G residue steadily decrease with increasing number of OE units. L-Alanine(L-A) slightly raises the melting and Krafft points, and sarcosine(S) has the least influence on the properties. This indicates that introducing a highly hydrogen bond-forming secondary amido linkage into the nonionic molecule increases both the crystallinity and hydrophilicity of POE nonionic.

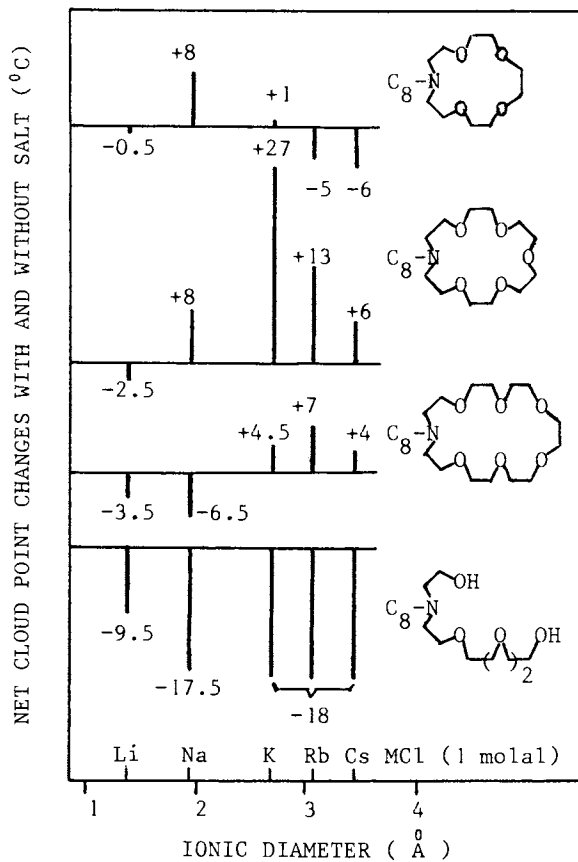


Figure 3. Salt effects on cloud points of N-alkyl monoaza crown ethers and the corresponding open chain derivatives (from Kuo and Okahara, Ref. 22. 1983)

Table VII. Melting Point, Krafft Point and Cloud Point of Nonionics

Compound ^{a)}	Melting point(°C)	Krafft point(°C)	Cloud point(°C)
C ₁₂ OE ₆ ^{b)}	25	< 0	51
C ₁₂ O ₂ E ₆ ^{c)}	21 - 23	< 0	54
C ₁₂ GE ₂	59 - 61	40	78
C ₁₂ GE ₃	56 - 58	24	46
C ₁₂ GE ₄	44 - 46	< 0	74 - 76
C ₁₂ G ₂ E ₄	102 - 103	52	>100
C ₁₂ AE ₃	33 - 34	14	22 - 23
C ₁₂ SE ₃	liq.	< 0	43 - 45

a) G : -NHCH₂COO- E_m : -(C₂H₄O)_mH G : -(NHCH₂CO)₂O- A : -NHCHMeCOO- (L-alanine) S : -NMeCH₂COO-

b) C₁₂H₂₅O(C₂H₄O)₆H c) C₁₁H₂₃COO(C₂H₄O)₆H

Table VIII. Cmc and Surface Properties of Nonionics (30°C)

Compound	cmc (mol l ⁻¹ x 10 ⁴)	Surface tension at cmc (mNm ⁻¹)	Area per molecule (nm ² x 10 ²)
C ₁₂ OE ₆	0.80 ^{a)}	31.5 ^{a)}	50 ^{a)}
C ₁₂ O ₂ E ₆	1.2 ^{a)}	31.5 ^{a)}	--
C ₁₂ GE ₃	2.9	28.2	44
C ₁₂ GE ₄	3.8	29.8	51
C ₁₂ AE ₃	3.6	28.8	53
C ₁₂ SE ₃	3.0	29.6	52

a) Measured at 20°C

Table VIII shows that G, L-A and S residues cause the same degree of increase in the cmc and only slightly affect surface tension reduction and molecular area on the adsorption film. For each series of this type of nonionic, plots of log cmc vs. number of carbon atoms(8 - 16) in the acyl chain gave a straight line with a slope similar to that for the usual type of nonionic. However, the former types differ distinctly from the latter type in

Table IX. Thermodynamic Data for Micellization of Nonionic Surfactants at 25°C

Compound	$-\Delta G_m$ (kJ mol ⁻¹)	ΔH_m (kJ mol ⁻¹)	ΔS_m (J mol ⁻¹ K ⁻¹)
C ₁₀ OE _{5.7}	28.1	+5.12	112
C ₁₀ SE ₄	24.3	+2.43	90
C ₁₀ AE ₄	23.7	0.0	80
C ₁₀ GE ₄	23.6	-2.10	72
C ₁₂ OE ₆	33.3	+10.0	146
C ₁₂ SE ₄	30.1	0.0	100
C ₁₂ AE ₄	29.4	-3.35	88
C ₁₂ GE ₄	29.7	-15.5	46

the temperature dependence of the cmc, as shown in Figure 4. The nonionics having G, L-A or S residues all gave a line with negative slope and a break point. Such temperature dependence of cmc has been reported not for the known POE nonionics, but for the zwitterionic N-alkyl betaines (26), the molecules of which are intermediate in polarity between ionics and POE nonionics.

Table IX shows the thermodynamic parameters of micellization, calculated from the cmcs and their temperature dependence, for two homologues of each of these types of nonionics. It can be seen that ΔH_m and ΔS_m progressively decrease in the order: usual-type > S > L-A > G type for both homologous series. This suggests that the high polarity of the amido linkage causes either less dehydration or exothermic association of the hydrophilic part on micelle formation.

Figure 5 shows plots of cloud point vs. number of OE units for each of these types of nonionics. These plots give four curves roughly parallel to one another, except for a part of the G type. From these curves, it is possible to estimate a contribution of the inserted residue to hydrophilicity of the nonionics. Namely, such contribution may be represented by the difference between usual and other types in OE unit number required to give the same cloud point in the temperature range 40 - 60°C. Thus, the equivalent number of OE units is about 3 for both G and S, and 2 for L-A, respectively. Only the G type gives an unusual curve with a minimum, which has not previously been reported for POE nonionics. A similar unusual behavior can also be observed regarding the acyl chain length (N) dependence of the cloud point, as shown in Figure 6. Only the S type, with tertiary amido linkage, gave a curve descending with increasing N, like the usual type. On the other

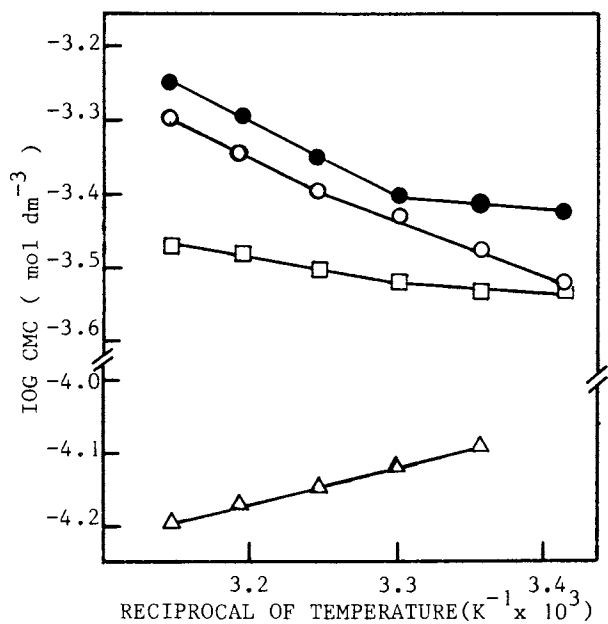


Figure 4. Plots of log cmc vs. the reciprocal of temperature for nonionics : $C_{12}GE_4$ (○), $C_{12}AE_4$ (●), $C_{12}SE_4$ (□) and $C_{12}OE_6$ (△)

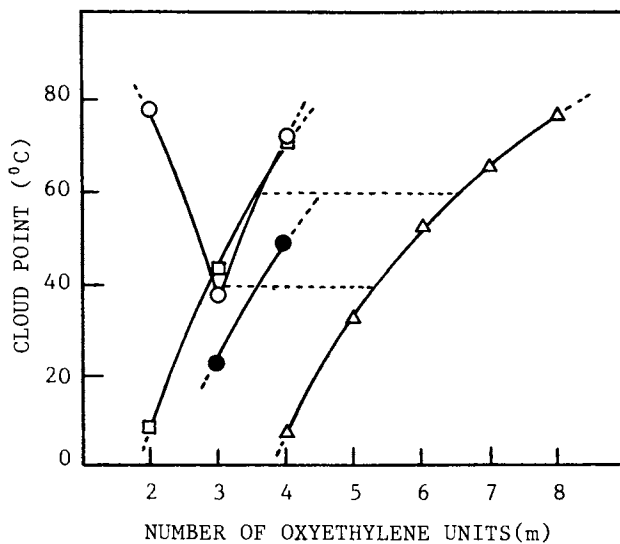


Figure 5. Plots of cloud point vs. number of oxyethylene units(m) for nonionics : $C_{12}GE_m$ (—○—), $C_{12}AE_m$ (—●—), $C_{12}SE_m$ (—□—) and $C_{12}OE_m$ (—△—)

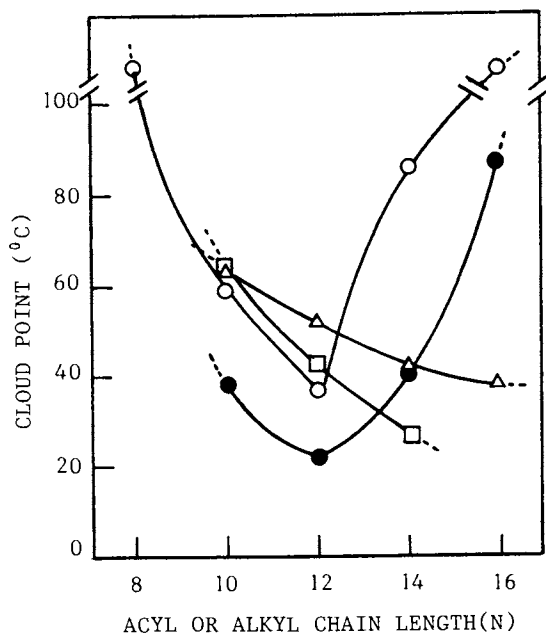


Figure 6. Plots of cloud point vs. number of carbon atoms in the acyl or alkyl group for nonionics : C_NGE_3 (—○—), C_NAE_3 (—●—), C_NSE_3 (—□—) and C_NOE_6 (—△—)

hand, the curves of G and L-A types having secondary amido linkages have a sharp minimum at the same $N(12)$. This problem will be discussed in relation to the phase diagram of the G type and water system.

Binary phase diagram of the G type-water system were determined by visual observations with polarizing microscopy and by differential-scanning-calorimetry. Several photographic illustrations of the liquid crystal phase of a 50 wt% $C_{14}GE_3$ dispersion in water over the temperature range 35 - 86°C are shown in Figure 7. We can see typical textures characteristic of a neat phase above the Krafft point(38°C). The textures partially disappear at 63°C, but new liquid crystals appear again with ascending temperature up to 85°C. At 86°C, a portion of the liquid crystals begin to melt and phase separation occurs, but the other portion remains up to 97°C.

Figure 8 shows the binary phase diagram of the $C_{14}GE_3$ -water system. This indicates that this nonionic has no middle phase and has a markedly wide area of neat phase over both composition and temperature ranges. On the other hand, the S type with the same N gives not so wide area of neat phase, and it has been reported that the $C_{12}OE_6$ -water system has middle and neat phases (27). The results suggest that G type nonionics with a secondary amido linkage and a long chain acyl group are particularly apt to form a lamellar liquid crystals due to highly orienting molecules.

Figure 9 shows the effect of acyl chain length (N) on the binary phase diagram of G type nonionics. The area of neat phase spreads with increasing N and the extension of the area takes rapid strides between N of 12 and 14. This N is just in accord with that of the sharp minimum in the cloud point - N curve of the G type. The same thing has also been found for the relation between the effect of OE number on the area of the neat phase and the minimum in the cloud point - OE number curve of $C_{12}GE_m$ ($m = 2 - 4$).

These facts may be explained as follows : The secondary amido linkage located near the alkyl chain contributes, together with hydrophobic bonding by the alkyl chain, to form a tight lamellar aggregate of the nonionic molecule, due to its intermolecular hydrogen-bonding ability. This is reflected in the wide area of neat phase over a great range of both temperature and composition for the higher members of the G type. Consequently, dehydration of the hydrophilic part of the nonionic fixed in the lamellar aggregate may be significantly restricted up to a high temperature. This results in raising the cloud point curve as a whole.

Concerning the effects of introducing amino acid residues into POE nonionics, it can be concluded that 1) amido groups do not lower surface-active properties, 2) amido groups generally increase the hydrophilicity of nonionics (giving a high cloud point), 3) secondary amido groups increase the crystallinity of nonionics (giving a high Krafft point and the ability to form lamellar liquid crystals). Thus, the insertion of amino acid

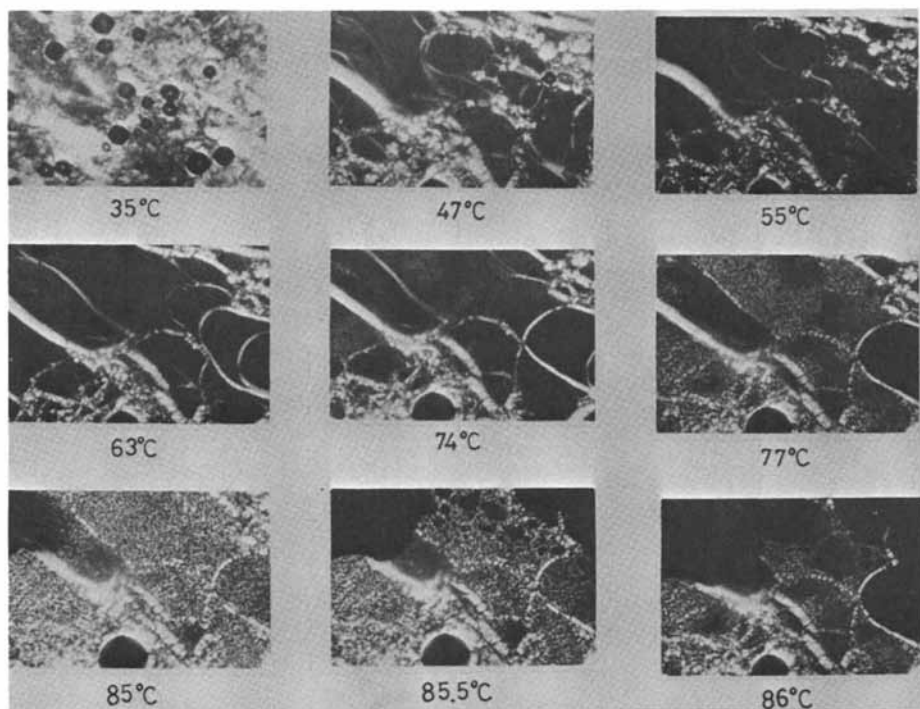


Figure 7. Photomicrographs with crossed polaroids of a 50 wt% $C_{14}GE_3$ dispersion in water over the temperature range 35 - 86°C. Magnification Ca x 100

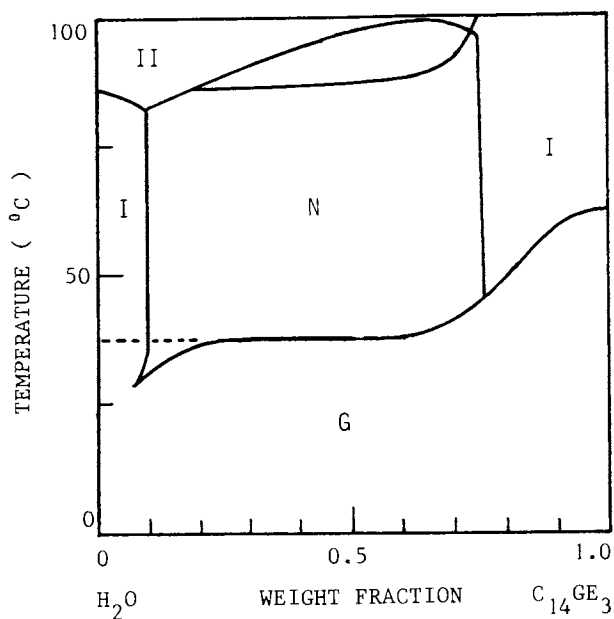


Figure 8. Binary phase diagram of C₁₄GE₃-water system. G : gel phase, N : neat phase, I : isotropic solution, II : two liquid phase

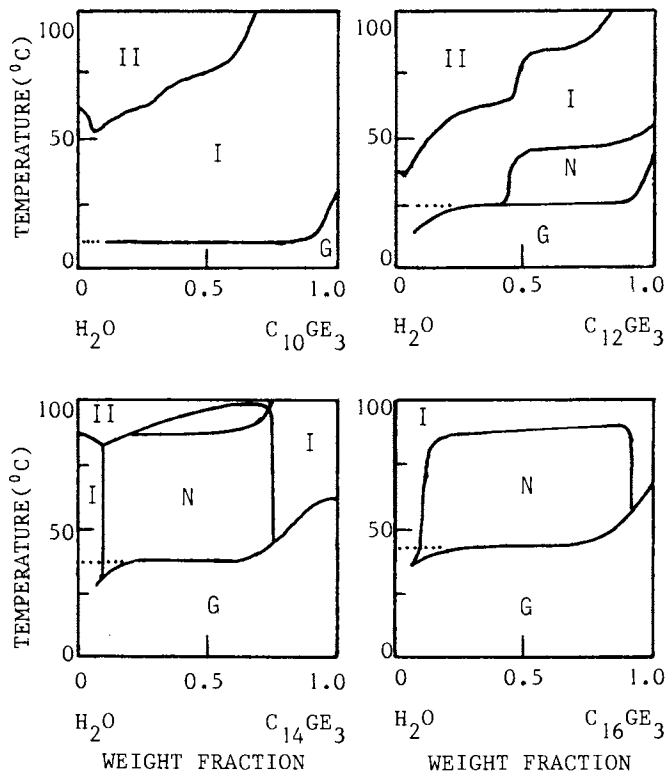


Figure 9. Effect of acyl chain length(N) on the binary phase diagram of C_NGE_3 -water systems

residues becomes a new structural factor for control of two important properties of POE nonionics, hydrophilicity and crystallinity, which have so far been controlled only with hydrocarbon and polyoxyethylene chain lengths.

Acknowledgments

The author wish to thank Professor M. J. Rosen, Brooklyn College of the City University of New York, for his kind editing of the manuscript. The author is also grateful to the following co-workers who at some time were responsible for part of the work presented from our laboratory : T. Suzuki, H. Tanaka, S. Inokuma and Dr. H. Takahashi.

Literature Cited

1. Ueno, M.; Takasawa, Y.; Tabata, Y.; Sawamura, T.; Kawahashi, N.; Meguro, K. Yukagaku 1981, 30, 421.
2. Meguro, K.; Takasawa, Y.; Kawahashi, N.; Tabata, Y.; Ueno, M. J. Colloid Interface Sci. 1981, 83, 50.
3. Rosen, M. J.; Cohen, A. W.; Dahanayake, M.; Hua, X-Y. J. Phys. Chem. 1982, 86, 541.
4. Cohen, A. W.; Rosen, M. J. J. Am. Oil Chem. Soc. 1981, 58, 1062.
5. Elworthy, P. H.; Florence, A. T. Kolloid-Zeit. 1964, 195, 23.
6. Schüring, S.; Ziegenbein, W. Tenside Detergents 1967, 4, 161.
7. Kuwamura, T.; Akimaru, M.; Takahashi, H.; Arai, M. Reports of Asahi Glass Foundation for Industrial Technology 1979, 35, 45; Chem. Abstr. 1981, 95, 61394q.
8. Tanford, C. J. Phys. Chem. 1972, 76, 3020.
9. Okahata, Y.; Tanamachi, S.; Nagai, M.; Kunitake, T. J. Colloid Interface Sci. 1981, 82, 401.
10. Le Moigne, J.; Gramain, P. J. Colloid Interface Sci. 1977, 60, 566.
11. Kuwamura, T.; Kawachi, T. Yukagaku 1979, 28, 195.
12. Moroi, Y.; Pramauro, E.; Grätzel, M.; Pelizzetti, E.; Tundo, P. J. Colloid Interface Sci. 1979, 69, 341.
13. Kuwamura, T.; Yoshida, S. Nippon Kagaku Kaishi 1980, 427.
14. Kuo, P.-L.; Ikeda, I.; Okahara, M. Tenside Detergents 1982, 19, 4.
15. Kuo, P.-L.; Ikeda, I.; Okahara, M. Tenside Detergents 1982, 19, 204.
16. Inokuma, S.; Hagiwara, Y.; Shibasaki, K.; Kuwamura, T. Nippon Kagaku Kaishi 1982, 1218.
17. Kuo, P.-L.; Ikeda, I.; Okahara, M. Bull. Chem. Soc. Jpn. 1982, 55, 3356.
18. Kuo, P.-L.; Miki, M.; Okahara, M. J. Chem. Soc. Chem. Commun. 1978, 504.
19. Kuo, P.-L.; Kawamura, N.; Miki, M.; Okahara, M. Bull. Chem. Soc. Jpn. 1980, 53, 1689.

20. Ikeda, I.; Yamamura, S.; Nakatsuji, Y.; Okahara, M. J. Org. Chem. 1980, 45, 5355.
21. Kuo, P.-L.; Miki, M.; Ikeda, I.; Okahara, M. J. Am. Oil Chem. Soc. 1980, 57, 227.
22. Kuo, P.-L. Ph. D. Thesis, Osaka University, Osaka, 1983.
23. Okahara, M.; Kuo, P.-L.; Yamamura, S.; Ikeda, I. J. Chem. Soc. Chem. Commun. 1980, 586.
24. Bluestein, B. R.; Cowell, R. D. J. Am. Oil Chem. Soc. 1981, 58, 173A.
25. Kuwamura, T. et al. unpublished data which have been presented at the meeting of Division of Colloid and Surface Chemistry in Japan Chemical Society and at the Japan Oil Chemists' Society meeting, 1981 - 1983.
26. Swarbrick, J.; Daruwara, J. J. Phys. Chem. 1967, 73, 2627.
27. Balmbra, R. R. et al. Trans. Faraday Soc. 1962, 58, 1661.

RECEIVED January 10, 1984

American Chemical
Society Library

1155 16th St. N. W.

In Structure/Performance Relationships in Surfactants; Rosen, M.;
ACS Symposium Series; American Chemical Society: Washington, DC, 1984.

Washington, D. C. 20036

Surface Properties of Zwitterionic Surfactants

1. Synthesis and Properties of Some Betaines and Sulfobetaines

M. DAHANAYAKE and MILTON J. ROSEN

Department of Chemistry, Brooklyn College, City University of New York, Brooklyn, NY 11210

Zwitterionic surfactants of structure $\text{RN}^+(\text{CH}_2\text{C}_6\text{H}_5)-(\text{CH}_3)\text{CH}_2\text{COO}^-$, where R is an alkyl chain of 10 or 12 carbon atoms, and $\text{RN}^+(\text{CH}_2\text{C}_6\text{H}_5)(\text{CH}_3)\text{CH}_2\text{CH}_2\text{SO}_3^-$, where R is 8, 10, or 12 carbon atoms, have been synthesized. From surface tension-concentration curves in aqueous solution at 10°, 25°, and 40°C, surface excess concentrations and areas/molecule at surface saturation, critical micelle concentrations, efficiency and effectiveness of surface tension reduction, and thermodynamic parameters of adsorption and micellization have been calculated. The areas/molecule indicate that the entire ionic head group in each series is lying flat in the aqueous solution/air interface. For the glycines, the standard free energies of micellization and of adsorption per methylene group at the aqueous solution/air interface are -2.80 kJ and -3.05 kJ, respectively; for the taurines, the standard free energy of adsorption per methylene is -3.15 kJ, all at 25°C.

The use of zwitterionic surfactants commercially has increased dramatically in recent years (1) because of their unique properties, such as compatibility and synergism when used in conjunction with most other types of surfactants. This type of surfactant is used in textile processing aids, cosmetic products, cleaning agents, and as antistatic agents. The sulfobetaines have been found to be very good lime soap disperants (2).

In spite of this wide applicability, a survey of the literature reveals that, compared to ionic and nonionic surfactants, there have been relatively few investigations of their surface and thermodynamic properties. Investigation has been hampered by the nonavailability of pure compounds and proper analytical techniques to determine their concentration in solution.

0097-6156/84/0253-0049\$06.00/0
© 1984 American Chemical Society

Tori and Nakagawa (3-7), in a series of papers, described the micellar properties of C_8 , C_{10} , and C_{12} C-alkylbetaines of the type $(CH_3)_3^+N-CH(R)COO^-$, and N-octylbetaine, $C_8H_{17}^+N(CH_3)_2CH_2COO^-$. From studies of the temperature dependence of the cmc, they were able to calculate ΔH_{mic}° . Herrmann (8) studied C_{10} , C_{12} , and C_{16} N-alkyl-sulfobetaines of the type, $R-^+N(CH_3)_2(CH_2)_3SO_3^-$ with regard to the chain length and ionic strength variation on the cmc. He calculated the standard free energy contribution to micellization of a methylene group to be $0.61 \text{ kcal mol}^{-1}$ and, thereby, concluded that the internal structure of the micelles of these zwitterionics is similar to all other ionic and nonionic surfactants studied. Thermodynamic parameters of micellization have also been investigated by Molyneux (9), and Swarbrick (10). They were able to estimate the standard free energy contribution to micellization of the head group of N-alkyl and C-alkylbetaines to be $+3.3$ and $+2.7 \text{ Kcal mol}^{-1}$, respectively. Molyneux et al. found the plot of $\log \text{ cmc}$ vs. $1/T$ for dodecyl N-methylbetaines to be linear, whereas Swarbrick et al. observed a minimum in the curve for the corresponding decyl and undecyl betaines. From these data, these workers were able to estimate the standard enthalpies and entropies of micellization and to compare these results with other nonelectrolyte amphophiles.

In contrast to this, there is little information available (11) on the thermodynamics of adsorption of alkylbetaines and no data on the thermodynamic parameters of adsorption or micellization for sulfobetaines.

In the present work, we have synthesized two betaines and three sulfobetaines in very pure form and have determined their surface and thermodynamic properties of micellization and adsorption. From these data on the two classes of zwitterionics, energetics of micellization and adsorption of the hydrophilic head groups have been estimated and compared to those of nonionic surfactants.

Experimental Section

N-alkyl N-benzyl N-methylglycines, $C_nH_{2n+1}N^+(CH_2C_6H_5)(CH_3)CH_2COO^-$.

Two homologues, in which $n = 10$ (C_{10} BMG) and 12 (C_{12} BMG), were synthesized by reacting N-methylbenzylamine (3 moles) and sodium chloroacetate (1 mole) in 95% ethanol overnight at 40°C . The resulting solution was treated with 0.5 moles of Na_2CO_3 and steam distilled to remove the excess N-methylbenzylamine. Water was removed by rotary evaporator and the crude residue N-methylbenzylglycine was recrystallized from isopropyl alcohol.

The tertiary amine thus obtained was dissolved in absolute ethanol and was refluxed for two days with five molar percent excess of the appropriate bromoalkane (97% Humphrey Chemical, North Haven, Conn.). Solvent was removed and the residue in aqueous Na_2CO_3 solution was extracted with hexane to remove any unreacted bromoalkane. Next, the N-alkyl N-benzyl N-methylglycine was extracted into chloroform from the aqueous layer. Solvent was stripped off and the crude material was recrystallized thrice from carbon tetrachloride and twice from THF/ $CHCl_3$ (60:40 v/v) mixture. The yields of the purified betaines were about 75% of the theoretical.

Analytical data for the compounds were as follows:

	calculated			found		
	C	H	N	C	H	N
C ₁₀ BMG	75.19	10.41	4.38	74.48	10.82	4.32
C ₁₀ BMG	76.03	10.73	4.03	75.70	10.76	3.92

N-alkyl N-benzyl N-methyltaurines, $C_nH_{2n+1}N^+(CH_2C_6H_5)(CH_3)CH_2CH_2SO_3^-$.

Three homologues in which $n = 8$ (C₈BMT), 10 (C₁₀BMT), and 12 (C₁₂BMT) were synthesized by a procedure similar to that for the N-alkylbetaines. Here, the N-methylbenzylamine and sodium salt of 2-chloroethanesulfonic acid were refluxed in 95% methanol for two days. After treatment with 0.5 M Na₂CO₃, the resulting solution was steam distilled to remove the excess N-methylbenzylamine. Water was removed and the crude residue was recrystallized from ethanol.

The tertiary amine thus obtained was dissolved in absolute ethanol and refluxed for five days with five molar percent excess of the appropriate bromoalkane. Thereafter, the procedure was similar to that for the N-alkylglycines. Crude product was recrystallized thrice from water and then from THF/CHCl₃ (50:50 v/v) mixture.

Analytical data for the compounds were:

	calculated			found		
	C	H	N	C	H	N
C ₁₀ BMT	64.99	9.55	3.79	65.20	9.92	3.74
C ₁₂ BMT	66.45	9.89	3.52	66.31	10.01	3.48

The molar absorptivities for the two betaines and the three sulfobetaines in aqueous solution are listed in Table I. Before being used for surface tension measurements, aqueous solution of surfactants were further purified by repeated passage (12) through minicolumns (SEP-PAK C₁₈ Cartridge, Waters Assoc., Milford Mass.) of octadecylsilanized silica gel. The concentration of surfactant in the effluent from these columns was determined by ultraviolet absorbance, using the molar absorptivities listed in Table I.

Table I. Molar Absorptivities for $R-N^+(CH_2C_6H_5)(CH_3)CH_2COO^-$ and $R-N^+(CH_2C_6H_5)(CH_3)CH_2CH_2SO_3^-$

Compound	λ_{max}	ϵ (dm ³ mol ⁻¹ cm ⁻¹ x 10 ⁻³)
C ₁₀ BMG	263	3.80
C ₁₂ BMG	263	3.55
C ₈ BMT	263	3.88
C ₁₀ BMT	263	3.80
C ₁₂ BMT	210	12.12

Surface tension measurements. Solutions of the betaines were prepared with quartz-condensed, distilled water, specific conductance, 1.1×10^{-6} mho cm^{-1} at 25°C . All surface tension measurements were made by Wilhelmy vertical plate technique. Solutions to be tested were immersed in a constant-temperature bath at the desired temperature $\pm 0.02^\circ\text{C}$ and aged for at least 0.5 h before measurements were made. The pH of all solutions was > 5.0 (usually, in the range 5.5-5.9), where surface properties show no change with pH.

Results and Discussions

Plots of surface tension, γ , vs. the log of the molar concentration, C , of the surfactant in the bulk phase at 10° , 25° , and 40°C for the N-alkyl glycines and the N-alkyltaurines are shown in Figures 1 and 2 respectively.

Surface excess concentration, Γ , in mol cm^{-2} , and area/molecule, A , in nm^2 , at the liquid/air interface were calculated from the relationships:

$$\Gamma = \frac{1}{2.303RT} \left(\frac{-\partial\gamma}{\partial \log C} \right)_T \quad \text{and} \quad A = \frac{10^{14}}{NT}$$

where $(\partial\gamma/\partial \log C)_T$ is the slope of the γ -log C curve at constant temperature, T , $R = 8.31 \text{ J mol}^{-1}\text{K}^{-1}$, and $N = \text{Avogadro's number}$. Values of the critical micelle concentration (cmc), minimum area per molecules (A_{min}), π_{cmc} , the effectiveness of surface tension reduction (13), and pC_{20} , the efficiency of surface tension reduction (14), are listed in Table II.

The $C_{10}\text{BMG}$ and $C_{12}\text{BMG}$ were found to have high solubility in water, whereas the corresponding N-alkyltaurines were sparingly soluble in water. As a result of the poor solubility, the only cmc determined in this series was for $C_{10}\text{BMT}$ at 40°C . The cmc of $C_8\text{BMT}$ was not determined due to its high cmc and insufficient material.

The areas per molecule for the glycines and for the taurines, when compared to the cross sectional areas of the compounds as obtained from molecular models, suggest that, at the aqueous solution/air interface, the ionic head groups, $-\text{N}^+(\text{CH}_2\text{C}_6\text{H}_5)(\text{CH}_3)\text{CH}_2\text{CH}_2\text{SO}_3^-$ (in the case of the taurines) and $-\text{N}^+(\text{CH}_2\text{C}_6\text{H}_5)(\text{CH}_3)\text{CH}_2\text{COO}^-$ (in the case of the glycines), are lying flat in the interface.

Although the efficiencies of surface tension reduction, pC_{20} , for the betaines and their corresponding sulfobetaines are almost the same, the former appear to show greater effectiveness in surface tension reduction, as indicated by the π_{cmc} values. This may be due to the smaller areas per molecule of the betaines as compared to the corresponding sulfobetaines.

Standard Thermodynamic Parameters of Micellization. Standard free energies of micellization were calculated by the relationship:

$$\Delta G_{\text{mic}}^\circ = RT \ln \text{CMC}$$

Standard entropies and enthalpies of micellization, $\Delta S_{\text{mic}}^\circ$ and $\Delta H_{\text{mic}}^\circ$, can be calculated from the relationships:

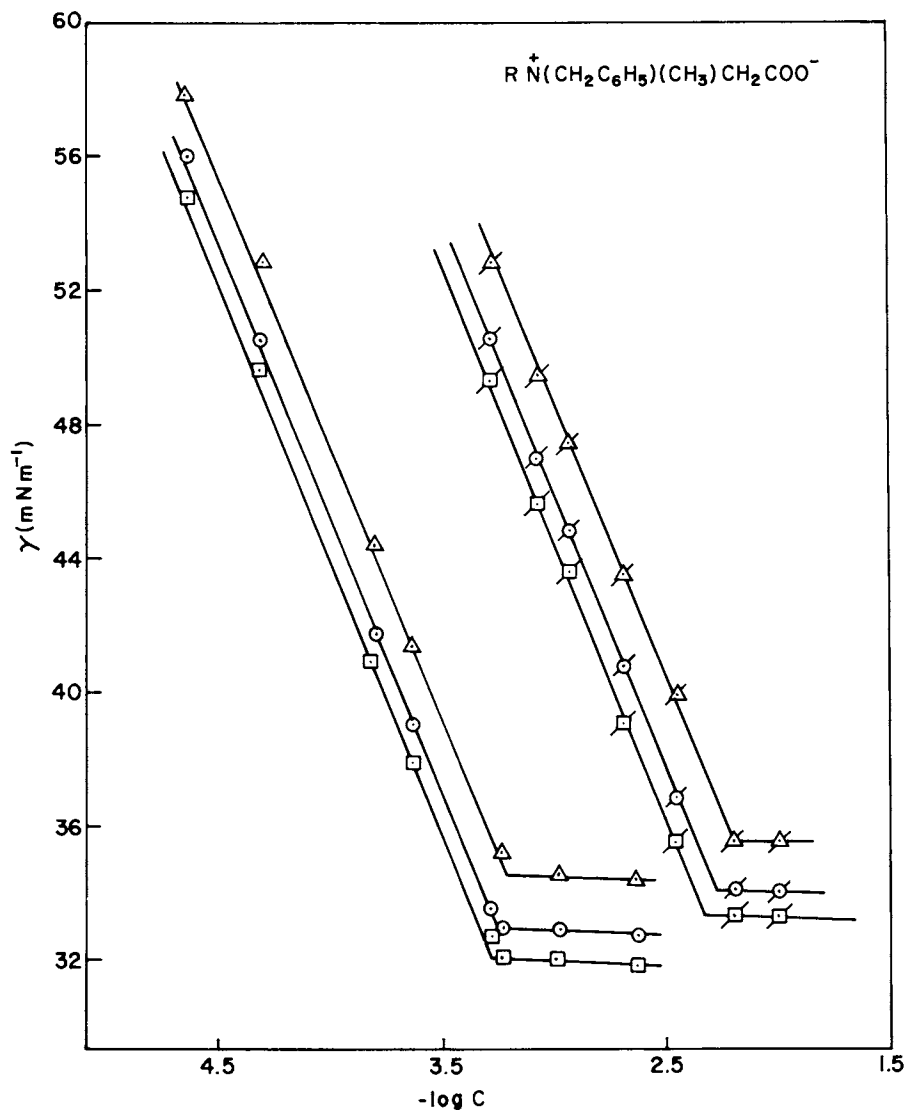


Figure 1. Surface tension vs. log concentration of C_{10} BMG in aqueous solution at 10° Δ , 25° \circ , and 40° \square ; of C_{12} BMG at 10° Δ , 25° \circ , and 40° \square .

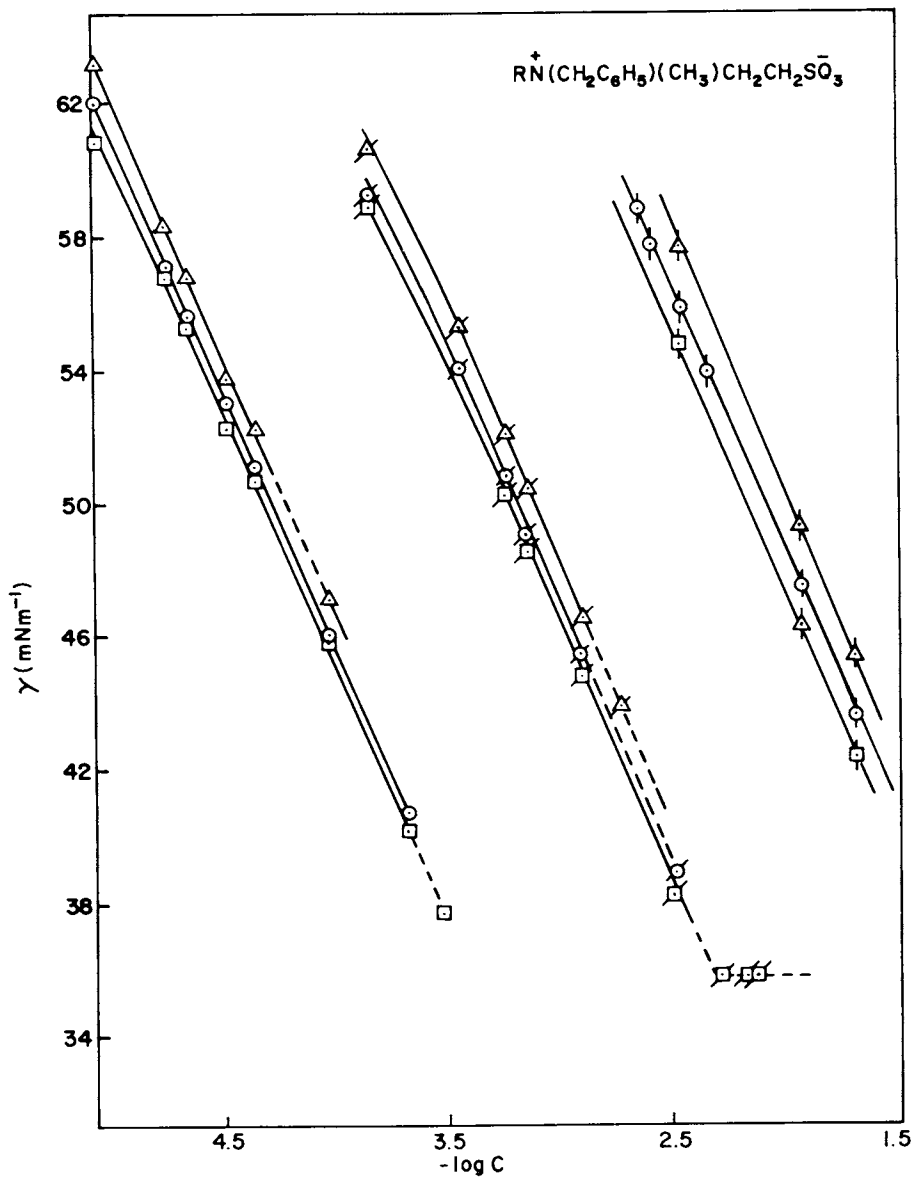


Figure 2. Surface tension vs. log concentration of C₈BMT at 10° △ , 25° ○ , and 40° ◻ ; of C₁₀BMT at 10° △ , 25° ○ , and 40° ◻ ; of C₁₂BMT at 10° △ , 25° ○ , and 40° ◻ .

Table II. Surface Properties of $R-N^+(CH_2C_6H_5)(CH_3)CH_2COO^-$ and $R-N^+(CH_2C_6H_5)(CH_3)CH_2CH_2SO_3^-$

Compound	T(°C)	cmc mole dm ⁻³	A _{min} nm ² x 100	pC ₂₀	π _{cmc} mN m ⁻¹
C ₁₀ BMG	10°	6.31 x 10 ⁻³	54.8	3.34	38.7
	25°	5.25 x 10 ⁻³	56.9	3.36	38.0
	40°	4.36 x 10 ⁻³	59.7	3.30	36.3
C ₁₂ BMG	10°	6.026 x 10 ⁻⁴	56.2	4.42	39.7
	25°	5.49 x 10 ⁻⁴	57.6	4.42	39.0
	40°	5.25 x 10 ⁻⁴	59.7	4.32	37.6
C ₈ BMT	10°	---	54.0	2.26	--
	25°	---	60.9	2.23	--
	40°	---	63.4	2.17	--
C ₁₀ BMT	10°	---	55.8	3.4	--
	25°	---	60.9	3.34	--
	40°	4.57 x 10 ⁻³	64.0	3.22	33.8
C ₁₂ BMT	10°	---	58.5	4.52	--
	25°	---	61.2	4.44	--
	40°	---	64.0	4.32	--

$$d(\Delta G^\circ/dt) = -\Delta S^\circ$$

and

$$\Delta H^\circ = \Delta G^\circ + T\Delta S^\circ$$

The ΔS_{mic}° values in Table III are all positive, indicating increased randomness in the system upon transformation of the zwitterionic surfactant molecules into micelles. The ΔH_{mic}° values, too, are positive, due to the endothermic desolvation associated with micellization. Smaller ΔH_{mic}° and ΔS_{mic}° values at 25-40°C than at 10-25° are due to the smaller hydration of the monomers at the higher temperatures. In the temperature range studied, no minimum in the variation of ΔH_{mic}° with temperature was observed, in agreement with the work of Swarbrick et al. (10).

From the variation of the ΔH_{mic}° values for the two alkyl betaines, it is seen that, for the shorter alkyl chain compounds, the enthalpy change is a significant factor in the process of micellization while, for the longer chain compounds, the free energy change is due almost entirely to the entropy change.

From the standard free energy of micellization of the N-alkylglycines, the ΔG_{mic}° per methylene group at 25°C is -2.80 kJ. This

Table III. Standard Thermodynamic Parameters of Micellization for $R-N^+(CH_2C_6H_5)(CH_3)CH_2COO^-$

Compound	T (°C)	ΔG° (kJ mol ⁻¹)	ΔH° (kJ mol ⁻¹)	ΔS° (kJ mol ⁻¹ K ⁻¹)
C ₁₀ BMG	10	-11.5		
	25	-13.0	+8.5	+0.070
	40	-13.9	+4.7	+0.044
C ₁₂ BMG	10	-17.4		
	25	-18.6	+4.6	+0.078
	40	-19.6	+0.9	+0.067

is in close agreement with the corresponding value of -2.85 kJ at 20°C obtained by Molyneux et al. (9).

Standard Thermodynamic Parameters of Adsorption. Table IV lists the standard thermodynamic parameters of adsorption. Values have been

Table IV. Standard Thermodynamic Parameters of Adsorption for $R-N^+(CH_2C_6H_5)(CH_3)CH_2COO^-$ and $R-N^+(CH_2C_6H_5)(CH_3)CH_2CH_2SO_3^-$

Compound	T (°C)	ΔG° (kJ mol ⁻¹)	ΔH° (kJ mol ⁻¹)	ΔS° (kJ mol ⁻¹ K ⁻¹)
C ₁₀ BMG	10	-24.7		
	25	-26.0	+0.2	+0.087
	40	-27.2	-2.6	+0.078
C ₁₂ BMG	10	-30.9		
	25	-32.1	-7.1	+0.082
	40	-33.2	-10.9	+0.071
C ₈ BMT	10	-18.7		
	25	-20.0	+5.9	+0.083
	40	-20.6	-9.2	+0.036
C ₁₀ BMT	10	-25.1		
	25	-26.3	-2.7	+0.079
	40	-27.0	-12.9	+0.045
C ₁₂ BMT	10	-31.5		
	25	-32.6	-10.6	+0.074
	40	-33.5	-14.8	+0.060

calculated by the relationship (15):

$$\Delta G_{ad}^{\circ} = RT \ln CMC - \pi_{cmc} \cdot A_{min}$$

From the data, ΔG_{ad}° per methylene group at 25°C is -3.05 kJ for the glycines and -3.15 kJ for the taurines. These are in agreement with values of -3.15 kJ for long-chain alcohols and 1,3-diols (15).

The ΔH_{ad}° values are less positive than the ΔH_{mic}° values for the same alkyl glycines. This shows less dehydration of the surfactant required for adsorption at the aqueous solution/air interface than for the process of micellization. This is consistent with previous observations on polyoxyethylenated nonionics and alkylpyridinium halides (16,17).

The ΔS_{ad}° values are all slightly more positive than the ΔS_{mic}° values for the same compound, reflecting the greater restriction of space in the micelle than at the aqueous solution/air interface.

The ΔS_{ad}° values and ΔH_{ad}° values are both more positive for the betaines than for the corresponding sulfobetaines. This shows that the sulfobetaines require less dehydration for adsorption at the aqueous solution/air interface.

Using $\Delta G^{\circ}(-CH_3) = \Delta G^{\circ}(-CH_2-) - 5.56 \text{ kJ mol}^{-1}$, on the basis of solubility data (9,18) for liquid N-alkanes in water at 25°C, standard free energies of adsorption and micellization, $\Delta G_{ad}^{\circ}(-W)$ and $\Delta G_{mic}^{\circ}(-W)$ respectively, for the hydrophilic head groups, $-N^+(\text{CH}_3)(\text{CH}_2\text{C}_6\text{H}_5)\text{CH}_2\text{CH}_2\text{SO}_3^-$ and $-N^+(\text{CH}_2\text{C}_6\text{H}_5)(\text{CH}_3)\text{CH}_2\text{COO}^-$, were calculated. These values are listed in Table V together with the standard free energy values for the head groups $-\text{CHOHCH}_2-\text{CH}_2\text{OH}$ and $-\text{OCH}_2\text{CH}_2\text{OH}$ (19).

The $\Delta G^{\circ}(-W)$ values for the two zwitterionics are comparable to each other. Both the $\Delta G_{ad}^{\circ}(-W)$ and $\Delta G_{mic}^{\circ}(-W)$ values for the two nonionics are less positive than for the two zwitterions, possibly due to the greater hydration of the zwitterions than of the ether oxygen and/or -OH groups.

From the solubility data of n-decane in water, the enthalpy for the process n-decane (H_2O) \rightarrow n-decane (pure) at 25°C has been estimated by Boddard et al. (20) to be $-5.85 \text{ kJ mol}^{-1}$. Subtracting this value from the calculated $\Delta H^{\circ}(25^\circ\text{C})$ values for C_{10}BMG and C_{12}BMT , in Tables III and IV, the $\Delta H^{\circ}(-W)$ values for micellization and for adsorption at the aqueous solution/air interface at 25°C can be estimated. Values are shown in Table V.

From the $\Delta H_{ad}^{\circ}(-W)$ term for the two types of hydrophilic groups, it is evident that there is an exothermic effect in the transfer of the $-N^+(\text{CH}_2\text{C}_6\text{H}_5)(\text{CH}_3)\text{CH}_2\text{CH}_2\text{SO}_3^-$ from aqueous medium to the interface. This exothermic enthalpy term, together with a larger negative entropy term for the N-alkyltaurine head group, is possibly due to the partial neutralization of the oppositely charged groups in the hydrophilic heads due to their arrangement in checkerboard fashion aqueous solution/air interface, as suggested by Beckett and Woodward (21). In the case of the N-alkylglycines, endothermic dehydration of the hydrophilic head may outweigh the neutralization effect, thus making $\Delta_{ad}^{\circ}(-W)$ positive.

Table V. Standard Thermodynamic Parameters of Adsorption and Micellization of Various Head Groups (-W) at 25°C

(-W)	ΔG_{ad} (kJ mol ⁻¹)	ΔH_{ads}° (kJ mol ⁻¹)	ΔS_{ads}° (kJ mol ⁻¹ K ⁻¹)	ΔG_{mic}° (kJ mol ⁻¹)	ΔH_{mic}° (kJ mol ⁻¹)	ΔS_{mic}° (kJ mol ⁻¹ K ⁻¹)
-N ⁺ (CH ₂ C ₆ H ₅)(CH ₃)CH ₂ COO ⁻	+10.0	+4.6	-0.018	+20.5	+12.4	-0.027
-N ⁺ (CH ₂ C ₆ H ₅)(CH ₃)CH ₂ CH ₂ SO ₃ ⁻	+10.6	-1.9	-0.042	--	--	--
-CH(OH)CH ₂ CH ₂ OH	+7.4	--	--	+10.0	--	--
-OCH ₂ CH ₂ OH	+8.8	--	--	+16.3	--	--

Literature Cited

1. Ernst, R.; Miller, E. J., Jr. "Amphoteric Surfactants"; Bluestein, B. R.; Hilton, C. L., Ed.; Marcel Dekker: New York, 1982; pp. 137-150.
2. Kaminiski, M.; Linfield, W. M. J. Am. Oil Chem. Soc. 1979, 56, 771.
3. Tori, K.; Nakagawa, T. Kolloid - Z. Z. Polym. 1963, 50, 187.
4. Tori, K.; Nakagawa, T. Kolloid - Z. Z. Polym. 1963, 188, 47.
5. Tori, K.; Nakagawa, T. Kolloid - Z. Z. Polym. 1963, 189, 50.
6. Tori, K.; Nakagawa, T. Kolloid - Z. Z. Polym. 1963, 191, 42.
7. Tori, K.; Nakagawa, T. Kolloid - Z. Z. Polym. 1963, 191, 48.
8. Herrmann, K. W. Colloid Interface Sci. 1966, 22, 352.
9. Molyneux, P.; Rhodes, C. T.; Swarbrick, J. Trans. Faraday Soc. 1965, 61, 1043.
10. Swarbrick, J.; Daruwala, J. J. Phys. Chem. 1969, 73, 2627.
11. Swarbrick, J., J. Pharm. Sci. 1969, 58, 147.
12. Rosen, M. J. J. Colloid Interface Sci. 1981, 79, 587.
13. Rosen, M. J. J. Colloid Interface Sci. 1976, 56, 32.
14. Rosen, M. J. J. Am. Oil Chem. Soc. 1974, 51, 461.
15. Rosen, M. J.; Aronson, M. Colloids Surfaces 1981, 3, 201.
16. Rosen, M. J.; Cohen, A. W.; Dahanayake, M.; Hua, X. J. Phys. Chem. 1982, 86, 541.
17. Rosen, M. J., Dahanayake, M.; Cohen, A. Colloids Surfaces 1983, 5, 159.
18. McAuliffe, C. Nature (London) 1963, 200, 1092.
19. Kwan, C.; Rosen, M. J. J. Phys. Chem. 1980, 84, 547.
20. Goddard, E. D.; Hoeve, C. A.; Benson, G. C. J. Phys. Chem. 1957, 61, 593.
21. Beckett, A. H.; Woodward, R. J. J. Pharm. Pharmacol. 1963, 15, 422.

RECEIVED January 20, 1984

Surface Properties of Zwitterionic Surfactants

2. Effect of the Microenvironment on Properties of a Betaine

MILTON J. ROSEN and BU YAO ZHU¹

Department of Chemistry, Brooklyn College, City University of New York, Brooklyn, NY 11210

The effect of pH and electrolyte on the surface properties of a betaine surfactant, $C_{12}H_{25}N^+(CH_2C_6H_5)(CH_3)CH_2COO^-$, were studied. The ΔG_{ad}° of both the zwitterionic form of the betaine and of the cationic protonated betaine were calculated. Surface activity decreases slightly with decrease in pH. As expected, the cationic form has somewhat lower surface activity than the zwitterionic form. Although the pK_a of the protonated betaine is 2.8, the properties of both the zwitterionic betaine and the cationic protonated betaine determine the surface properties, even in distilled water (pH = 5.85). At pH = 5.85, the betaine interacts more strongly with Na_2SO_4 than with NaCl or $CaCl_2$; anionic surfactants also show stronger interaction with the betaine than do cationic surfactants. These effects cannot be attributed to the zwitterion, but to the presence of the protonated cationic form in equilibrium with the zwitterion.

There has been a recent revival of interest in zwitterionic surfactants (1-4) because of certain useful properties shown by these molecules, including: 1) mild behavior on the skin, 2) compatibility with both anionics and cationics, 3) adsorption onto skin and hair, and 4) lime soap dispersing ability. Although this type of surfactant has been produced and used industrially for the last few decades, there have been few studies of the properties of well purified surfactants of this type (5-11) and almost all of these have been concerned with the micellar properties of these compounds rather than with their behavior at interfaces.

One of the problems associated with the study of the physico-chemical properties of these materials is the lack of analytical methods of determining accurately their concentrations in dilute solution. In order to permit such determinations, an N-betaine type surfactant was synthesized with a benzyl group attached to the quaternary nitrogen. This permitted analysis of dilute aqueous

¹Current address: Colloid Chemistry Laboratory, Department of Chemistry, Peking University, Beijing, People's Republic of China

solutions of the compounds by ultraviolet spectrometry. The present work describes the effect of pH and various electrolytes on the surface properties of the betaine, N-dodecyl-N-benzyl-N-methylglycine, $C_{12}H_{25}N^+(CH_3)(CH_2C_6H_5)CH_2COO^-(C_{12}BMG)$.

Experimental

The synthesis and purification of $C_{12}BMG$ by the reaction of N-methylbenzylamine with sodium chloroacetate followed by the quaternization of the resulting tertiary ammonioacetate with 1-bromododecane is described elsewhere (12). Purification of aqueous solutions of the surfactant for surface tension measurements and determination of the surface tension of the solutions by the Wilhelmy method using a sand-blasted platinum blade were by techniques previously described (13). The concentration of $C_{12}BMG$ in aqueous solution was determined by measuring its absorbance at 263 nm ($\epsilon = 350.5$).

The ionization constant, K_a , of the protonated betaine, $C_{12}H_{25}N^+(CH_3)(CH_2C_6H_5)CH_2COOH(BH^+)$, was obtained by adding V_{H^+} ml of an aqueous hydrochloric acid solution of hydrogen ion concentration $C_{H^+}^0$, in moles dm^{-3} , to V_B^0 ml of the surfactant betaine solution of concentration C_B^0 at a pH of 5-6 and measuring the hydrogen ion concentration, $[H^+]$, of the resulting mixture with a pH meter. The ionization constant was calculated by use of the following relationship:

$$K_a = [H^+] \times \left[\frac{V_B^0 \cdot C_B^0}{V_{H^+} \cdot C_{H^+}^0 - [H^+](V_B^0 + V_{H^+})} - 1 \right]$$

The average of 10 different measurements was $1.6 \pm 0.2 \times 10^{-3}$ ($pK_a = 2.8$). The K_1 of N-propylglycine is 4.46×10^{-3} (14).

Results and Discussion

Effect of pH. Surface tension (γ) as a function of log of the molar concentration of $C_{12}BMG$ ($\log C_B$) in aqueous solution ($25^\circ C$) at various pHs is shown in Figure 1. Table I shows the effect of change in the pH of the solution on the surface properties of the betaine. With decrease in the pH of the solution, the material which, at a pH of 5.85, is 99.9 mole percent in the zwitterionic form, B^\pm , is converted more and more to the cationic protonated form, BH^+ . From the K_a value of BH^+ , its solution phase concentration will exceed that of the zwitterion, B^\pm , when the pH of the solution is below 2.8. However, the cation, BH^+ , is less surface-active than the zwitterion, B^\pm , (see below) as is to be expected, and therefore there is little change in some of the surface properties of the mixture until a pH considerably below that value is reached. The smaller activity of BH^+ , compared to B^\pm , at the aqueous solution/air interface is indicated by the steady decrease in the pC_{20} , the bulk phase molar concentration of surfactant required to produce a surface

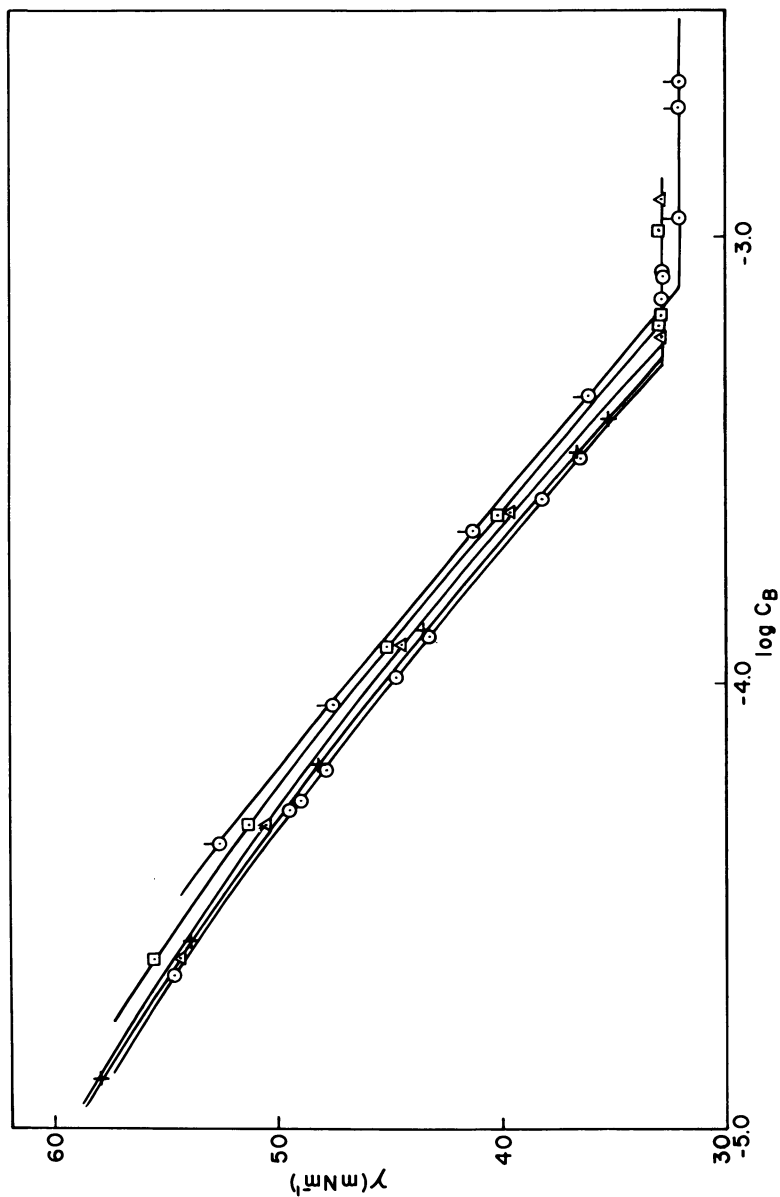


Figure 1. Surface tension versus log concentration of $C_{12}\text{BMG}$ in aqueous solution (25°C) at various pHs. \odot pH = 3.0; \oplus pH = 4.0; \ominus pH = 5.0; \triangle pH = 2.0; \square pH = 1.0; \ominus pH > 5.0.

pressure, π , of 20 mN m^{-1}) with increase in the H^+ content of the solution. At constant surface area per molecule, the pC_{20} value is a linear function of the $-\Delta G_{\text{ad}}^\circ$ of the mixture (15).

The critical micelle concentration (c.m.c.) of the material increases with decrease in pH of the solution below 5, as is to be expected as the ratio of BH^+ to B^\pm increases. The increase in the c.m.c. is somewhat greater than the increase in the C_{20} value with pH decrease as shown by the cmc/C_{20} ratio, indicating somewhat greater inhibition of micellization than of adsorption at the aqueous solution/air interface as the BH^+/B^\pm ratio increases. This may reflect some steric inhibition of micellization resulting from the increased size of the protonated hydrophilic head.

On the other hand, the value of Γ_{max} shows no significant change in the pH range investigated. Since an increase in the BH^+/B^\pm ratio at the aqueous solution/air interface would be expected to cause an increase in the surface area per molecule, due to increased electrical repulsion between the cationic head groups of BH^+ , the lack of change must be due to a compensatory compression of the electrical double layer surrounding these groups as a result of the increase in the ionic strength of the solution with decrease in the pH.

From molecular models, the minimum cross-sectional area of the C_{12}BMG molecule with an orientation normal to the interface is a trapezoid of 0.41 nm^2 . The minimum rectangular area is 0.54 nm^2 . The latter value agrees well with the experimental values shown in Tables I and II. Tori (2) obtained a value of 0.54 nm^2 for the C-dodecyl betaine, $\text{C}_{12}\text{H}_{25}\text{CH}(\text{COO}^-)\text{N}^+(\text{CH}_3)_3$ in water at 27°C .

The value of π_{cmc} shows almost no change until pH 1 is reached. Since the value of π_{cmc} is determined by the values of Γ_{max} and the cmc/C_{20} ratio (16) and there is no change in Γ_{max} with change in pH, the increase in π_{cmc} reflects the sharp increase in the cmc/C_{20} ratio at pH 1.

TABLE I. Effect of pH on the Surface Properties of C_{12}BMG

pH	cmc (mol dm^{-3} $\times 10^4$)	Γ_{max} (mol dm^{-2} $\times 10^{10}$)	A_{min} (nm^2 $\times 10^2$)	Π_{cmc} (mN m^{-1})	pC_{20}	$\frac{\text{cmc}}{\text{C}_{20}}$
5.85*	5.11	2.96	56.1	39.0	4.45	14.2
5.0	5.11	2.96	56.1	39.0	4.45	14.2
4.0	5.33	3.00	55.3	39.2	4.43	14.4
3.0	5.78	2.96	56.1	39.1	4.41	14.8
2.0	6.37	2.94	56.4	39.2	4.37	14.8
1.0	7.71	2.94	56.4	40.1	4.32	16.1

* Data at pH = 9.0 indicate no change in surface properties above pH = 5.85.

Effect of Electrolyte. Surface tension- $\log C_B$ curves in solutions of different electrolytes at pH = 5.85 and pH = 3.0 (25°C) are shown in Figure 2 and 3, respectively. Table II shows the effect of various electrolytes on the surface properties of the betaine at the two different pHs. From the data, it is apparent that, at both pHs, the

TABLE II. Effect on Electrolyte on the Surface Properties of C_{12} BMG

electro- lyte conc.	pH	cmc (mol dm ⁻³ x 10 ⁴)	Γ_{\max} (mol dm ⁻² x 10 ¹⁰)	A_{\min} (nm ² x 10 ²)	Π_{cmc} (mN m ⁻¹)	pC ₂₀	$\frac{\text{cmc}}{C_{20}}$
0	5.85	5.11	2.96	56.1	39.0	4.45	14.2
0.1 N NaCl	5.85	4.24	3.00	55.3	39.2	4.54	14.6
0.1 N CaCl ₂	5.85	4.24	3.00	55.3	39.2	4.54	14.6
0.1 N Na ₂ SO ₄	5.85	4.04	3.00	55.3	39.3	4.58	15.2
0	3.0	5.78	2.96	56.1	39.1	4.41	14.8
0.1 N NaCl	3.0	4.21	3.10	53.6	40.2	4.58	14.9
0.1 N CaCl ₂	3.0	4.21	3.10	53.6	40.2	4.58	14.9
0.1 N Na ₂ SO ₄	3.0	3.86	3.10	53.6	40.3	4.62	15.1

addition of electrolyte increases the surface activity of the material, i.e., it decreases the c.m.c. and increases both the pC₂₀ value and π_{cmc} . However, the effect of electrolyte on the surface properties of the product is greater at the lower pH where the BH⁺/B[±] ratio is larger. There is a larger decrease in the c.m.c., a larger increase in Γ_{\max} , and a larger increase in π_{cmc} . The greater effect of electrolyte in depressing the cmc of C-octyl betaine C₈H₁₇CH(COO⁻)N⁺(CH₃)₃, at a lower pH was noted by Tori (9).

In contrast to the effect of HCl in the absence of other added electrolyte, discussed above, the addition of electrolyte at constant pH results in a decrease in the surface area per molecule at the aqueous solution/air interface, presumably due to compression of the electrical double layer surrounding the ionic head groups. The effect is more pronounced at pH 3 than at pH 5.85. This slightly larger Γ_{\max} at pH 3 in the presence of electrolyte accounts for the higher π_{cmc} value under those conditions, since the cmc/C₂₀ ratio is virtually unchanged.

A noteworthy feature is that, in their effects on all these properties, equivalent amounts of NaCl and CaCl₂ are identical,

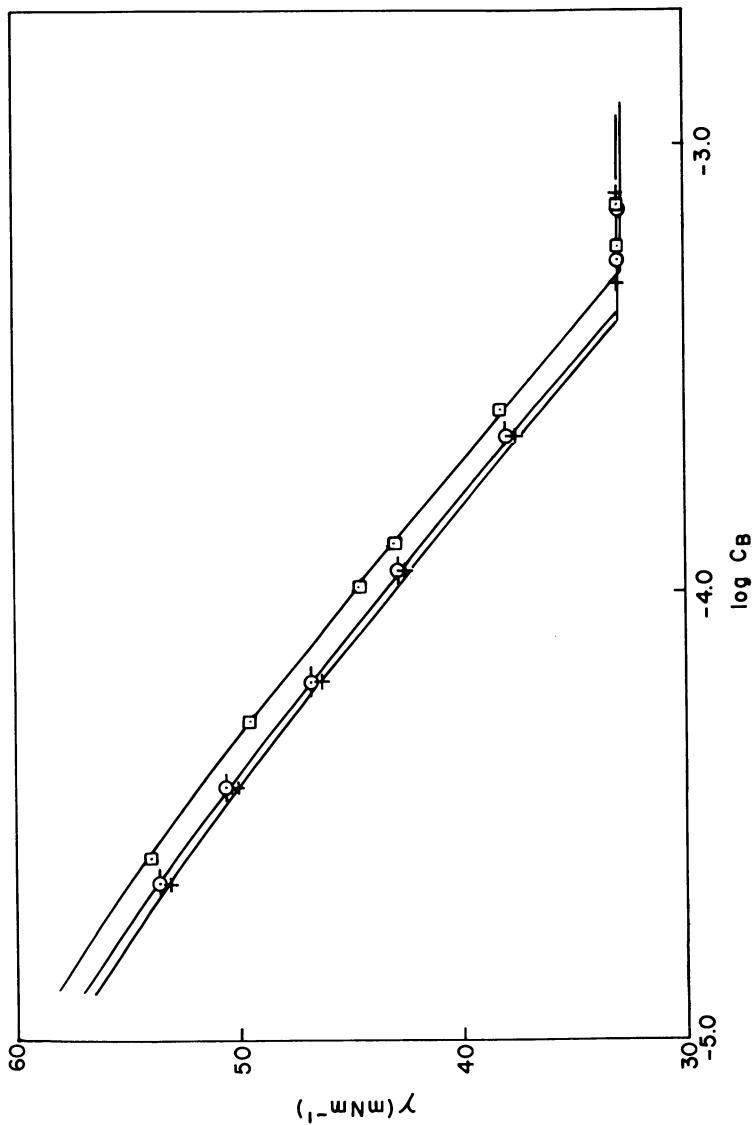


Figure 2. Surface tension versus log concentration of C_{12}BMG in aqueous solutions of various electrolytes at $\text{pH} = 5.85$ (25°C),
 □ 0.1 N NaCl ; ○ $0.1 \text{ N CaCl}_2 + 0.1 \text{ N Na}_2\text{SO}_4$.

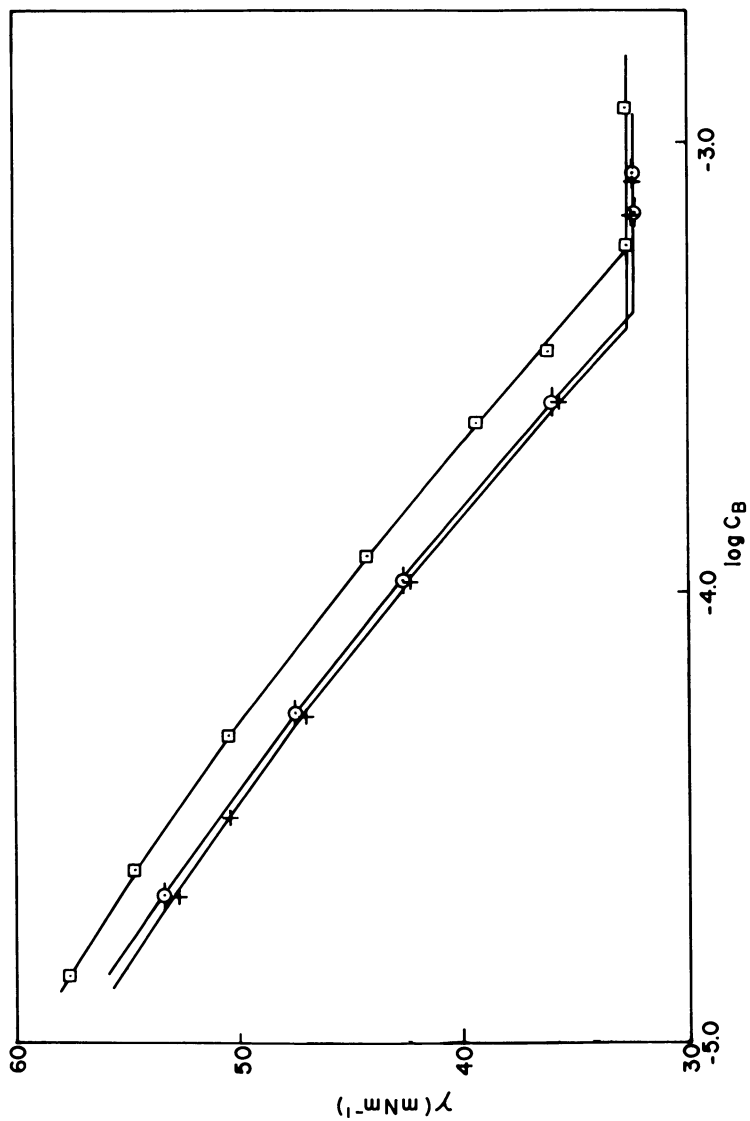


Figure 3. Surface tension versus log concentration of $C_{12}\text{BMG}$ in aqueous solutions of various electrolytes at $\text{pH} = 3.0$ (25°C).

□ H_2O ; ○ 0.1 N NaCl ; × $0.1 \text{ N CaCl}_2 + 0.1 \text{ N Na}_2\text{SO}_4$.

whereas an equivalent amount of Na_2SO_4 has a greater effect. This indicates that the betaine, at both pHs, shows a stronger electrostatic interaction with anions than with cations. The greater effect of Na_2SO_4 compared to NaCl or CaCl_2 on the c.m.c. of C-octylbetaine, is seen also in the data of Tori (9).

This greater interaction of the betaine with anions than with cations is seen also in its interaction with other surfactants (17) as measured by the molecular interaction parameter for mixed monolayer formation, β , using non-ideal solution theory (18). Whereas the degree of interaction of C_{12}BMG with the cationic surfactant, $\text{C}_{12}\text{H}_{25}\text{N}(\text{CH}_3)_3\text{Br}$, yields a value of $\beta = -1.3$, not much greater than that with the nonionic surfactant, $\text{C}_{12}\text{H}_{25}(\text{OC}_2\text{H}_4)_8\text{OH}$, ($\beta = -0.60$), its interaction with the anionic surfactant, $\text{C}_{12}\text{SO}_3\text{Na}$, is considerably greater ($\beta = -5.7$) and increases with decrease in the pH of the solution.

It is believed that this greater interaction of C_{12}BMG with anions than with cations is due, not to the zwitterionic betaine, B^\pm , but to the cationic protonated betaine, BH^+ , in equilibrium with it. Although the concentration of BH^+ at $\text{pH} = 5.8$ is very small, it is felt that strong electrostatic interaction between it and an anion can displace the zwitterion-cation equilibrium sufficiently to cause an appreciable effect.

Bulk and Surface Phase Concentrations of B^\pm and BH^+ . The mole fractions of the zwitterion, $x_{\text{B}^\pm}^b$, and of the protonated betaine, $x_{\text{BH}^+}^b$, in the total surfactant in the bulk phase were calculated by combining

$$K_a = \frac{C_{\text{H}^+} \times C_{\text{B}^\pm}}{C_{\text{BH}^+}} \quad (1)$$

and
$$x_{\text{B}^\pm}^b = \frac{C_{\text{B}^\pm}}{C_{\text{B}^\pm} + C_{\text{BH}^+}} \quad (2)$$

from which,
$$x_{\text{B}^\pm}^b = \frac{K_a}{K_a + C_{\text{H}^+}} \quad (3)$$

and
$$x_{\text{BH}^+}^b = \frac{C_{\text{H}^+}}{K_a + C_{\text{H}^+}} \quad (4)$$

Values of $x_{\text{BH}^+}^b$ as a function of pH are tabulated below:

pH	5.85	5.0	4.0	3.0	2.0	1.0
$x_{\text{BH}^+}^b$	0.0009	0.006	0.059	0.385	0.86	0.984

The surface phase mole fractions of zwitterion, $x_{\text{B}^\pm}^s (= \frac{\Gamma_{\text{B}^\pm}}{\Gamma_t})$,

and of protonated betaine, $x_{\text{BH}^+}^{\text{S}} (= \frac{\Gamma_{\text{BH}^+}}{\Gamma_{\text{t}}})$, where Γ_{B^\pm} , Γ_{BH^+} , and Γ_{t} are the surface (excess) concentrations of B^\pm , BH^+ , and their mixture at the aqueous solution/air interface were calculated from surface tension data at constant C_{B^\pm} at $\text{pH} < 3$. The Gibbs absorption equation for a mixture of B^\pm and BH^+ in dilute HCl solution at constant C_{B^\pm} is:

$$-d\gamma = RT(\Gamma_{\text{BH}^+}d \ln C_{\text{BH}^+} + \Gamma_{\text{H}^+}d \ln C_{\text{H}^+} + \Gamma_{\text{Cl}^-}d \ln C_{\text{Cl}^-}) \quad (5)$$

Since H^+ is a non-surface-active ion of similar charge to BH^+ , we can assume that $\Gamma_{\text{H}^+}d \ln C_{\text{H}^+} \approx 0$. If we assume that $\Gamma_{\text{BH}^+} = \Gamma_{\text{Cl}^-}$ to maintain electroneutrality, then

$$-d\gamma = RT\Gamma_{\text{BH}^+}(d \ln C_{\text{BH}^+} + d \ln C_{\text{Cl}^-}) \quad (6)$$

When $C_{\text{B}^\pm} \ll C_{\text{H}^+}$ (i.e., at low pH), $d \ln C_{\text{Cl}^-} = d \ln C_{\text{H}^+}$. Moreover, at constant C_{B^\pm} , from equation (1), $d \ln C_{\text{BH}^+} = d \ln C_{\text{H}^+}$. Therefore,

$$-d\gamma = 2RT\Gamma_{\text{BH}^+}d \ln C_{\text{BH}^+} \quad (7)$$

or

$$\Gamma_{\text{BH}^+} = \frac{1}{2RT} \left(\frac{-\partial\gamma}{\partial \ln C_{\text{BH}^+}} \right)_{C_{\text{B}^\pm}} \quad (8)$$

and

$$x_{\text{BH}^+}^{\text{S}} = \frac{\Gamma_{\text{BH}^+}}{\Gamma_{\text{t}}} \quad (9)$$

$$\Gamma_{\text{t}} = \frac{1}{RT} \left(\frac{-\partial\gamma}{\partial \ln C_{\text{B}}} \right)_{\text{pH}} \quad (10)$$

where C_{B} is the total concentration of C_{12}BMG in the aqueous phase. $x_{\text{BH}^+}^{\text{S}}$ can, consequently, be determined from the data in Figure 1 by selecting from the curves at pHs 1, 2, and 3, points at constant C_{B^\pm} , calculating C_{BH^+} and plotting γ versus C_{BH^+} .

Values of $x_{\text{BH}^+}^{\text{b}}$ and $x_{\text{BH}^+}^{\text{S}}$ at pHs 1 and 2 are tabulated below:

pH	1	2
$x_{\text{BH}^+}^{\text{b}}$	0.984	0.86
$x_{\text{BH}^+}^{\text{S}}$	0.345	0.257

It is apparent from these values that BH^+ is considerably less surface-active than B^\pm .

Standard Free Energies of Adsorption of B^\pm and BH^+ . The standard free energy of adsorption of $C_{12}BMG$ was calculated from the surface tension data in Figures 1 and 2 by use of the equation:

$$\Delta G_{ad}^\circ = RT \ln C_B - \pi A_{min} \quad (11)$$

where C_B is the bulk phase concentration of $C_{12}BMG$ to produce a given surface pressure, π , in the region just below the c.m.c. where the γ -log C curve is essentially linear. The standard state for the surface phase is a hypothetical monolayer at its closest packing ($A = A_{min}$) and at zero surface pressure (15).

The standard free energy of adsorption of the zwitterion, $\Delta G_{ad,B^\pm}^\circ$, was calculated from the surface tension data at $pH \approx 5$, where the concentration of BH^+ is negligible. The value of $\Delta G_{ad,B^\pm}^\circ$ at 25°C is $-32.04 \text{ kJ mol}^{-1}$ from the data in water and $-32.10 \text{ kJ mol}^{-1}$ from the data in 0.1 N NaCl. The ΔG_{ad}° for a series of nonionics, $C_{12}H_{25}(OC_2H_4)_xOH$, containing the same ($C_{12}H_{25}$) hydrophobic group as $C_{12}BMG$, ranges from -35.2 ($x = 2$) to -37.4 ($x = 8$) kJ mol^{-1} , using the same standard state for the surface phase (13).

The standard free energy of adsorption of the protonated betaine, $\Delta G_{ad,BH^+}^\circ$, was calculated from the surface tension data at pH s 1 and 2 by use of the relationships:

$$\Delta G_{ad}^\circ = X_{BH^+}^S \cdot \Delta G_{ad,BH^+}^\circ + X_{B^\pm}^S \cdot \Delta G_{ad,B^\pm}^\circ \quad (12)$$

The average value of $\Delta G_{ad,BH^+}^\circ$ was $-29.8 \text{ kJ mol}^{-1}$ in aqueous hydrochloric acid solution of 0.1 N total ionic strength ($pH = 1$).

Acknowledgment

This material is based upon work supported by the National Science Foundation under Grant No. ENG-7825930.

Literature Cited

1. Hidaka, H. *J. Amer. Oil Chem. Soc.* 1979, 56, 914; 1980, 57, 382.
2. Takai, M.; Hidaka, H.; Ishikawa, S.; Takada, M.; Moriya, M. *J. Amer. Oil Chem. Soc.* 1980, 57, 183.
3. Takai, M.; Hidaka, H.; Moriya, M. *J. Amer. Oil Chem. Soc.* 1979, 56, 537.
4. Weil, J. K.; Linfield, W. M. *J. Amer. Oil Chem. Soc.*, 1976, 53, 60; 1977, 54, 339; 1979, 56, 85.
5. Tori, K.; Nakagawa, T. *Kolloid Z. Z. Polym.*, 1963, 187, 44.
6. Tori, K.; Wakagawa, T. *Kolloid Z. Z. Polym.*, 1963, 188, 47.
7. Tori, K.; Nakagawa, T. *Kolloid Z. Z. Polym.*, 1963, 191, 42.
8. Tori, K.; Kuriyama, K.; Nakagawa, T. *Kolloid Z. Z. Polym.*, 1963, 191, 48.
9. Tori, K.; Nakagawa, T. *Kolloid Z. Z. Polym.*, 1963, 189, 50.

10. Molyneaux, P.; Rhodes, C. T.; Swarbrick, J. Trans. Faraday Soc. 1963, 61, 1043.
11. Evans, N. G.; Pilpel, N. J. Pharm. Sci. 1969, 1228.
12. Dahanayake, M.; Rosen, M. J. In Chapter 3, this book.
13. Rosen, M. J.; Cohen, A. W.; Dahanayake, M.; Hua, X. Y. J. Phys. Chem. 1982, 86, 541.
14. "Handbook of Chemistry and Physics"; 61st ed., CRC Press: Boca Raton, Florida, 1980; p. D-161.
15. Rosen, M. J.; Aronson, S. Colloids Surfaces 1981, 3, 201.
16. Rosen, M. J. Colloid Interface Sci. 1976, 56, 320.
17. Rosen, M. J.; Zhu, B. J. Colloid Interface Sci., in press.
18. Rosen, M. J.; Hua, X. Y. J. Colloid Interface Sci. 1982, 86, 164.
19. Rosen, M. J.; Dahanayake, M.; Cohen, A. W. Colloids Surfaces 1982, 5, 159.

RECEIVED January 20, 1984

Effect of Structure on Activity at the Critical Micelle Concentration and on the Free Energy of Micelle Formation

Ionic and Nonionic Surfactants

M. NAKAGAKI and T. HANDA

Faculty of Pharmaceutical Sciences, Kyoto University, Kyoto, 606 Japan

The slope of the linear relationship between $\log \text{cmc}$ and number of carbon atoms in the chain, n_c , is -0.5 for nonionic and zwitterionic surfactants, whereas the slopes are -0.3 and -0.25 for univalent and bivalent ionic surfactants, respectively. When the activity of the surfactants at cmc , cma , is used instead of cmc , the slopes are -0.5 — -0.58 irrespective of head group. This results in a value of -680 — -777 cal/mol for the free energy of micelle formation per CH_2 group. Furthermore, the linear relationship between $\log \text{cmc}$ and $\log[\text{counter ion}]$ shows a slope of -0.6 for potassium dodecanoate, -0.67 for sodium dodecyl sulfate, and -0.95 for disodium dodecyl phosphate. When the critical micelle activity, cma , is used instead of cmc , the slopes are -0.9 for the univalent surfactants and -1.8 for the bivalent surfactants. These results indicate that the cma is substantially constant regardless of the counter ion concentration.

Performance of surfactants is closely related to surface activity and to micelle formation. Both these are due to amphiphilic nature of the surfactant molecule. The molecule contains a nonpolar hydrophobic part, usually, a hydrocarbon chain, and a polar hydrophilic group, which may be nonionic, zwitterionic, or ionic. When the hydrophobic group is a long straight chain of hydrocarbon, the micelle has a small liquid like hydrocarbon core(1,2). The primary driving

0097-6156/84/0253-0073\$06.00/0
© 1984 American Chemical Society

force for micelle formation has been considered to be the hydrophobic effect (1-4), that is, the tendency of the hydrocarbon chains to associate together with themselves rather than to remain in the aqueous phase. A thermodynamic equilibrium is established between micellar and monomeric states.

To understand micelle formation quantitatively, critical micelle concentrations (cmc) have to be determined for a large number of surfactants (5). When the cmc values of the surfactants with the same hydrophilic group (a homologous series) are examined, a nearly 3-fold decrease in cmc is observed for nonionic and zwitterionic surfactants (1,2) upon the addition of a methylene group into the hydrocarbon chain, whereas, a 2-fold or only 1.8-fold reduction in cmc can be observed for univalent (1,2) and bivalent (6) ionic surfactants, respectively.

In this work, the critical micelle activity, cma, which is the activity of the surfactant at the cmc, is introduced and used instead of the cmc to investigate the free energy of micelle formation. It is found that upon the addition of an extra methylene group into the hydrocarbon chain, an approximately 3-fold reduction in cma is observed, irrespective of the hydrophilic head group. The effect of added electrolyte on cmc is also examined by the use of cma.

Experimental

Materials and Method. Aqueous solutions of disodium alkyl phosphates were prepared by dissolving the corresponding acids in sodium hydroxide solutions. The alkyl phosphoric acids were synthesized by the reaction of pyrophosphoric acid with the respective alcohol in benzene at room temperature for 4 days. Details of the purification procedures are given elsewhere (7).

The capillary-rise method was employed to measure the surface tension of aqueous solutions of disodium alkyl phosphate at 25 °C. The cmc values of the solutions were obtained from the discontinuity in the surface tension - concentration curves (7).

Other cmc data than those of disodium alkyl phosphates investigated in this study are taken from the extensive tables by Mukerjee and Mysels (5).

Theoretical Background

Nonionic Micelle Formation. Micelle formation in aqueous solution was first considered to be an equilibrium between monomer and micelle (1). The law of mass action controls the equilibrium



where L is the surfactant monomer, M is the micelle, and n expresses the number of monomers associated in the micelle (the association number). The equilibrium constant, K, for the process can be written as

$$K = f_M[M]/(f_L[L])^n \quad (2)$$

Here f_M and f_L are the activity coefficients of micelle and monomer. The free energy of micelle formation ΔG is, therefore,

$$\Delta G = -(RT/n) \ln K \quad (3)$$

and from equation 2, ΔG is rewritten as

$$\Delta G = -(RT/n) \ln(f_M[M]) + RT \ln(f_L[L]) \quad (4)$$

At the critical micelle concentration, $[L] = \text{cmc}$. The first term of the right hand side of equation 4 is usually negligible when n is large ($n = 50\text{---}100$). If f_M and f_L are regarded to be unity, Equation 4 reduces to

$$\Delta G = RT \ln[L] = RT \ln \text{cmc} \quad (5)$$

Equations 4 and 5 are derived by completely ignoring electrostatic contributions to micelle formation, and can be applied only to nonionic and zwitterionic micelle formation.

On the other hand, micelle formation has sometimes been considered to be a phase separation of the surfactant-rich phase from the dilute aqueous solution of surfactant. The micellar phase and the monomer in solution are regarded to be in phase equilibrium and cmc can be considered to be the solubility of the surfactant. When the activity coefficient of the monomer is assumed to be unity, the free energy of micelle formation, ΔG , is calculated by an equation similar to equation 5 (8—11). Detailed examinations of micelle formation have indicated the phase separation model to be only an approximation (4,12).

In Figure 1, the log of the cmc is shown as a function of the number of carbon atoms in the hydrocarbon chain, n_c . It is clear that the nonionic surfactants (hexaethyleneglycol alkyl ethers) and the zwitterionic surfactants (N-alkyl betaines) exhibit linear relations with similar slopes of about -0.5

(hexaethyleneglycol alkyl ethers: -0.517; N-alkyl betaines: -0.49), while the ionic surfactants without added electrolyte show different slope values.

The free energy of micelle formation of a methylene group, $\Delta \Delta G(\text{CH}_2)$, is

$$\begin{aligned} \Delta \Delta G(\text{CH}_2) &= \Delta G(\text{C}_n\text{H}_{2n+1}\text{-Y}) - \Delta G(\text{C}_{n-1}\text{H}_{2n-1}\text{-Y}) \\ &= 2.303 \text{ RT}X \text{ (slope of log cmc vs. } n_c) \end{aligned} \quad (6)$$

$\Delta \Delta G(\text{CH}_2)$ thus calculated is -705 cal/mol and -657 cal/mol for hexaethyleneglycol alkyl ethers and N-alkyl betaines, respectively, as shown in Table 1.

For the transfer of one methylene group in a hydrocarbon chain from aqueous to hydrocarbon liquid environment, the free energy have been calculated to be -825 cal/mol (at 25°C) (4). For the transfer (adsorption) of the same group from the aqueous phase to air-water and hydrocarbon-water interfaces (sparsely covered interfaces), the free energies are -620 and -820 cal/mol, respectively(13). The free energy gained by removing a methylene group in the hydrocarbon chain of the surfactant from the aqueous phase and placing it in the micelle may be less than that of complete transfer to bulk liquid hydrocarbon, because one end of the hydrocarbon chain is anchored to the hydrophilic head group in the micellar surface and there is restricted freedom of motion inside the micelle(3). Values of $\Delta \Delta G(\text{CH}_2)$ obtained here for nonionic and zwitterionic micelle formation are , therefore, reasonable. Values between -650 and -720 cal/mol are indicated by Mukerjee(4) and also by Tanford(3). Values of $\Delta \Delta G(\text{CH}_2)$ for various transfers are shown in Figure 2.

Ionic Micelle Formation. Even for ionic micelle formation, the free energy of transfer of one methylene group to a micelle should have a value similar to those for nonionic and zwitterionic micelle formation. The negative slope of log cmc vs. n_c is, however, smaller for nonionic surfactants, as shown in Figure 1. The univalent ionic surfactants, alkyl trimethylammonium bromide, sodium alkyl sulfate, and sodium alkyl carboxylate give slopes of about -0.3. The bivalent anionic surfactant, disodium alkyl phosphate has the slope of -0.25. These values correspond to the 3-, 2-, and 1.8-fold lowering of the cmc for nonionic and zwitterionic , univalent ionic, and bivalent ionic surfactants, respectively, upon addition of one methylene group to the hydrocarbon chain.

The direct application of Equation 6 therefore results in $\Delta \Delta G(\text{CH}_2)$ values of -400 cal/mol for uni-

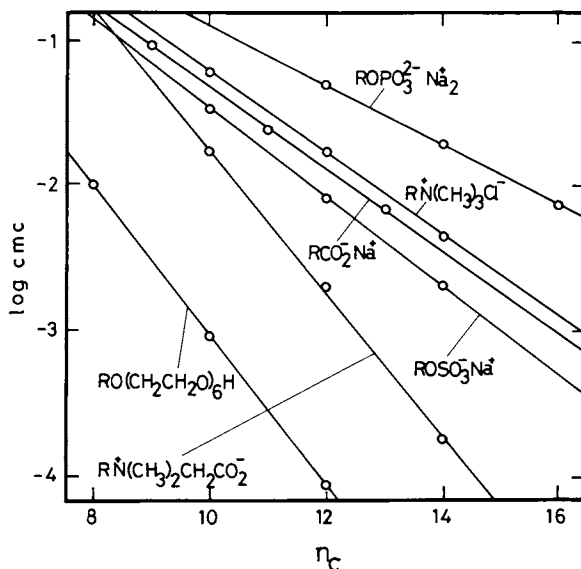
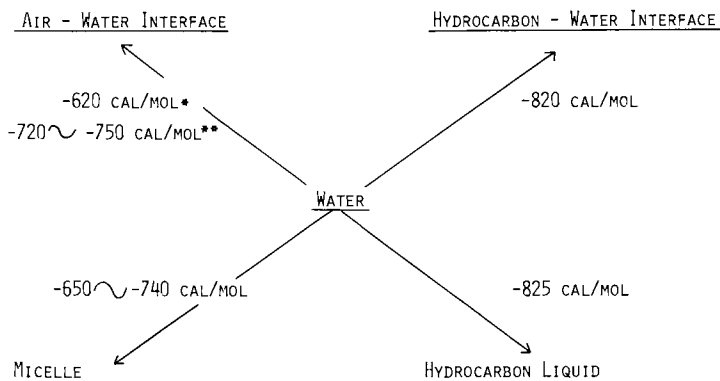
Figure 1. Log cmc vs. n_c 

Figure 2. The free energy of transfer of a methylene group in a hydrocarbon chain

* The value for the adsorption to the sparsely covered surface.

** The value for the adsorption to the monolayer at its minimum surface area per molecule (17).

Table 1. Slopes of log cmc and log cma vs. n_c and the Free Energy of Micelle Formation of a Methylene Group, $\Delta\Delta G(\text{CH}_2)$

Surfactant	Slope (log cmc vs. n_c)	Slope (log cma vs. n_c)	$\Delta\Delta G(\text{CH}_2)$ (cal/mol)
Hexaethyleneglycol alkyl ether (non- ionic)	-0.517		-705**
N-Alkyl betaine (zwitterionic)	-0.49		-657**
Alkyl trimethyl- ammonium bromide (cationic)	-0.29	-0.54	-736***
Sodium alkyl sulfate (univalent anionic)	-0.30	-0.57	-777***
Sodium alkyl carboxylate (univalent anionic)	-0.28	-0.52	-708***
Disodium alkyl phosphate (divalent anionic)*	-0.25	-0.50	-681***

Data used here are taken from reference 5.

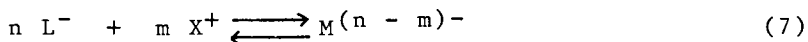
* Data taken from references 6 and 7.

** Calculated by Equation 6 (25 °C)

*** Calculated by Equation 21 (25 °C)

valent and -350 cal/mol for bivalent ionic surfactants. These differences could be due to electrical interactions in ionic micelle formation. The exact evaluation of the electrostatic part of the free energy of micelle formation is considered to be a very complicated problem and our present position seems to be far removed from that necessary to offer a well founded calculation of it (3,4).

We may begin the examination of ionic micelle formation by reviewing the main theories already presented. First of all, the mass action law is extended to ionic micelle formation(14—16) as



Considerations analogous to those used in the derivation of Equation 5 lead to Equation 8, if f_L and f_X are assumed to be unity.

$$\Delta G = RT \ln[L] + \frac{m}{n} RT \ln[X] \quad (8)$$

Here, X indicates the counter ions of the ionic surfactant. When there is no added electrolyte, $[L] = [X] = \text{cmc}$ and

$$\Delta G = \left(1 + \frac{m}{n} \right) RT \ln \text{cmc} \quad (9)$$

Although, ΔG evaluated by Equation 9 takes into account the loss in translational entropy of counter ions upon micellar association(3,4), it is doubtful that the term $(m/n) RT \ln[X]$, can include all the effects of interionic interaction in micelle formation.

On the basis of Equation 9, $\Delta \Delta G(\text{CH}_2)$ is derived as

$$\Delta \Delta G(\text{CH}_2) = 2.303 \left(1 + \frac{m}{n} \right) RT X (\text{slope of } \log \text{cmc vs. } n_c) \quad (10)$$

To obtain -650—-720 cal/mol for $\Delta \Delta G(\text{CH}_2)$ from the calculation with the slope of -0.3, the value of (m/n) should be in the range between 0.62 and 0.80. The values of (m/n) (the degree of association of counter ion) have been experimentally determined from the measurements of electromotive force(18—22), electric conductivity(23), and light scattering(24,25) of micellar solution. Though, these measurements gave 0.75—0.85 for the degree of association of counter ion, (m/n) , the theoretical vagueness inherent in Equations 8 and 9 have not been setteled yet.

In contrast to Equations 7 and 8, based on the binding of counter ion to micelle, an equation including a form for the electrostatic part of free energy of micelle formation, F_{e1} , evaluated from double

layer theory, has been used to calculate ΔG . In this method, the equilibrium between micellar and monomer states is represented as



The free energy of micelle formation, ΔG , is written as

$$\Delta G = RT \ln \text{cmc} - F_{e1} \quad (12)$$

The phase separation model for nonionic micelle formation has been modified for ionic micelle formation to give an equation close to Equation 12 for ΔG (26). In this modification, the ionic micelle has been considered as the charged phase, which has difficulties from the thermodynamic viewpoint. The precise measurement of the surface tension of aqueous sodium dodecyl sulfate solutions revealed the continuous decrease of surface tension above the cmc and indicated that the charged phase separation model is not correct (27).

Hobbs(28), and later, Shinoda(26) investigated F_{e1} by assuming the charged micellar surface to be flat. The assumption of very high electrical potential gave rise to the relationship between cmc and counter ion concentration, [X]:

$$\log \text{cmc} = - \log[X] + k \quad (13)$$

The direct application of Equation 13 did not explain experimental results. Hobbs, and also Shinoda, introduced a factor, K_g , whose meaning has not been theoretically elucidated(26,28), yielding

$$\log \text{cmc} = - K_g \log[X] + k \quad (14)$$

Tanford examined the application of Debye-Hückel theory and found the theory not to be valid because the high charge density generated by the closely spaced head groups leads to substantial charge neutralization by counter ions(3). Alternatively, he equated the work of compression of the charged surfactant monolayer at a hydrocarbon-water interface to F_{e1} (29).

Later, Stigter evaluated F_{e1} on the basis of the Stern-Göuy model of ionic double layer with a substantial part of the counter ions in a regular distribution between ionic head groups and the remaining counter ions in a diffuse layer. In this calculation, he also introduced the correction for the discreteness of charge at the micellar surface. Finally, the free energy of micelle formation contributed by hydrophobic interaction was related to the change of hydrocarbon -

water contact area in micelle formation and the value of $\Delta G(\text{CH}_2)$ was estimated as -740 cal/mol (30,31).

As mentioned above, a substantial part of the electrical charge of the micelle surface has been shown to be neutralized by the association of the counter ions with the micelle. In the calculation based on Equation 12, however, the loss in entropy arising from this counter ion association is not taken into account. This is by no means insignificant in comparison to F_{e1} of Equation 12 (4). A major part of the counter ions are condensed on the ionic micelle surface and counteract the electrical energy assigned to the amphiphilic ions on the micellar surface. The minor part of the counter ions, in the diffuse double layer, are also restricted to the vicinity of the micellar surface.

More complete neutralization by counter ions has sometimes been observed in micellar solutions with added electrolyte (32). In explaining the specific binding of counter ions, Stigter has used the "image force" resulting when the counter ion approaches the micellar core which has a low dielectric constant (30). On the other hand, Lindman proposed hydrogen bonding between (polarized) water molecules in the primary hydration sheath of the bound counter ion and the head group of the surfactant to account for the sequence of counter ion binding to micelle (33,34).

Application of Activity at cmc. The above consideration suggested us to propose a new treatment for ionic micelle formation. According to thermodynamics, the micelle-monomer equilibrium is achieved when the chemical potential of surfactant in the micelle is equal to that in the bulk solution. The free energy of micelle formation can be represented by the use of the critical micelle activity, c_{ma} , which is the activity of surfactant at the cmc, as

$$\Delta G = RT \ln c_{ma} \quad (15)$$

The c_{ma} is calculated as

$$c_{ma} = a_{\pm}^{\nu} = f_{\pm}^{\nu} [L]^{\nu_-} [X]^{\nu_+} \quad (16)$$

where ν_- and ν_+ are the numbers of anions and cations in the surfactant molecule, $\nu (= \nu_+ + \nu_-)$ is the total number of ions in the surfactant molecule, and a_{\pm} is the mean ionic activity of the surfactant at the cmc. According to Equation 15,

$$\Delta G = \nu RT \ln f_{\pm} + \nu_- RT \ln [L] + \nu_+ RT \ln [X] \quad (17)$$

If c' is the concentration of added electrolyte that has the same cation as the surfactant, the c_{ma} is expressed as follows

$$c_{ma} = f_{\pm}^{\nu} c_{mc}^{\nu} (c_{mc} + c')^{\nu} \quad (18)$$

For univalent ionic surfactants, e.g., alkyl trimethylammonium bromide and chloride, sodium alkyl sulfate, and sodium alkyl carboxylate,

$$c_{ma} = f_{\pm}^2 c_{mc} (c_{mc} + c') \quad (18a)$$

and for bivalent ionic surfactant, e.g., disodium alkyl phosphate

$$c_{ma} = f_{\pm}^3 c_{mc} (c_{mc} + c')^2 \quad (18b)$$

In Equations 16—18, f_{\pm} represents the mean ionic activity coefficient of the surfactant and may be calculated according to the Güntelberg approximation of the Debye-Hückel equation(6,7),

$$\log f_{\pm} = -\frac{A |z_+ z_-| \sqrt{I}}{1 + \sqrt{I}} \quad (19)$$

where

$$A = 1.825 \times 10^6 \times (DT)^{3/2} \quad (20)$$

Here, I is the ionic strength based on the free ions in the micellar solution and D is the dielectric constant of solvent.

On the basis of Equation 15, the increment in ΔG by the addition of a methylene group to the hydrocarbon chain of surfactant, $\Delta \Delta G(\text{CH}_2)$, is written as

$$\Delta \Delta G(\text{CH}_2) = 2.303RT \times (\text{slope of } \log c_{ma} \text{ vs. } n_c) \quad (21)$$

in which c_{mc} in the Equation 6 has been replaced with c_{ma} .

Results and Discussion

In Figure 3, the logarithm of c_{ma} is represented as a function of the number of carbon atoms in the hydrocarbon chain, n_c . It is found that the $\log c_{ma}$ values for the various surfactants at the same n_c value, except N-alkyl betaine, become closer compared to $\log c_{mc}$, and ΔG calculated by Equation 15 is -4.91 — -6.54 cal/mol for $n_c = 12$. For N-alkyl betaines, higher values of ΔG compared to other surfactants have been recognized in the literature and were ascribed to the

ordering of the zwitterionic head group on the micellar surface (35,36). Also the contact of the hydrocarbon chain with water molecules at the micellar surface has been considered to be an important factor (3,30,31).

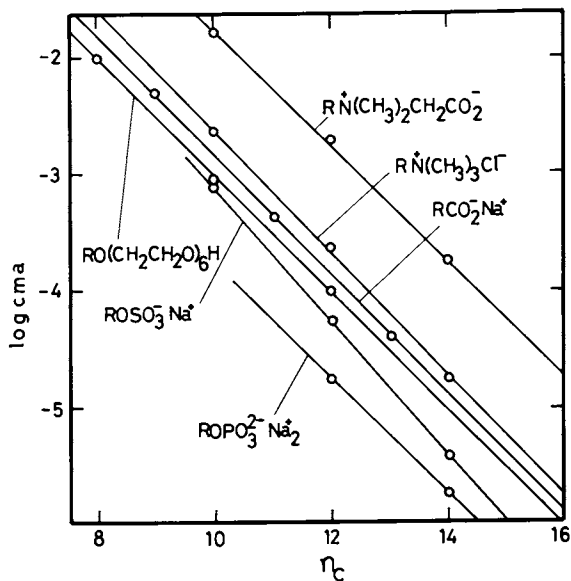
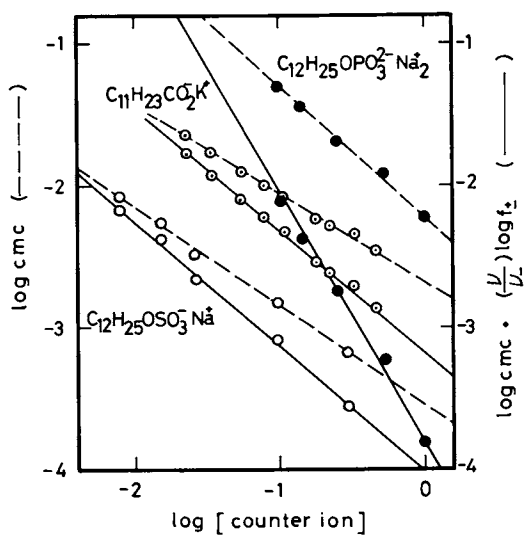
On the other hand, the slopes obtained were -0.5 for disodium alkyl phosphate, -0.54 for alkyl trimethylammoniumchloride, -0.52 for sodium alkyl carboxylate, and -0.58 for sodium alkyl sulfate. These values are close to those for nonionic and zwitterionic surfactants, obtained from the linear relation of $\log \text{cmc}$ and n_c . The $\Delta \Delta G(\text{CH}_2)$ values calculated from Equation 21 are in the range of -708—-777 cal/mol and have good agreement with the values for nonionic and zwitterionic surfactants, as shown in Table 1.

In the calculation of ΔG by Equation 15, the cma values for a homologous series of surfactants are evaluated at different ionic strengths and the results obtained for $\Delta \Delta G(\text{CH}_2)$, therefore, indicate that ΔG thus calculated is independent of the ionic strength of the micellar solution. Equation 17, derived from Equation 15, is rewritten as

$$\nu_- \log \text{cmc} + \left(\frac{\nu_+}{\nu_-} \right) \log f_{\pm} = - \left(\frac{\nu_+}{\nu_-} \right) \log [X] + G / (2.303 \nu_- RT) \quad (22)$$

In Figure 4, the values of $\log \text{cmc}$ are presented as a function of the logarithm of total concentration of counter ion, $\log [X]$. The slopes of these plots are -0.67 for sodium dodecyl sulfate, -0.6 for potassium dodecanoate, and -0.9 for disodium dodecyl phosphate. In accordance with Equation 22, the values of $\log \text{cmc} + (\nu_+/\nu_-) \log f_{\pm}$ are also plotted against $\log [X]$ in the same figure. The linear relations obtained now give slopes of -0.9 for sodium dodecyl sulfate and potassium dodecanoate, and -1.8 for disodium dodecyl phosphate, which are in fairly good agreement with the theoretical values of -1 and -2, respectively. The results obtained here suggest that the condensation of counter ions on the ionic micellar surface and the reduction of electrostatic energy play important roles in the ionic micelle formation.

The application of the activity of the surfactant has been examined also for the surface tension and adsorption of disodium alkyl phosphate (6,7), sodium dodecyl sulfate (37), alkyl trimethylammonium bromide (35), and sodium perfluorooctanoate (13) solutions. These studies show that the surface tension and the adsorption amount are controlled by the activity of surfactant, irrespective of the added electrolyte concentration.

Figure 3. Log cma vs. n_c Figure 4. Log cmc and $\log \text{cmc} + \left(\frac{v}{v_{\bar{c}}}\right) \log f_{\pm}$ as a function of $\log[\text{counter ion}]$

It is also noteworthy that the surface tension of mixed solutions of anionic and cationic surfactants is controlled by the activity of the salt(38). These results indicate that, in adsorption of an ionic surfactant at the solution surface, the accompanying adsorption of the counter ion also plays an important role.

In conclusion, micelle formation of an ionic surfactant is found to take place at a constant activity, i.e., critical micelle activity, *cma*, irrespective of counter ion concentration.

Literature Cited

1. Hartley, G.S. "Aqueous Solutions of Paraffin Chain Salts" Hermann et Cie : Paris, 1936.
2. Debye, P. J. Colloid Sci. 1948, 3, 407.
3. Tanford, C. "The Hydrophobic Effect" 2nd Ed., John Wiley & Sons: New York, 1980.
4. Mukerjee, P. Advan. Colloid Interface Sci. 1967, 1, 241.
5. Mukerjee, P; Mysels, K.J. "Critical Micelle Concentration of Aqueous Surfactant Systems" NSRDS-NBS 36, US Nat. Bur. Stand., 1971.
6. Nakagaki, M; Handa, T; Shimabayashi, S. J. Colloid Interface Sci. 1973, 43, 521.
7. Nakagaki, M; Handa, T. Bull. Chem. Soc. Jpn. 1975, 48, 630.
8. Stainsby, G; Alexander, A.E. Trans. Faraday Soc. 1950, 46, 587.
9. Hutchinson, E; Inaba, A; Bailey, L.G. Z. Physik. Chem. 1955, 5, 344.
10. Matijevic, E; Pethica, B.A. Trans. Faraday Soc. 1958, 54, 587.
11. Herrman, K.W. J. Phys. Chem. 1962, 66, 295.
12. White, P; Benson, G.C. Trans. Faraday Soc. 1959. 55, 1025.
13. Mukerjee, P; Handa, T. J. Phys. Chem. 1981, 85, 2298.
14. Murray, R.C; Hartley, G.S. Trans. Faraday Soc. 1935, 31, 183.
15. Mysels, K. J. Colloid Sci. 1955, 10, 507.
16. Mukerjee, P. J. Phys. Chem. 1962, 66, 33.
17. Rosen, M.J; Aronson, S. Colloid Surf. 1981, 3, 201.
18. Shedlovsky, L; Jakob, C.W; Epstein, M.B, J. Phys. Chem. 1963, 67, 2075.
19. Botre, C; Cresenzi, V.L; Mele, A. J. Phys. Chem. 1969, 63, 650.
20. Ingram, T; Jones, M.N. Trans. Faraday Soc. 1969, 65, 297.
21. Mathews, W.K; Larsen, J.W; Pikai, M.J. Tetrahedron Letter, 1972, 6, 513.

22. Malik, W.U; Srivastava, S.K; Gupa, D. J. Electro-annal. Chem. 1072, 34, 540.
23. Anderson, J.E; Taylor, H. J. Pharm. Pharmacol. 1971, 23, 311.
24. Philips, J.N; Mysels, K.J. J. Phys. Chem. 1955, 59, 325.
25. Barry, B.W; Morrison, J.C. Pikai, M.J. Tetrahedron Letter. 1972, 6, 513.
26. Shinoda, K; Nakagawa, T; Tamamushi, B; Isemura, T. "Colloid Surfactant" Academic Press; New York, 1963; Chap.1.
27. Elworthy, P.H; Mysels, K. J. Colloid Sci. 1966, 21, 331.
28. Hobbs, M.E. J. Phys. Chem. 1951, 55, 675.
29. Tanford, C. Proc. Nat. Acad. Sci. U.S.A. 1974, 71, 1811.
30. Stigter, D. J. Phys. Chem. 1975, 79, 1008, 1015 and 1020.
31. Stigter, D. J. Colloid Sci. 1974, 47, 473.
32. Kresheck, G.C. in "water"; Franks, F. Ed.; plenum Press: New York, 1975, Vol.4, Chap.2.
33. Gustavsson, H; Lindman, B. J. Am. Chem. Soc. 1975, 97, 3923.
34. Lindman, G; Lindman, B ; Tiddy, G.T.J. J. Am. Chem. Soc. 1978, 100, 2299.
35. Molyneux, P; Rhodes, C.T; Swarbrick, J. Trans. Faraday Soc. 1965, 61, 1043.
36. Beckett, A.H; Woodward, R.J. J. Pharm. Pharmacol. 1963, 15, 422.
37. Lucassen-Reynder, E.H. J. Phys. Chem. 1966, 70, 1977.
38. Rosen, M.J. Friedman, D; Gross, M. J. Phys. Chem. 1964, 68, 3219.

RECEIVED January 10, 1984

Relationship of Solubilization Rate to Micellar Properties

Anionic and Nonionic Surfactants

Y. C. CHIU, Y. C. HAN, and H. M. CHENG

Department of Chemistry, Chung Yuan Christian University, Chung-Li, Taiwan 320, Republic of China

This paper presents a new finding that the oil solubilization rate is a function of surfactant aggregate size. Light scattering and conductance measurements were used in the experiments. Alcohol ethoxylates and SDS were used as surfactants. The aggregate size was changed by changing the surfactant structure or by adding chemicals. The solubilization rate shows a maximum at a certain aggregate size for a given surfactant and a given oil. Thus, we have found a measurable and controllable factor (size) in the process of oil solubilization. A theory was proposed to relate solubilization rate with micellar properties and surfactant structure. By using this theory, we can explain the performance of petroleum sulfonate in enhanced oil recovery and improve current formulation in achieving ultra-low interfacial tension. We can also explain the nonionic detergent performance as a function of surfactant structure.

This paper presents a new finding that the oil solubilization rate is a function of the surfactant aggregate size. This idea originated from Chiu's observation on solubilization phenomena in tertiary oil recovery.

During experiments with petroleum sulfonates in surfactant flooding, it was found that the surfactant solutions in the optimum electrolyte region, containing large surfactant aggregates, are effective in oil recovery (1). These solutions give fast solubilization of oil and exhibit ultralow interfacial tension when they are in contact with oil (1). A theory was proposed that the large surfactant aggregates are important in obtaining rapid solubilization and ultralow interfacial tension (1). In order to test this theory, medium molecular weight alcohols were used to replace electrolyte in increasing surfactant aggregate size. The resulting solutions also gave good oil recovery (2). This theory has been

0097-6156/84/0253-0089\$08.00/0
© 1984 American Chemical Society

used to explain the detergent performance of alcohol ethoxylates with respect to surfactant structure (3).

Although the proposed theory has been used effectively in several practical applications, no experimental proof has been given that the oil solubilization rate is a function of surfactant aggregate size. In view of the importance of solubilization and the existence of practical methods of measuring and controlling surfactant aggregate size, we decided to correlate the solubilization rate with micellar properties for some anionic and nonionic surfactants.

Although solubilization (4) has been a subject of many investigations, most of the studies were made on the final equilibrium solubilization. Only a few studies concern about the kinetics and mechanism. In recent publications, Carrol (5) measured solubilization rate of nonpolar oils by nonionic surfactant solutions using a microscopic observation of the change of oil droplet adhering on a fiber. Chan et al (6,7) studied the kinetics and mechanism of solubilization in detergent solutions by radio tracer technique. These methods are either tedious or requiring safety precaution. For large scale laboratory operation using simple equipments, we have developed a light scattering technique to measure the solubilization rate and particle size.

Experimental

Light scattering technique was used in determining the oil solubilization rate. Debye's equation (8) was used in the interpretation. The basic principle involves the measurement of the surfactant aggregate size during the solubilization. As the oil goes into the surfactant micelle, the increased size will be reflected by the turbidity of the solution.

The instrument used in the turbidity measurement was Hatch Model 2100 A Turbidimeter. A Hotech Shaker Bath, Model 901 (Hotech Instruments Corp.) was used in mixing the oil and surfactant solution. The nonionic surfactants, Newcol 1102, 1103 and 1105 were produced by Sino-Japan Chemical Co., Ltd. The active ingredient is dodecanol ethoxylate. Sodium dodecyl sulfate (SDS, No. L. 5750, Sigma Chemical Co. 95% active, containing 65% C₁₂, 27% C₁₄ and 6% C₁₆) was used as the anionic surfactant. Oleic Acid (Extra pure reagent, Kanto Chemical Co., Tokyo, Japan), Triolein (glycerol trioleate (C₁₇H₃₃COO)₃C₃H₅, Technical, BDH Chemicals, England) and n-decane (E. Merck, G.C., 95%) were used as oil. Sodium chloride (E. Merck, purity 100 ± 0.05%) was used as electrolyte.

The experiment was done by adding a given amount of oil to 14.0 g of 0.05% nonionic surfactant solution. The oil was first added to the surfactant solution and dispersed into tiny droplets by hand and was then mixed with the surfactant solution by the Hotech Shaker at 120 cycles/min for 20 minutes. The turbidity of the solution was measured. The solution was shaken and turbidity

was measured repeatedly until the turbidity reached a constant value. For anionic surfactant experiments, 15.0 g of 0.5% surfactant solution was used and the shaking time was 5 minutes.

Some experiments concerning the solubilization of triolein in SDS solutions were done by adding triolein dropwise to the surfactant solution. 15.0 g of 0.5% SDS solution was used. One drop of triolein (0.006 ± 0.001 g) was added to the surfactant solution. The oil was dispersed, shaken and turbidity measured as it was mentioned above. When turbidity reached a constant value, another drop of triolein was added and the process repeated until the turbidity value did not change with the addition of triolein.

It should be mentioned here that the nonionic surfactant solutions were used within 1-10 days after the preparation. The anionic surfactant solutions were used after aging for two days.

All experiments were done at room temperature, 25 ± 1 °C.

Result and Discussion

A Proposed Theory. In earlier publications (1-3), a theory was proposed to correlate solubilization rate, interfacial tension and size of the surfactant aggregate: (1) the interfacial tension lowering between the oil-surfactant solution interface is a function of the rate of solubilization of oil, and (2) the rate of solubilization ($\Delta S/\Delta t$) is a function of the effective volume for solubilization:

$$\Delta S/\Delta t = k n V_{\text{eff}} \quad (1)$$

Where k = constant.

n = number of aggregates in unit volume of surfactant solution.

V_{eff} = effective volume for solubilization by an aggregate.
 $= f$ (accessible volume of the hydrocarbon core, chemical nature of the surfactant molecule, chemical nature of the oil).

The effective volume for solubilization may or may not be proportional to the geometrical size of the aggregate. It depends on the packing of the molecules in the aggregate and the mutual compatibility of the surfactant and oil molecules. In most cases, V_{eff} is proportional to the size of the micelle (or aggregate). When the aggregate size is too large and the packing of monomer becomes too tight, V_{eff} may decrease with the aggregate size.

Interpretation of Light Scattering. We used Debye's equation (8) for micellar solution as a basis for the light scattering measurement:

$$\tau = \frac{32\pi^3}{3} \frac{\mu_o^2}{N\lambda^4} \left(\frac{d\mu}{dC} \right)^2 M (C-C_o) \quad (2)$$

Where τ = Turbidity.

μ = refractive index of the solution.

μ_0 = refractive index of the solvent.

C = concentration (g/ml).

C_0 = critical micellar concentration (CMC).

M = aggregate weight.

N = Avogadro's number.

λ = wave length of the light.

When $(d\mu/dC)^2(C-C_0)$ becomes constant, τ would be proportional to M . For nonionic surfactant, we used Newcol 1102, 1103 and 1105. These surfactants contain dodecanol ethoxylate. The last digit in the Newcol number represents the ethylene oxide (EO) number. The CMC values for pure dodecanol ethoxylate (3) with EO number from 3 to 5 are in the concentration range of 0.001-0.003%. C value in our experiment is 0.05%. Therefore, $C-C_0$ can be considered as constant. Values (3) of μ as a function of C also show that $d\mu/dC$ is almost constant. Thus in the nonionic surfactant measurement in this paper, τ is considered to be proportional to M .

For anionic surfactant, we used sodium dodecyl sulfate (SDS). The CMC values were measured by conductance method. The CMC values were taken from the breaks of curves from plots of K/C versus $N^{1/2}$. Where K is the specific conductance, C is molar concentration and N is the equivalence. Figure 1 shows the CMC values of SDS at 25 °C. The curve showing in the lower left side represents data taken from literature for pure SDS. The curve showing in the upper right side represents measurements for our impure sample. Table I shows some values of $(d\mu/dC)^2(C-C_0)$ for pure SDS at 25 °C. The values for NaCl concentrations of 0.03 M to 0.50 M are not far from constant. Therefore, in this concentration region, τ is also considered to be proportional to M . The C value used in our experiments is 0.5% (0.0171 M, average molecular weight was taken as 293).

Table I. Some SDS Properties at 25 °C

System	Data from Fig.1	Data from Ref.12	$(d\mu/dC)^2(C-C_0)$
	Lower Left Curve $C - C_0$	$\lambda = 4358$ $(d\mu/dC)^2$	
H ₂ O	0.0091	0.01426	0.000130
0.03M NaCl	0.0141	0.01421	0.000200
0.20M NaCl	0.0163	0.01339	0.000218
0.50M NaCl	0.0162	0.01199	0.000194

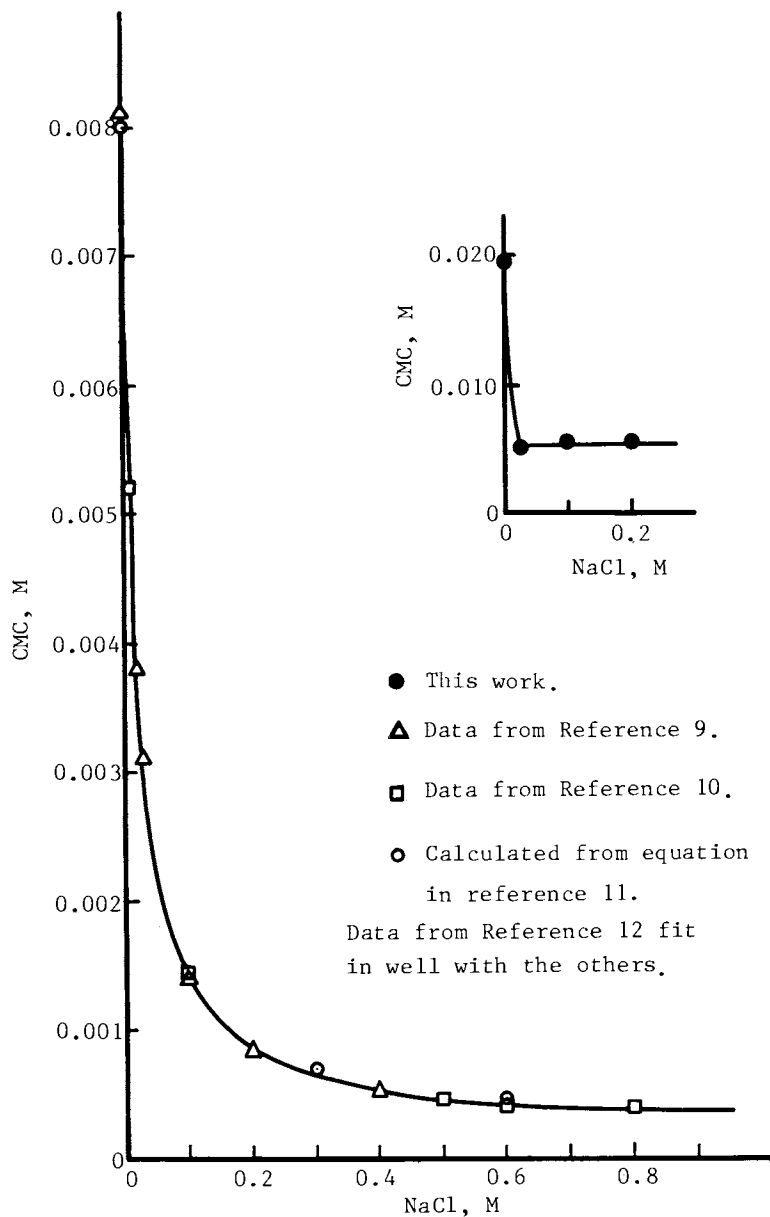


Figure 1. CMC Values of SDS at 25 °C.

During the solubilization experiment, oil continues to solubilize in the surfactant micelle and the M value continues to increase. The change of M is reflected by the change of τ . And $d\tau/dt$ (t = time) is taken as the rate of solubilization in our experiments.

The contribution to τ by emulsified oil in our experiments is considered negligible in the nonionic surfactant solutions due to the very low CMC values. In SDS solutions, the emulsification occurs at the very beginning when no NaCl is added to the solution and the turbidity introduced by emulsification does not change with time. When NaCl is added to SDS solutions, the CMC becomes low and emulsification becomes unimportant as it will be shown in the following sections.

Solubilization in Nonionic Surfactant. Figure 2 shows the solubilization of oleic acid in Newcol nonionic surfactants. Turbidity was plotted against shaking time. The first number on the curve represents the surfactant. 1102 means dodecanol ethoxylate containing 2 EO. The second number on the curve represents the amount of oleic acid added to the surfactant solution.

For dodecanol ethoxylate, when EO number is larger than 8, the aggregate weight decreases with the increase in EO number (13). For the low EO members, water solubility becomes low. For example, when EO = 4, the cloud point (3) is about 8 °C. When EO = 5, the cloud point (3) is about 30 °C. In Figure 2, the turbidity in zero shaking time reflects the aggregate weight in the surfactant solution before the addition of oil. The turbidity is very high in 1102 indicating large aggregates in the solution. The turbidity for the original solution is slightly higher for 1103 than 1105 indicating larger aggregates existing in 1103 solution.

$d\tau/dt$ (slope of the curve) in Figure 2 represents solubilization rate and the steady turbidity showing at the end of each curve signifies the solubilization of oil at that particular condition. Among these 6 curves, the 1102 curve should be discussed separately. Since our experiments were carried out at 25 °C, the temperature is far above the 1102 cloud point. Although the aggregate size is large, the aggregate is packed tight and should have low solubilization volume. The addition of a small amount of oleic acid (0.002 g) increases the aggregate size tremendously. Further addition of oleic acid results in coagulation and decreases turbidity. For curves representing Newcol 1103 and 1105, several trends are shown in Figure 2: (1) for surfactant solutions containing the same amount of oleic acid, $d\tau/dt$ is higher for 1103 than 1105, showing good agreement with Equation 1 and (2) when the same surfactant is used, $d\tau/dt$ is higher for more oil addition. This is expected from kinetics rules.

Figure 3 shows the solubilization of triolein in Newcol surfactants. Figure 4 shows the solubilization of n-decane in the same surfactant solutions. The general characteristics of the curves in Figures 3 and 4 are the same as those shown in Figure 2.

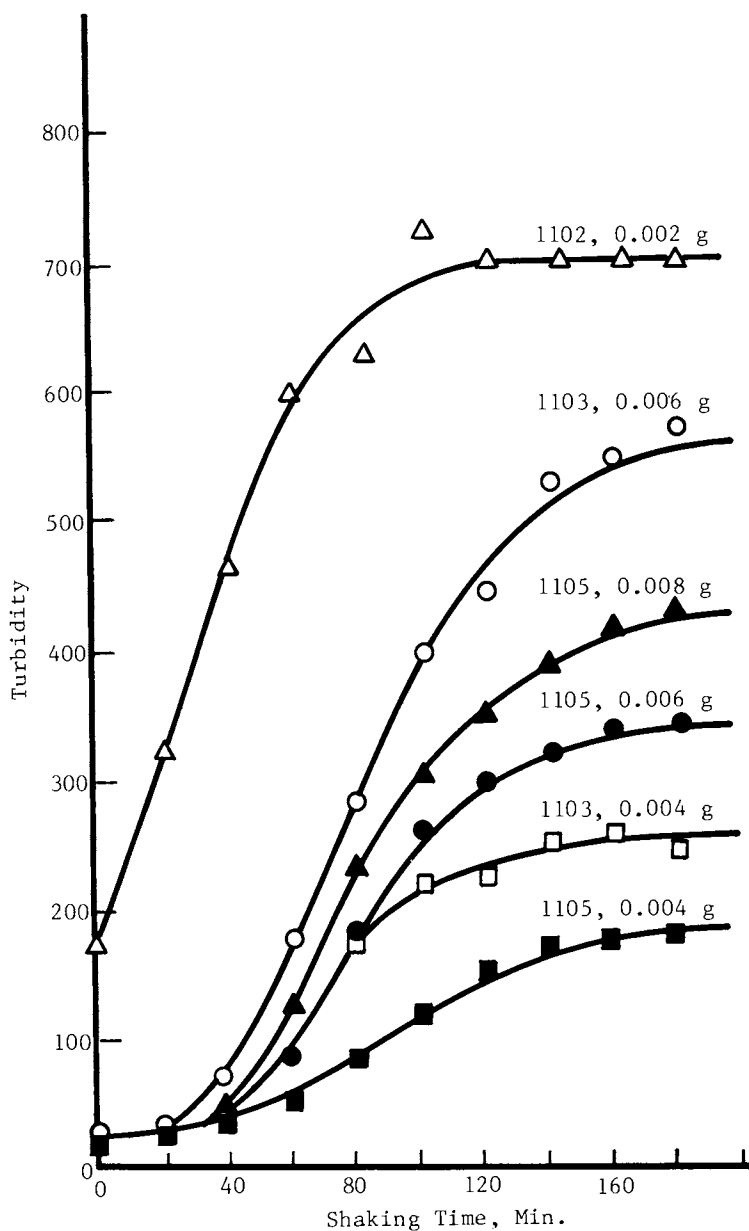


Figure 2. Solubilization of Oleic Acid in Nonionic Surfactant.

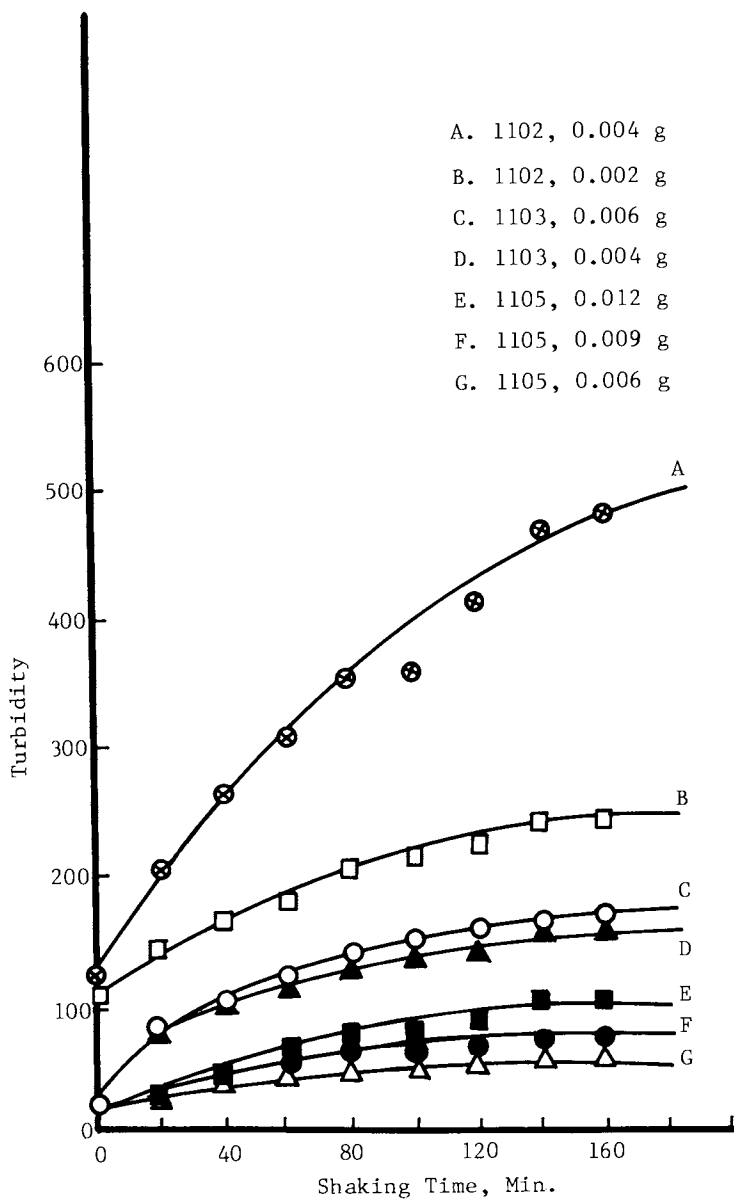
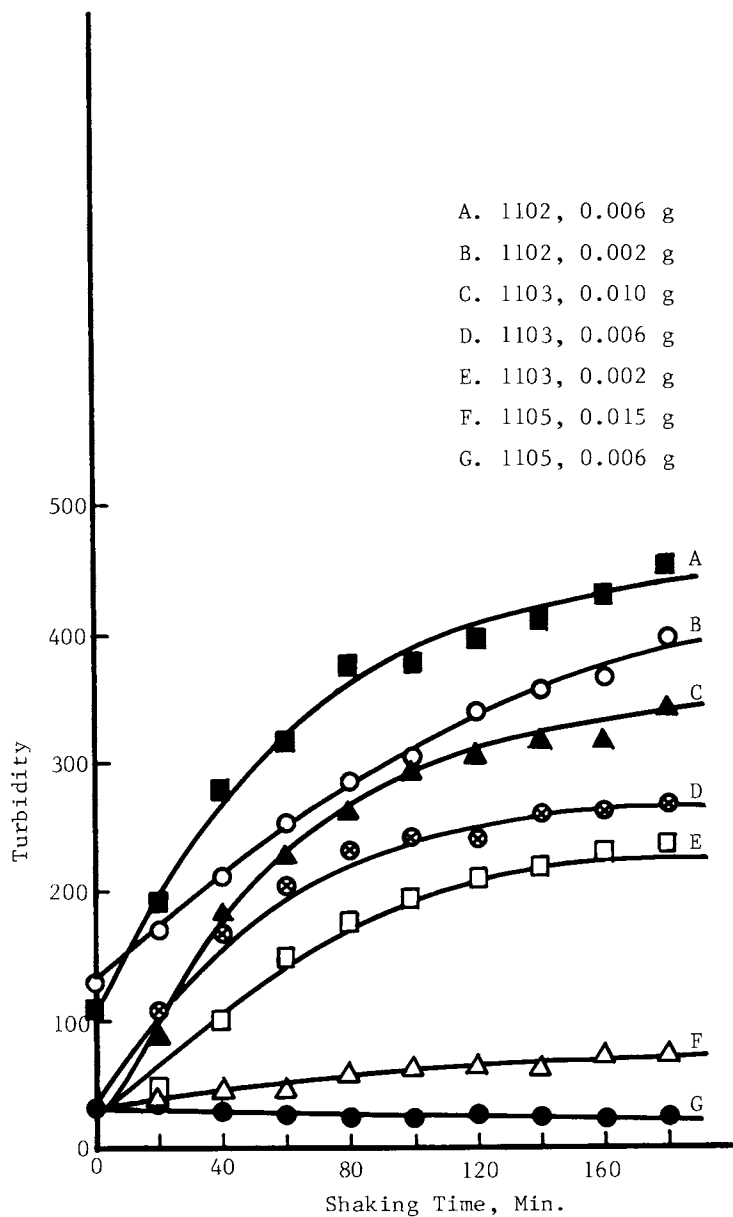


Figure 3. Solubilization of Triolein in Nonionic Surfactant.

Figure 4. Solubilization of *n*-Decane in Nonionic Surfactant.

From the lower turbidity values shown in Figures 3 and 4, one may estimate that the solubilization of oleic acid is higher than triolein or n-decane in Newcol surfactant solutions. It is difficult to make further distinction between triolein and n-decane from Figures 3 and 4.

Solubilization in Anionic Surfactant. Figures 5 and 6 show the solubilization of oleic acid in SDS solutions. The surfactant aggregate size is varied by changing NaCl concentration in the surfactant solution. Table II shows the aggregation number of SDS micelles at 25°C as reported by various authors. The aggregation number is in general increases with the NaCl concentration. When the NaCl concentration is above 0.4M, the aggregation number increases more rapidly. The micellar shape changes from spherical to rod (14,15).

Table II. Aggregation Number of SDS Micelles at 25°C

Solution	Aggregation Number			
	Ref. 9	Ref. 10	Ref. 12	Ref. 14
Water	80	-	62	-
0.01M NaCl	-	70-77	-	-
0.02M NaCl	94	-	-	-
0.03M NaCl	100	-	72	-
0.10M NaCl	112	97-101	-	-
0.15M NaCl	-	-	-	90
0.20M NaCl	118	-	101	-
0.30M NaCl	-	-	-	110
0.40M NaCl	126	-	-	-
0.45M NaCl	-	-	-	200
0.50M NaCl	-	148	142	-
0.55M NaCl	-	-	-	600
0.60M NaCl	-	174-528	-	940
0.80M NaCl	-	1630	-	-

The turbidity values at zero shaking time reflects the turbidity for the SDS solutions before the addition of oil. Usually, hand dispersion of oil does not increase turbidity of the surfactant solution. Turbidity increases only when mechanical shaking is applied. But in SDS solutions when no NaCl is added, the dispersion of oleic acid by hand increases turbidity and subsequent mechanical shaking causes no further change. The initial turbidity for SDS solution containing 0-0.4 M NaCl before the addition of oil ranges from 1-3 and is hardly distinguishable in the drawing. Figures 5 and 6 show similar characteristics. Each curve in Figure 5 represents the solubilization of 0.050 g oleic acid in SDS solution containing the specified NaCl. In Figure 6, 0.062 g oleic acid is used. In general, higher turbidity is observed in Figure 6 than in Figure 5.

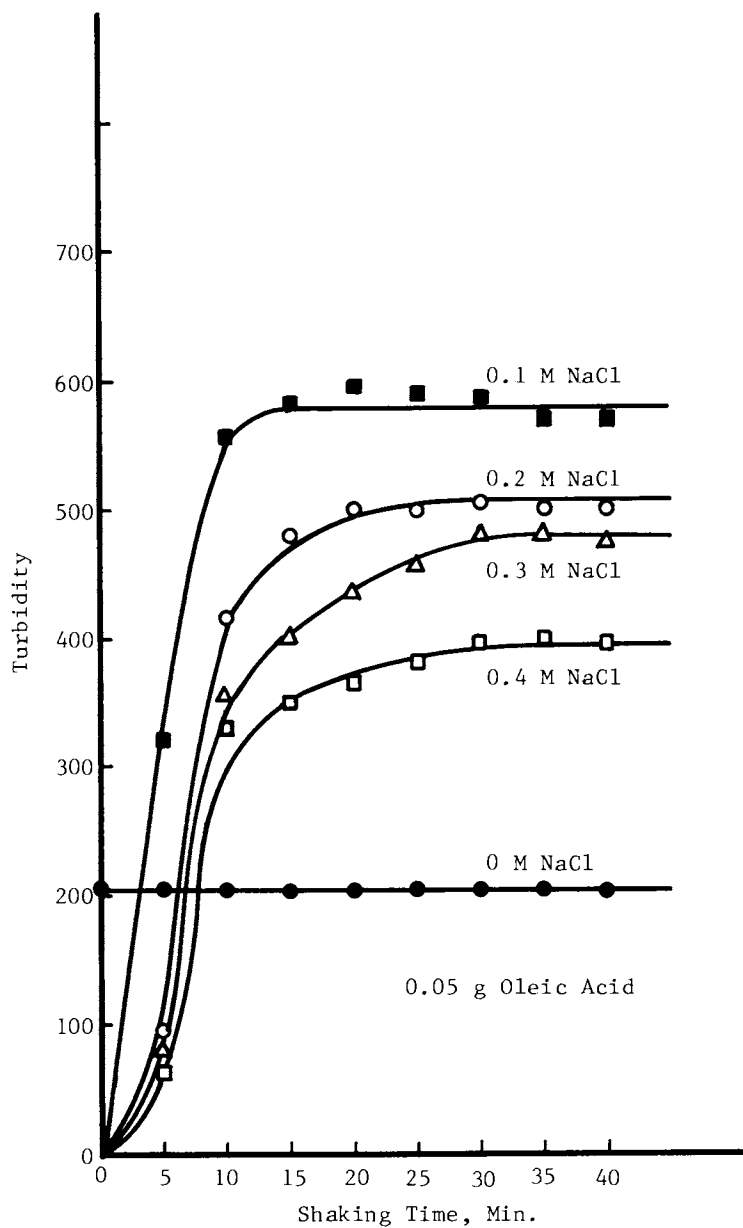


Figure 5. Solubilization of Oleic Acid in Anionic Surfactant.

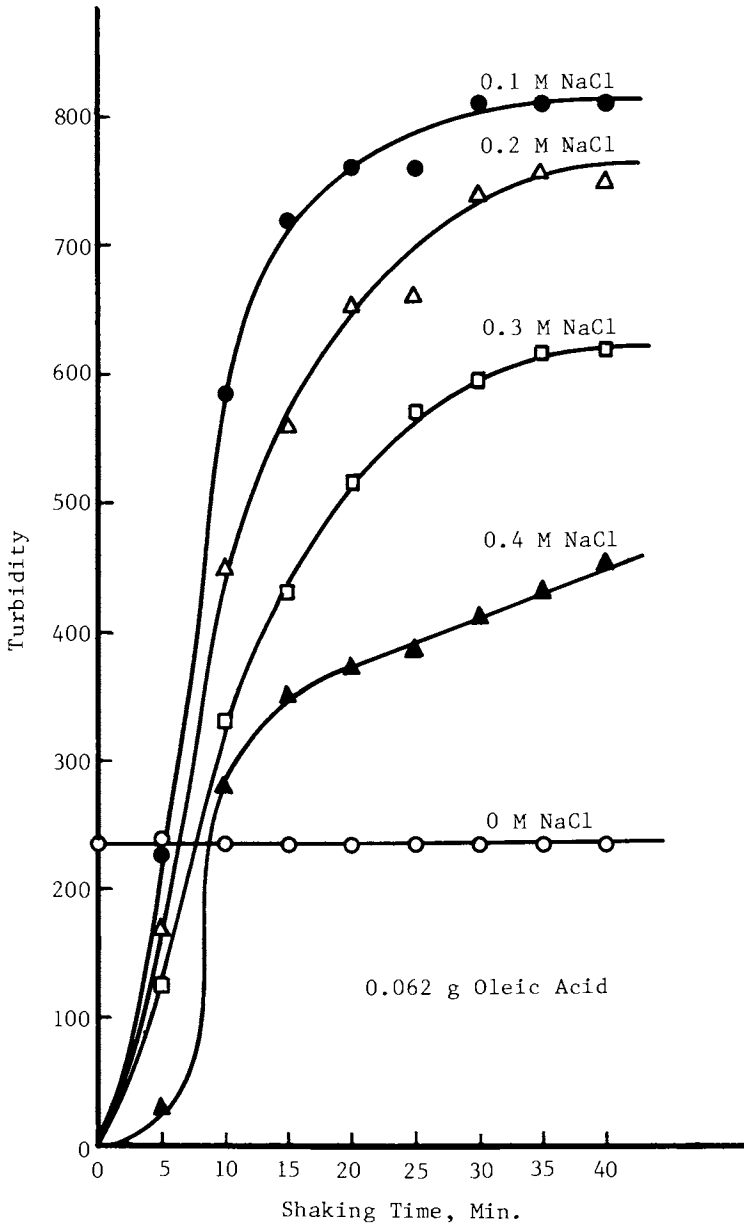


Figure 6. Solubilization of Oleic Acid in Anionic Surfactant.

Among the SDS solutions with different NaCl concentrations, the micellar properties in these solutions require some discussion. From Figure 1, one can see the CMC values of our SDS solutions in the upper right side. Since the conductance method for CMC determination can be used only in electrolyte concentration of not more than 0.1 M, we may use the values obtained only in this concentration region. In SDS solution without NaCl, the CMC value is 0.56-0.60%. For NaCl concentration of 0.025-0.1 M, CMC values are around 0.15%. From literature data showing in the same figure, one may predict only small decrease of CMC would occur in NaCl concentration range of 0.1-0.4 M. In the SDS solutions we used in the experiments, the surfactant concentration is 0.5%. This value lies below the CMC when no NaCl is added. In the presence of 0.1-0.4 M NaCl, 70% of the surfactant will be in the micellar form.

When no NaCl is added to the SDS solution, the turbidity increase with slight dispersion of oleic acid is probably due to the monomer emulsification of the oleic acid. The process does not seem to require as much time and energy as solubilization. In the SDS solutions containing 0.1-0.4 M NaCl, the turbidity increase is mainly due to micellar solubilization. The solubilization rate ($d\tau/dt$) of the solutions seems to be in this order: 0.1 M > 0.2 M > 0.3 M > 0.4 M NaCl. The final solubilization of the solutions is also in the same order. The size of the pure SDS micelles in solutions containing NaCl has been shown to increase with the NaCl concentration (Table II). Our instrument is not sensitive enough to distinguish the size between these small micelles at different NaCl concentrations. In the solubilization of oleic acid in 0.5% SDS solutions, the maximum V_{eff} seems to occur when the NaCl concentration is around 0.1 M. The maximum may occur in NaCl concentration below 0.1 M or between 0.1 M and 0.2 M which we have not studied.

Figure 7 shows some turbidity data as a function of triolein addition in SDS solutions containing varying amount of NaCl. Each point was taken from experiments such as described in the experimental section by dropwise addition of triolein. The turbidity increases with the addition of triolein to a steady value for all SDS solutions containing different amount of NaCl. The highest turbidity (or the highest solubilization) and the highest solubilization rate ($d\tau/dt$) occur at 0.5 M NaCl. At higher NaCl concentrations, coagulation occurs with shaking and turbidity decreases. Figure 7 also shows some data taken from experiments performed in the same way as described above for the solubilization of oleic acid in SDS solutions. In these experiments, 0.050 g triolein was added to the SDS solution containing a specified amount of NaCl. The final turbidity values were plotted along the line corresponding to 0.050 g triolein addition with the specified NaCl concentration. These values are not too far from the values obtained by dropwise addition of triolein as shown in the same diagram.

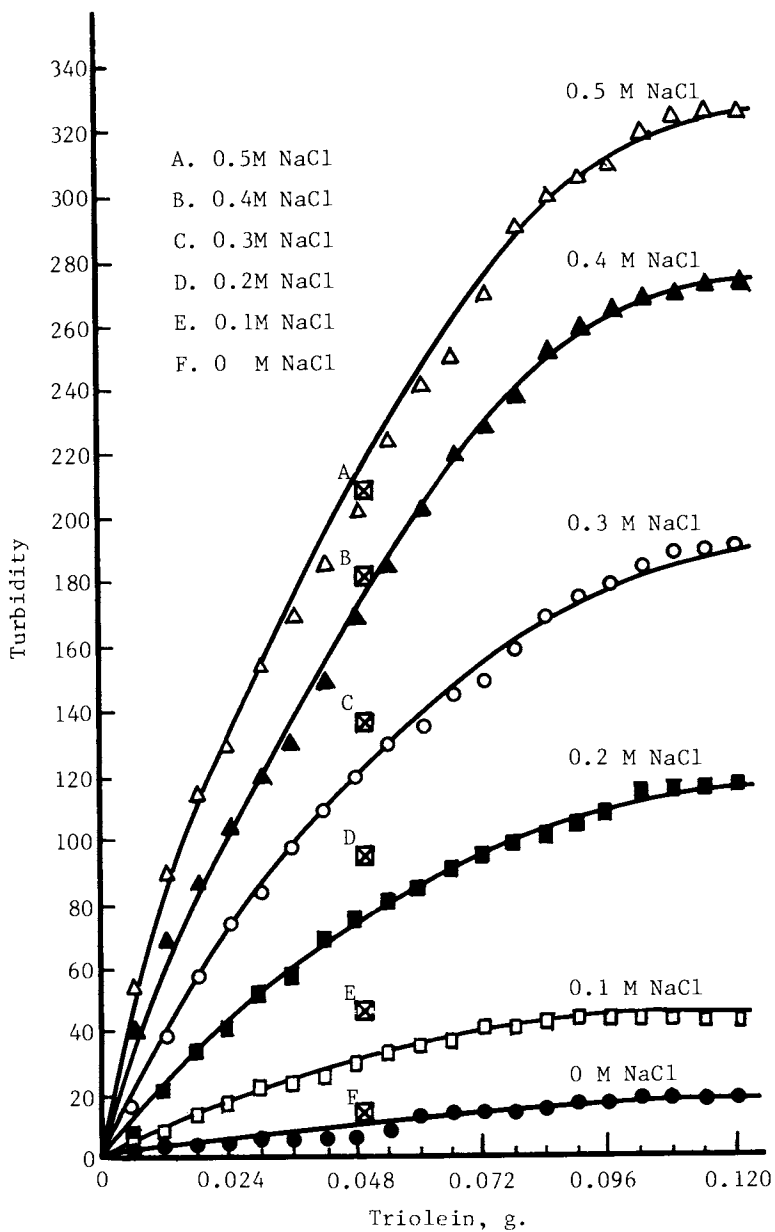


Figure 7. Solubilization of Triolein in Anionic Surfactant.

Up to this moment we have studied the solubilization rate of several oily materials in some nonionic and anionic surfactants. In general we found that the oil solubilization rate is a function of the surfactant aggregate size. The maximum V_{eff} for a series of surfactant solutions seems to occur at the condition that the surfactant associates to the maximum aggregate volume without increasing the density of the aggregate. The V_{eff} value seems to parallel the final solubilization value of the surfactant.

All the results we obtained are qualitative in nature. The materials used in the experiments are mostly not 100% pure but should be usable in comparing performance result of industrial applications. And the conclusions we obtained do not have the limitation of a pure oil (or surfactant) or a particular oil (or surfactant). One important factor we have not discussed is the electrical effect. This may contribute significantly in anionic surfactant solubilization with polar oil. We have neither discussed the mechanism of solubilization nor the specific effect of a certain oil to a certain surfactant. To understand clearly such specific effects and to derive more quantitative relations governing the result of solubilization, we are planning to conduct future experiments with pure sample.

Relation Between Structure and Performance of Surfactants. In a detergent paper (3), we have repeated the detergency work of The Proctor and Gamble Company of some narrow range dodecanol ethoxylates with EO number from 2 to 8. A detergency maximum at EO number 4 for 24 °C (at EO number 5 for 38 °C) was found for triolein removal. For oleic acid removal, a steady increase of detergency was found for dodecanol ethoxylates from EO number 2 to EO number 5 at 38 °C and no significant change from EO number 5 to EO number 8. From cloud point measurement, it was found that the temperature at which the indicated surfactant showing the maximum detergency is 7-15 °C above the surfactant cloud point. Since triolein is relatively non-polar, its removal depends mainly on solubilization. The large aggregates formed at temperature somewhat above the cloud point are obviously very effective in solubilization. We have attributed this to the increase of solubilization rate with the surfactant aggregate size. The evidence has been shown by this paper.

Carroll (5) studied the kinetics of solubilization of nonpolar oil by nonionic surfactant solutions and found that the solubilization rate is strongly temperature dependent in the region of the nonionic cloud point: 15 °K below the cloud point, the rate is extremely small relative to that at the cloud point. Nakagawa and Tori (16) have found a tremendous increase in aggregate weight for nonionic surfactants near the cloud point and the increase in aggregate weight correlated with increased solubilization of long chain alkyl compounds at constant total surfactant concentration. These independent studies show more evidences to what we have just described in this paper.

Since oleic acid is relatively polar, it may become emulsified by the surfactant monomer. The removal of oleic acid comes mainly from two contributions: monomer emulsification and micellar solubilization. Although the V_{eff} has been decreased with increasing EO number in dodecanol ethoxylates, in higher EO numbers than 5, this factor has been compensated by the increase of monomer with increasing EO number (CMC decreases with EO number). The levelling of detergency of dodecanol ethoxylates from EO number 5 to EO number 8 has been interpreted by these reasons. The monomer emulsification of oleic acid has been clearly shown in this paper in SDS solution. The nonionic surfactants we used here have low EO numbers and show mainly the effect of solubilization.

It also appears that larger solubilize prefers larger micelles for solubilization. This is shown in the SDS solubilization. Triolein solubilizes more effectively in SDS solutions containing higher NaCl concentration while oleic acid solubilizes better in lower NaCl concentration. The distinction of the size preference between different solubilizes is not so obvious in the nonionic surfactant solutions reported here. With EO number between 2-5, the sizes of the nonionic surfactant aggregates are so much larger than the SDS micelles (or the oil molecules) that even the smallest nonionic aggregates are more effective solubilizers than the SDS micelles. Thus they show a levelling effect for the different solubilizes. The electrical charge on anionic surfactants may also have some contribution to the difference in solubilization of oleic acid and triolein.

Another example showing the preference for large surfactant aggregates is demonstrated in tertiary oil recovery (1). When a 5% Bryton 430 petroleum sulfonate solution was used, the ultralow interfacial tension between oil and water and fast solubilization of crude oil appeared around 0.3 M NaCl. By Coulter counter measurement, surfactant aggregates around 1μ in size was found. Below 0.3 M NaCl, the aggregate sizes were smaller and the solubilization rates were slower. Above 0.3 M NaCl, the aggregates became unstable and tended toward separation from water. We have not had an opportunity to measure the solubilization rate of petroleum sulfonate solutions. The statement made here is mainly from observation. The oil solubilization in 5% Bryton 430 containing 0.3 M NaCl is too fast to be measured by ordinary methods. In order to bring the solubilization rate in a measurable range, we used much smaller surfactant aggregates (SDS) in the experiments. The phenomenon exhibited by triolein solubilization resembled the phenomenon observed in Bryton 430 except the rate was much slower.

It is well known that SDS and many commercial surfactants can not be used to recover oil. In our opinion these surfactants can not associate to form large enough aggregates is one important reason. In most cases, when electrolyte is added to the surfactant solution to increase the size of the aggregate, surfactant separation occurs before large enough aggregates can be built up.

This paper presents a very basic principle in surfactant solubilization. More quantitative measurement in correlating solubilization rate with micellar properties and more applications of this principle to improve performance of various solubilization processes remain the subject of our investigation.

Acknowledgments

Shu-Mei Ann, Venice Hu, Dao-Shinn Hwang, Peter Hwang, Jing-Ming Hsu, Tian-Tsain Wu, Huann-Jang Hwang and Ruey-Jing Cheng have made contribution to this paper.

Literature Cited

1. Chiu, Y. C. in "Solution Behavior of Surfactants: Theoretical and Applied Aspects"; Mittal, K. L.; Fendler, E. J., Ed.; Plenum: New York, 1982; Vol. II, pp. 1415-1440.
2. Chiu, Y. C. Oilfield and Geothermal Chemistry Symposium, Denver, Co., U.S.A., June 1-3, 1983; SPE paper 11783.
3. Benson, H.L.; Chiu, Y. C. "Relationship of Detergency to Micellar Properties for Narrow Range Alcohol Ethoxylates", Technical Bulletin, SC: 443-80, Shell Chemical Co. Houston, Texas, U.S.A., 1980.
4. McBain, M.E.; Hutchinson, E. "Solubilization and Related Phenomena"; Academic Press: New York, 1955.
5. Carroll, B. J. J. Colloid and Interface Sci. 1981, 79, 126.
6. Chan, A. F.; Evans, D. F.; Cussler, E. L. AICHE 1976, 22, 1006.
7. Shaeiwitz, J. A.; Chan, A. F-C.; Cussler, E. L.; Evans, D. F. J. Colloid and Interface Sci. 1981, 84, 47.
8. Debye, P. Ann. N. Y. Acad. Sci. 1949, 51, 575.
9. Phillips, J. N. Trans. Faraday Soc. 1955, 51, 561.
10. Hayashi, S.; Ikeda, S. J. Phys. Chem. 1980, 84, 744.
11. Emerson, M. F.; Holtzer, A. J. Phys. Chem. 1967, 71, 1898.
12. Mysels, K. J.; Princen, L. H. J. Phys. Chem. 1959, 63, 1696.
13. Becher, P. J. Colloid Sci. 1961, 16, 49.
14. Mazer, N. A.; Benedek, G. B.; Carey, M. C. J. Phys. Chem. 1976, 80, 1075.
15. Missel, P. J.; Mazer, N. A.; Benedek, G. B.; Young, C. Y.; Carey, M. C. J. Phys. Chem. 1980, 84, 1944.
16. Nakagawa, T.; Tori, K. Koll. Z. 1960, 168, 132.

RECEIVED January 20, 1984

Hydrotropic Function of a Dicarboxylic Acid

STIG E. FRIBERG and TONY D. FLAIM

Chemistry Department, University of Missouri-Rolla, Rolla, MO 65401

The hydrotropic action of a dicarboxylic acid is discussed against the general features of hydro-tropic action; the liquid crystal/isotropic solution equilibrium. It is shown that the hydrotropic action of the dicarboxylic acid in question, 8-[5(6)-carboxy-4-hexyl-cyclohex-2-enyl] octanoic acid, depends on its conformation at an interface.

The word hydrotrope was introduced 67 years ago by Neuberg (1). In his treatment and in the subsequent ones the hydrotropes were investigated for their solubilizing power in aqueous solutions (2-6).

A change in the perception of their mechanism of action came in the sixties when Lawrence (7) pointed out that short chain surfactants would delay the gelling to a liquid crystalline phase which takes place at high surfactant concentrations. Friberg and Rydhag (8) showed that hydrotropes, in addition, prevent the formation of lamellar liquid crystals in combinations of surfactants with hydrophobic amphiphiles, such as long chain carboxylic acids and alcohols. The importance of this finding for laundry action was evident.

The hydrotropes in this era were short chain aromatic sulfonates, with the p-xylene sodium sulfonate as a typical example. Their action is preventing the formation of liquid crystals is easily understood from a direct comparison of their molecular geometry (Fig. 1).

The short bulky aromatic compound does not pack well in a lamellar liquid crystalline structure, the mutual stabilizing action of the straight hydrocarbon chains is lost, and instability results.

0097-6156/84/0253-0107\$06.00/0
© 1984 American Chemical Society

During the 1970's, a new kind of hydrotrope was introduced, WESTVACO DIACID® (9), (Fig. 2). It is a dicarboxylic acid with a total of twenty-one carbon atoms. Its basic properties have been investigated by Matijevec and collaborators (10), who determined its cmc and the association constants for the diacid in water.

This new hydrotrope posed an intriguing problem; the explanation of the hydrotropic action of such a long chain dicarboxylic acid. The problem was solved in a series of articles (11-14) which contain the essential experimental information for this article. These articles each provided a part of the total framework of the problem and we considered a unified treatment essential in order to present a systematic pattern for the different aspects involved.

The analysis of hydrotropic action is conveniently divided into two parts: (1) The isotropic liquid/liquid crystalline equilibrium between essential phases and (2) The molecular mechanism for the influence of the hydrotrope on the equilibrium.

The Isotropic Liquid/Liquid Crystalline Equilibrium

Hydrotropes with their gel-prevention action are an essential part of liquid cleaners for which they provide two essential functions: (a) they allow high surfactant concentrations in the formulation by preventing its gelling at the low water concentrations employed, and (b) they prevent gel formation in extremely water-rich systems under laundering conditions.

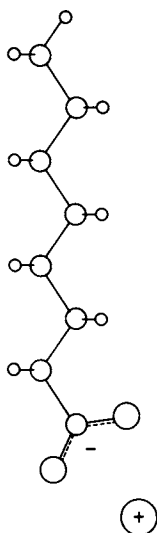
Low Water Content

The gel-prevention action in the water-poor part of the system is illustrated by a comparison between the dicarboxylic acid and a monocarboxylic acid of approximately the same carboxylic/methylene group ratio.

The carboxylic acids were combined with hexylamine and water in order to study the association structures formed. The hexylamine was chosen because it did not by itself form a liquid crystalline phase with water, Fig. 3A. Water dissolves in the amine to a maximum of 60% to form an isotropic solution. The liquid crystal is formed first at a certain octanoic acid: amine ratio, approximately 0.1. The liquid crystalline phase forms a large region reaching to a weight fraction of 0.61 of the acid, corresponding to a 1:1 molar ratio of the two species.

The combination of the hexylamine with the dicarboxylic acid on the other hand, Fig. 3B, does not give a liquid crystalline phase for any combination between the acid and the amine or the water. The entire area, Fig. 3B, is an isotropic liquid.

SODIUM OCTANOATE



SODIUM XYLENE SULFONATE

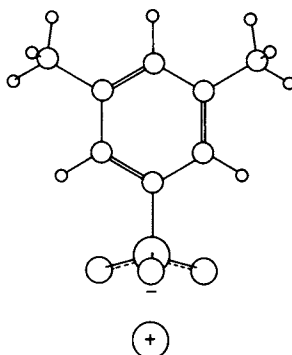


Figure 1. The structure of a conventional hydrotrope (right) inhibits the formation of a lamellar structure with the common straight-chain surfactants.

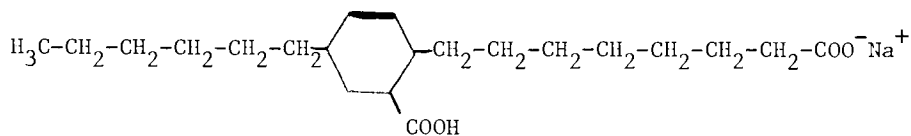
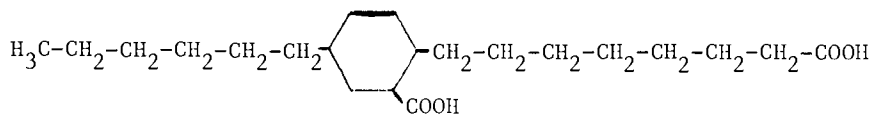


Figure 2. The structure of 8-[5-carboxy-4-hexyl-cyclohex-2-enyl] octanoic acid (top) and its monos soap (bottom).

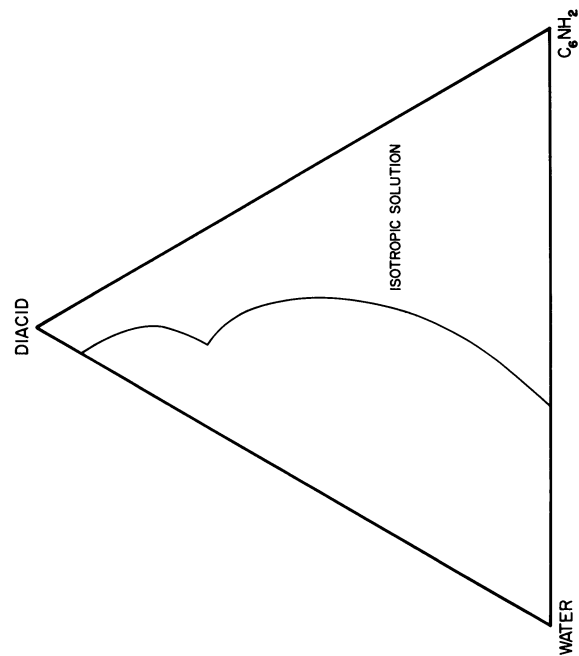


Figure 3A.

The combination of water and hexylamine forms only an isotropic liquid phase. In combination with octanoic acid, a large liquid crystalline area is found.

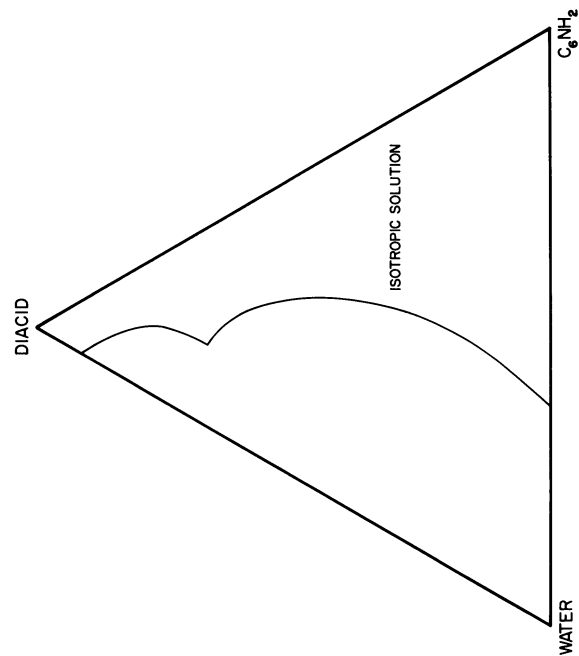


Figure 3B.

A combination of water and hexylamine with the dicarboxylic acid, 8-[5(6)-carboxy-4-hexyl]-cyclohex-2-enyl] octanoic acid, gives no liquid crystalline phase.

These results showed an important feature of the dicarboxylic acid in question. Contrary to the corresponding monocarboxylic acid, it prevents the formation of a liquid crystalline phase in water-poor systems. The implications of this fact for the formulations of liquid cleaners is obvious.

High Water Content

The question of gelling in the water-rich systems, which are typical of laundering conditions, was probed using a simplified model system. The surfactant used was of shorter chain length than normally applied under laundry conditions. The eight carbon chain of sodium octanoate gives a cmc considerably higher than that of the normally used twelve to eighteen carbon chain varieties. The choice was made with the view of facilitating the experimental situation. The phase equilibria at the cmc and concentrations below become simpler to evaluate with a wider concentration range to explore. Octanol was used as a model for oily dirt, following the use of decanol in a recent contribution from Unilever (15).

The phase condition for concentrations in the range close to the cmc are found in Fig. 4A. For the lowest soap concentrations, a liquid isotropic alcohol solution separated, when the solubility limit of the alcohol was exceeded. This was changed at concentrations approximately one half the cmc, when a lamellar liquid crystalline phase appeared instead. After the relatively narrow three-phase region had been transversed, this liquid crystalline phase was the only phase in equilibrium with the aqueous solution. Solubilization of the long chain alcohol increased at the cmc, as expected.

Replacing part of the soap with the dicarboxylic acid at a sufficiently high pH value to ensure its complete ionization gave the results in Fig. 4B. At the site for the onset of the 3-phase area in Fig. 4A with the liquid crystal, the alcohol and the aqueous solution, solubilization of the alcohol now showed a sudden maximum.

The results are straight forward and the interpretation immediately evident. The liquid crystalline phase formed in these extremely water rich systems was destabilized by the dicarboxylic acid and transformed to an isotropic solution. The conclusion that the hydrotropic action of the dicarboxylic acid is intimately related to its capacity to destabilize a liquid crystalline phase also under the water-rich conditions during actual laundering conditions appears well justified.

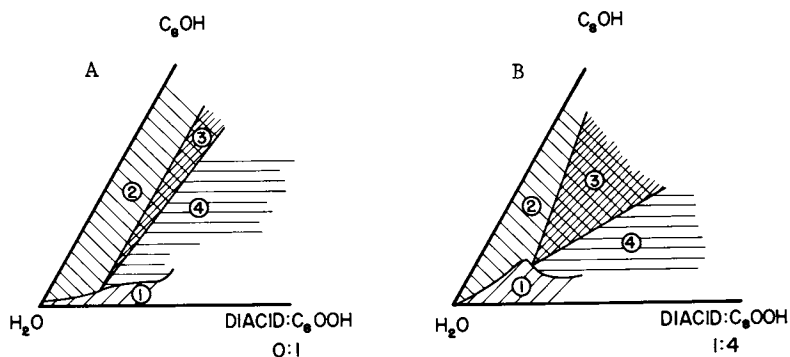


Figure 4. Addition of the dicarboxylic acid to a water/detergent combination prevents (B) the gelling caused by a model dirt (octanol, C_8OH) below the cmc (A). A The model dirt octanol (C_8OH) forms a liquid crystalline phase with water and sodium octanoate (C_8OOH at pH 10) in area 3 and 4. Partial substitution of the sodium octanoate with the diacid soap (pH 10) leads to an increase of solubilization of the octanol (B). 1: aqueous solution, 2: two-phase region of 1 + octanol solution, 3: three-phase region of 1 + alcohol solution + lamellar liquid crystal and 4: two-phase region of 1 + lamellar liquid crystal.

The Molecular Mechanism For The Hydrotropic Action

The remaining problem of the molecular mechanisms of this action was judged to be related to the conformation of the dicarboxylic acid at the interface. This conformation is usually determined directly with the use of a Langmuir trough (16-18). The disadvantage of such a method for the present problem lies with the restrictions of the environment of the molecule to be investigated. The basic requirement is that the molecule must be virtually insoluble in the liquid substrate on which the monolayer is supported. For the dicarboxylic acid in question, this meant a pH value as low as 2 and also a high electrolyte content in the aqueous substrate.

Although it may be argued that the conformation of the dicarboxylic acid under such conditions may be of pronounced scientific interest, several factors suggested a different approach. The interest in the conformation of the hydrotrope is primarily related to its behavior at an oil/water interface in conjunction with surfactant molecules. In addition, molecules from an "oily dirt" may be present. Finally, it is essential to realize that the action of the hydrotrope is to destabilize a liquid crystalline phase and transform it to an isotropic liquid.

With these factors in mind, a new method to evaluate the conformation of an amphiphilic molecule at the site of interest was introduced. The method is built on the fact that the determination of interlayer spacings of a lamellar liquid crystal using low angle X-ray diffraction methods in combination with density measurements will provide sufficient information to calculate the cross-sectional areas occupied by each amphiphile (19).

This means that the partial molar area may directly be determined from the change in molecular area, when an amphiphilic molecule is introduced into a host liquid crystalline pattern. Of course, this area is the change of area per molecule at the introduction of one molecule of the substance in question and may be influenced by the interaction between the host molecules and the guest molecules. Since this interaction is an essential part of the present problem, it appears obvious that the method exactly meets the requirements.

The host liquid crystalline matrix was composed of water, sodium octanoate and octanol. This combination was chosen in order to create an environment as closely matching the specific requirements of the problem as possible. In the first instance, the surfactant was identical to the one used for the solubilization determinations (12) and the alcohol was present in order to resemble actual laundering conditions with "oily dirt" molecules present (12).

The conformational distinction which was sought was the location of the middle carboxylic group relative to the interface. If the middle carboxylic group were found at the interface, the interlayer spacing as influenced by the dicarboxylic acid would be comparable to the one from sodium octanoate. A straight conformation of the diacid, on the other hand, would give an increment to the interlayer spacing similar to the one from sodium oleate.

The influence of sodium oleate on the interlayer spacing is found in Fig. 5A. The distance between layers is increased by an average of 2.5Å and 0.5 moles of the sodium oleate are added to the liquid crystal. The corresponding addition of the monosoap of the dicarboxylic acid gives only an insignificant increase of the distance (Fig. 5B). This result shows the length of the monosoap of the diacid to be comparable to the length of octanoic acid.

The evaluation of the conformation of the diacid monosoap from these results is unambiguous. Both the polar groups of the monosoap are located at the water surface, giving a conformation such as the one in Fig. 6. This conformation readily provides an explanation for the hydrotropic action of the dicarboxylic acid. When acting at an interface, the molecule does not possess the extended conformation of Fig. 2; its conformation is as shown in Fig. 6. Hence, the destabilizing action may be intuitively understood in the same manner as for the traditional aromatic hydro-trope, Fig. 1.

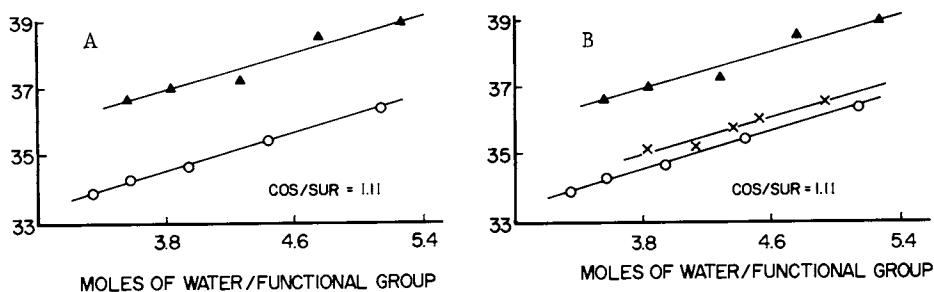


Figure 5. Sodium oleate (▲) added to a lamellar liquid crystalline phase of water, sodium octanoate, and octanol (O) increases the interlayer spacing (A). Addition of the dicarboxylic acid monosoap (X) does not give the same change (B).

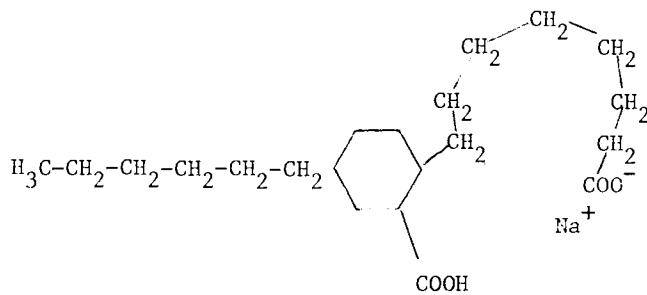


Figure 6. The conformation of the dicarboxylic acid mono-soap at the interface.

Acknowledgments

The authors express their gratitude to Westvaco Co. for financial support and stimulating interactions.

Literature Cited

1. Neuberg, C., Biochem. Z. 76, 107 (1916).
2. Durand, R., C. R. hebdom. Seances Acad. Sci. 225, 409 (1948).
3. Krasnic, I. Wiss. Z. Martin-Luther Univ. Halle-Wittenberg math-naturwiss k. VIII, 205 (1959).
4. Booth, H. S. and H. E. Everson, Ind. Engng. Chem. 41, 2627 (1959).
5. Rath, H., Tenside 2, 1 (1965).
6. Winsor, P. A., Trans. Faraday Soc. 44, 376-398, 451-471 (1948).
7. Lawrence, A.S.C., B. Baffey and K. Talbot, Proc. Internat. Congr. Surface Active Substances, Brussel, II, 673 (1964).
8. Friberg, S and L. Rydhag, Tenside 7, 80 (1970).
9. Ward, B. F. Jr., C. G. Force, A. M. Bills and F. E. Woodward, J. Am. Oil Chem. Soc. 52, 219 (1975).
10. Mino, J., E. Matijevic and L. Meites, J. Colloid Interface Sci. 60, 148 (1977).
11. Friberg, S. and L. Rydhag, J. Am. Oil Chem. Soc. 48, 113 (1971)
12. Cox, J. M. and S. E. Friberg, J. Am. Oil Chem. Soc. 58, 743 (1981).
13. Flaim, T., Friberg, S., Force, C. G. and Bell, A., Tenside Detergents 20, 177 (1983).
14. Flaim, T. and Friberg, S., J. Colloid Interface Sci. (In press).
15. Kielman, H. S. and P. J. F. van Steen "Surface Active Agents" Soc. Chem. Ind. London, 1979; p. 191.
16. Gershfeld, N. L. and Pak, Y. G., J. Colloid Interface Sci. 23, 215 (1967).
17. Bruun, H. H., Acta Chem. Scan. 9, 1721 (1955).
18. Parreira, H. C., J. Colloid Interface Sci. 20, 742 (1965).
19. Fontell, K. "Liquid Crystals and Plastic Crystals", Ellis Horwood Ltd., 1974; p. 80.

RECEIVED March 6, 1984

Aqueous Solution Properties of a Fatty Dicarboxylic Acid Hydrotrope

A. BELL

Westvaco Corporation, Charleston Research Center, North Charleston, SC 29406

K. S. BIRDI

Fysisk-Kemisk Institut, Technical University of Denmark, DK-2800 Lyngby, Denmark

Aqueous solution properties of the twenty-one carbon dicarboxylic acid 5(6)-carboxyl-4-hexyl-2-cyclohexene-1-yl octanoic acid (C_{21} -DA) in salt form - alone and in the presence of a nonionic, anionic or cationic detergent - are reported. Membrane osmometry results indicate that C_{21} -DA alkali salt forms low molecular weight aggregates or micelles, its aggregation behavior appearing to resemble that of certain polyhydroxy bile salts. In the presence of detergent, small aggregates are also formed provided the weight fraction of C_{21} -DA salt in the micelles exceeds ca. 0.5. Phase equilibrium studies show that C_{21} -DA (as the dipotassium or full triethanolamine salt) acts as a hydrotrope above certain concentration levels in concentrated detergent solutions, retarding build-up of anisotropic aggregates responsible for mesophase formation, in accordance with previous investigations by Friberg and co-workers.

In recent studies, Friberg and co-workers (1,2) showed that the 21 carbon dicarboxylic acid 5(6)-carboxyl-4-hexyl-2-cyclohexene-1-yl octanoic acid (C_{21} -DA, see Figure 1) exhibited hydrotropic or solubilizing properties in the multicomponent system(s) sodium octanoate (decanoate)/n-octanol/ C_{21} -DA aqueous disodium salt solutions. Hydrotropic action was observed in dilute solutions even at concentrations below the critical micelle concentration (CMC) of the alkanolate. Such action was also observed in concentrates containing pure nonionic and anionic surfactants and C_{21} -DA salt. The function of the hydrotrope was to retard formation of a more ordered structure or mesophase (liquid crystalline phase).

0097-6156/84/0253-0117\$06.00/0

© 1984 American Chemical Society

As is well known, hydrotropes are incorporated in liquid detergent formulations in order to produce transparent (isotropic) solutions at high solids concentrations which will be stable under varying conditions of temperature and composition. Depending upon its structure, the hydrotrope may also assist in solubilizing components added in small amounts (e.g., perfumes, colorants, bactericides) and, depending upon the nature of the soil, enhance detergency.

In order to better understand the molecular basis of hydrotropic action, it is useful to investigate phase properties of multicomponent regions of interest, specifically the micellar or isotropic regions. Recently, a powerful technique has again emerged for characterizing micellar formation in detergent solutions - membrane osmometry (3-6). With this technique, the effect of additives (electrolytes, organic solutes, etc.) can also be explored (7,8).

Here, utilizing membrane osmometry, we report on micelle formation in solutions of C₂₁-DA alone (in dilute electrolyte) and in the presence of surface active ingredients incorporated in commercial liquid detergent formulations. Phase diagrams of 3-component blends (detergent/C₂₁-DA salt/H₂O) are also presented.

Experimental

Materials. The dicarboxylic acid was Westvaco DIACID R 1550, or H-240, its partially neutralized 40% solids aqueous potassium salt solution (9,10). Linear fatty alcohol ethoxylate (LE-9), prepared from alcohols containing 12-15 carbon atoms and containing an average of 9 ethylene oxide groups per molecule, was obtained commercially. Sodium dodecylbenzenesulfonate (SDBS, technical grade) and cetyltrimethylammonium bromide (CTAB) were obtained from Fluka, triethanolamine (TEA) from Fisher. Inorganic chemicals were reagent grade. Water was Milli-Q R deionized.

Membrane Osmometry. The apparatus has been described in detail elsewhere (5). The concentration of detergent in the solution compartment was many times the CMC (10 to 100) whereas the concentration in the solvent compartment was somewhat above (i.e., 5 to 10 times) the CMC. Under these conditions, the following limiting equation applies (3-6):

$$\frac{\pi}{(C-C')}_{C \rightarrow C'} = \frac{RT}{M_n} + 2 RTB(C'-CMC)$$

where π is the osmotic pressure, C the detergent concentration in the solution compartment, C' the detergent concentration in the solvent compartment, R the universal gas constant, T the absolute temperature, M_n the number average molecular weight, and B the second virial coefficient. As shown previously (3-5), the term involving B is small compared to RT/M_n , and thus a plot of $\pi/RT(C-C')$ versus $(C-C')$ gives the value $1/M_n$ at the intercept. Recent fluorescent probe studies (11) indicate that in pure detergent solutions, M_n does not change appreciably in dilute electrolyte medium as concentration is increased well above the CMC. This suggests that in aqueous micellar regions containing mixtures of C₂₁-DA salt, detergent and dilute electrolyte, the micellar aggregation number should remain essentially constant (except perhaps near phase boundaries) at a given weight ratio of hydrotrope to detergent. A recent investigation by Kratochvil and co-workers (12) on the concentration-dependent aggregation of conjugated bile salts (especially taurodeoxycholate) in concentrated electrolyte media ($> 0.1M$ NaCl), however, appears to indicate otherwise.

CMC values were obtained from dye (azobenzene) solubilization and surface tension measurements. Values of π used in the above equation were obtained via extrapolation (4-5). For very low values of M_n , there is concern about leakage through the membrane (13). Assuming that leakage did occur within the timeframe of the measurements, M_n (and hence N_n) values would be lower than those calculated. For this reason, all values of M_n and N_n are reported as being apparent.

Phase Regions. Phase regions were determined by visual inspection of blended components stored in tightly capped vials. The blends were prepared by mixing the components together, with stirring, at 60-100°C, followed by cooling in air to 25°C. The C₂₁-DA dipotassium salt was fully neutralized (with 45% KOH) Westvaco H-240 (acid value equivalent), the final solids content being ca. 45% by weight. Higher concentrations of this salt were obtained via evaporation at 90-100°C. Anhydrous C₂₁-DA full triethanolamine salt is an isotropic liquid at 25°C. Anisotropic regions were determined by viewing the samples between crossed polarizers (1,2) or under a polarizing microscope. In the vicinity of phase boundaries, many weeks were often required before equilibrium was attained.

Results

CMC values in 0.05M electrolyte at pH 10 are given in Table I. Apparent number average molecular weights M_n of aqueous detergent mixtures in the same medium are listed in Table II. The maximum concentration of surface active agents in any given system was 50 g/l. Figure 2 is a plot of $\pi/RT(C-C')$ versus $(C-C')$ for the system CTAB:C₂₁-DA salt. Figure 3 shows the

variation of N_n , the apparent micellar aggregation number (calculated by dividing M_n by the average molecular weight of the detergent mixture), as a function of weight fraction of detergent in the micelle, assuming that the ratio of detergent to C_{21} -DA salt in the micelle is equal to that of the overall surfactant inventory. This assumption is essentially valid well above the CMC of the mixture (14).

Results of phase equilibrium studies are shown in Figures 4-6.

Table I. Results of CMC Determinations (0.05M NaCl or NaBr, pH 10, 25°C)

Weight Ratio Detergent in Solution	CMC Value (g/l; obtained via extrapolation)		
	LE-9	SDBS	CTAB
0.00	0.4	0.4	0.4
0.25	0.4	0.25	0.3
0.50	0.3	0.15	0.2
0.75	0.25	0.25	0.15
1.00	0.2	0.2	0.1

Table II. Results of Membrane Osmometry (0.05M NaCl or NaBr, pH 10, 25°C)

Weight Ratio Detergent in Micelle	Apparent M_n Values (g/mol)		
	LE-9	SDBS	CTAB
0.00	2400	2400	2400
0.25	3000	3100	2700
0.50	2600	3000	6800
0.75	7000	10800	14400
1.00	48000	14000	90000

Discussion

The aggregation behavior of C_{21} -DA salt in dilute electrolyte medium appears to resemble that of certain polyhydroxy bile salts (15,16). That C_{21} -DA, with a structure quite different from bile acids, should possess solution properties similar to, e.g., cholic acid is not entirely surprising in light of recent conductivity and surface tension measurements on purified (i.e., essentially monocarboxylate free) disodium salt aqueous solutions, and of film balance studies on acidic substrates (17). The data in Figure 3 suggest that C_{21} -DA salt micelles incorporate detergents - up to an approximate weight fraction of 0.5 - much like cholate incorporates lecithin or soluble

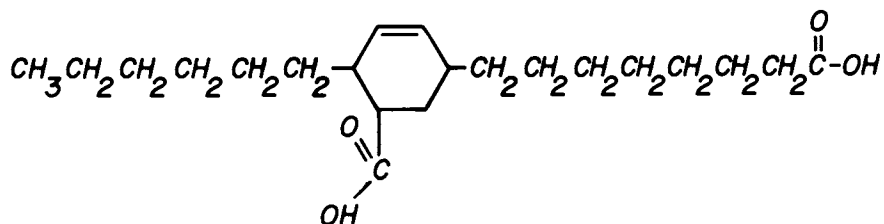


Figure 1. Structure of the dicarboxylic acid 5-carboxy-4-hexyl-2-cyclohexene-1-octanoic acid (C_{21} -DA).

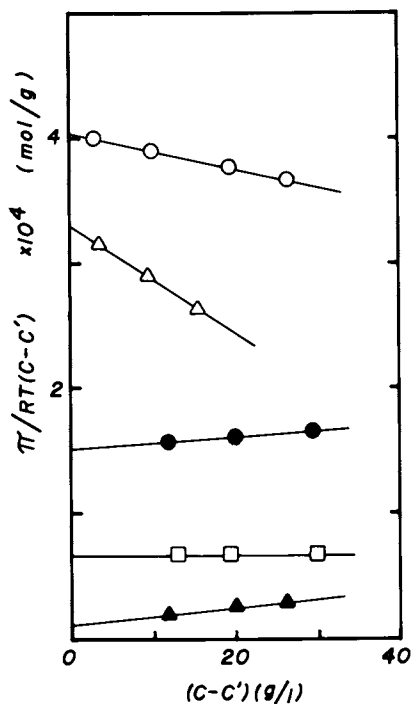


Figure 2. Plots of $\pi/RT(C-C')$ vs. $(C-C')$ for mixtures of cetyltrimethylammonium bromide (CTAB) and C_{21} -DA alkali salt in 0.05M NaBr, pH 10, 25°C. Weight ratio CTAB: C_{21} -DA salt 0:1 (○); 1:3 (▲); 1:1 (●); 3:1 (□); 1:0 (▲).

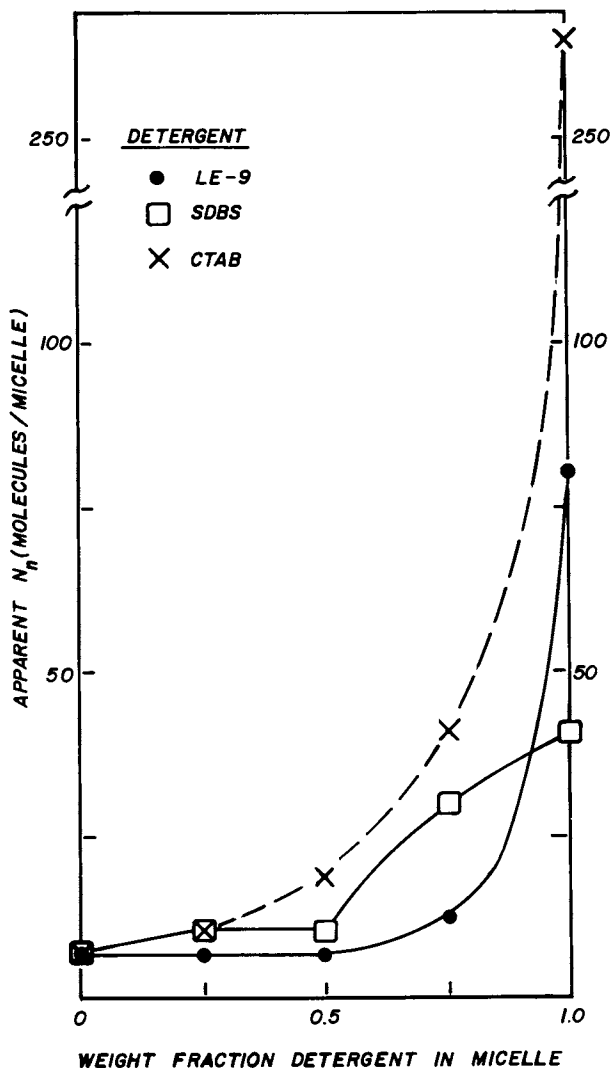


Figure 3. Apparent aggregation number (N_n) of mixed micelles containing detergent and/or C_{21} -DA alkali salt. Aqueous medium: 0.05 M NaCl or NaBr, pH 10, 25°C. LE-9, linear fatty alcohol ethoxylate; SDBS, sodium dodecylbenzenesulfonate; CTAB, cetyltrimethylammonium bromide.

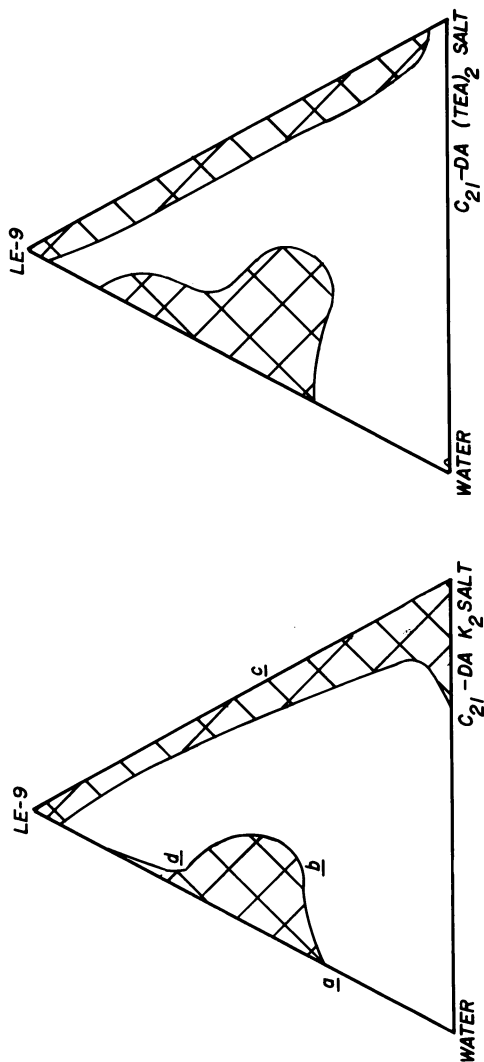




Figure 4. Phase diagrams, 25°C: linear fatty alcohol ethoxylate (LE-9)/C₂₁ dicarboxylic acid dipotassium (C₂₁-DA K₂) or full triethanolamine (C₂₁-DA (TEA)₂) salt/water. Anisotropic region (liquid crystalline and/or solid material present) ; isotropic region .

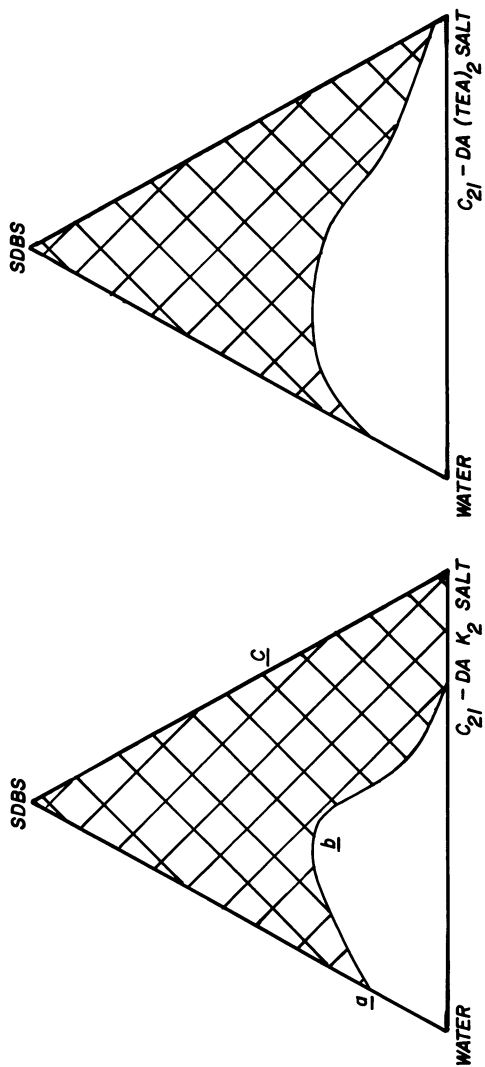


Figure 5. Phase diagrams, 25°C: sodium dodecylbenzenesulfonate (SDBS)/C₂₁ dicarboxylic acid dipotassium (C₂₁-DA K₂) or full triethanolamine (C₂₁-DA (TEA)₂) salt/water.

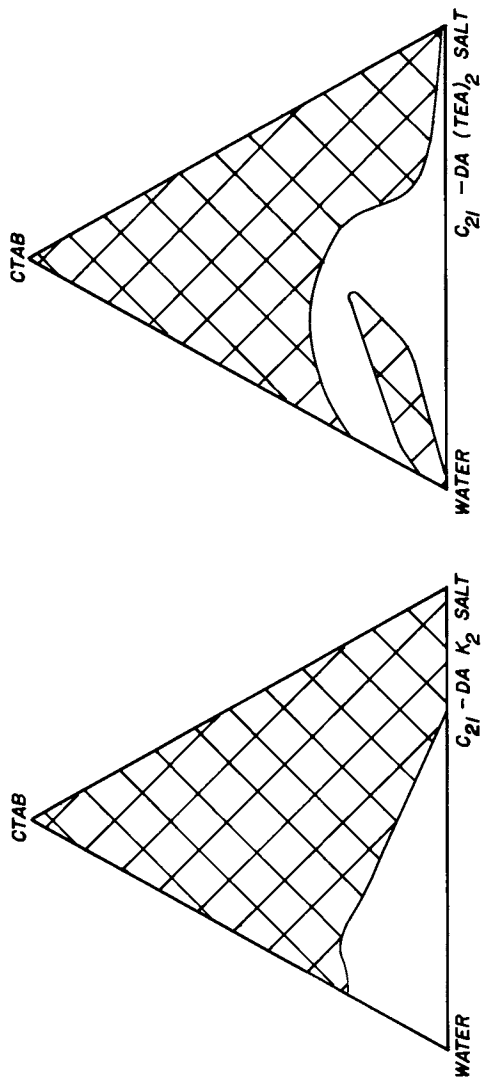


Figure 6. Phase diagrams, 25°C: cetyltrimethylammonium bromide (CTAB)/C₂₁ dicarboxylic acid dipotassium (C₂₁-DA K₂) or full triethanolamine (C₂₁-DA (TEA)₂) salt/water.

amphiphiles (e.g., oleate, monolein) in micellar solutions (15,18). As the weight fraction of detergent approaches unity, the size (and presumably the shape) of the aggregates is altered, reflecting the influence of the main constituent.

It is probable that at higher weight fractions of C_{21} -DA salt, the shape of the mixed micelles is roughly spherical at concentrations not too far removed from the CMC (16). However, as the weight fraction of detergent and/or total solids concentration is increased, it is likely that the shape changes. Whether Small's model (15) (wherein all the C_{21} -DA salt molecules would be at the micelle exterior) or the "mixed-disc" model (18) (wherein some C_{21} -DA salt molecules would also enter the interior of the micelle) is not known. In the case of bile salt(cholate)/detergent micelles, recent calorimetric studies (19) suggest that the "mixed-disc" model is favored, with hydrogen bonding taking place in the interior. If this model applies to detergent/ C_{21} -DA salt micelles (with accompanying hydrogen bonding), the less acidic C_{21} -DA secondary carboxyl group (20) should be only partially ionized within the micelle.

Concentrated systems are now considered. Here, we define a hydrotrope as a substance capable of increasing the absolute amount of detergent in an isotropic formulation. For both the nonionic (Figure 4) and anionic (Figure 5) systems, addition of C_{21} -DA K_2 salt to the onset of the water-rich liquid crystalline region (composition a) results in an increase of solubilized detergent up to a point where the weight ratio detergent: C_{21} -DA salt is ca. 1:1 (composition b). (Note that at composition c, obtained via extrapolation of the line joining a and b, the ratio is also ca. 1:1). Comparison with the results of membrane osmometry (Table II) suggests that there is a correlation between dilute solution properties and the tendency to form anisotropic aggregates or mesophases in water-rich concentrated systems.

In the nonionic system (Figure 4), C_{21} -DA K_2 salt also acts as hydrotrope in the water-poor (reversed) micellar region (i.e., in the vicinity of composition d). Indeed, in this region, its efficiency appears to be greater than in the water-rich region.

As might be expected, there is a greater interaction in concentrated systems between cationic detergent (CTAB) and the negatively charged C_{21} -DA K_2 salt, resulting in a diminution of the isotropic region or in the case of the full TEA salt, formation of an anisotropic phase within the region (Figure 6). The maximum hydrotropic action is observed when the ratio detergent: C_{21} -DA salt is ca. 0.8:1, again in line with osmometry results (Table II).

Employing x-ray methods, Flaim and Friberg (21) studied the conformation of C_{21} -DA as the acid or monosoap in a lamellar liquid crystalline matrix. At low water concentrations, the conformations are the same (extended). At somewhat higher water

concentrations, the monosoap becomes coiled, occupying a larger area within the matrix, thus tending to disrupt close packing; under similar conditions, the acid remains extended. These findings point to the influence of structure on hydrotropic action.

Summarizing, past and present investigations indicate that C₂₁-DA salt acts as a hydrotrope in both concentrated and dilute systems by retarding build-up of anisotropic aggregates or micelles responsible for mesophase formation (1,2,21). Hydrotropic action appears to be pronounced in the system containing nonionic detergent (water-rich and water-poor regions). In liquid systems containing both anionic and cationic detergents, C₂₁-DA salt could serve to enhance compatibility, especially near phase boundaries, as a result of its unusual hydrotropic properties.

Acknowledgments

The authors are grateful to Professor S. E. Friberg for helpful comments, to Mr. R. A. Stanton for experimental assistance, and to Mrs. L. M. Baldwin for typing the manuscript.

Literature Cited

1. Cox, J. M.; Friberg, S. E. J. Amer. Oil Chemists' Soc. 1981, 58, 743.
2. Flaim, T.; Friberg, S. E.; Force, C. G.; Bell, A. Tenside Detergents 1983, 20, 177.
3. Coll, H. J. Phys. Chem. 1970, 74, 520.
4. Attwood, D.; Elworthy, P. H.; Keyne, S. B. J. Phys. Chem. 1970, 74, 3529.
5. Birdi, K. S. Kolloid Z. u. Z. Polymere 1972, 250, 731.
6. Birdi, K. S. In "Proceedings of the International Conference on Colloid and Surface Science", Wolfram, E., Ed.; Academic Kado: Budapest, 1976; p.473.
7. Birdi, K. S.; Backlund, S.; Sorensen, K.; Krag, T.; Dalsager; S. J. Colloid Interface Sci. 1980, 76, 2035.
8. Birdi, K. S.; Dalsager, S.; Backlund, S. J. Chem. Soc. Faraday I 1980, 76, 2035.
9. Ward, B. F, Jr.; Force, C. G.; Bills, A. M.; Woodward, F. E. J. Amer. Oil Chemists' Soc. 1975, 52, 219.
10. "DIACID^R Surfactants"; Westvaco Chemical Division: Charleston Heights, S. C., 1981.
11. Lianos, P.; Zana, R. J. Colloid Interface Sci. 1981, 84, 100.
12. Kratochvil, J. P.; Hsu, W. P.; Jacobs, M. A.; Aminabhavi, T. M.; Mukunoki, Y. Colloid & Polymer Sci. 1983, 261, 781.
13. Billmeyer, F. W., Jr. "Textbook of Polymer Science", 2nd ed.; Wiley-Interscience: New York, 1971; pp.72-73.

14. Holland, P. R., paper presented at this Symposium.
Funasaki, N.; Hada, S. J. Phys. Chem. 1979, 83, 2471.
15. Small, D. M. In "The Bile Acids"; Nair, P. P.; Kritchevsky, D., Eds.; Plenum Press: New York, 1971; Vol. I, Chap. 8.
16. Carey, M. C.; Small, D. M. Am. J. Med. 1970, 45, 590.
17. Pethica, B. A.; Pallas, N. R.; Bell, A., unpublished data.
18. Mazer, N. A.; Benedek, G. B.; Carey, M. C. Biochemistry 1980, 19, 601.
19. Zimmerer, R. O., Jr.; Lindenbaum, S. J. Pharm. Sci. 1979, 68, 581.
20. Mino, J.; Matijevic, E.; Meites, L. J. Colloid Interface Sci. 1977, 60, 148.
21. Flaim, T.; Friberg, S. E., paper presented at this Symposium.

RECEIVED February 3, 1984

Interaction of Long Chain Dimethylamine Oxide with Sodium Dodecyl Sulfate in Water

DAVID L. CHANG and HENRI L. ROSANO

Department of Chemistry, City College, City University of New York, New York, NY 10031

Lauryl, myristyl, cetyl and stearyl-dimethylamine oxide (LDAO) aqueous solutions alone and in combination with sodium dodecyl sulfate (SDS) have been investigated by surface tension, viscosity and pH measurements. 1) LDAO solutions: At any particular pH, the amine oxide is in equilibrium with its protonated form. The viscosity of the solution depends strongly on the degree of ionization (β) and maximum viscosity was observed when $\beta = 0.5$, due to the formation of elongated structure. 2) LDAO/SDS solutions: Progressive addition of SDS to dodecyl or myristyl DAO results in pH and viscosity increases, both values reach their maximum values at a 3:1 LDAO/SDS molar ratio. However, the change in pH remains constant over a wide range of molar ratios, while the viscosity value depends strongly on that ratio. The viscous mixture is non-Newtonian in nature, and exhibits liquid crystalline behaviour. In the case of cetyl- and stearyl-DAO/SDS mixtures, solutions are turbid with low viscosity. This difference in behaviour is attributed, in part, to the compatibility in chain length of the LDAO and SDS.

Binary mixtures of surfactant solutions have been studied extensively (1-5). Such mixtures can exhibit appreciable surface and bulk synergistic effects. In general, cationic/anionic surfactant mixtures produce the largest effects. Surface activity related synergistic phenomena are of technological and marketing interests (6). In the present study, the interaction between a long chain dimethylamine oxide (LDAO) and sodium dodecyl sulfate (SDS) in aqueous solution has been investigated.

The aggregation characteristics of LDAO in aqueous solutions (7-12) and their interaction with anionic surfactants

0097-6156/84/0253-0129\$06.00/0
© 1984 American Chemical Society

(1,2,13) have been studied previously. Goddard and Kung (14) have investigated the monolayer properties of docosyldimethyl amine oxide. LDAO, a weak base having about the same basicity as the acetate anion (15), can exist in both nonionic and cationic form depending upon the pH of the solution. At any particular pH, an equilibrium is established between the cationic and nonionic form, viz.,



According to Kolp et al. (1), K_a , the monomeric equilibrium constant has been determined by potentiometric titration to be

$$K_a = \frac{[\text{H}^+][\text{LDAO}]}{[\text{LDAOH}^+]} = 10^{-4.9} \quad [2]$$

where the quantities in brackets are the activities of the indicated species relative to a standard state such that, at infinite dilution, the activity equals the molar concentration.

Tokiwa and Ohki (10) have shown that 1) the K_a value of the micellized LDAO is different from the molecular form, viz., $10^{-5.9}$ 2) while the values of K_a are independent of the degree of protonation (β) below the critical micelle concentration (CMC), they are dependent on β at concentrations above the CMC. These authors did not explain why the micellar pK_a (5.9) at $\beta = 0$ is different from the molecular value ($pK_a = 4.9$).

Difference between micellar and molecular pK_a 's has been reported for other systems (16,17), however, no explanations were provided. Recently, Mille (18) has concluded from a theoretical approach that for the case of LDAO, assuming only a charge-charge interaction in the nearest-neighbor model can not explain the difference in pK_a 's satisfactorily and that additional attractive interaction must be included, suggesting possible hydrogen bonding formation.

EXPERIMENTAL

Long chain dimethylamine oxides with alkyl chain length = 12, 14, 16, 18 carbons (Onyx Chem. Co., Jersey City, N.J.) and laboratory grade sodium dodecyl sulfate (Fisher Chem. Co., Fairlawn, N.J.) were used without further purification.

For the titration of LDAO, solutions were made with their pH adjusted to 12 with NaOH and titrated with HCl. Binary mixtures of LDAO and SDS solutions were prepared by mixing different volumes of the surfactant solutions at equal molar concentration.

pH Measurement. For amine oxide titration, pH was monitored with an Orion Research Ionalyzer (Model 801 A, Orion Res. Inc., Cambridge, Mass.). All other pH measurements were made with a Photovolt pH meter (Photovolt Corp., New York, N.Y.).

Surface Tension Measurement. Surface tension was determined with a Rosano Tensiometer (Arenberg-Sage Inc., Jamaica Plain, Mass.) utilizing a sand-blasted platinum blade.

Viscosity Measurement. A Brookfield Viscometer (Model LVT, Brookfield Engineering Lab., Inc., Stoughton, Mass.) was employed for the measurement of relative viscosity.

Electrical Resistance and Percent Light Transmittance. Low frequency electrical resistance measurements were made on a conductivity bridge (Model RC-18, Industrial Instrument, Cedar Grove, N.J.) at a line frequency of 1 KC. Beckman conductivity cell with cell constant 1.0 cm^{-1} was used. The percent transmission was also monitored for each of the mixtures at 490 nm (Spectronic 20, Bausch & Lomb Co., Rochester, N.Y.).

Wettability Test of Glass Surface. Glass surface in water is negatively charged. When the corner of a cleaned and water covered microscope cover slide touches the surface of a solution containing cationic surfactant just below its CMC, instantaneous dewetting occurs; the positive charge of the surfactant interacts electrostatically with the negative charge of the glass surface, the solid surface is then covered by a thin layer of the surfactant molecules with their hydrophobic tails pointing outward and the surface is no longer wettable. This effect is not observed with anionic and nonionic surfactant solutions.

In addition, viscoelasticity of solution was determined qualitatively by the simple method of swirling a vial containing the solution and observe the recoiling of air bubbles entrapped in the solution (19).

RESULTS

Titration of LDAO. Fig. 1 represents the titration curves of C_{14}DAO at 0.2 M, $8 \times 10^{-4}\text{M}$, and $4 \times 10^{-5}\text{M}$ concentration and $3\text{C}_{14}\text{DAO}/1\text{SDS}$ mixture at 0.2 M total concentration with HCl at 25°C . For comparison, the four curves are plotted on a same HCl equivalent scale.

The CMC of C_{14}DAO is about $1 \times 10^{-3}\text{M}$ at 25°C . Below the CMC a typical buffering action is observed ($4 \times 10^{-5}\text{M}$), above the CMC the titration curves are slanted toward lower pH's with increasing HCl concentration; 0.2 M having a steeper slope than $8 \times 10^{-3}\text{M}$. Addition of SDS to a solution of C_{14}DAO affects the HCl titration curve markedly and will be discussed later.

Also plotted is the viscosity variation with HCl added for 0.2 M C_{14}DAO . Maximum viscosity is observed when half of the amine oxide molecules are in the cationic form. However, in the absence of NaOH the change in viscosity with HCl added is

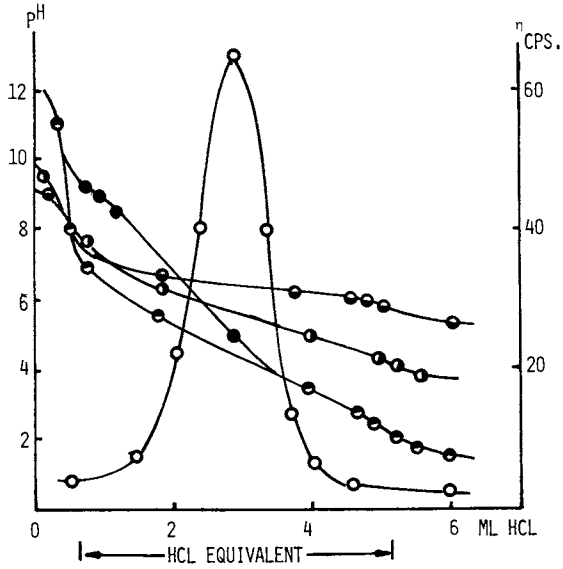


Figure 1.

Titration curves of C_{14} DAO @ 0.2M, \ominus ; 8×10^{-4} M, \bullet ; 4×10^{-5} M, \bullet and $3C_{14}$ DAO/1SDS mixture @ 0.2M, \bullet .

Relative viscosity (η : \circ) vs. ml HCl added is also plotted for C_{14} DAO @ 0.2M.

much less pronounced (by about an order of magnitude). C_{12} DAO gives similar results. The fact that an increase in viscosity of the solution is observed in the vicinity of a 1:1 molar ratio of the nonionic form to the cationic form of the LDAO is similar to that observed in an acid-soap (20).

LDAO-SDS Interactions. Mixtures of C_{12}^- or C_{14} -DAO with SDS show a surface tension minimum at an 1:1 molar ratio, as shown on Fig. 2 for C_{14} DAO. Also shown is the variation in pH for different mixing ratios. The increase in pH of the mixed solution seems to indicate that the addition of SDS to a LDAO solution favor the protonation of the amine oxide, water being the proton donor. This point will be discussed more fully below. The change in viscosity of the mixture at different compositions is plotted in Fig. 2 as well, the maximum of which corresponds to a $3C_{14}$ DAO/ISDS association. Similar behavior is observed for C_{12} DAO/SDS mixtures.

Minimum surface tension at a 1:1 cationic/anionic ratio has been observed in the system containing SDS and dodecyltrimethyl ammonium bromide (3). In addition, 1:1 association has been observed for C_{12} DAO with long-chain sulfonates (1,2). The latter two cases, hydrogen bonding between the protonated amine oxide and the anionic sulfonate has been shown to exist in the solid salt. The salt may separate out in crystalline form, as reported in (1,2,20), but no precipitation is observed in this work when the pH of the solution is kept above 9.

Figs. 3 and 4 show the interaction between C_{16} DAO and C_{18} DAO with SDS respectively. For LDAO/SDS ratio greater than 1, these mixed solutions are turbid and birefringent; addition of SDS results in production of filament-like structures. When the molar amount of SDS is equal to or greater than that of the LDAO, the solutions become isotropic and clear. AT 3:1 LDAO/SDS molar composition, the change in pH reaches its maximum value. Minimum surface tension is reached when the LDAO content is still in excess, unlike the cases of C_{12}^- and C_{14} -DAO. This observation indicates that the surface of the solution has already been saturated with a mixed molecule formed between C_{16}^- or C_{18} -DAO and SDS, although the bulk concentrations of the individual species are different, and that the composition of the bulk must be the same throughout the low surface tension region. Enhancement in viscosity is still observed with C_{16} DAO. However, C_{18} DAO shows a rapid decrease in viscosity upon mixing with SDS, the value of which reaches that of the SDS solution at equal molar composition.

The 3:1 C_{12}^- or C_{14} -DAO/SDS mixture exhibits non-Newtonian fluid characteristics; its viscosity decreases with increased shear rate. At high pH (~ 12), the mixture is still non-Newtonian and its viscosity is enhanced by about an order of magnitude (at high shear rate) to two orders of magnitude (at low shear rate) compared to the values at its natural pH (~ 10). The

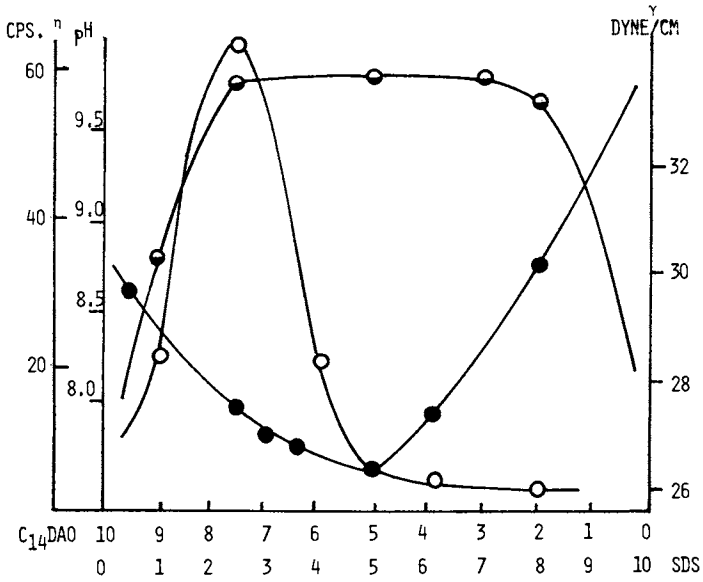


Figure 2.

Relative viscosity (η :○), surface tension (γ :●) and pH (●) variations at different $C_{14}DAO/SDS$, molar ratios. The total concentration equals 0.5M.

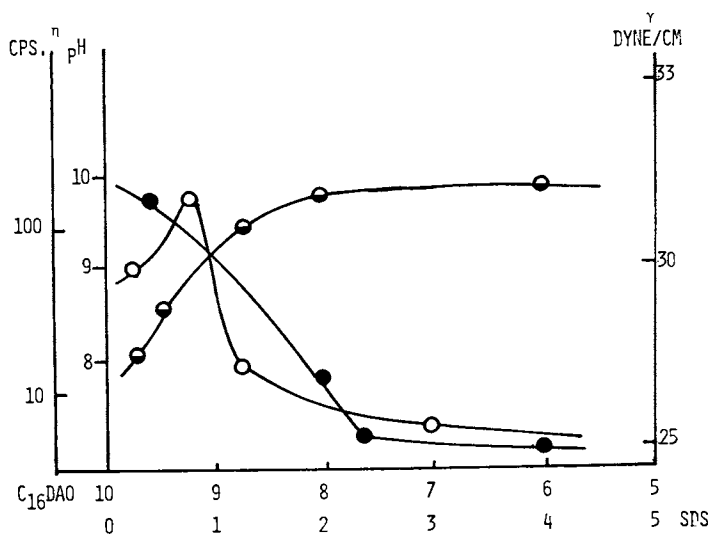


Figure 3.

Relative viscosity (η :○), surface tension (γ :●) and pH (◐) variations at different $C_{16}DAO/SDS$ molar ratios. The total concentration equals 0.05M.

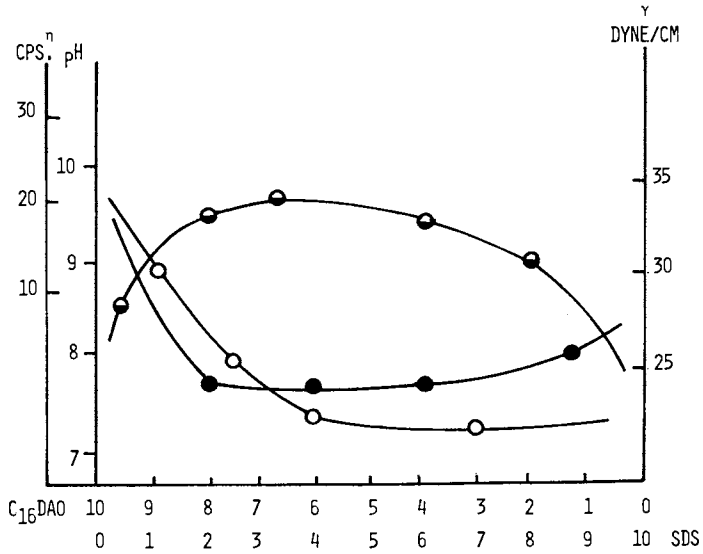


Figure 4.

Relative viscosity (η :○), surface tension (γ :●) and pH (◐) variations at different $C_{18}DAO/SDS$ molar ratios.

The total concentration equals 0.005M.

solution exhibits birefringency when the solution is shaken. Upon cooling, the solution becomes milky, indicating possible crystal formation, and this behavior is reversible when the temperature is raised. These observations suggest that the mixed solution can probably be categorized as liquid crystal. Below pH 9, precipitation occurs. Analysis of the ir, nmr and mass spectra of the precipitate reveals that its composition is $\text{CH}_3(\text{CH}_2)_{13}\text{N}(\text{CH}_3)_2\text{OH O}_3\text{SO}(\text{CH}_2)_{11}\text{CH}_3$, with the proton of the cationic amine oxide involved in hydrogen bonding with the sulfonate anion.

The 3:1 LDAO/SDS mixture becomes viscoelastic and rheopectic when a small amount of NaCl is added. Its viscosity shows a reversible increase with time of shearing at constant shear rate. The rheopectic behavior is probably due to long thread-like micelles that are aligned parallel to the flow in weakly bound clusters, as in the case of cetyltrimethyl ammonium bromide and monosubstituted phenol mixed solutions (21).

DISCUSSION

Titration of LDAO. When hydrogen ions are added to a LDAO solution at high pH, the excess hydroxide ions are neutralized first. Then two reactions occur: protonation of the monomer, and protonation of the micelle. The former is probably more favored; the buffering-action region for concentrations below the CMC occurs at a higher pH value than for concentrations above the CMC. Tokiwa and Ohki (10) have shown that for C_{12}DAO , the $\text{pK}_{\text{micelle}}$ decreases from 5.95 to about 4 with increasing degree of protonation (β), implying that the micelle is even less favored as a proton acceptor compared to its monomer (which has a $\text{pK} = 4.95$) with diminishing nonionic character. They calculated the surface potential of C_{12}DAO micelles as a function of β and found an increase from 0 to +120 mV as β is varied from 0 to 1. These authors concluded that the micelles were becoming more and more positively charged. The light-scattering data obtained by Ikeda et al. (12) suggest the formation of large rod-like micelles of C_{12}DAO at $\beta = 0.5$ in the presence of NaCl, while at high and low pH's, the micelles are small and probably spherical. There is a spherical \rightarrow elongated \rightarrow spherical transition of the amine oxide micelles as β is varied from 0 to 0.5 and then to 1. As has been pointed out by Nagarajan and Ruckenstein (22), transition from spherical to cylindrical micelle is favored by factors which contribute to an increase in the attractive component or a decrease in the repulsive component of the free energy of micellization. In the case of ionized amine oxide, the ionizable proton is capable of hydrogen bonding to the neighboring oxygen thereby decreasing the average distance between adjacent head groups effectively. As a result, the tail groups have to readjust spatially thus leading to a breakage of the spheroid. In addition, protona-

tion of the monomer can also lead to a breakage of the spheroid if the assumption is made that the concentration of the monomer remains constant above the CMC (23). Both mechanisms contribute to the production of elongated structure.

From the study of monolayer properties of a long chain (C_{22}) amine oxide, Goddard and Kung (14) have found that above pH 7.5 of the aqueous substrate, the monolayer is quite expanded, ($55 \text{ \AA}^2/\text{molecule}$ at 10 dyne/cm surface pressure), while the area per molecule equals 33 \AA^2 for the same surface pressure at pH = 4.8; LDAO yields a less expanded film when some of the molecules are ionized than when they are all nonionic. They remarked that the quaternary ammonium group in protonated amine oxide is unusual in possessing a hydroxy group; the strong electron-attracting, positively charged nitrogen substantially augments the polarization of this OH group.

With increased proton character, the H^+ has a tendency to hydrogen bond. Below pH 7.5, the appearance of the cationic form has a marked condensing effect in association with unionized amine oxide and results in the production of elongated structures replacing progressively the small and spherical micelles of LDAO in the nonionic form. Below pH 4.5, the elongated structures are progressively converted into low viscosity, small spherical micelles made of LDAOH.

The present results also show that there is a discrepancy between the monomeric pK_a values found in this work and the previous studies; ours being higher (6.6 vs 4.9, respectively). The cause of this is believed to be due to the presence of bicarbonate ions in the solution (27).

LDAO/SDS Interaction. Mixing of cationic and anionic surfactant solutions results in the formation of a mixed species that is more surface active than the individual species. The enhanced synergistic effect has been explained (2,3) by showing that a close-packed adsorption of electroneutral R^+R^- takes place (R^+ and R^- represent the long chain cation and anion respectively). In the case of C_{12} - and C_{14} -DAO, a 1:1 LDAO/SDS molar ratio produces a minimum in surface tension and is accompanied by an increase in pH in the bulk solution; the association seems to be of the type R^+R^- , and the absence of visible precipitate may be attributed to the solubilization of the R^+R^- complex in the solution. In the region where LDAO is in excess, the structure is probably [cationic (LDAOH⁺) anionic (SDS)] nonionic (LDAO), while [cationic (LDAOH⁺) anionic (SDS)] anionic (SDS) is formed when SDS is in excess. Equal molar concentration results in cationic (LDAOH⁺) anionic (SDS) complex which should favor precipitation. However, at pH >9, there is no indication of precipitation (even when the total solute concentration is 0.35 M). When the pH is below 9, then precipitation will take place.

Another possibility is the interaction between neutral LDAO

and SDS with adsorption of H_3O^+ ions on the aggregate surface. This type of combination not only explains an increase in the pH but also explains the absence of precipitation for any given mixing ratio in the concentration range studied. This interpretation is supported by the titration behavior of, for example, a 3:1 LDAO/SDS mixture (see Fig. 1) above pH 12 addition of HCl neutralizes the OH^- ions in the bulk, when more H^+ ions are added, the concentration of H^+ ions increases until surface neutralization occurs below pH 10, and below pH 9 precipitation of the 1:1 $LDAOH^+$ /SDS complex takes place. Since the LDAO is in excess, below pH 7 when all the SDS molecules have been reacted, protonation of LDAO occurs, reminiscent of the titration of pure LDAO solution.

Another feature of surfactant-water systems is that they can also aggregate into lyotropic liquid crystalline phases when intermicellar interactions are significant. Typically, non-Newtonian behavior is usually found for these liquid crystalline phases. For the 3LDAO/ISDS mixed system, all evidence suggests that they do form liquid crystalline phase.

The difference in properties when the aliphatic chain of amine oxide contains more than 14 carbons is attributed to the mismatch of the hydrophobic chain with that of the SDS. The extra terminal segment results in a disruptive effect on the packing of the surface active molecules. The observed association behavior in the case of C_{12} - or C_{14} -DAO with SDS is then also due to the maximum cohesive interaction between hydrocarbon chains in addition to the reduced electrostatic repulsion in the head groups. Solubilization of the 1:1 association is also determined by this chain length compatibility effect which may contribute to the absence of visible precipitation in C_{12}/C_{12} and C_{12}/C_{14} mixtures. Chain length compatibility effects in different systems have been discussed by other investigators (24,25,26).

Acknowledgments

The authors are grateful to Dr. M. Aronson and Dr. E. D. Goddard for helpful discussions. D. L. C. also wishes to thank Lever Brothers Company and the Gillette Corporation for their financial support.

Literature Cited

1. Kolp, D. G.; Laughlin, R. G.; Krause, R. P.; Zimmere, R. E. J. Phys. Chem. 1963, **67**, 51.
2. Rosen, M. J.; Friedman, D.; Gross, M. J. Phys. Chem. 1964, **68**, 3219.
3. Lucassen-Reynders, E. H.; Lucassen, J.; Giles, D. J. Colloid Interface Sci. 1982, **81**, 150.

4. Al-Saden, A. A.; Florence, A. T.; Whateley, T. L.; Puisieux, F.; Vaution, C. J. Colloid Interface Sci. 1982, 86, 51.
5. Hua, X. Y.; Rosen, M. J. J. Colloid Interface Sci. 1982, 90, 212.
6. Rosano, H. L.; U.S. Patent Application 473078 07, 1983.
7. Herrmann, K. W. J. Phys. Chem. 1962, 66, 295.
8. Ibid., 1964, 68, 1540.
9. Benjamin, L. J. Phys. Chem. 1964, 68, 3575.
10. Tokiwa, F.; Ohki, K. J. Phys. Chem. 1966, 70, 3437.
11. Ikeda, S.; Tsunoda, M. A.; Maeda, H. J. Colloid Interface Sci. 1978, 67, 336.
12. Ibid., 1979, 70, 448.
13. Tokiwa, F.; Ohki, K. J. Colloid Interface Sci. 1968, 27, 247.
14. Goddard, E. D.; Kung, H. C. J. Colloid Interface Sci. 1973, 43, 511.
15. Nylen, P. Z. Anor. Allgem. Chem. 1941, 246, 227.
16. Tokiwa, F.; Ohki, K. J. Phys. Chem. 1967, 71, 1824.
17. Corkill, J. M.; Gemmel, K. W.; Goodman, J. F.; Walker, T. Trans. Faraday Soc. I. 1970, 66, 1817.
18. Mille, M. J. Colloid Interface Sci. 1981, 81, 169.
19. Gravsholt, S. J. Colloid Interface Sci. 1976, 57, 575.
20. Rosano, H. L.; Brendel, K.; Schulman, J. H.; Eydt, A. J. J. Colloid Interface Sci. 1966, 22, 58.
21. Hyde, A. J.; Maguire, D. J.; Stevenson, D. M. Proc. Vith Intern. Congr. Surface Active Substances, Zurich, 1972, Vol. II(2).
22. Nagarajan, R.; Ruckenstein, E. J. Colloid Interface Sci. 1979, 71, 580.
23. Hutchinson, E.; Sheaffer, V. E.; Tokiwa, F. J. Phys. Chem. 1964, 68, 2818.
24. Schick, M. J.; Fowkes, F. M. J. Phys. Chem. 1957, 61, 1062.
25. Fort, T., Jr. J. Phys. Chem. 1962, 66, 1136.
26. Cameron, A.; Crouch, R. F. Nature (London) 1936, 198, 475.
27. Chang, D. C.; Rosano, H. L., to be published.

RECEIVED February 3, 1984

Effects of Surfactant Structure on the Thermodynamics of Mixed Micellization

PAUL M. HOLLAND

Miami Valley Laboratories, The Procter & Gamble Company, Cincinnati, OH 45247

Calorimetric measurements are used to examine interactions between different surfactant components in nonideal mixed micelles and assess the effects of surfactant structure on the thermodynamics of mixed micellization. Results for some anionic/nonionic surfactant mixtures show that variations in surfactant structure can have important effects on heats of mixing in the micelles and significantly influence the critical micelle concentration (cmc) of the mixed surfactant systems. Here, both the heats of mixing and deviations of the cmc from ideality are smaller for alkyl ethoxylate sulfates than alkyl sulfates when mixed with alkyl ethoxylate nonionics. The calorimetric results for these systems are also used to examine the appropriateness of the regular solution approximation used in pseudo-phase separation models for treating mixed micellization. The failure of the regular solution approximation to account for the observed heats of mixing in these systems suggests that the net interaction parameter of the nonideal mixed micelle models be interpreted as an excess free energy parameter in such cases.

The formation of mixed micelles in surfactant solutions which contain two or more surfactant components can be significantly affected by the structures of the surfactants involved. The observed critical micelle concentration (cmc) is often significantly lower than would be expected based on the cmc's of the pure surfactants. This clearly demonstrates that interactions between different surfactant components in the mixed micelles are taking place.

0097-6156/84/0253-0141\$06.00/0
© 1984 American Chemical Society

Nonideal mixed micelle models based on the pseudo-phase separation approach and a regular solution approximation have been developed (1-4) to describe this behavior. Here, the details of micellar structure are ignored and the interactions between two different surfactant components are accounted for by a single generalized parameter which represents an excess heat of mixing. This approach has been successfully applied (2,3,5) to a considerable variety of binary nonideal surfactant mixtures including mixed nonionic and ionic surfactants even though the model neglects effects due to the bonding of counterions. In the description of nonideal mixed ternary surfactant systems (3) no adjustable parameters beyond those for the binary mixtures are required to obtain good results. Together these results show that the net interaction parameters (β) obtained for binary surfactant mixtures can provide a useful measure of nonideal mixing in micelles. However, it is not as clear how well this approach (using the regular solution approximation) actually reflects the thermodynamics of mixed micellization.

Calorimetric measurements represent a promising way of gaining thermodynamic information about mixed micellization. Of the possible types of measurements, heats of micellar mixing obtained from the mixing of pure surfactant solutions are perhaps of the greatest interest. Also of interest is the titration (dilution) of mixed micellar solutions to obtain mixed cmc's. While calorimetric measurements have been applied in studies of pure surfactants (6,7) and their interaction with polymers (8), to our knowledge, applications of calorimetry to problems of nonideal mixed micellization have not been previously reported in the literature.

Among the purposes of this paper is to report the results of calorimetric measurements of the heats of micellar mixing in some nonideal surfactant systems. Here, attention is focused on interactions of alkyl ethoxylate nonionics with alkyl sulfate and alkyl ethoxylate sulfate surfactants. The use of calorimetry as an alternative technique for the determination of the cmc's of mixed surfactant systems is also demonstrated. Besides providing a direct measurement of the effect of the surfactant structure on the heats of micellar mixing, calorimetric results can also be compared with nonideal mixing theory. This allows the appropriateness of the regular solution approximation used in models of mixed micellization to be assessed.

Theory

The derivation of a pseudo-phase separation model for treating nonideal mixed micellization is given in detail in reference 3. This leads to the generalized result

$$\frac{1}{C^*} = \sum_{i=1}^n \frac{\alpha_i}{f_i C_i} \quad (1)$$

which can be used to relate the mixed cmc (C^*) of a nonideal surfactant system to the activity coefficients (f_i) of the surfactant components in the mixed micelles, their mole fractions (α_i) and pure cmc's (C_i). In the case where the activity coefficients equal unity this expression reduces in form to that previously derived for ideal mixed micelles (1,9).

Consideration of the thermodynamics of nonideal mixing provides a way to determine the appropriate form for the activity coefficients and establish a relationship between the measured enthalpies of mixing and the regular solution approximation. For example, the excess free energy of mixing for a binary mixture can be written as

$$G^E = RT(x_1 \ln f_1 + (1 - x_1) \ln f_2) \quad (2)$$

Taking the partial derivative with respect to the mole fractions in the micelle (x_i) and using the Gibbs-Duhem relation to eliminate some of the resulting terms gives

$$\left(\frac{\partial G^E}{\partial x_1} \right)_{T,P} = RT (\ln f_1 - \ln f_2) \quad (3)$$

Combining these relationships then allows the activity coefficients to be expressed in terms of the excess free energy of mixing

$$\ln f_1 = \frac{1}{RT} \left(G^E + (1 - x_1) \frac{\partial G^E}{\partial x_1} \right) \quad (4)$$

$$\ln f_2 = \frac{1}{RT} \left(G^E - x_1 \frac{\partial G^E}{\partial x_1} \right) \quad (5)$$

The regular solution approximation is introduced by assuming (by definition) that the excess entropy of mixing is zero. This requires that the excess free energy equal the excess enthalpy of mixing. For binary mixtures the excess enthalpy of mixing is ordinarily represented by a function of the form

$$H^E = \beta x_1(1 - x_1)RT \quad (6)$$

where β times RT represents a difference in interaction energy between the mixed and unmixed systems. This corresponds to the leading term in the lattice model description of liquid mixtures (10). When this expression is substituted for G^E in equations 4 and 5 the resulting binary activity coefficients (in the regular solution approximation) take the form

$$f_1 = \exp \beta (1 - x_1)^2 \quad (7)$$

$$f_2 = \exp \beta x_1^2 \quad (8)$$

with β providing a measure of the nonideality of mixing in the system.

The β parameters in the above expressions are determined from the experimental mixed cmc's of binary systems. This requires solving iteratively for x_1 (at the cmc) using a relationship such as

$$x_1^2 \ln \left[\frac{\alpha_1 C^*}{x_1 C_1} \right] = (1 - x_1)^2 \ln \left[\frac{\alpha_2 C^*}{(1-x_1) C_2} \right] \quad (9)$$

followed by substitution into the expression

$$\beta = \frac{\ln \left[\frac{\alpha_1 C^*}{x_1 C_1} \right]}{(1 - x_1)^2} \quad (10)$$

While this treatment is strictly developed for nonionic surfactant mixtures it can often be applied empirically to mixtures containing ionic surfactants with success. Some examples of the types of surfactant mixtures to which this model has been successfully applied and the corresponding β parameters are given in Table I. It is readily seen that negative values are typically seen for deviation from ideal behavior. These would correspond to exothermic heats of mixing in the micelles. Assuming the validity of the regular solution approximation, it should then be possible to directly relate heats of mixing in the micelles (as a function of mole fraction) to the value of the β parameter via equation 6.

Table I. Values of the Net Interaction Parameter β for Some Binary Surfactant Mixtures (from Ref. 3)

β	Binary Mixture	Conditions
-3.7	$C_{10}(\text{CH}_3)_2\text{PO}/C_{12}\text{OSO}_3 \cdot \text{Na}^+$	1mM Na_2CO_3 (24°C)
-2.4	$C_{10}(\text{CH}_3)\text{SO}/C_{12}\text{OSO}_3^- \cdot \text{Na}^+$	" " "
0	$C_{10}(\text{CH}_3)_2\text{PO}/C_{10}(\text{CH}_3)\text{SO}$	" " "
-4.4	$C_{12}(\text{CH}_3)_2\text{NO}/C_{12}\text{OSO}_3^- \cdot \text{Na}^+$	0.5mM Na_2CO_3 (23°C)
-3.6	$C_{10}(\text{OCH}_2\text{CH}_2)_4\text{OH}/C_{12}\text{OSO}_3^- \cdot \text{Na}^+$	" " "
-0.8	$C_{12}(\text{CH}_3)_2\text{NO}/C_{10}(\text{OCH}_2\text{CH}_2)_4\text{OH}$	" " "
-13.2	$C_{10}\text{N}^+(\text{CH}_3)_3 \cdot \text{Br}^-/C_{10}\text{OSO}_3^- \cdot \text{Na}^+$.05M NaBr (23°C)
-4.1	$C_8(\text{OCH}_2\text{CH}_2)_4\text{OH}/C_{10}\text{OSO}_3^- \cdot \text{Na}^+$	" " "
-1.8	$C_{10}\text{N}^+(\text{CH}_3)_3 \cdot \text{Br}^-/C_8(\text{OCH}_2\text{CH}_2)_4\text{OH}$	" " "

Experimental Section

Isoperibol calorimetric measurements were carried out using a Tronac, Inc. Model 550 Calorimeter interfaced with a digital voltmeter and micro-computer for data acquisition. In these experiments a Dewar flask reaction vessel was stirred at a constant rate while immersed in a constant temperature bath (at 25°C) with mixing initiated by either injection or titration of another solution held at bath temperature into the vessel. The experiments were initiated when the bath and reaction vessel temperatures were equal and the changes in temperature were monitored by a thermistor referenced to the bath. A slightly modified version of a software package developed by Grime et al. (11) was used for data acquisition and reduction (i.e., correction for stirring heat, etc.). The compounds used in this study were pure single specie surfactants determined to be greater than 98% purity by thin-layer or gas chromatography.

Heats of mixing for micellar solutions were determined by mixing various ratios of pure equimolar surfactant solutions by injection. These measurements were carried out for pentaoxyethylene glycol monodecyl ether (C₁₀E₅) with sodium dodecyl sulfate (SDS), sodium dodecyl dioxyethylene sulfate (C₁₂E₂S) and sodium decyl pentaoxyethylene sulfate (C₁₀E₅S), respectively at 25°C. In order to subtract out effects due to additional micellization of pure surfactant monomers on mixing, the experiments were carried out at two concentrations above the cmc (.02M and .08M) and the difference in the results taken. Under these conditions the composition of the mixed micelles and solution should be approximately equal since the concentrations are on the order of 20 to 100 times the mixed cmc in each case. The final differenced results should then correspond to the mixing of pure micelles to form mixed micelles, and therefore to good approximation, to the excess heats of micellar mixing as a function of mole fraction.

The mixed cmc's of micellar solutions of tetraoxyethylene glycol mono-octyl ether (C₈E₄) with SDS and C₁₂E₂S, respectively were also determined by calorimetry. Mixtures with C₈E₄ were chosen due to the higher cmc and consequent larger and more adequate total enthalpies of demicellization compared to mixtures with C₁₀E₅. The measurements were carried out by the titration (dilution) of mixed surfactant solutions with varying ratios of components and .12M total concentration into distilled water. Under these conditions the heat of demicellization is observed as a function of titrant added, with a sharp break occurring once the cmc is reached in the reaction vessel. Values for the cmc endpoint were taken from the intersection of least squares fits of line segments immediately before and after the break in the titration results (corrected for stirring heat and volume changes). Cmc's were determined for the pure surfactants in a similar manner except for that of SDS. Here, the heat of

micellization is quite small and dilution effects are significant making an accurate determination of the cmc by calorimetry difficult. Therefore the cmc of SDS in distilled water was determined by surface tension measurements using a tensiometer with du Nouy ring, as in previous work (3).

Results and Discussion

Results from the heats of micellar mixing experiments are shown in Figure 1. Here, the heat of mixing per mole (after differencing to correct for monomer contributions) is plotted versus the mole fraction of $C_{10}E_5$ in the mixed micellar system. It is clearly seen that the interaction of SDS with $C_{10}E_5$ is significantly stronger than that of the alkyl ethoxylate sulfate surfactants with $C_{10}E_5$. In addition, the symmetry in the heat of mixing curves is strikingly different with those for $C_{12}E_2S$ and $C_{10}E_5S$ showing an asymmetric maximum at about a 1:2 mole ratio with $C_{10}E_5$, while the SDS results are symmetric about a 1:1 ratio. These observations clearly demonstrate that the presence of ethoxylation in the structure of the sulfate surfactants has a pronounced effect on their heats of mixing.

Titration results for the mixed cmc's of the SDS/ C_8E_4 and $C_{12}E_2S/C_8E_4$ systems as a function of their relative mole fraction in solution are shown in Figures 2 and 3, respectively. Here, the experimentally determined points are compared with calculated results from the nonideal mixed micelle model (solid line) and the ideal mixed micelle model (dashed line). Good agreement with the nonideal model is seen in each case. Figure 2 shows that the binary SDS/ C_8E_4 system deviates significantly from ideality with a β value of -3.3. This result is comparable to the parameters found for other alkyl sulfate/alkylethoxylate nonionic systems (see Table I). In the case of the $C_{12}E_2S/C_8E_4$ system (see Figure 3) a significantly smaller deviation from ideality is observed, giving a value of -1.6 for β . This seems to be consistent with the smaller heats of mixing observed for $C_{12}E_2S$ compared to SDS in Figure 1.

Together these results show that the nonideal behavior of sulfate surfactants can be significantly affected by the presence or absence of ethoxylation in their structures. Here, both the heats of mixing and deviations of the cmc from ideality are smaller for alkyl ethoxylate sulfates than alkyl sulfates when mixed with alkyl ethoxylate nonionics. This is presumably due to improved screening or separation of charge in pure alkyl ethoxylate sulfate micelles compared to alkyl sulfate micelles. This interpretation would be compatible with the "charge separation" effect previously used in explaining the mixed cmc data of unethoxylated sulfate/alkyl ethoxylate nonionic surfactant mixtures (5,12). The surprising differences

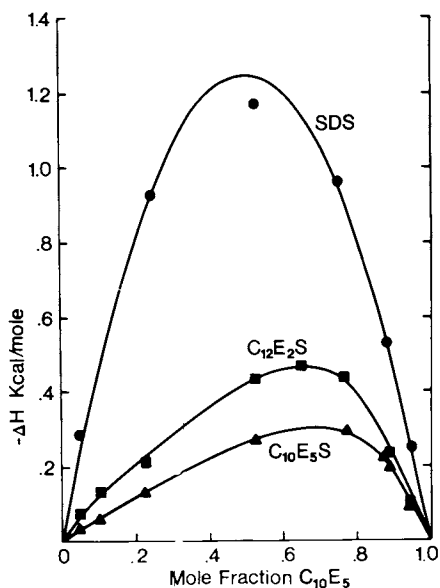


Figure 1. Heats of micellar mixing after correction for monomer contributions (see text) as a function of composition for SDS, $C_{12}E_2S$ and $C_{10}E_5S$ with $C_{10}E_5$ (at 25°C).

American Chemical
Society Library

1155 16th St. N. W.

In Structure/Performance Relationships in Surfactants; Rosen, M.;
ACS Symposium Series; American Chemical Society: Washington, DC, 1984.

Washington, D. C. 20036

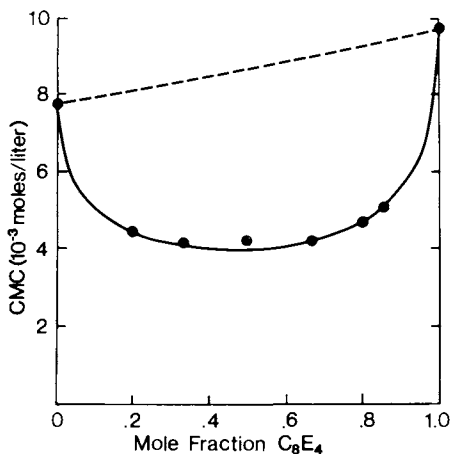


Figure 2. Cmc's of mixtures of SDS and C_8E_4 in distilled water (at 25°C). The plotted points are experimental data, the solid line is the result for the nonideal mixed micelle model with $\beta = -3.3$, and the dashed line is the result for ideal mixing.

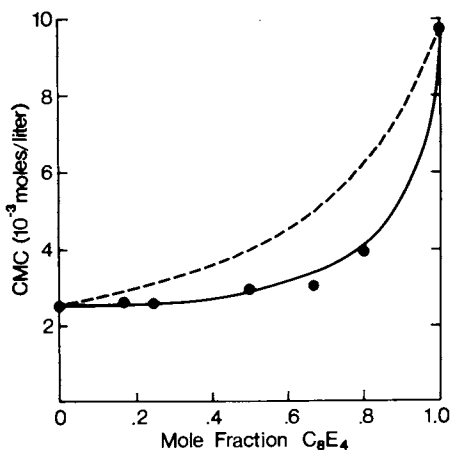


Figure 3. Cmc's of mixtures $C_{12}E_2OSO_3^-.Na^+$ and C_8E_4 in distilled water (at 25°C). The plotted points are experimental data, the solid line is the result for the nonideal mixed micelle model with $\beta = -1.6$, and the dashed line is the result for ideal mixing.

observed in the symmetry of the micellar mixing heats with composition (Figure 1) are more difficult to understand. Here, it may be possible that differences in the ratio where the maximum in the heat of mixing occurs arise from differences between the preferred minimum energy packing geometry of the alkyl ethoxylate sulfate and alkyl sulfate surfactants with alkyl ethoxylates in the micelle.

The information obtained about the heats of mixing in nonideal mixed micelles can also be used to examine the appropriateness of the regular solution approximation used in nonideal mixed micelle models. Here, equation 6 allows a comparison between the observed calorimetric results and both the symmetry and magnitude of the excess heats of mixing that would be predicted by the regular solution approximation used in the models. Referring to Figure 1, the SDS/C₁₀E₅ results show a good fit to the form of the regular solution approximation (solid line) calculated from equation 6 with $\beta = -8.4$. While it is seen that the predicted symmetry of the regular solution approximation is reproduced quite well, the magnitude of the β parameter necessary to obtain the fit is significantly outside the range of β values normally found when applying the nonideal micelle model to mixtures of alkyl sulfates and alkyl ethoxylate nonionics (see Figure 2 and Table 1). This indicates that the regular solution approximation does not adequately describe mixing in this system. An examination of the heats of mixing for C₁₂E₂S and C₁₀E₅S with C₁₀E₅ clearly shows that the predicted symmetry of the regular solution approximation used in the mixed micelle models is not observed. Together these results clearly demonstrate that in spite of the success of the nonideal mixed micelle models in describing nonideal behavior, the regular solution approximation does not properly account for the heats of mixing in these systems.

This conclusion implies that the excess entropy of mixing is non-zero and that the mixed micelles presumably acquire more internal order than they would by random mixing. An examination of the magnitude of the deviations from the regular solution approximation shows that there must be a large TS^E contribution to the excess free energy of mixing. A similar situation is commonly observed in mixtures of liquids, where the regular solution approach often gives good results for the excess free energies, but poor results for the heats of mixing (13). Unfortunately, the excess entropies cannot be easily extracted from calorimetric measurements of micellar mixing heats such as those in Figure 1 and measurements of the mixed cmcs to obtain G^E . This is because the composition of the micelles at the cmc are not known and may vary significantly from the composition of the overall surfactant mixture.

The finding that the assumptions of the regular solution approximation do not hold for the mixed micellar systems investigated here suggests a re-examination of how the thermodynamics of mixing enter the nonideal mixed micelle model. For example, it is readily seen (equations 4 and 5) that when the functional form of equation 6 is substituted for G^E , the form of the activity coefficients in equations 7 and 8 results. It is clear then that for cases where the excess entropy is not zero, empirically assuming the form

$$G^E = \beta x_1(1 - x_1)RT \quad (11)$$

for the excess free energy of mixing (as in reference 4), will give the same form for the activity coefficients. Under these circumstances, the β value from the nonideal mixed micelle model should be interpreted as a dimensionless excess free energy parameter, rather than an excess heat of mixing parameter.

Conclusions

Calorimetric measurements can be used to obtain heats of mixing between different surfactant components in nonideal mixed micelles and assess the effects of surfactant structure on the thermodynamics of mixed micellization. Calorimetry can also be successfully applied in measuring the cmc's of nonideal mixed surfactant systems. The results of such measurements show that alkyl ethoxylate sulfate surfactants exhibit smaller deviations from ideality and interact significantly less strongly with alkyl ethoxylate nonionics than alkyl sulfates.

The mixed cmc behavior of these (and many other) mixed surfactant systems can be adequately described by a nonideal mixed micelle model based on the pseudo-phase separation approach and a regular solution approximation with a single net interaction parameter β . However, the heats of micellar mixing measured by calorimetry show that the assumptions of the regular solution approximation do not hold for the systems investigated in this paper. This suggests that in these cases the net interaction parameter in the nonideal mixed micelle model should be interpreted as an excess free energy parameter.

Acknowledgments

The author wishes to thank Mr. R. P. Burwinkel and Mr. D. F. Etson for experimental work in the author's laboratory, Dr. J. B. Kasting for allowing his Calvet isothermal calorimeter to be used for some preliminary measurements and Dr. D. N. Rubingh for helpful discussions.

Legend of Symbols

f_i	activity coefficient of surfactant i in mixed micelles
x_i	mole fraction of surfactant i in mixed micelles
C_i	cmc of pure surfactant i
α_i	mole fraction of surfactant i in total mixed solute
C^*	cmc of mixed system
β	dimensionless net interaction parameter
G^E	excess free energy of mixing
H^E	excess enthalpy of mixing
S^E	excess entropy of mixing
R	gas constant
T	absolute temperature

Literature Cited

1. Lange, H.; Beck, K. H. Kolloid Z.Z. Polym. 1973, 251, 424.
2. Rubingh, D. N., in "Solution Chemistry of Surfactants"; Vol. 1, Mittal, L., Ed.; Plenum Press: New York, 1979; p. 337.
3. Holland, P. M.; Rubingh, D. N. J. Phys. Chem. 1983, 87, 1984.
4. Kamrath, R. F.; Franses, E. I. Ind. Eng. Chem. Fundam. 1983, 22, 230.
5. Scamehorn, J. F.; Schechter, R. S.; Wade, W. H. J. Disp. Sci. Tech. 1982, 3, 261.
6. Benjamin, L. J. Phys. Chem. 1964, 68, 3575.
7. Mazer, N.A.; Olofsson, G. J. Phys. Chem. 1982, 86, 4584.
8. Kresheck, G. C.; Hargraves, W. A. J. Colloid Interface Sci. 1981, 83, 1.
9. Clint, J. J. Chem. Soc. 1975, 71, 1327.
10. Münster, A. "Statistical Thermodynamics"; Springer-Verlag: Berlin-Heidelberg-New York, 1974, Vol. 2, p. 650.
11. Grime, J. K.; Staab, R. A.; Wernery, J. D., SAC '83 International Triennial Conference and Exhibition on Analytical Chemistry, Univ. of Edinburg July 1983.
12. Schick, M. J.; Manning, D. J. J. Amer. Oil Chem. 1966, 43, 133.
13. Hildebrand, J. H.; Prausnitz, J. M.; Scott, R. L. "Regular and Related Solutions"; Van Nostrand: New York, 1970; Chap. 7.

RECEIVED January 10, 1984

Influence of Structure and Chain Length of Surfactant on the Nature and Structure of Microemulsions

TH. F. TADROS

ICI Plant Protection Division, Jealott's Hill Research Station, Bracknell, Berkshire, RG12 6EY, England

The theories of microemulsion formation and stability have been reviewed. Three main approaches, namely mixed film, solubilisation and thermodynamic theories, have been briefly discussed. This is then followed by a section on factors determining w/o versus o/w microemulsion formation. The influence of surfactant and cosurfactant structure and chain length on the structure of microemulsions was described. In particular the cosurfactant chain length and structure has a considerable effect on the structure of the microemulsion. With short chain alcohols ($<C_6$) and/or surfactants, there is no marked separation into hydrophobic and hydrophilic domains and the structure is best described by a bicontinuous solution with easily deformable and flexible interfaces. With long chain alcohols ($>C_6$), well defined "cores" may be distinguished with a more pronounced separation into hydrophobic and hydrophilic regions. It was also concluded that microemulsions can be formed by a single surfactant provided this has the right geometry for packing at the interface and is capable of reducing the interfacial tension to low values. Addition of a cosurfactant is necessary in some cases to ensure packing of the surfactant molecule and to lower the interfacial tension.

0097-6156/84/0253-0153\$06.25/0

© 1984 American Chemical Society

The term microemulsion was first introduced by Hoar and Schulman (1) to describe the "transparent" or "translucent" systems, formed spontaneously when oil and water were mixed with relatively large amounts of an anionic surfactant (such as potassium oleate) and a cosurfactant (medium chain alcohol such as pentanol or hexanol). These systems are dispersions of very small drops (radius of the order of 5-50 nm) of water in oil (w/o) or oil in water (o/w). Microemulsions differ from ordinary emulsions (sometimes referred to as macroemulsions) in two main respects, namely their lack of turbidity and thermodynamic stability. For small particles, light scattering is proportional to the square of the volume of particles (2) and hence these systems with small droplets scatter little light and are not turbid. The thermodynamic stability of such systems is the consequence of the zero or negative free energy of their formation (see below), since the interfacial tension is so low that the remaining free energy of the interface is over compensated by the entropy of the dispersion of the droplets in the medium.

In spite of the advances made in recent years in the theoretical basis of explaining the physics and chemistry of microemulsions (3), the science of their formation has not reached the point of their exact formulation (4). The mechanics of microemulsion formation differ somewhat from those used in making macroemulsions. The most significant difference lies in the fact that putting work into a macroemulsion or increasing the surfactant concentration usually improves their stability; but this is not the case with microemulsions which appear to be dependent for their formation on specific interactions among the constituent molecules and with the interface. If these interactions are not realised, neither the work input nor increasing the surfactant concentration will produce a microemulsion (4). On the other hand, once the conditions are right, spontaneous formation occurs and no mechanical work is required. Thus, the crucial step in formulating the required microemulsion lies in the choice of emulsifiers. In other words, the nature (whether w/o or o/w) and structure of microemulsions depend to a large extent on the structure and chain length of the surfactant and co-surfactant used in their preparation. This is the subject of the present review.

Before describing how microemulsion nature and structure are determined by the structure and chain length of surfactant and cosurfactant, it is necessary first to briefly review the theories of microemulsion formation and stability. These theories will highlight the important factors required for microemulsion formation. This constitutes the first part of this review. The second part describes the factors that determine whether a w/o or o/w microemulsion is formed. This is then

followed by a section on the effect of structure and chain length of surfactant and cosurfactant on the structure of the microemulsion formed. Finally, the question of whether a microemulsion can be formulated with a single surfactant will be raised.

Theories of Microemulsion Formation and Stability

As discussed before (4) it is perhaps convenient to classify these theories into three main categories : interfacial or mixed film theories, solubilisation theories and thermodynamic theories. Below a brief description of each of these classes will be given with particular emphasis on the role of surfactant nature and structure.

Mixed film theories (4-8) The essential feature of the mixed film theories is to consider the film as a liquid, two dimensional third phase in equilibrium with both oil and water, implying that such a monolayer could be a duplex film, i.e., one giving different properties on the water side than on the oil side (4). According to these theories, the interfacial tension γ is given by the expression,

$$\gamma = (\gamma_{o/w})_a - \pi \quad (1)$$

where $(\gamma_{o/w})_a$ is the o/w interfacial tension, which is reduced by the presence of the alcohol cosurfactant (hence the subscript a), and π is the two dimensional spreading pressure of the mixed film. Contributions to π were considered to be the crowding of the surfactant and cosurfactant molecules and penetration of the oil phase into the hydrocarbon part of the interface. According to equation (1) if $\pi > (\gamma_{o/w})_a$, γ_T becomes negative leading to expansion of the interface until γ reaches zero.

The above concept of duplex film can be used to explain both the stability of microemulsions and the bending of the interface. Considering that initially the flat duplex film has different tensions (i.e., different π values) on either side of it, then the deriving force for film curvature is the stress of the tension gradient which tends to make the pressure or tension in both sides of the curved film the same. This is schematically shown in Figure 1. For example if $\pi'_w > \pi'_o$ on the flat film, then the film has to be expanded much more at the water side than at the oil side (which indeed contracts as a result of the curvature effect) until the surface pressures become equal on both sides of the duplex film (i.e. $\pi_w = \pi_o = 1/2 (\gamma_{o/w})_a$). This means that an o/w microemulsion results in this case. On the other hand, if $\pi_o > \pi_w$, then the film expands at the oil side and contracts at the water side of the interface resulting in the formation of a w/o microemulsion.

The above simple theory can be applied to predict the nature of the microemulsion. In a duplex film, the surface pressures at the oil and water sides of the interface depend on the interactions of the hydrophobic and hydrophilic portions of the surfactant at both sides respectively. For example, if the hydrophobic portions are bulky in nature relative to the hydrophilic groups, then for a flat film, such hydrophobic portions tend to crowd forming a higher surface pressure at the oil side of the film. In this case bending occurs to expand the oil side forming a w/o microemulsion. On the other hand, with a surfactant molecule with a relatively bulky hydrophilic group, crowding occurs at the water side of the interface, tending to form an o/w microemulsion.

A quantitative theory based on the lateral stress gradient resulting from the difference in swelling of the heads and tails across the interface was developed by Robbins (9). This stress gradient was expressed in terms of physically measurable quantities, namely, surfactant molecular volume, interfacial tension and interfacial compressibility. Relating the pressure difference across a curved interface to the activity of water in a w/o microemulsion, Robbins (9) established criteria for spontaneous water uptake without postulating a negative interfacial tension. It should be mentioned, however, that any duplex film theory has the drawback that two interfacial tensions must be defined at the oil side and water side of the interface (this is certainly difficult to define in a thermodynamic sense). Moreover, there is no way that such interfacial tensions can be measured and, therefore, the mixed film theory must only be regarded as approximate and is of only historical interest.

Solubilisation Theories (10-13) The solubilisation concept introduced by Shinoda and coworkers (10-13) who preferred to treat microemulsions as swollen micellar systems, thus relating them directly to the phase diagrams of the components. For example, the phase diagram of a three component system of water, ionic surfactant and alcohol usually displays one isotropic aqueous liquid region L_1 , from the water corner and one isotropic liquid region L_2 , from the alcohol corner (reverse micelles). The latter can dissolve a large amount of a hydrocarbon oil. Alternatively, such inverse micelles may be produced if the alcohol is dissolved in the oil followed by the addition of water and surfactant. Since the final solution is isotropic and no phase separation takes place when going from the pure hydrocarbon state to the microemulsion state, Shinoda and coworkers (10-13) preferred to describe these systems as swollen micelles.

Solubilisation can best be illustrated by considering the phase diagrams of non-ionic surfactants containing poly(oxyethylene oxide) head groups. Such surfactants do not generally need a cosurfactant for microemulsion formation. At low temperatures, the ethoxylated surfactant is soluble in water

and at a given concentration is capable of solubilising a given amount of oil. The oil solubilisation increases rapidly with increase of temperature near the cloud point of surfactant. This is clearly illustrated in Figure 2a which shows both the solubilisation curve and cloud point curve of the surfactant. Between the two curves, an isotropic region of o/w solubilised system exists. At any given temperature any increases in the oil weight fraction above the solubilisation limit results in oil separation i.e. o/w solubilised + oil, whereas at any given surfactant concentration any increase in temperature above the cloud point of surfactant results in separation into oil water and surfactant.

On the other hand, if one starts from the oil phase with dissolved surfactant and add water, solubilisation of the latter takes place and hence solubilisation increases rapidly with reduction of temperature near the haze point of the surfactant. This is illustrated in Figure 2b which shows both the haze point and solubilisation curve. Between the two curves, an isotropic region of w/o solubilised system exists. At any given temperature, any increase in water weight fraction above the solubilisation limit results in water separation, i.e. w/o solubilised + water, whereas at a given surfactant concentration, any decrease in temperature below the haze point result in separation into water, oil and surfactant.

Thus, with nonionic surfactants, both types of micremulsions can be formed depending on the conditions. As shown above, with such systems temperature is the most crucial factor since the solubility of the surfactant in water or in oil depends on the temperature. One should remember that in aqueous solutions, the solubility of nonionic ethoxylated surfactants decreases with increase of temperature, whereas the reverse is true with oil solutions.

Thermodynamic Theories (14-18) Two main treatments have been considered, namely by Ruckenstein et al (14-16) and Overbeek et al (17,18). The treatments follow roughly the same procedure, but vary somewhat in detail (3). Ruckenstein et al (14,15) considered the free energy of formation of microemulsions ΔG_m , to consist of three main contributions ΔG_1 an interfacial energy term, ΔG_2 an energy of interaction between the droplets term and ΔG_3 an entropy term accounting for the dispersion of droplets into the continuous medium. The interfacial free energy term ΔG_1 was considered to consist of two contributions due to the creation of an uncharged surface (given by the product of area created and specific surface free energy of the interface) and a contribution due to the formation of electrical double layers (which is given by the product of the interfacial area and the specific surface free energy due to creation of an electrical

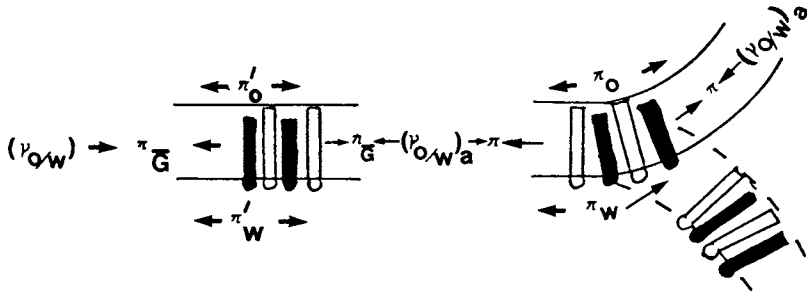


Figure 1. Schematic representation of film bending

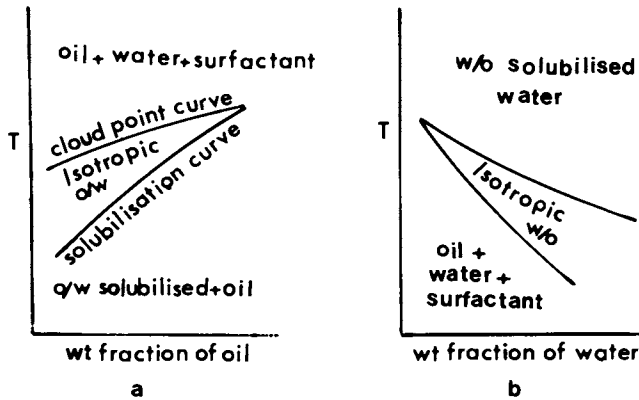


Figure 2. Schematic representation of solubilisation (a) oil solubilised in a nonionic surfactant solution; (b) water solubilised in an oil solution of nonionic surfactant

double layer). The double layer contribution was calculated using the Debye-Huckel approximation. For the calculation of ΔG_2 a pairwise additivity of interaction potentials was assumed, whereas for the calculation of the entropy contribution term ΔG_3 , a lattice model was used to calculate the number of configurations of droplets in the continuous medium. From the variation of ΔG_m with droplet radius R , various states could be distinguished which illustrated the transition from instability kinetic stability thermodynamic stability. This transition may be obtained by reducing the value of ΔG_1 , i.e. reducing the specific surface energy, f_s . The reduction of f_s to sufficiently small values was accounted for by Ruckenstein (15) in terms of the so called "dilution effect". Accumulation of surfactant and cosurfactant at the interface not only causes significant reduction in the interfacial tension, but also results in reduction of the chemical potential of surfactant and cosurfactant in bulk solution. The latter reduction may exceed the positive free energy caused by the total interfacial tension and hence the overall ΔG of the system may become negative. Further analysis by Ruckenstein and Krishnan (16) have showed that micelle formation encountered with water soluble surfactants reduces the dilution effect as a result of the association of the surfactants molecules. However, if a cosurfactant is added, it can reduce the interfacial tension by further adsorption and introduces a dilution effect. The treatment of Ruckenstein and Krishnan (16) also highlighted the role of interfacial tension in the formation of microemulsions. When the contribution of surfactant and cosurfactant adsorption is taken into account, the entropy of the drops becomes negligible and the interfacial tension does not need to attain ultralow values before stable microemulsions form.

In Overbeek theory (17,18) the free energy of microemulsion formation was also considered to consist of three main contributions; ΔG_1 due to mixing of surfactant with water and co-surfactant with oil; ΔG_2 due to the interfacial area in forming the droplets and ΔG_3 due to the mixing of droplets into the continuous phase. ΔG_1 is simply given by the sum of the product of number of moles of each component and its chemical potential with reference to the standard state. The interfacial area term ΔG_2 is given by the final interfacial tension and final area of the interface plus a chemical potential term due to adsorption of surfactant and co-surfactant. Finally, the free energy term due to mixing of droplets into the continuous medium have been obtained using the hard-sphere model of Percus Yevick (19) and Carnahan and Starling (20) which was originally used by Agterof et al (21) to describe the non-ideal behaviour of microemulsions.

Taking the above three contributions into account, Overbeek (17) derived the following expression for the free energy dG_m for microemulsion formation,

$$dG_m = dA \left[\gamma_{\text{uncharged}} + \int \psi_o d\sigma + \frac{A^2 kT}{12 (n_w v_w)^2} \left(\ln \phi - 1 + \phi \frac{4-3\phi}{(1-\phi)^2} + \ln \frac{v_o}{v_{hs}} \right) \right] \quad (2)$$

where dA is the change in interfacial area. The first term between the square brackets is the interfacial tension term, $\gamma_{\text{uncharged}}$ that is obtained if no double layers had been formed. $\int \psi_o d\sigma$ is the electrical contribution to the interfacial tension as a result of formation of an electrical double layer, with ψ_o being the surface potential and σ the surface charge density. The third term is the osmotic contribution due to mixing of microemulsion droplets (treated as hard spheres) and v_{hs} is their molar volume. The number of hard sphere droplets is given by,

$$n_{hs} = \frac{A^3 N_{av}}{36 \pi (n_w v_w)^2} \quad (3)$$

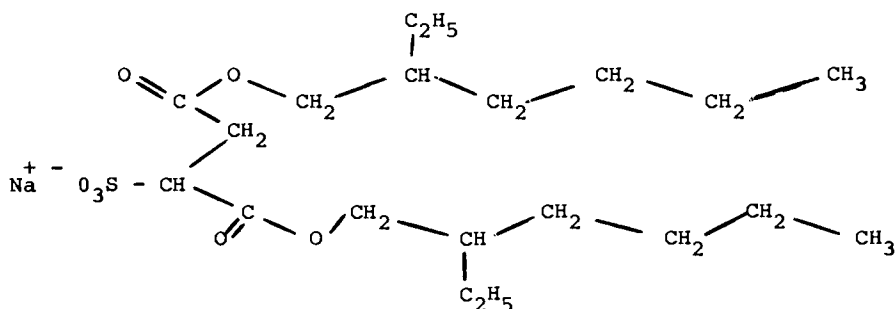
where A is the area, n_w is the number of water molecules and v_w is their molar volume.

The three terms of equation (2) are unequal in magnitude. The last term is always negative. For example, for a high ratio of surfactant to water $n_s/n_w = 0.04$ (corresponding to a mass ratio of 0.7) and $\phi = 0.5$, this term is $\sim 0.2 \text{ m Nm}^{-1}$. For $\phi = 0.1$, the value would be $\sim 0.5 \text{ m Nm}^{-1}$ and to make this term -1.0 m Nm^{-1} , ϕ has to be below 10^{-5} , i.e. a very dilute microemulsion.

On the other hand, the electrical free energy per unit area of double layer (second term) is high and positive even for relatively low surface potential. The contribution of this term could be tens of m Nm^{-1} . This requires $\gamma_{\text{uncharged}}$ to have a high negative value to reach the condition $dG = 0$. The conclusion so far reached from this analysis is that in a microemulsion the interfacial tension, including the electrical term must have very low but positive value. The small variations in the total interfacial tension required to balance the variation in the free energy of mixing (osmotic term) can be easily obtained by small variations in the amount of surfactant and cosurfactant at the interface leading to variations in $\gamma_{\text{uncharged}}$.

Factors Determining w/o versus o/w Microemulsion Formation

Several factors play a role in determining whether a w/o or o/w microemulsion is formed. These factors may be considered in the light of the theories described in section 2. For example, the duplex film theory predicts that the nature of the microemulsion formed depends on the relative packing of the hydrophobic and hydrophilic portions of the surfactant molecule, which determines the bending of the interface. For example, a surfactant molecule such as Aerosol OT, having the structure shown below, is favourable for formation of w/o microemulsion, without the need of adding a cosurfactant. As a result of the presence of a stumpy head group and large volume to length (V/l) for the non-polar group, the interface tends to bend with the head groups facing inwards thus forming a w/o microemulsion. This geometric constraint for the Aerosol OT molecule was considered in detail by Oakenfull (22) who showed that the molecule has a $V/l > 0.7$, which was considered to be necessary for microemulsion formation.



With ionic surfactants for which $V/l < 0.7$, microemulsion formation needs the presence of a cosurfactant. The latter has the effect of increasing V without affecting l (if the chain length of the cosurfactant does not exceed that of the surfactant). These cosurfactant molecules act as "padding" separating the head groups.

The importance of geometric packing on the nature of the microemulsion has also been considered by Mitchell and Ninham (23). According to these authors the nature of the aggregate unit depends on the packing ratio $v/a_0 l_c$ where v is the partial molecular volume of the surfactant, a_0 is the head group area of a surfactant molecule and l_c is the maximum chain length. Thus, this packing ratio provides a measure of the hydrophobic-hydrophilic balance (HLB). For values of $v/a_0 l_c < 1$, normal i.e., convex aggregates are predicted, whereas for $v/a_0 l_c > 1$ inverse drops are expected. The packing ratio is affected by many factors including hydrophobicity of head group, ionic strength of solution, pH, temperature and the

addition of lipophilic compounds such as cosurfactants. Addition of electrolyte or increase of temperature causes a change in the area per head group and hence effects the packing ratio. With the Aerosol OT molecule $v/a_o l_c$ is greater than 1 since both a_o and l_c are small. Thus, this molecule is favourable for formation of w/o microemulsion.

The packing ratio also explains the nature of microemulsion formed by using nonionic surfactants. If $v/a_o l_c$ increases with increase of temperature (as a result of reduction of a_o), one would expect the solubilisation of hydrocarbons in nonionic surfactant to increase with temperature as observed, until $v/a_o l_c$ reaches the value of 1 where phase inversion would be expected. At higher temperatures, $v/a_o l_c > 1$ and water in oil microemulsions would be expected and the solubilisation of water would decrease as the temperature rises again as expected.

The influence of surfactant structure on the nature of the microemulsion formed can also be predicted from the thermodynamic theory by Overbeek (17,18). According to this theory, the most stable microemulsion would be that in which the phase with the smaller volume fraction forms the droplets, since the osmotic term increases with increasing ϕ . For w/o microemulsion prepared using an ionic surfactant, the hard sphere volume is only slightly larger than the water volume, since the hydrocarbon tails of the surfactant may interpenetrate to a certain extent, when two droplets come close together. For an oil in water microemulsion, on the other hand, the double layer may extend to a considerable extent, depending on the electrolyte concentration (the thickness of the double layer $1/\kappa$ is of the order of 100 nm for 10^{-5} mol dm^{-3} and 10 nm for 10^{-3} mol dm^{-3} 1:1 electrolyte). Thus, the hard sphere radius can be increased by 5 nm or more unless the electrolyte concentration is high (say 10^{-1} mol dm^{-3} where $1/\kappa \sim 1$ nm). Thus this factor works in favour of the formation of w/o microemulsions especially for small droplets. Furthermore, establishing a curvature of the adsorbed layer at a given adsorption is easier with water as the disperse phase, since the hydrocarbon chains will have more freedom around than if they were inside the droplet.

Influence of Surfactant and Cosurfactant Structure and Chain Length on the Structure of Microemulsions

Both the structure and chain length of surfactants and cosurfactants have a striking influence on the structure of the microemulsion formed. The most systematic studies have been on the influence of the cosurfactant chain length and structure on the nature of the microemulsion region. Two main studies have been carried out to elucidate the difference obtained, namely electrical conductivity and NMR investigations. As we will see

later, the results of such investigations led to the classification of microemulsions into two main systems, namely those with well defined "cores" with pronounced separation into hydrophobic and hydrophilic regions and those systems in which there is no marked separation into hydrophobic and hydrophilic domains and the structure is best described by a bicontinuous solution with easily deformable and flexible interface.

One of the best examples of the influence of chain length and structure of the cosurfactant on the nature of the microemulsion region is that obtained by Clause and coworkers (24,25). Figure 3 shows the phase diagrams of the system water/sodium dodecylsulphate/alkanols benzene at various chain length of the alkanol from C_2 to C_7 (i.e. ethanol to heptanol). In such systems, the molar ratio of surfactant to alcohol was kept constant (1:2) at the temperature was 25°C . The phase diagrams may be classified into two distinct systems. In the first case, with cosurfactant chain length C_1 to C_4 (Figure 3a-d), the transparent domain (sometimes referred to as the Winsor IV domain) consists of a unique area that has the shape of a curvilinear triangle leaning against a large portion of the surfactant (S) - water (W) side of the phase diagram. These systems were referred to by Clause *et al* (21) as Type U systems. On the other hand, with cofurfactants with chain length C_5 to C_7 (Figur 3 e-g), the Winsor IV domain is split into two disjointed areas that are separated by a composition zone over which viscous turbid and birifringent media are encountered. This second class of systems was referred as Type S systems (24). It can also be seen that the Winsor IV domain reaches its maximum extension at C_4 reducing in size below and above C_4 . Moreover, at C_5 , one observes a small monophasic region near the W apex (probably o/w microemulsion of the Schulman's type) which vanishes as the alcohol chain length is increased to C_6 .

The influence of cosurfactant structure is best illustrated by using various isomeric alcohols with the same chain length. This is shown in Figure 4 for the system water, benzene, potassium oleate and amylic alcohols (25). The mass ratio of potassium oleate to COH is 3:5 and the temperature was 22°C . This figure shows the progressive geometrical deformation undergone by the monophasic transparent domain upon substitution of a C_5 alcohol for one of its isomers. It appears that the substitution of one isomeric pentanol for another induces a transition from systems displaying a unique Winsor IV domain to systems displaying a Winsor IV domain split into two disjointed areas. Thus, the substitution of an isomeric pentanol for another one, induces a progressive transition between the case of Type U systems and that of Type S systems, in contrast with the sharp transition observed upon substituting a longer straight alkanol for a shorter one (Figure 3).

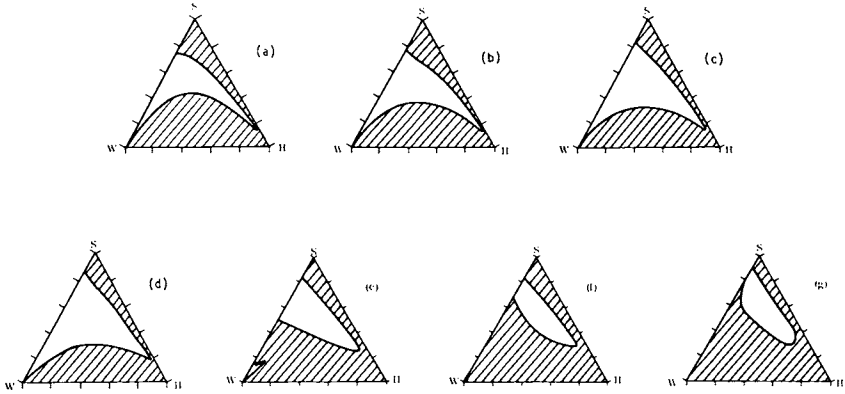


Figure 3. Phase diagrams of the system water sodium dodecyl sulphate/alkanols benzene (a) ethanol; (b) 2-propanol; (c) 1-propanol; (d) 1-butanol; (e) 1-pentanol; (f) 1-hexanol; (g) 1-heptanol.

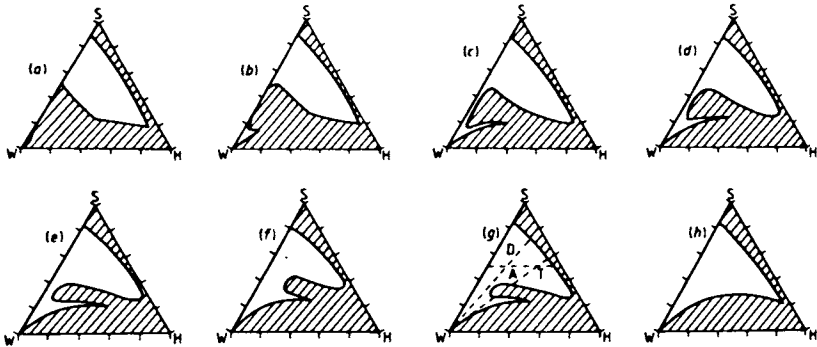


Figure 4. Phase diagrams of the system water benzene potassium oleate/amylic alcohols (a) 1-pentanol (1P); (b) 3-methyl-1 butanol (3M1B); (c) 2-methyl-1-butanol (2M1B) (d) 2,2-dimethyl-1-proptanol (22M1P); (e) 2-pentanol (2P); (f) 3-pentanol (3P); (g) 3 methyl-2-butanol (3M2B); (h) 2-methyl-2-butanol (2M2B).

The above differences observed with the various cosurfactants are reflected in the conductivity - water volume fraction (ϕ_w). This is shown in Figures 5 and 6. It can be seen that the conduction behaviour is strongly influenced by the nature of the alcohol. For example Figure 5 shows that for the shorter alcohols ethanol, 1-propanol and 1-butanol (which give Type U systems) the conductivity increases rapidly as the water content increases above a certain ϕ_w value, which is smaller the shorter the alcohol. In contrast with the larger alcohol, 1-pentanol, the conductivity does not take high values and its variation with ϕ_w is more smooth. With even higher chain length alcohols, namely 1-hexanol and 1-heptanol (which give Type S system), the conductivity is very low ($<0.05 \text{ Sm}^{-1}$) and hence appears close to zero on the scale of Figure 5. However, if the scale is expanded, the conductivity of such S-Type shows a maximum. This is illustrated in Figure 7 for the system water/hexadecane/potassium oleate/hexanol which shows the trend. Similar results have been recently obtained for the system xylene/water/sodium dodecyl benzene sulphonate/hexanol (26). Thus, the difference in conductive behaviour between the two systems must reflect a difference between the structural units involved.

With the U-Type systems (i.e. with the low chain alcohols) the trends in the conductivity - ϕ_w curve are consistent with percolative conduction originally proposed to explain the behaviour of conductance of conductor-insulator composite materials (27). In the latter model, the effective conductivity is practically zero as long as the conductive volume fraction is smaller than a critical value ϕ_w^P , called the percolation threshold, beyond which κ suddenly takes a non-zero value and rapidly increases with increase of ϕ_w . Under these conditions,

$$\kappa \sim (\phi_w - \phi_w^P)^{8/5} \quad \text{when } \phi_w > \phi_w^P \quad (4)$$

$$\text{and } \kappa \sim (\phi_w^C - \phi_w)^{-0.7} \quad \text{when } \phi_w < \phi_w^P \quad (5)$$

By fitting the conductivity data to the above equations, one usually finds a ϕ_w^P value for droplets (which should also include surfactant) near to the theoretical limit of 0.29. At this volume fraction, charge transfer between w/o globular micelles submitted to attractive interactions take place. Moreover, as we will see later, such systems contain easily deformable and flexible interfaces.

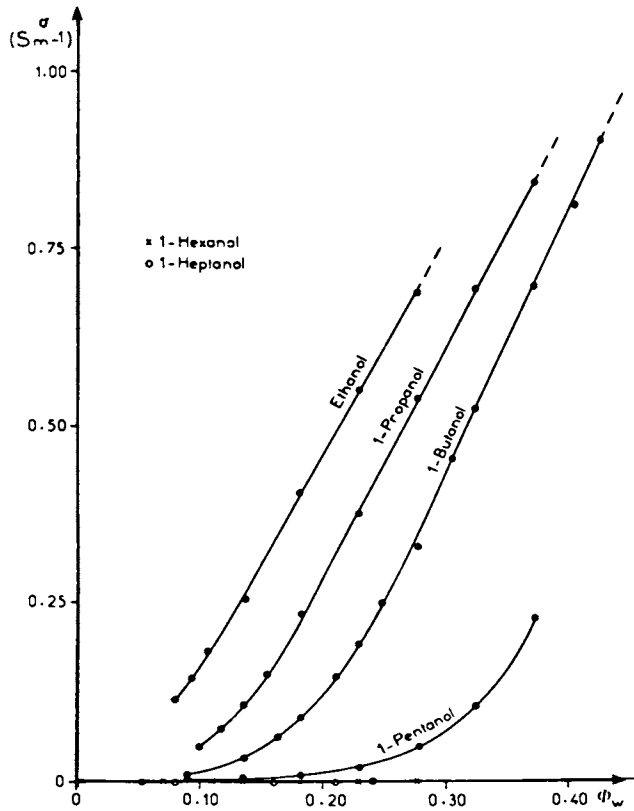


Figure 5. Influence of alcohol chain length on the conductivity - water volume fraction curves

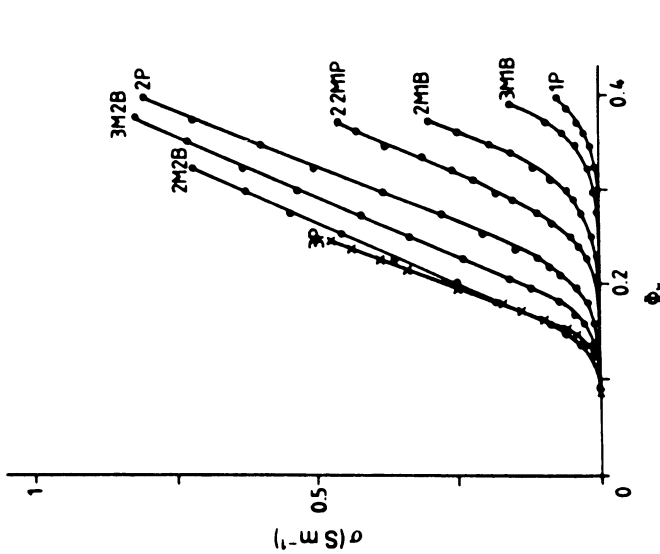


Figure 6. Influences of alcohol isomery on the conductivity - water volume fraction curve: (symbols are the same as those for Figure 4).

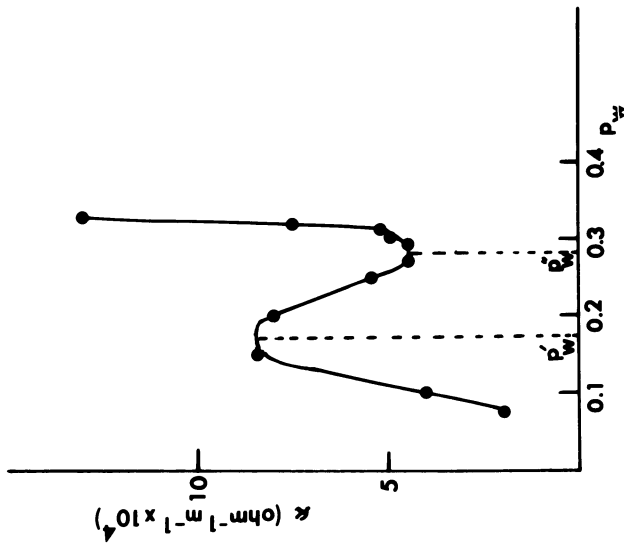


Figure 7. Variation of κ with p_w for the system water/hexadecane/potassium oleate/hexanol.

With the S-type system, the trend in conductivity - p_w (which p_w is the water weight fraction) (Figure 7) is more complex showing a number of transitions indicating more subtle changes in the conduction units as the water concentration is increased. It seems that in the low water concentration region i.e. below the maximum, inverted swollen micelles or microdroplets do not exist (premicellar region) and the increase in conductivity with p_w in this region is likely to be due to the increase in the dissociation of the surfactant on the addition of water (26). The region beyond the maximum, i.e. where the conductivity decreases with increase of p_w , is the region of the existence of w/o microemulsion of the Schulman type. The sharp increase at the second p_w region (i.e. p_w) may be associated with a "facilitated" path for ion transport. This can be ascribed to the formation of non spherical particles resulting from swollen micelle clustering and subsequent cluster interlinking, a process that is indicative of system stability breakdown and of crystalline structure organisation (26). Thus, these systems represent those of "true" microemulsions, i.e., with definite water cores and therefore are non-percolating.

The maximum in the conductivity - ϕ_{H_2O} curves for the Type S systems can be explained in terms of the model proposed by Eicke and Denss (28). These authors considered charge production to be caused by two processes. The first by dissociation of the surfactant molecules inside the micellar entities, a process thought to be independent of the medium in which the aggregates are embedded. The second process is a transfer of charges, i.e., of an anion which stems from the dissociation of the surfactant inside the droplet, to another (originally neutral) micellar aggregate. This latter process is considered to represent a phase transfer between the droplet pseudo phase (built-up by the ensemble of microemulsion droplets) and the solution phase consisting of a very dilute solution of charged micellar aggregates in the non-polar solvent. The charge transfer will actually proceed in two steps: ion (droplet phase) \rightarrow ion (non-polar solvent) and ion (non-polar solvent) \rightarrow ion (resolubilised in micellar aggregate).

Further information on the dependence of structure of microemulsions formed on the alcohol chain length was obtained from measurement of self diffusion coefficient of all the constituents using NMR techniques (29-34). For microemulsions consisting of water, hydrocarbon, an anionic surfactant and a short chain alcohol (C_4 and C_5) the self diffusion coefficient of both water, cosurfactant and hydrocarbon was quite high (of the order of $10^{-9} \text{ m}^2 \text{ s}^{-1}$) being two orders of magnitude higher than the value to be expected for a discontinuous medium ($10^{-11} \text{ m}^2 \text{ s}^{-1}$ and below). This can be

attributed to three alternative effects or a combination of all of them: (i) bicontinuous solutions, i.e., both oil and water continuous, (ii) easily deformable and flexible interface, or (iii) absence of large aggregates. Lang *et al* (35) have shown that addition of short chain alcohol to a micellar solution results in a considerable reduction of the life time of surfactant monomer in the micelle. This result is consistent with the picture of disorganised and flexible interfaces. Thus, the picture of microemulsion based on an anionic surfactant and short chain alcohols is that of very small aggregates with any internal interface with very limited spatial extension or very dynamic and flexible structure which breaks up and reform at very high speed, or both.

On the other hand, with microemulsions based on an anionic surfactant and a long chain alcohol, D_w was fairly low for certain concentrations, indicating that distinct water droplets in a hydrophobic medium may form. The system investigated by Lindman *et al* (29-34) was based on octanoic acid - decanol - octane-water. This means that the anionic "surfactant" used contains only seven carbon atoms in the alkyl chain which is fairly short. With longer chain surfactants, one would expect well defined "water cores" provided the alcohol is also long-chain. Such well defined "water cores" have also been confirmed by Lindman *et al* (34) for the Aerosol OT - hydrocarbon system. In that case the self diffusion coefficient - concentration curve shows a behaviour distinctly different from the cosurfactant microemulsions. D_w has a quite low value throughout the extension of the isotropic solution phase up to the highest water content. This implies that a model with closed droplets surrounded by surfactant anions in a hydrocarbon medium gives an adequate description of these solutions. However, since D_w was found to be significantly higher than D_s , the authors came to the conclusion that a non-negligible amount of water must exist between the emulsion droplets.

Thus, in summary, self diffusion measurements by Lindman *et al* (29-34) have clearly indicated that the structure of microemulsions depends to a large extent on the chain length of the cosurfactant (alcohol), the surfactant and the type of system. With short chain alcohols ($< C_6$) and or surfactants there is no marked separation into hydrophobic and hydrophilic domains and the structure is best described by a bicontinuous solution with easily deformable and flexible interfaces. This picture is consistent with the percolative behaviour observed when the conductivity is measured as a function of water volume fraction (see above). With long chain alcohols ($> C_6$) on the other hand, well defined "cores" may be distinguished with a more pronounced separation into hydrophobic and hydrophilic regions.

The same is true with other specific systems such as that based on Aerosol OT without the presence of a cosurfactant. This structure is also consistent with the non-percolative nature of such systems (see above).

Thus it can be concluded that the structure of microemulsions depends on the structure of surfactant and cosurfactant. Moreover, this structure also determines the amount of solubilisation of oil and or water in microemulsions. In recent studies by Gracia et al (36) and Baraket et al (37) the criteria for structuring surfactants to maximise solubilisation of oil and water were investigated. Using a number of ethoxylated alkyl phenols with the same HLB, but different molecular weight i.e. in which both the hydrophilic and hydrophobic moieties of the surfactant were increased simultaneously, Gracia et al (36) found that solubilisation increases with increase of molecular weight. On the other hand, Baraket et al (37) showed that branching of the surfactant hydrocarbon tail has a significant effect on solubilisation; the less the branching the higher the solubilisation.

Microemulsions Based on a Single Surfactant and the role of the cosurfactant. It is interesting now to raise the following question. Can microemulsions be prepared using a single surfactant?. This question can be answered in the light of the criteria needed for the formation microemulsion discussed above. Two main criteria are important: surfactant geometry and low interfacial tension. As mentioned above the relative packing of the hydrophobic and hydrophilic portion of the surfactant molecule, plays a major role. Such packing is favourable with molecules such as Aerosol OT with a stumpy head group and a large volume to length ratio for the non-polar group, which tend to bend with the head groups facing inwards. Moreover such a molecule when adsorbed at the w/o interface lowers the interfacial tension sufficiently such that a w/o microemulsion can be formed without the need of a cosurfactant.

As mentioned before, nonionic surfactants also form microemulsions without the need of adding a cosurfactant. This is still the case with "pure" nonionic surfactants which consist of a single chain length. Under conditions whereby a microemulsion is formed, nonionic surfactants satisfy the above mentioned criteria, namely packing and low interfacial tension. For example, in the homogeneous isotropic region between the solubilisation and cloud point curve (Figure 2a), geometric packing of the molecules favours the formation of oil in water microemulsions and in this region the interfacial tension also falls to very small values. Similarly, between the haze point and solubilisation curve (Figure 2b) water in oil microemulsion

form since geometric packing favours bending with the larger polyethylene oxide head group solubilising the water. In this region, the interfacial tension also falls to very small values.

The cosurfactant plays two major roles; firstly it effects the packing of the surfactant molecule at the interface and secondly it brings the necessary reduction in interfacial tension, if this could not be produced by the surfactant molecules alone. As mentioned before, the packing of the surfactant molecules depends on the ratio of the volume to the length of the non-polar group. Addition of a cosurfactant increases the volume without affecting the length and hence it enables the geometrical packing of the molecules at the interface. Moreover, such molecules act as "padding" separating the head groups.

The role of the cosurfactant in reducing the interfacial tension can be understood from application of the Gibbs adsorption equation in the form (14).

$$\left(\frac{\partial \gamma}{\partial \mu^i}\right)_{T,P, \text{ all } n_j \text{ except } n_i, A} = -\left(\frac{\partial n^i}{\partial A}\right)_{T,P, \text{ this all } n_j \text{ except } n_i, A} = \Gamma_i \quad (6)$$

By using equation (6) twice for the cosurfactant ($i = Co$) and for the surfactant ($i = Sa$), the following equation can be derived,

$$\gamma = \gamma_0 - \left[\int_{C(Co=0)}^{C(Co)} Co \, d\mu_{Co} \right]_{T,P, C(Sa) = 0} - \left[\int_{C(Sa=0)}^{C(Sa)} Sa \, d\mu_{Sa} \right]_{T,P, n(Co), n_{oil}, n_w} \quad (7)$$

It is clear from equation (7) that the addition of a second surfactant results in further decrease in γ ; the essential requirements being a not too small adsorption of the second surfactant. Whether it replaces the first surfactant or is adsorbed in addition to it is immaterial, just as it is not essential for the two surfactants to form a complex. If the two surfactants are of the same type e.g. both water soluble anionic surfactants, they will form mixed micelles and this will lower the activity of the second surfactant added and decrease both its Γ and $d\mu$. However, if the two surfactants are different in nature, e.g. one predominantly water soluble and the other oil soluble, they will only slightly affect each other's activity and their combined effect on the interfacial tension may be large enough to bring γ to zero at finite concentrations.

Literature Cited

1. Hoar, T.P. and Schulman, J.H., *Nature (London)* 152, 102 (1943)
2. Kerker, M., "The Scattering of Light" Academic Press, New York (1969) pp. 30-39.
3. Tadros, Th. T., "Microemulsions - An Overview"., in "Solution Properties of Surfactants" Editor Mital, K.L., Plenum Publishing Corporation (in Press).
4. Prince, L. M., "Microemulsions, Theory and Practice" Academic Press, New York (1977).
5. Bowcott, J.E. and Schulman, J.H., *J. Electrochem.* 54, 283, (1955)
6. Schulman, J.H., Stoeckenhuis, W. and Prince, L. M., *J. Phys. Chem.* 63, 1677 (1959)
7. Prince, L.M., *J Colloid Interface Sci* 23, 165 (1967)
8. Prince, L.M., *J. Cosmet Chem.* 21, 183 (1970)
9. Robbins, M. L., "Theory for the Phase Behaviour of Microemulsions", Paper No 5839, presented at the Improved Oil Recovery Symposium of the Society of Petroleum Engineers of AIME, Tulsa, Oklahoma, March 22-24 (1976).
10. Shinoda, K and Friberg, S., *Adv. Colloid Interface Sci.* 4, 281 (1975)
11. Saito, H. and Shinoda, K., *J Colloid Interface Sci* 24, 10 (1967); 26; 70 (1968)
12. Shinoda, K. and Kunieda, H., *J Colloid Interface Sci.* 42, 381 (1973)
13. Ahmed, S.I., Shinoda, K and Friberg, S., *J. Colloid Interface Sci.* 47, 32 (1974)
14. Ruckenstein, E. and Chi, J.C., *J. Chem. Soc. Faraday Trans.* 71, 1690 (1975)
15. Ruckenstein, E, *J Colloid Interface Sci* 66, 369 (1978)
16. Ruckenstein, E and Krishnan, R, *J Colloid Interface Sci* 71, 321 (1979); 75, 476 (1980) ; 76, 188, 201 (1980)
17. Overbeek, J. Th. G., *Farraday Disc. Chem. Soc* 65, 7 (1978)
18. Overbeek, J. TH. G., de Bruyn. P.L. and Verhoeckx, F., in "Surfactants" Editor Tadros, Th. F., Academic Press (in Press)
19. Percus, J. K. and Yevick, G. J., *Phys. Rev.* 110, 1 (1958)
20. Carnahan, N. F. and Starling, K. E., *J Chem Phys.* 51, 635 (1969).
21. Agterof, W. G. M., Van Zameren, J. A. J. and Vrij, A., *chem Phys. Letters*, 43, 363 (1976)
22. Oakenfull, D., *J. Chem Soc. Faraday Trans I*, 76, 1875 (1980)
23. Mitchell, D. J. and Ninham, B. W., *J Chem Soc. Farradey Trans II*, 77, 601 (1981)

24. Clause, M., Peyrelasse, J., Boned, C., Heil, J., Nicolas-Margantine, L. and Zradba, A., in "solution properties of surfactants" Editor Mittal, K. L., Plenum Corporation (in Press)
25. Peyrelasse, J., Boned, C., Heil, J. and Clause, M., *J Phys C: Solid State Phys.*, 15, 7099 (1982)
26. Baker, R. C., Florence, A. T. and Tadros, Th. F., *J. Colloid Interface Sci*, submitted.
27. Kilpatrick, S., *Mod. Phys.* 45, 574 (1983)
28. Eicke, H. F. and Denss, A., in "Solution Chemistry of Surfactants, K. L. Mittal, editor, Vol 2 Plenum Press, New York (1979) p607
29. Lindman, B., and Wennerstrom, H., in "Topics in current chemistry" (F.L. Boschke Ed) 87, 1-83, Springer-Verlag, Heidelberg (1980).
30. Winnerstrom, H. and Lindman, B., *Phys. Rep* 52, 1 (1970)
31. Lindman, B., Kamenka, N., Kalhopoulis, T.M., Brumand, B, and Nilsson, P. G., *J. Phys Chem* 84, 1485 (1980)
32. Fabre, H., Kamenka, N., Lindman, B., *J. Phys. chem.* 85, 3493 (1981)
33. Stilbs, P., Mosely, M. E. and Lindman, B., *J. Magn. Reson. Sci.* 401 (1981)
34. Lindman. B., Stilbs, P. and Moseley, M.E., *J. Colloid Inteface Sci.* 83, 569 (1981)
35. Lang, J., Djavanbakht, A, and Zana, R. in "Microemulsions", Rubb, I.D., Editor, Plenum Press, New York (1982) pp 233-255.
36. Gracia, A., Fortney, L. N., Schechter, R. S., Wade, W. H. and Yiv, S., *Soc, Pet. Eng. SPE* 9815 (1980)
37. Barakat, Y., Fortney, L. N., Schechther, R. S., Wade, W. H., and Yiv, S. H., *J. Colloid Inteface Sci* 92, 561 (1983)

RECEIVED January 20, 1984

Reaction of *N*-Dodecyl-3-carbamoyl Pyridinium Ion with Cyanide in Oil-Water Microemulsions

LEONA DAMASZEWSKI and R. A. MACKAY¹

Department of Chemistry, Drexel University, Philadelphia, PA 19104

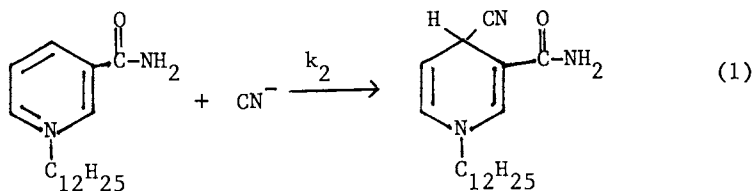
The rate constants for the reaction of a pyridinium ion with cyanide have been measured in both a cationic and nonionic oil in water microemulsion as a function of water content. There is no effect of added salt on the reaction rate in the cationic system, but a substantial effect of ionic strength on the rate as observed in the nonionic system. Estimates of the ionic strength in the "Stern layer" of the cationic microemulsion have been employed to correct the rate constants in the nonionic system and calculate effective surface potentials. The ion-exchange (IE) model, which assumes that reaction occurs in the Stern layer and that the nucleophile concentration is determined by an ion-exchange equilibrium with the surfactant counterion, has been applied to the data. The results, although not definitive because of the ionic strength dependence, indicate that the IE model may not provide the best description of this reaction system.

A pseudophase ion exchange model has been applied to reactions in micellar systems with varying success (1-7). According to this model, the distribution of nucleophile is considered to depend on the ion-exchange equilibrium between the nucleophile and the surfactant counterion at the micelle surface. This leads to a dependence on the ion-exchange constant (K_{IE}) as well as on the degree of dissociation (α) of the surfactant counterion. The ion exchange (IE) model has recently been extended to oil in water microemulsions (8).

¹Current address: Chemical Branch, Research Division, Chemical Research and Development Center, Aberdeen Proving Ground, Aberdeen, MD 21010

0097-6156/84/0253-0175\$06.00/0
© 1984 American Chemical Society

Ion exchange constants have been calculated from kinetic data for the reaction of p-nitrophenyl diphenyl phosphate with hydroxide and fluoride in a cationic microemulsion, and from acid-base equilibrium data in an anionic microemulsion (8-9) using the ion exchange model for microemulsions. Although the kinetic data can be fit to the IE model, they can also be explained by means of the effective surface potential (ESP) model which considers the local nucleophile concentration to be a function only of α . Thus, if the ESP model is valid, attempts to fit kinetic data to the IE model should produce similar values of the ion-exchange constant (K_{IE}) for any nucleophile. This was in fact observed for the above reaction. However, hydroxide and fluoride have similar ion exchange constants with respect to bromide. Therefore, a reaction involving a nucleophile having a significantly different ion exchange constant should provide a more definitive test of the model. Unfortunately, attempts to react nucleophiles such as cyanide or thiophenoxide with the phosphate ester used in the above studies were unsuccessful. Thus, it was decided to employ a different substrate, and to that end we have followed the reaction of interphase-bound N-dodecyl 3-carbamoyl pyridinium bromide with cyanide ion at $\text{pH} \geq 11.8$ (equation 1) in a cationic and in a nonionic microemulsion.



This reaction has been used as a test of the ion-exchange model in micelles (2), and the value of K_{IE} for cyanide differs from that of fluoride or hydroxide by about an order of magnitude.

Experimental

Systems and materials. The reaction was carried out at several compositions in an ionic and in a nonionic system. The ionic system consisted of an emulsifier (49.6 wt % cetyltrimethyl ammonium bromide (CTAB)/50.4% n-butanol), hexadecane, and water. The nonionic emulsifier consisted of 65.7% polyoxyethylene (10) oleyl ether (Brij 96) and 34.4% n-butanol, again with hexadecane and water. In both systems, microemulsion (μE) compositions used were obtained by diluting an initial 90 weight percent (%) emulsifier/10% oil mixture with varying amounts of water. Microemulsion samples thus obtained had final compositions of 30 to 80% water. Phase maps describing these systems have been published (10-11).

N-dodecyl 3-carbamoyl pyridinium bromide (I) was prepared from vacuum-distilled n-dodecyl bromide (K&K) and nicotinamide (Kodak) according to a published procedure (15) and identified by IR spectrum and melting point (218–220°C). The molar extinction coefficient of (I) at 264.5 nm was determined as $4120 \text{ m}^{-1} \text{ cm}^{-1}$ (methanol), 4250 (water), and 4220 (60% water CTAB μE). Fisher technical grade CTAB was recrystallized before use (16). Brij 96, obtained from Sigma, was neutralized and deionized before use (17) to remove buffering impurities. Aldrich reagent grade KCN, Aldrich 99% hexadecane, Aldrich gold label n-butanol (99 + %), and Fisher certified 0.200 N and 0.0200 N NaOH were used as received.

Kinetics. The reaction of N-dodecyl 3-carbamoyl pyridinium bromide (I) with cyanide ion in the microemulsions was observed by following the 340 nm absorption maximum of the 4-cyano adduct (II). See equation (1). Following the work of Bunton, Romsted and Thamavit in micelles (2), a 5/1 mole ratio of KCN to NaOH was employed to prevent cyanide hydrolysis. The pH of each reaction mixture was measured on a Coleman 38A Extended Range pH meter to insure that the system was sufficiently basic to allow essentially complete ionization of the cyanide. The appropriate amounts of cyanide and hydroxide were added to the microemulsion sample within 10 minutes of running a reaction. Cyanide concentration varied between 0.02 and 0.08 M with respect to the water content. Substrate was injected via a Unimetrics model 1050 syringe directly into a known volume of the μE -nucleophile mixture in a 1.0 cm UV quartz cell. Absorbance at 340 nm was followed as a function of time on a Perkin-Elmer model 320 spectrophotometer at $25.0 \pm 0.3^\circ\text{C}$. Since the initial bulk concentration of substrate was 10^{-4} M , cyanide was always present in considerable excess.

The reaction is reversible (12–13). However, it was possible to monitor approximately 60 percent of the reaction without any significant contribution from the reverse reaction. At most μE compositions, infinite-time absorbance readings could be obtained by the addition of small amounts of solid KCN. For those compositions which could not be forced to completion, the average value of the available final (infinite time) absorbance measurements in the μE system was used with only a small decrease in the accuracy of the results. It is known that rearrangement (12–13) or hydrolysis (14) of the product (II) may occur in various media. In our experiments, however, these secondary reactions did not interfere with observation of the reaction of interest over the time span involved. Also, hydroxide was not found to react appreciably with the substrate (I) at the concentrations employed.

As a check on the method, the reaction was run in aqueous CTAB micelles. The results obtained were in agreement ($\pm 5\%$) with

those previously reported (2, 15). It should also be noted that the molar extinction coefficient which corresponds to our infinite-time absorption measurements in the above CTAB ($7100 \text{ M}^{-1}\text{cm}^{-1}$) and Brij ($6900 \text{ M}^{-1}\text{cm}^{-1}$) μE systems corresponds closely to the extinction coefficient ($7120 \text{ M}^{-1}\text{cm}^{-1}$) obtained for the hexadecyl analog of (II) in CTAB micelles (15).

At each composition, at least three separate runs were performed. In most cases, the reported rate constant is the average of four to five runs and up to eight runs were carried out at some compositions. In all cases, the (n-1) standard deviation was less than 15%, and most often 10% or less.

Effect of Ionic Strength. Both μE systems were examined for ionic strength effects. Microemulsion compositions were prepared at 70% water, with a cyanide concentration of 0.032 M with respect to the water content. Potassium bromide was used to vary the ionic strength of the reaction mixtures. Ionic strength in the CTAB μE was varied from 0.04 to 0.34. Since the Brij μE tolerated a much higher salt concentration without phase separation, ionic strength in that system was varied between 0.04 and 1.80. As will be seen, the Brij system exhibits a salt effect, while the CTAB μE does not. Rate constants obtained for reaction (1) in the Brij μE were therefore corrected to take into account the effect of ionic strength in that system (vide infra).

Results

Kinetics. With nucleophile present in large excess, pseudo-first-order rate constants were obtained for reaction (1) in both μE systems employed. As already noted, the reverse and the possible successive reactions did not interfere with observation of the reaction of interest over the observed time span. The levels of hydroxide ion employed held the pH in the reaction mixtures at 11.8 or greater, thus insuring essentially complete ionization without itself producing any significant reaction.

The reaction is second order overall. The second order rate constant corrected for phase distribution of cyanide ion, $k_{2\phi}$, is given by $k_1/(\text{CN}^-)_w$, where k_1 is the observed pseudo-first-order rate constant and $(\text{CN}^-)_w$ is the concentration of cyanide ion with respect to the water content. Polarographic data on the N-dodecyl-3-carbamoyl pyridinium ion in μE shows that the substrate is completely associated with the hydrophobic region (18), making it unnecessary to consider the effect of phase distribution of substrate on the measured reaction rate. The kinetic results are summarized in Table I. The microemulsion composition is expressed as phase volume $\phi = 1 - wg$, where w is the weight fraction of water and g is the specific gravity of the μE .

Table I. Phase volume corrected second order rate constants ($k_{2\phi}$) as a function of phase volume (ϕ) for the reaction of cyanide with N-dodecyl-3-carbamoyl-pyridinium ion in CTAB and Brij 96 microemulsions

ϕ	CTAB ^a	BRIJ ^b
0.73	0.067	1.10
0.63	0.077	0.67
0.53	0.094	0.67
0.43	0.13	0.55
0.32	0.18	0.54
0.23	0.29	0.53

a. $M^{-1}s^{-1}$. Average standard deviation \pm 10%.

b. $M^{-1}s^{-1}$. Average standard deviation \pm 12%.

As expected, $k_{2\phi}$ increases by a factor of 4 with decreasing phase volume in the CTAB μ E over the composition range studied (Figure 1). In the Brij system $k_{2\phi}$ quickly becomes approximately linear (within experimental accuracy) at the various compositions. An anomalously high value in the Brij μ E occurs at $\phi = 0.72$. In this high-emulsifier region, however, the μ E may have a different structure.

The average rate constant in the nonionic μ E is, however, considerably higher than all the rate constants in the cationic system, rather than lower. As discussed above, this is due to the effect of ionic strength on the reaction rate and a correction must be made for it if a meaningful comparison of the data is to be made. The dependence of the rate constant $k_{2\phi}$ on the ionic strength (I) is shown in figure 2. Within experimental error, $-\log k_{2\phi} = 0.78 I + 0.16$. In order to estimate the value of I to employ for the correction, it was assumed that the reaction took place in an outer shell (e.g. Stern Layer) of thickness s using a droplet radius of 34A and corrected for the fraction of free counterion α . The value of I thus obtained varied with water content since α varies with ϕ . However, the variation was not significant, and an average value of I of 3.0 ($s = 4A$) and 6.0 ($s = 2A$) was used. The corrected values of $k_{2\phi}$ for Brij were 0.03 and 0.01 $M^{-1}s^{-1}$ respectively (Figure 1).

Reaction models. The effective surface potentials (ψ_ϕ) as defined by equation (2) are given in Table II, along with the values of α . The values of ψ_ϕ for the reaction of p-nitrophenyl diphenyl

$$k_{2\phi}(\text{CTAB})/k_{2\phi}(\text{Brij, corrected}) = \exp(e\psi_\phi/kT) \quad (2)$$

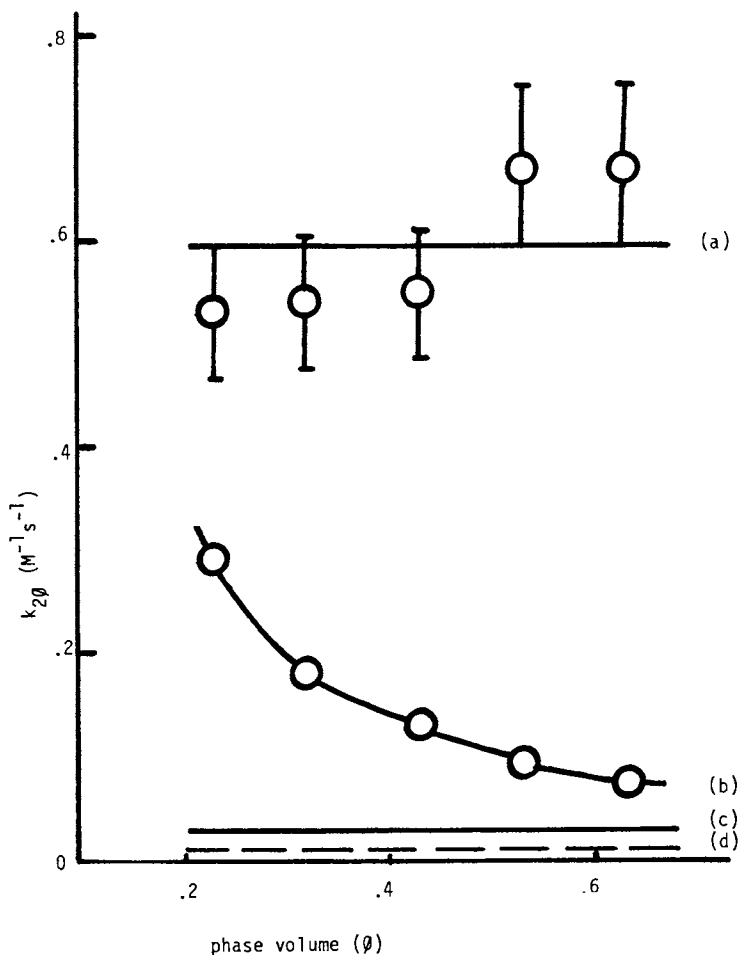


Figure 1. Phase volume corrected rate constant ($k_{2\phi}$) vs. phase volume (ϕ) for the N-dodecylnicotinamide-cyanide reaction in (a) Brij μ E and (b) CTAB μ E. Curves (c) and (d) are the ionic strength corrected Brij rate constants for Stern layer thicknesses of 4A and 2A, respectively (vide text).

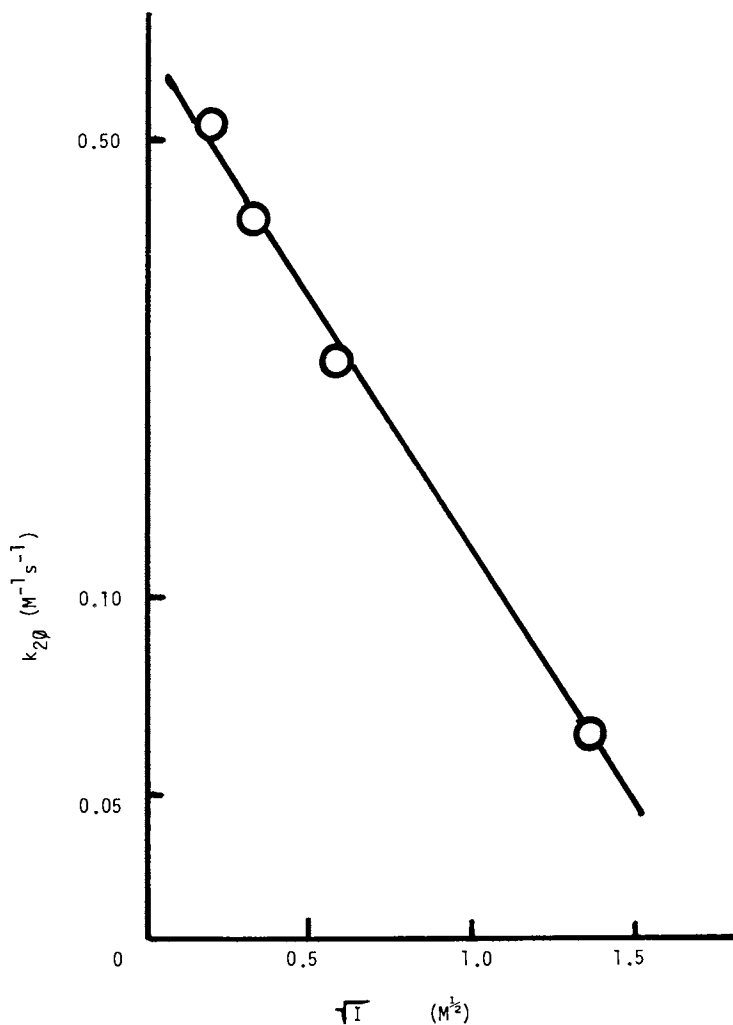


Figure 2. Dependence of the rate constant ($k_{2\phi}$) for the cyanide reaction (c.f. figure 1) in Brij μ E at a phase volume $\phi = 0.32$ on ionic strength (I) adjusted by means of added potassium bromide.

phosphate (PNDP) are also presented for purposes of comparison. It is immediately evident that the values of ψ_ϕ using $s = 4A$ for

Table II. Effective surface potential (ψ_ϕ) and degree of dissociation (α) as a function of phase volume (ϕ)

ϕ	α^a	$(\text{CN}^-)^{b,c}$	$(\text{CN}^-)^{b,d}$	$(\text{OH}^-)^e$	$(\text{F}^-)^e$
.63	.10	48	20	26	30
.53	.12	53	25	30	33
.43	.14	66	38	34	36
.32	.16	76	48	41	43
.23	.18	88	60	49	54

- a. reference 18.
 b. substrate N-dodecyl-3-carbamoyl pyridinium bromide.
 (ψ_ϕ in mV. \pm 22%).
 c. $s \pm 2A^\circ$.
 d. $s = 4A^\circ$.
 e. substrate PNDP (ψ_ϕ in mV, \pm 20%).

cyanide are comparable to those for fluoride and hydroxide, and thus consistent with the ESP model. The values for $s = 2A$ are higher, as would be expected based on the IE model. Additional insight may be obtained from an attempt to fit the data to equation (3), obtained from the microemulsion IE model (8).

$$\psi_\phi = \frac{kT}{e} \left\{ \ln \left[\left(\frac{1-\phi}{\phi} \right) \left(\frac{K_\phi}{1+K_\phi} \right) \right] + \ln \frac{r}{3s} \right\} \quad (3)$$

Here, $K_\phi = K_{IE} (1-\alpha)/\alpha$, $kT/e = 25.6$ mV at 25°C , and all other symbols have their previously defined meanings. A plot of ψ_ϕ vs $\ln \left[\frac{(1-\phi)/\phi}{K_\phi/(1+K_\phi)} \right]$ using the data in Table II is shown in Figure 3 for three different values of K_{IE} . The values of the slope and the value of s calculated from the intercept using the theoretical slope of 25.6 mV and a radius of 34A are given in Table III.

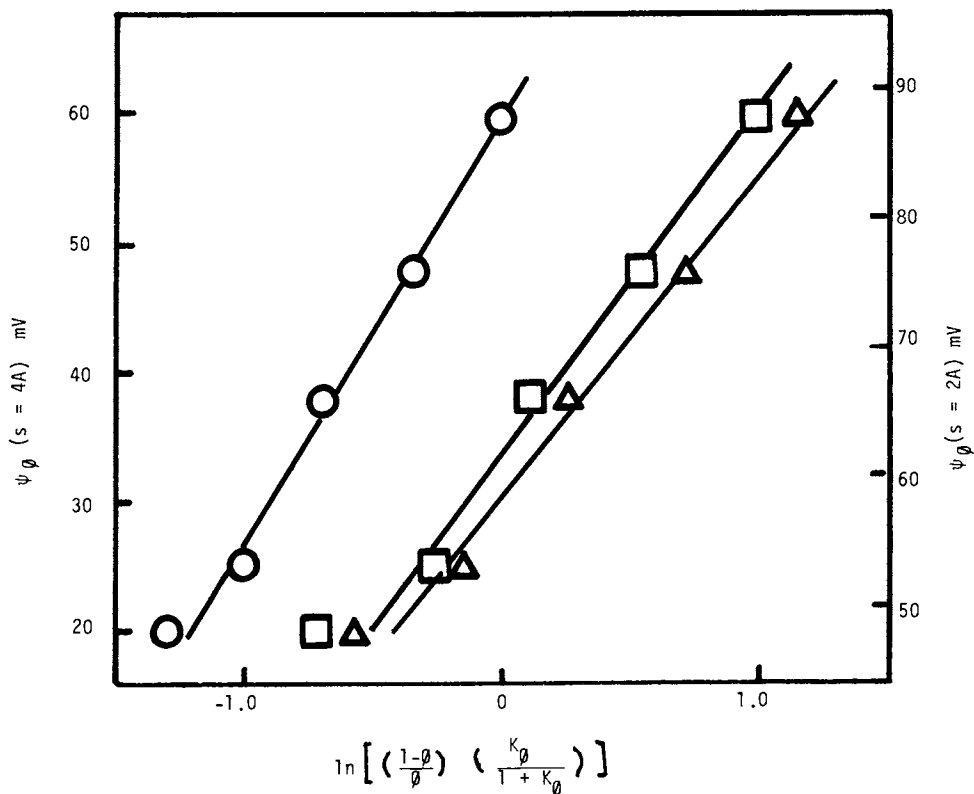


Figure 3. Ion-exchange model plot (vide text). The data are for values of K_{IE} of 0.1 (circles), 1.0 (squares), and 10 (triangles).

Table III. Values of the slope and reaction region thickness (s) for the values of K_{IE} from figure 3.

K_{IE}^a	Slope (mv)	Thickness (A) ^b	
		S = 2A	S = 4A
0.1	34	0.4	1.1
1.0	26	1.0	3.0
10	25	1.2	3.5

a. $K_{IE} = (\text{CN}^-)_{\text{free}} (\text{Br}^-)_{\text{Stern}} / (\text{CN}^-)_{\text{Stern}} (\text{Br}^-)_{\text{free}}$

b. Determined using values of ψ_ϕ obtained from the ionic strength corrected Brij $k_2\psi_\phi$ values, where I was estimated assuming a thickness $s = 2A$ or $4A$.

The values of s obtained from the higher set of ψ_ϕ values are unrealistically small. The values of the slope and s for $K_{IE} = 1$ using the lower ψ_ϕ values are acceptable, but again this set of ψ_ϕ values is also in accord with the ESP model.

The major difficulty here is of course the ionic strength effect. It is clear that a reasonably definitive test of the model will require a reaction which (a) is relatively insensitive to ionic strength and (b) can employ the same oil soluble substrate with reactant ions of widely varying K_{IE} , preferably over two orders of magnitude. It should be noted that the pyridinium ion substrate is more water soluble than the ester, and in addition has a positive charge. This may result in the protrusion of part of the head group out of the Stern layer, which in turn means that the nucleophile concentration should be governed by the ESP model. There is precedent for this type of behavior in the reaction of an alkylated pyridine derivative with hydroxide in an anionic system (19). A neutral, oil soluble substrate such as the ester may be more likely to react in the Stern layer. This is illustrated in Figure 4. There may also be substrate - nucleophile systems which are distributed such that they exhibit behavior intermediate between the two extremes of the IE and ESP models.

Conclusion

The rate constants for the reaction of N-dodecyl-3-carbamoyl-pyridinium ion with cyanide in both cationic and nonionic o/w microemulsions have been measured as a function of phase volume. Added salt has no effect in the cationic system, but the rate constants in the nonionic system depend upon ionic strength as would be expected for a reaction between two ions. In order to compare the two microemulsions, the ionic strength in the reaction region has been estimated using thicknesses of 2-4A. The former produces values of the effective surface potential which yield

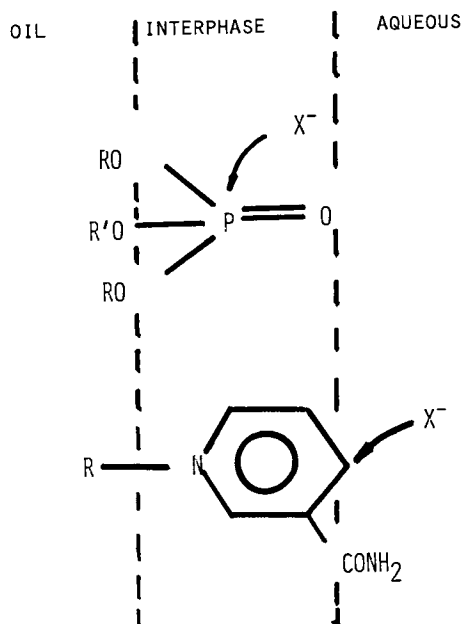


Figure 4. Schematic diagram illustrating the attack of an anionic nucleophile on a substrate located in an interface with a net positive charge, where the attack occurs (a) in the Stern layer or (b) in the double layer.

small s values, while the latter yield reasonable s values but are also in accord with the ESP model. It must be concluded that at present there is no compelling evidence in favor of the IE model. Definitive experiments must utilize the employment of substrate - nucleophile combinations which meet the criteria discussed above.

Acknowledgment. The authors wish to thank Dr. N. S. Dixit for valuable technical assistance, and the US Army Research Office for financial support.

Literature Cited

1. Chaimovich, H.; Bonilha, J.B.S.; Politi, M.J.; Quina, F.H. J. Phys. Chem. 1979, 83, 1851.
2. Bunton, C.A.; Romsted, L.S.; Thamavit, C. J. Am. Chem. Soc. 1980, 102, 3900.
3. Quina, F.H.; Politi, M.J.; Cuccovia, I.M.; Baumgarten, E.; Martins-Franchetti, S.M.; Chaimovich, H. J. Phys. Chem. 1980, 84, 361.
4. Bunton, C.A.; Romsted, L.S.; Sepulveda, L. ibid, 1980, 2611.
5. Bunton, C.A.; Romsted, L.S.; Savelli, G. J. Am. Chem. Soc. 1979, 101, 1253.
6. Bunton, C.A.; Frankson, J.; Romsted, L.S. J. Phys. Chem. 1980, 84, 2607.
7. Rupert, L.A.M.; Engberts, J.B.F.N. J. Org. Chem. 1982, 47, 5015.
8. Mackay, R.A. J. Phys. Chem. 1982, 86, 4756.
9. Mackay, R.A., in proceedings of 4th International Symposium on Surfactants in Solution, Lund, Sweden, 1982. Plenum Press, Mittal, K.L., ed, in press.
10. Hermansky, C.; Mackay, R.A., in "Solution Chemistry of Surfactants", Mittal, K.L., ed, Plenum Press, NY 1979.
11. Hermanski, C.; Mackay, R.A. J. Coll. Interface Sci., 1980, 73, 324.
12. Bruice, T.C.; Benkovic, S.J. "Bioorganic Mechanisms", Chapter 9, W.A. Benjamin, New York, 1966.
13. Lindquist, R.N.; Cordes, E.H. J. Am. Chem. Soc. 1968, 90, 1269.
14. Rappaport, Z., in "Chemistry of the Cyano Group", Patai, S., ed., Interscience, New York, 1970.
15. Baumrucker, J.; Calzadilla, M.; Centeno, M.; Lehrmann, G.; Urdaneta, M.; Lindquist, P.; Dunham, D.; Price, W.; Sears, B.; and Cordes, E.H. J. Am. Chem. Soc., 1972, 94, 8164.
16. Mukerjee, P.; Mysels, K.L. J. Org. Chem. 1955, 77, 2937.
17. Mackay, R.A.; Hermansky, C. J. Phys. Chem. 1981, 85, 739.
18. Mackay, R.A., in "Microemulsions", Robb, I.D. ed., Plenum Press, London, 1982.
19. Mackay, R.A.; Dixit, N.S. and Agarwal, R. "Inorganic Reactions in Microemulsions", ACS Symposium Series No. 177, Holt, S.L. ed., 1982, 179-194.

RECEIVED January 20, 1984

Interactions of Nonionic Polyoxyethylene Alkyl and Aryl Ethers with Membranes and Other Biological Systems

ALEXANDER T. FLORENCE, IAN G. TUCKER¹, and KENNETH A. WALTERS²

Department of Pharmacy, University of Strathclyde, Glasgow G1 1XW, Scotland

Many nonionic surfactants of the poly(oxyethylene) alkyl and aryl ether class interact with biological membranes increasing their permeability and causing increased trans-membrane solute transport. The mechanisms of such effects are not fully understood. Studies of the interaction of homologous series of nonionic surfactants (varying either in hydrophobic or hydrophilic chain length) with a variety of biological substrates, reviewed here, indicate there to be an optimal lipophilicity for maximal membrane activity. Problems with the hydrophile-lipophile balance (HLB) as an index of lipophilicity result from the structural non-specificity of this value. The biological effects of surfactants are concentration dependent and structure dependent. In many cases C₁₂ hydrocarbon chain compounds appear to exert maximal effects and in all series a parabolic relationship between membrane activity and lipophilicity is observed. The effects are complex resulting from penetration of the membrane, its fluidization and, at high surfactant concentrations, solubilization of structural components.

Many formulated food and pharmaceutical products contain nonionic surfactants as emulsifiers, suspending, wetting or solubilizing agents (1). As nonionic surface active agents may have intrinsic biological activity or may influence the biological activity of other molecules the optimisation of formulations cannot be carried out without consideration of the biological

¹Current address: C.S.I.R.O. Division of Animal Production, Box 239, Blacktown 2148, Australia

²Current address: Fisons Pharmaceuticals plc, Loughborough, England

properties of the surfactants and indeed the whole formulation.

It has been recognised for some time (see for example reference 1), that surfactants can increase the rate and extent of transport of solute molecules through biological membranes by fluidisation of the membrane. It is only recently, however, that sufficient work has been carried out to allow some analysis of structure-action relationships. In this overview an attempt is made, by reference to our own work and to work in the literature, to define those structural features in polyoxyethylene alkyl and aryl ethers which give rise to biological activity, especially as it is manifested in interactions with biomembranes and subsequent increase in the transport of drug molecules. This paper is largely confined to the alkyl and aryl polyoxyethylene ethers, as these form series variable in both hydrophobic and hydrophilic chain length, and hence HLB, with minimal structural variation.

Structure-activity relationships are generally applied in the pharmaceutical sciences to drug molecules. The value of any structure-activity correlation is determined by the precision of the biological data. So it is with studies of the interaction of nonionic surfactants and biomembranes. Analysis of results is complicated by the difficulty in obtaining data in which one can discern small differences in the activity of closely related compounds, due to i) biological variability in tissues and animals, ii) potential differential metabolism of the surfactants in a homologous series (2), iii) kinetic and dynamic factors such as different rates of absorption of members of the surfactant homologous series (2) and iv) the typically biphasic concentration dependency of nonionic surfactant action (3). Few, if any, of the studies of the biological properties of nonionic surfactants have been carried out with purified non-ionic poly(oxyethylene) ethers, rendering comparison of work from different laboratories somewhat difficult. Nevertheless it is clear from the work reviewed here that in homologous series of surfactants with constant ethylene oxide chain length, there will be found an optimal hydrocarbon chain length for biological activity, most often C₁₂, and given a constant hydrophobic chain length, an optimal hydrophilic chain length will be observed. (Figure 1a,b). As in most work on structure-activity relationships of drug series a parabolic activity curve is also obtained with nonionic surfactant series, (Figure 1c), so it appears that data on surfactant activity fits conventional wisdom. However, with drug molecules increasing biological activity is always found with increasing lipophilicity (log P) until beyond the maximum (log P₀) a decrease in activity is brought about by limitations in solubility, protein binding, drug association etc. Not all of the surfactants considered in this paper are freely soluble, e.g. the E₂ derivatives are dispersible at the 0.1% level, and C₁₆E₁₀ and C₁₈E₁₀ have solubilities below 1%.

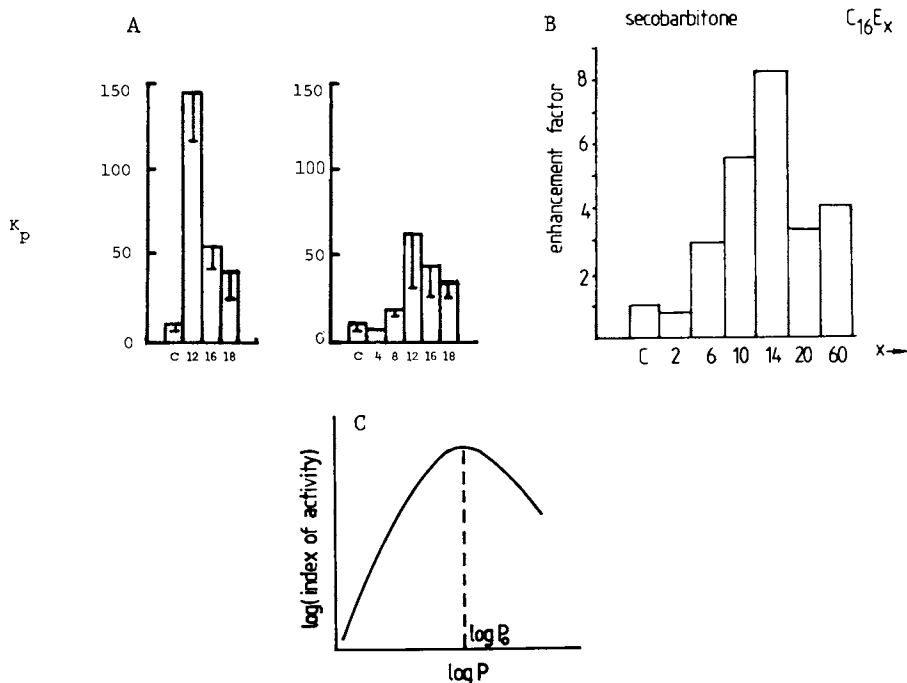


Figure 1.

- a) The effect of hydrocarbon chain length of (left) 1% C_xE₁₀ and (right) 1% C_xE₂₀ on paraquat transport through isolated rabbit gastric mucosa. (Walters, Dugard and Florence, 1981).
- b) The increase in the absorption of secobarbital in goldfish in the presence of 0.1% C₁₆E_x alkyl ethers as a function of ethylene oxide chain length, x. (Walters, Florence and Dugard, 1982a).
- c) An idealised log (activity) - log P profile showing optimal biological activity at a partition coefficient of P₀.

However the reduction in biological activity with increasing hydrocarbon chain length beyond the optimum (Figure 1a) and the increase in biological activity on initially increasing the hydrophilic nature of the surfactants (Figure 1b) requires elucidation, especially at lower concentrations.

Studies with homologous series of alkyl and aryl polyoxyethylene ethers

In this section several recently published studies on the interaction of nonionic surfactants with a variety of biological systems, including enzymes, bacteria, erythrocytes, leukocytes, membrane proteins, low density lipoproteins and membranes controlling absorption from the gastrointestinal tract, nasal and rectal cavities, will be assessed. This is a selective account, work having been reviewed that throws light on structure-activity relationships and on mechanisms of surfactant action.

Reference will be made to the hydrophile-lipophile balance (HLB) of the surfactants studied as a convenient index of hydrophilicity. Early attempts to observe correlations between activity and HLB include those by Marsh and Maurice (4) and Florence and Gillan (5, 6). Marsh and Maurice found that the compounds most efficient in effecting increased penetration of fluorescein into the anterior chamber of the eye had HLB values in the range 16-17, but several surfactants with HLB numbers in that range were inactive or poorly active. Florence and Gillan (5) proposed from work on the goldfish (*Carassius auratus*) gill membrane that "bulky" surfactants had low membrane activity and suggested that there might be a physical blocking mechanism as a result of the adsorption at the membrane surface of long chain ethylene oxide derivatives.

The difficulty with HLB as an index of physicochemical properties is that it is not a unique value, as the data of Zaslavsky *et al.* (7) on the haemolytic activity of three alkyl mercaptan polyoxyethylene derivatives clearly show in Table 1. Nevertheless data on promotion of the absorption of drugs by series of nonionic surfactants, when plotted as a function of HLB do show patterns of behaviour which can assist in pin-pointing the necessary lipophilicity required for optimal biological activity. It is evident however, that structural specificity plays a part in interactions of nonionic surfactants with biomembranes as shown in Table 1. It is reasonable to assume that membranes with different lipophilicities will "require" surfactants of different HLB to achieve penetration and fluidization; one of the difficulties in discerning this optimal value of HLB resides in the problems of analysis of data in the literature. For example, Hirai *et al.* (8) examined the effect of a large series of alkyl polyoxyethylene ethers (C₄, C₈, C₁₂ and C₁₂ series) on the absorption of insulin through the nasal mucosa of rats. Some results are shown in Table II.

Table I. Haemolytic activity of some nonionic surfactants

$R_m S (OCH_2CH_2)_n OH$	m	n	HLB	C*
	8	8	12.6	10.7
	10	10	12.6	30.0
	12	12	12.6	2.9

from B. Yu Zaslavsky *et al.* (1978) *Biochim.Biophys.Acta*, 507,1.

*concentration required to produce 50% haemolysis compared with concentration of standard $R_{12}S (OCH_2CH_2)_7.8OH$ required to do the same.

Table II. Effect of 1% nonionic surfactants on nasal absorption of insulin in rats

Surfactant	HLB	n	D%*
Control	-		6.0 ± 0.9
$C_{12}E_5$	8.6	5	59.3 ± 3.0
$C_{12}E_9$	11.5	9	60.9 ± 2.9
$C_{12}E_{10}$	12.1	4	63.3 ± 2.5
$C_{12}E_{20}$	15.5	5	50.8 ± 2.3
$C_{16}E_5$	7.2	4	13.5 ± 3.6
$C_{16}E_{10}$	10.6	4	64.0 ± 1.3
$C_{16}E_{20}$	14.1	4	54.6 ± 2.4

from S. Hirai *et al.* *Int. J. Pharmaceutics*, 1981, 9, 165.

*D is the percentage decrease in glucose levels. n = number of experiments.

In the C_{12} series optimum activity is seen with the $C_{12}E_{10}$ compound (HLB 12.1), whereas in the C_{16} series the peak activity is achieved with $C_{16}E_{10}$ whose HLB is only 10.6. This might be explained by the fact that the $C_{16}E_{14}$ compound with an HLB of 12.8 was not included in the study. These data when combined produces impressive corroboration of the previously suggested parabolic behaviour (see Figure 2).

Results with some esters are included in Figure 2. The activity of the esters is generally lower possibly due to their rapid metabolism (hydrolysis) in the mucosal layer. Also it is evident on close examination of the data that (as with the data

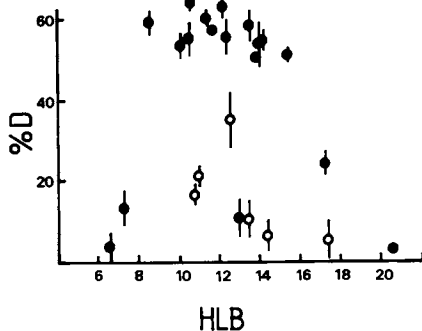


Figure 2.

Relationship between HLB values of nonionic surfactant ethers and esters and the nasal absorption of insulin (10U/kg) in rats measured as a percentage reduction (D) in glucose levels from 0-4h. Surfactant applied at a concentration of 1%. ● ethers, ○ esters. Data redrawn from Hirai et al. (1982a) as mean datum points \pm SE n = 4-9.

of Marsh and Maurice (4) some apparent anomalies occur in the ether series. The low activity of two surfactants with HLB values of 13.7 and 16.8 represent C_4 compounds with short ethylene oxide chains; this is in agreement with the previously demonstrated lack of activity of short hydrocarbon chain analogues. (Figure 1).

The promotion of insulin absorption from the rectal cavity has been studied by Touitou *et al.* (9). Figure 3 illustrates the marked influence of ethylene oxide chain length in the C_{12} series and of alkyl chain length in the C_xE_9 series. This striking demonstration of the structural dependence of activity is indicated with the loss of activity when the $C_{12}E_{25}$ and $C_{12}E_{40}$ compounds are used. Here $C_{12}E_9$ appears to be the most active of the series in promoting insulin absorption, although time dependent effects make it appear (see Figure 3) that another compound ($C_{16}E_9$) is more active. This may point to differences in the rate of absorption and interaction.

Several studies indicate the special nature of the dodecyl chain in interactions with a variety of biomembranes: Zaslavsky's (7) data on the haemolysis caused by alkyl ethers, our own data (10) on the absorption of paraquat by gastric mucosa, Walters and Olejnik's (11) data on methyl nicotinate transfer through hairless mouse skin. All indicate maximal activity residing with the C_{12} ether. Not only do the latter two studies indicate a falling off in effectiveness as the chain length is increased to C_{16} and C_{18} but they also indicate that the oleyl (unsaturated chain) ethers are more active than their saturated analogues.

In some biological systems nonionic surfactants have an intrinsic biological activity; the C_{12} alkyl ethers were too toxic to be used in the experiments of drug absorption with goldfish. The activity of the C_{12} ethers was quantified by measurement of the fish turnover time, T . When the reciprocal of the turnover time is plotted against alkyl chain length for the series C_x and E_{10} and C_{12} compound is distinguished by its marked effect. (12).

In all of these data what requires explanation is the effectiveness of the dodecyl chain, the decreasing activity with increasing ethylene oxide chain length above E_{10-14} the increase in activity when we move from a very hydrophobic surfactant with short ethylene oxide chain to the optimum, and the decrease in activity with increasing lipophilicity of compounds with alkyl chain lengths greater than C_{12} .

Penetration of the biomembrane is undoubtedly essential for most membrane activity. Araki and Rifkind (13) obtained esr spectra of stearic acid spin labelled erythrocyte membranes in the presence of diverse compounds including Triton X100, chlorpromazine and glutaraldehyde. The two surfactants chlorpromazine and Triton X100 both increase the rate of haemolysis and are shown to increase membrane fluidity. Glutaraldehyde as expected decreases fluidity and decreases the rate of haemolysis.

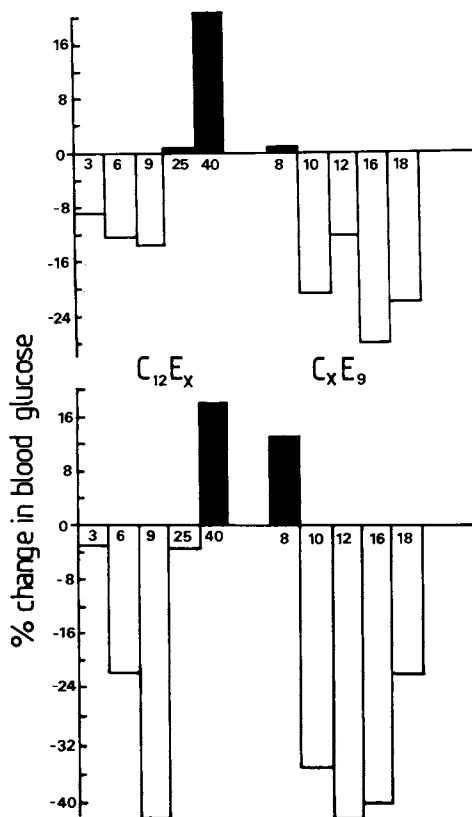


Figure 3.

The influence of hydrophilic chain length and alkyl chain length of a series of alkyl ethers ($C_{12}E_x$ and C_xE_9 respectively) on the percentage change in blood glucose on administration rectally of insulin with the surfactants. The upper plot shows the results 30 minutes after administration and the lower plot results after 60 minutes. (Redrawn from data in Touitou *et al*, 1978).

Surfactant lipophilicity

Penetration of the surfactant demands a certain minimum lipophilicity. Partitioning of nonionic surfactants into simple organic phases has been measured for a limited range of nonionics. Crook *et al.* (14) and Harusawa *et al.* (15, 16) have studied the partition coefficients (P) of homogeneous octyl phenyl ethers and nonyl phenyl ethers, the former between isooctane and water at 25° and the latter between cyclohexane and water. Harusawa *et al.* (16) observe, assuming a linear relationship between $\log P$ and ethylene oxide chain length (n):

$$\log P = 5.19 - 0.418n$$

Using this relationship one can calculate $\log P$ values of the nonyl phenyl ethoxylates used by Cserhati *et al.* (17) in their study on the effect of the surfactants on the growth of *Coronilla rhizobium* and *Bacillus subtilis* var *niger* and interaction with dipalmitoyl phosphatidylcholine liposomes containing tracer amounts of ^{42}KCl . Results on growth inhibition of the organisms and efflux of ^{42}K from the liposomes are plotted as a function of $\log P$ in figure 4.

These results are obtained with a constant hydrophobic head group, whereas most activity - $\log P$ plots in biological (drug) systems are derived by variation of this head group. The nature of the membrane interacting with the surfactant will play a role in determining the optimal lipophilicity, $\log P_0$; peak activity is noted in *C. rhizobium* at $\log P_0 = 1.0$, in the liposomes at $\log P_0 = 1.55$ and in *B. subtilis* at 1.90. While such shifts can indicate the differing degrees of hydrophobic nature of the target membrane they can also reflect differences in the structure of the barrier membrane. (18).

Concentration dependence of effects

Fig. 5 shows the concentration dependence of the effect of three alkyl polyoxyethylene ethers, C_{16}E_2 , $\text{C}_{16}\text{E}_{10}$ and $\text{C}_{16}\text{E}_{20}$, on the absorption of secobarbitone by the goldfish. The latter two compounds are active at very low temperatures. No obvious change in activity occurs at the critical micelle concentrations of the surfactants. Other data appended to the graph are the areas/molecule of the surfactant at the air water interface (27,110 and 148\AA^2 respectively) and calculated $\log P$ values using π values from Hansch (19). Calculated values are only valid below the CMC as Harusawa's (16) data shows. It must be assumed, therefore, that because of the lack of effect of C_{16}E_2 on this system at any concentration in spite of its extreme lipophilicity, a certain degree of amphipathicity is required for activity. This may be because the site of action of the surfactant is not directly

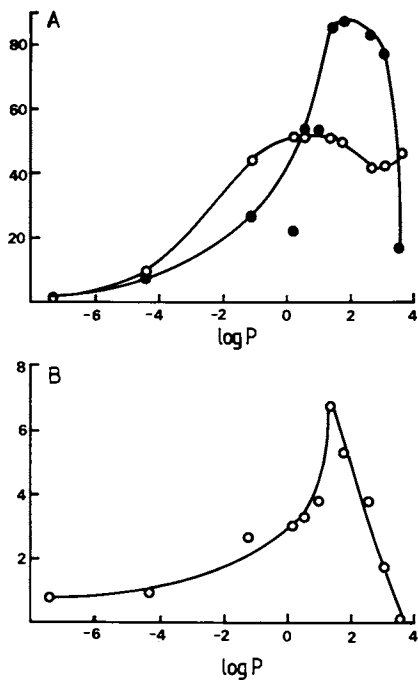


Figure 4.

Results of Cserhati et al. (1982) plotted as a function of the calculated log P of the surfactants used A) in determining the % reduction in growth of ● B. subtilis var niger and ○ C. rhizobium and B) the change in efflux of ^{42}K from liposomes prepared from dipalmitoyl phosphatidyl choline.

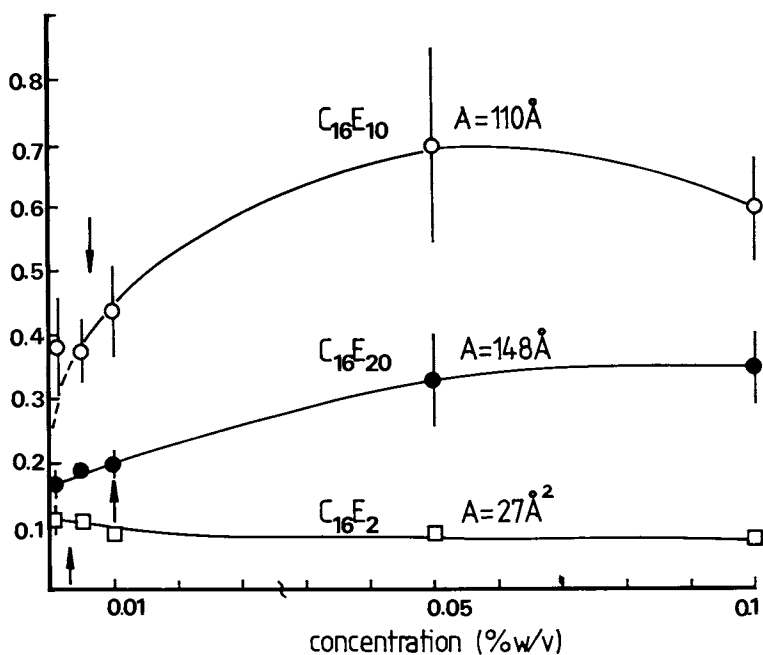


Figure 5.

Concentration dependent effects of surfactants $C_{16}E_2$, $C_{16}E_{10}$ and $C_{16}E_{20}$ on the reciprocal turnover times (T^{-1} , min^{-1}) of goldfish in the presence of secobarbital showing the areas/molecule of the surfactants at the air/water interface and calculated log P values for the surfactant molecules. Data from Walters, Florence and Dugard, (1982b).

on the lipid bilayer but may be mediated by adsorption and interaction with membrane proteins. $C_{16}E_2$ is however not freely soluble and its dispersion rather than solution might complicate interpretation. Tiddy has, in fact, suggested (20) that the existence of lamellar mesophases in short ethylene oxide chain species might account for the low biological activity. Mitchell *et al.* (21) have studied the phase behaviour of a range of pure C_mE_n compounds ranging from C_8 to C_{16} . Whereas normally they appear only at high concentrations, mesomorphous L_α phases exist over a large concentration range for $C_{16}E_4$. Extensive L_α phases occur only with surfactants with less than 5 ethylene oxide units. The L_α phase is extremely sensitive to ethylene oxide chain length as $C_{12}E_4$ has an extensive lamellar phase at 37° while $C_{12}E_5$ does not. The meltingpoints of the L_α phase are shown in Figure 6 as a function of hydrocarbon chain length and hydrophilic chain length; there is an interesting structural dependence here which might well throw light on the interactions of the molecules with the lipid bilayer.

Evidence from studies on the penetration of cholesterol monolayers by nonionic surfactants of two Brij series suggests penetration occurs at extremely low concentrations (22), the C_{12} compounds interacting at lower concentrations than C_{18} compounds. (Figure 7).

Haemolytic activity and the permeability-enhancing activity of nonionic alkyl ethers correlate well (23). Ponder in his classic work on haemolysis (24) has proposed that haemolysis by surfactants involves various stages viz, i) approach of the surfactant, ii) contact with surface i.e. adsorption, iii) reorientation of the molecule to allow film penetration and iv) "complex" formation in the membrane bilayer. This complex may either remain part of the altered surface ultrastructure or may become detached and solubilized in the external phase. Adsorption and membrane changes are essential but do not necessarily follow. Dahlgren *et al.* (25) used a series of fatty acid (C_2 - C_{18}) esters of polyoxyethylene glycol 6000 to modulate the activity of polymorphonuclear leukocytes. Binding first becomes apparent with the C_{12} derivative but as expected increases with increasing hydrocarbon chain thereafter, yet the C_{14} derivative was most effective in causing the release of the superoxide anion, a measure of the activation of cell metabolism. Superoxide production was negligible below C_{12} .

The question of optimal hydrocarbon chain length

In many of the experiments described C_{12} compounds have generally proved to be most active when a series of surfactants with identical hydrophilic tails are studied. Schott (26) suggested that the particular effectiveness of the lauryl surfactants is due to the balance of two properties. As the homologous series is ascended the lipophilicity of the compounds

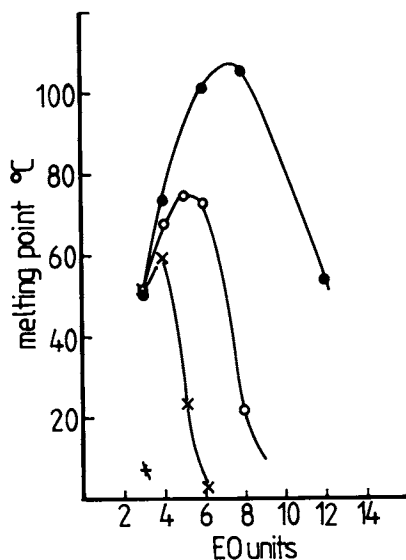


Figure 6.

The melting point of the L mesomorphic phase of alkyl ether nonionic surfactants taken from the results of Mitchell et al. (1983) showing the influence of alkyl and hydrophilic (EO) chain lengths.

● C₁₆; ○ C₁₂; × C₁₀; + C₈.

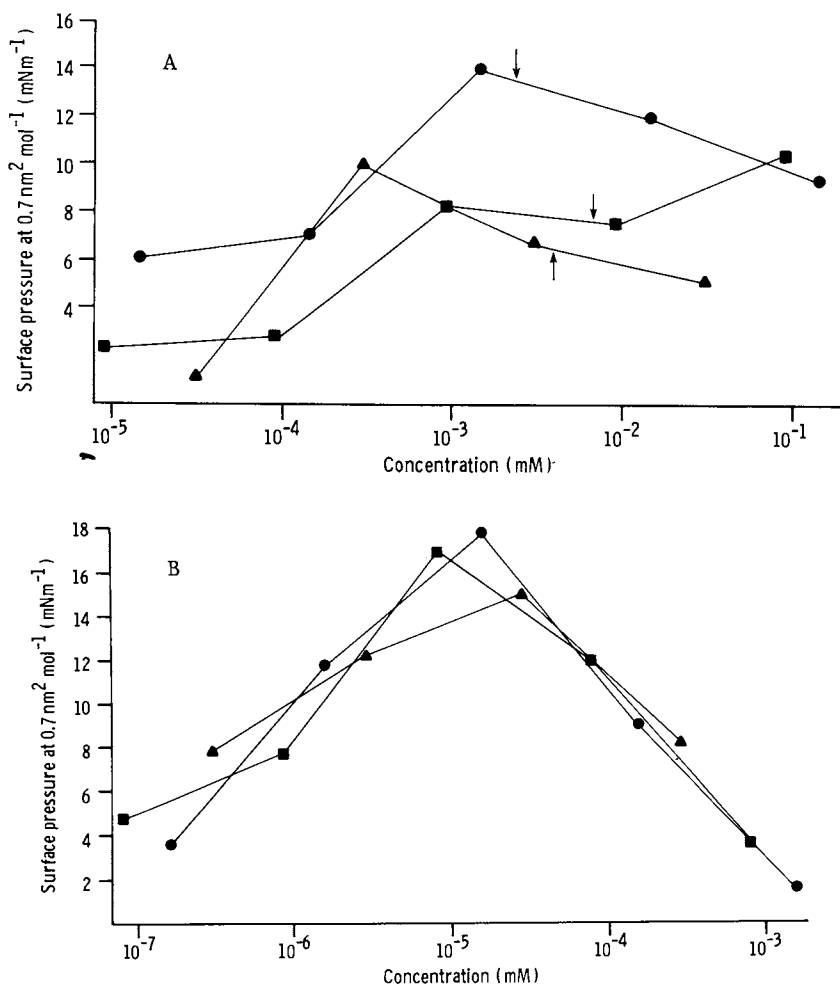


Figure 7.

- a) Plot of surface pressure at constant molecular area against surfactant concentration. ▲, Brij 72 ($C_{18}E_2$); ● Brij 76 ($C_{18}E_{10}$), ■ Brij 78 ($C_{18}E_{20}$). Arrows denote the CMC for each surfactant.
- b) Plot of surface pressure at constant molecular area against surfactant concentration. ▲, Brij 30 ($C_{12}E_4$); ●, Brij 36T ($C_{12}E_{10}$), ■, Brij 35 ($C_{12}E_{23}$).

increases, but the CMC decreases, thus limiting the concentration of monomers which can exist in the aqueous phase in the case of higher members of the series. From C₈ to C₁₂ as the partition coefficient increases there is an increased opportunity for the surfactants to enter the biophase, whereas from C₁₂ to C₁₈, while the thermodynamic tendency to partition into non-aqueous environments increases the decreasing concentration of monomers (the active species of surfactant) may elicit a smaller response. Adsorption of surfactant onto the high available surface areas of membrane components can also influence behaviour. (27).

Some workers have suggested that the lauryl chain is of intrinsic biological importance in relation to its ability to disrupt lipid bilayers, having the optimal physical properties of lipophilicity and size, but as C₁₂ compounds are also maximally irritant to the skin (28) where simple lipoidal barrier membranes are probably not involved, other factors are no doubt implicated. Dominguez et al. (29) have considered Schott's (26) approach to the biological uniqueness of the dodecyl chain, but have postulated that its properties of skin penetration are related to the conformation of the chain, especially when adsorbed to or interacting with protein. Dominguez et al. postulate that by adopting a compact configuration the dodecyl chain can migrate deeper into skin structure and thereby be more active than more lipophilic compounds. This is very speculative and requires more experimental and theoretical study.

Schott's arguments should apply to a homologous series in which the hydrophilic chain length alters too. In Figure 8 experimentally determined CMC's of a series of nonionic surfactants are employed with idealised diagrams of monomer concentrations as a function of total surfactant concentration. When measurements of surfactant activity in a biological system are made at 0.01% concentration levels, the monomer concentrations will approximate the CMC. It seems likely that at such low concentrations the activity of the hydrophobic members of the series is limited by micellisation, and in the case of C₁₆E₂, by low solubility. Hydrophilic members of the series have very low values of P and are unlikely to have much affinity for the membrane, in addition to having a larger surface area. If it is assumed that the monomer is the active species, a maximum in activity is readily shown by choice of partition coefficients such as those shown for members of the homologous series. (3). But these assumed values are very different from those calculated using the Hansch approach. It is likely then that partitioning of the complete surfactant molecule into the membrane is not necessary for activity.

It could well be that many of the results of increased transport rates are determined by membrane damage, rather than by reversible physical effects when surfactants are used above their CMC. Studies on the solubilization of protein have in several cases demonstrated a remarkable parallel between solubilizing ability and membrane action (30).

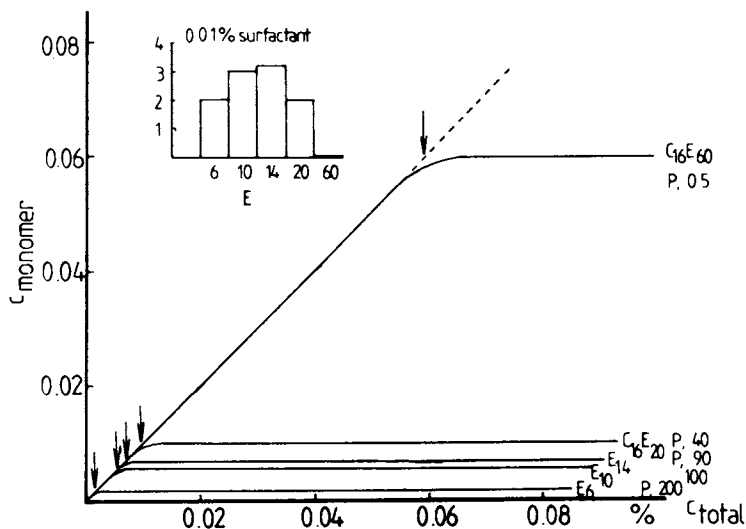


Figure 8.

Monomer concentrations as a function of total surfactant ($C_{16}E_x$) concentration. Experimental CMC's are marked by arrows. At 0.01% total surfactant levels, the monomer concentrations will be approximately given by the CMC values except for $C_{16}E_{60}$ whose CMC is 0.06.. Inset shows absorption profile if values of partition coefficient (P) shown apply. From Florence (1982).

Model membranes: surfactant in low density lipoprotein interactions

According to Helenius and Simons (30) solubilization of the membrane is preceded by saturation of the bilayer with surfactant. Certainly critical surfactant/phospholipid ratios must be attained before membrane disruption occurs.

Photon correlation spectroscopy was used to study the effects of a series of nonionic surfactants on the Stokes radius (R) of low density lipoprotein (LDL₂) particles (31, 32). LDL₂ interacted with surfactants in a manner similar to membranes. That is, nonionic surfactants caused an increase in the Stokes radius (R) of the particles due to penetration of the phospholipid surface layer and unfolding of apoprotein B molecules leading to particle asymmetry at molar ratios of surfactant LDL₂ of ca. 1000/1. At higher molar ratios, corresponding to 1-2 moles surfactant per mole of phospholipid, ionic surfactants and nonionics with HLB values < 14.6 caused rapid decreases in the Stokes radius due to breakdown of LDL₂ into the lipid surfactant and protein surfactant micelles.

The data suggest that surfactant HLB is important in determining ability to delipidate LDL₂ rapidly. Nonionic surfactants with HLB values < 14.6 caused a fall in R which can be interpreted as due to delipidation of LDL₂. Umbreit and Strominger (33) found that surfactants with HLB values of 12.5 - 14.5 are most effective in solubilizing membranes. Thus LDL₂ is responding like a biological membrane and this is supported by the fact that the fall in R starts at approximately one mole of surfactant per mole of phospholipid, a typical value for membranes (30). However, kinetic data suggest that surfactants with higher HLB values (e.g. C₁₂E₂₃, HLB 16.9) might delipidate membranes over a prolonged period (20 hours). The reason for these differences is not well known but it is interesting to speculate. The lower HLB surfactants tested are also those with the shortest hydrophilic chains, and so the smallest molecular areas (10). They should therefore have the highest concentrations at the LDL₂ surface at saturation causing disruption and solubilization. The slow action of C₁₂E₂₃ could be due to slow replacement of C₁₂E₂₃ molecules by lower HLB impurities in the surfactant samples.

Conclusions

A parabolic relationship between membrane activity and lipophilicity of nonionic surfactants is clearly established in series of surfactants in which either the hydrocarbon chain length or ethylene oxide chain length is varied. Activity at low and high concentrations should be considered separately.

membranes can occur at very low surfactant concentrations; structural specificity is demonstrated by the superior action of compounds with the C_{12} moiety. Depth of penetration of the hydrocarbon chain may not be equal in any homologous series varying in ethylene oxide chain length, hence even in the $C_{12}E_x$ series biological activity varies considerably. When x is below the optimum this is probably due to the low CMC which limits monomer activity and perhaps is also due to penetration of a portion of the EO chain into the membrane. When x is above the optimum number, increasing ethylene oxide chain length leads to increasing molecular area, decreasing surface activity and a likely less efficient penetration of the membrane by the hydrocarbon chain. If, as seems likely, the molecular dimensions of the C_{12} chain intercalate most efficiently with the bilayer structure than any alteration in the depth of penetration will change its activity. There is no direct evidence, however, to support this concept, and further detailed work is necessary to determine mechanisms of action at sub-solubilizing surfactant concentrations.

At concentrations well above the CMC, these effects are complicated by solubilization, but while it seems clear that protein solubilizing effectiveness and membrane activity correlate well, the structural basis for protein solubilization has not yet been clarified either.

Literature Cited

1. Attwood, D.; Florence, A.T. in "Surfactant Systems: their Chemistry, Pharmacy and Biology"; Chapman and Hall, London. 1983.
2. Drotman, R.B. Toxicol. Appl. Pharmacol. 1980, 52, 38-44.
3. Florence, A.T. Pure and Applied Chem. 1982, 53, 2057-2068.
4. Marsh, R.J.; Maurice, D.M. Exp. Eye Res. 1971, 11, 43-48.
5. Florence, A.T.; Gillan, J.M.N. Pesticide Sci. 1975, 6, 429-439.
6. Florence, A.T.; Gillan, J.M.N. J. Pharm. Pharmacol. 1975, 27, 152-159.
7. Zaslavsky, B. Yu. et al. Biochim. Biophys. Acta. 1978, 507, 1.
8. Hirai, S.; Yashiki, T.; Mima, H. Int. J. Pharmaceutics, 1981, 9, 175-182.
9. Touitou, M.; Donbrow, M.; Azaz, E. J. Pharm. Pharmacol. 1978, 30, 662-663.
10. Walters, K.A.; Dugard, P.H.; Florence, A.T. J. Pharm. Pharmacol. 1981, 33, 207-213.
11. Walters, K.A.; Olejnik, O. J. Pharm. Pharmacol. 1983, 35, Suppl. 81P.
12. Florence, A.T.; Walters, K.A.; Dugard, P.H. J. Pharm. Pharmacol. 1979, 30, Suppl. 29P.
13. Araki, J.; Rifkind, J.M. Biochim Biophys. Acta, 1981, 645, 81-90.

14. Crook, E.H.; Fordyce, D.B.; Trebbi, G.F. J. Colloid Sci. 1965, 20, 191-204.
15. Harusawa, F.; Saito, T.; Nakajima, H.; Fukushima, S. J. Colloid Interface Sci. 1980, 74, 435-440.
16. Harusawa, F.; Nakajima, H.; Tanaka, M. J. Soc. Cosmet. Chem. 1982, 33, 115-129.
17. Cserhati, T.; Szogyi, M.; Bordas, B. Gen. Physiol. Biophys. 1982, 1, 225-231.
18. Kubinyi, H. in "Drug Research"; Jucker, E., Ed.; Birkhauser: Basel, 1979; 23, 97-198.
19. Hansch, C. in "Drug Design"; Ariens., Ed.; Academic: New York, 1971: Vol. 1.
20. Tiddy, G.J.T.; Personal Communication, 1983.
21. Mitchell, D.J.; Tiddy, G.J.T.; Waring L.; Bostock, T.; McDonald, M.P. J.C.S. Faraday Trans. I, 1983, 79, 975-1000.
22. Walters, K.A.; Florence, A.T.; Dugard, P.H. J. Colloid Interface Sci. 1982a, 89, 584-587.
Walters, K.A.; Florence, A.T.; Dugard, P.H. Int. J. Pharmaceutics, 1982b, 10, 153-163.
23. Hirai, S.; Tashiki, T.; Mima, H.M. Int. J. Pharmaceutics, 1981b, 9, 1973.
24. Ponder, E. in "Haemolysis and Related Phenomena", Grume and Stratton: New York, 1984, 138 et. seq.
25. Dahlgren, C.; Rundquist, J.; Stendahl, O.; Magnusson, K.E. Cell Biophysics, 1980, 2, 253-267.
26. Schott, H. J. Pharm. Sci. 1973, 62, 341-343.
27. Kirkpatrick, F.H.; Gordesky, S.E.; Marinetti, G.V. Biochim. Biophys. Acta, 1974, 345, 154-161.
28. Ferguson, T.F.M.; Prottey, C. Fd. Cosmetic Toxicol. 1976, 14, 431-434.
29. Dominguez, J.C.; Parra, J.L.; Infante, M.R. et al. J. Cosmetic Chem. 1977, 28, 165-182.
30. Helenius, A.; Simons, K. Biochim. Biophys. Acta. 1975, 415, 29-79.
31. Tucker, I.G.; Florence, A.T.; Stuart, J.F.B. J. Pharm. Pharmacol. 1982, 34, 19P.
32. Tucker, I.G.; Florence, A.T. J. Pharm. Pharmacol. 1983, 35, 705-711.
33. Umbreit, J.N.; Strominger, J.L. Proc. Natl. Acad. Sci. U.S.A. 1973, 70, 2997-3001.

RECEIVED March 6, 1984

Modification by Surfactants of Soil Water Absorption

RAYMOND G. BISTLINE, JR., and WARNER M. LINFIELD

Agricultural Research Service, U.S. Department of Agriculture, Philadelphia, PA 19118

This work describes the application of a previous study which dealt primarily with organic synthesis and physical properties of reaction products of pure fatty acids with DETA. Derivatives to amplify the previous study were prepared from various industrial fatty materials. The reaction product, from 1 mole diethylenetriamine (DETA) with 2 moles fatty acid, was thought to be the primary amine, $\text{RCON}(\text{CH}_2\text{CH}_2\text{NH}_2)\text{-CH}_2\text{CH}_2\text{NHCOR}$, rather than the secondary amine, as cited in the literature. The amine was readily dehydrated to the imidazoline, $\text{RC} = \text{NCH}_2\text{CH}_2\text{NCH}_2\text{CH}_2\text{NHCOR}$. The imidazolines in the presence of moisture hydrolyzed upon standing, to the open chain derivatives. These cationic surfactants were examined as water repellents for soil. Water repellency was evaluated by contact angle measurements and water infiltration through sand, sandy soil, and soil containing 30% clay. A large number of derivatives made clay soil hydrophobic, whereas only a few caused this effect on sandy soils. The following factors influenced soil water repellency. Open chain derivatives were more hydrophobic than the corresponding imidazolines. Hydrophobicity intensified with increasing molecular weight of the saturated fatty acids. Unsaturation, as in the oleic acid derivatives, enhances hydrophilicity. Hydrocarbon branching in the fatty acid

This chapter not subject to U.S. copyright.
Published 1984, American Chemical Society

also reduces water repellency. The soil hydrophobic agents in treated soils greatly restrict seed germination.

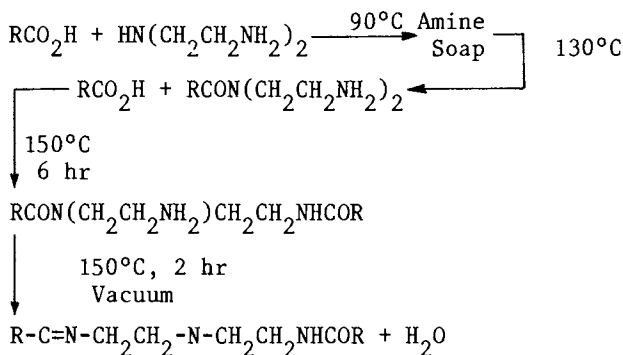
Farming, particularly in arid areas, requires efficient utilization of water. Over the years several methods have been developed to harvest water. Water harvesting is the process of collecting water from plots that have been made water repellent so that the runoff from these plots may be employed in agriculture. Physical waterproofing methods, such as coating the ground with nylon sheets, asphalt, fuel oil, and paraffin wax (1) have appeared in the literature; however, references to chemical interactions with the soil to produce hydrophobic surfaces are few (2, 3). A chemical soil treatment would provide an alternative means of harvesting water.

A search of the chemical literature suggested that surfactants, containing amine groups, might impart water repellent properties to soils. While studying the cation exchange mechanism of large substituted ammonium ions on clay, Gieseck (4) found that clays saturated with the organic ammonium ions did not show the water absorption, swelling, and dispersion characteristics of untreated clay. Subsequently, Law and Kunze (5) examined the effects of three different types of surfactants on clays. They reported that commercial cationic surfactants were strongly adsorbed on clay through ionic bonding, in amounts equal to or even greater than the cation-exchange capacities of the clays. According to these authors, the presence of surfactants on clays significantly reduced hydration and water content at high treatment rates. Furthermore, Greenland (6) observed that cationic surfactants created a layer of increased hydrophobic character beneath the soil's surface.

Various types of cationic surfactants were reviewed by us to select one, relatively low in cost and readily prepared on a large scale, for which the relationship of chemical structure to surface active properties could be conveniently studied.

One type of cationic surfactant was the fatty acid derivatives of polyamines. The properties of the derivatives of fatty acids and ethylenediamine have been described in the literature (7-9). It appeared from these reports that the 2-alkyl-2-imidazolines would not impart sufficient hydrophobicity to soils. However, the analogous series of homologous compounds from the fatty acids and diethylenetriamine (DETA) appeared likely to do so because of their higher molecular weight.

In 1940, Ackley (10) reacted fatty acids with DETA to form precursors for fabric softeners. However, it was not until recently (11) that the course of the reaction between fatty acids and DETA, and properties of the reaction products were studied. The reaction appears to proceed, according to the following scheme:



Initially, one molecule of fatty acid reacted with the secondary amine of DETA, followed by a second fatty acid molecule, reacting with one of the two primary amines. The product formed was the N-(2-aminoethyl) diamide, which will be referred to as the diamide. The diamides could be cyclized by heating under vacuum to form imidazolines, which were unstable to hydrolysis. In the presence of water, or upon exposure to atmospheric moisture, they revert back to the diamide.

DETA derivatives of C₉-C₂₂ saturated fatty acids, as well as the C₁₈ unsaturated acids, oleic and elaidic, were prepared and evaluated in the previous publication (11). Hydrophobicity determination, via contact angle measurements, proved to be nondiscriminatory and, therefore, a more meaningful test, the sand penetration test was devised. The results of this test demonstrated that the diamides of the C₁₄ and higher saturated fatty acids were water repellents. On the other hand, the unsaturated oleic acid derivatives enhanced hydrophilicity.

Materials and Methods

Apparatus. Infrared spectroscopy, Perkin-Elmer Model 257 infrared spectrophotometer, Perkin-Elmer Corporation (Norwalk, CT); ultraviolet spectroscopy, Perkin-Elmer Model 559 UV-vis spectrophotometer, Perkin-Elmer Corporation, Coleman

Instruments Div. (Oak Brook, IL); Fisher-Johns melting point apparatus, Fisher Scientific Company (Pittsburgh, PA); contact angles, Gaertner goniometer, Gaertner Scientific Corporation (Chicago, IL).

Reagents. The following chemicals were used: diethylenetriamine, Aldrich Chemical Company (Milwaukee, WI); C₁₂, C₁₄, C₁₆, C₁₈ saturated fatty acids, ArmaK Industrial Chemicals Division (Chicago, IL); oleic acid, A. Gross & Company (Newark, NJ); elaidic acid, laboratory preparation (12); tallow, Corenco Corporation (Philadelphia, PA) (titer, t = 42°, iodine no. 40); tallow fatty acid (T - 22) and partially hydrogenated tallow fatty acid (T - 11), Proctor & Gamble, Industrial Chemicals Division (Cincinnati, OH) (T - 22, t = 40°, I. no. = 60) (T - 11, t = 46°, I. no. = 41); hydrogenated tallow fatty acids, Acme-Hardesty Company, Incorporated (Jenkintown, PA), (t = 62°, I. no. = —); tall oil fatty acids, Arizona Chemical Company (Wayne, NJ) (t = 24°, I. no. = 75); MO-5 fatty acid, Union Camp Corporation (Jacksonville, FL) (t = 33°, I. no. 75); isostearic acid, Emery Industries Incorporated (Cincinnati, OH) (t = liquid, I. no. = 12).

Drierite, W. A. Hammond Drierite Company (Xenia, OH); Ottawa Sand ASTM, Arthur H. Thomas Company (Philadelphia, PA); SYLON-CT Silylating Reagent, Supelco, Incorporated (Bellefonte, PA).

Soils. Granite Reef soil is a sandy loam soil, supplied by the U.S. Water Conservation Laboratory, USDA, Phoenix, AZ. Walla Walla soil is a soil which contains 30% clay and organic matter, supplied by the Columbia Plateau Conservation Research Center, USDA, Pendleton, OR.

Experimental

Preparation of commercial fatty acid-DETA derivatives: the previously described procedure (11) was slightly modified, using a 5% excess fatty acid to ascertain that all DETA was consumed. Amine analysis was conducted, according to AOCs test method (13). The reaction products were used without purification.

Procedures for infrared and ultraviolet absorption and contact angle measurements are reported in the previous publication (11).

Infiltration Tests

Sand Penetration Test

Ten grams of indicating Drierite was placed in a 120-mL silylated jar and covered with 80 g treated ASTM Ottawa sand, prepared according to the previous report (11). The depth of the soil was 35 mm. Distilled water, 8 mL, was then placed on the surface of the sand. The time required to change the indicating Drierite completely from blue to pink was recorded as the infiltration time.

Soil Infiltration Test

A soil infiltration test was devised to screen a large number of compounds within a limited time span. The amounts used are far in excess of quantities used in field application. A 5% diamide solution in isopropanol, 15 mL, was added to 50 g soil, air dried overnight, and then placed in a vacuum oven at 50° for 1 hr to remove traces of isopropanol. The treated soil, 10 g, was placed in a 25 X 500 mm glass chromatographic column with a coarse porosity fritted disc on top of a detachable adapter base. The soil was tapped down lightly with a wooden dowel to a depth of 12 mm in order to prevent channeling. Forty-five cm of water covered the soil. The period required for 200 mL distilled water to penetrate through 10 g of treated soil was recorded as the infiltration time. The test was arbitrarily discontinued after 2 weeks.

Glycerine Effect on Hydrophobicity. The partially hydrogenated tallow fatty acid-DETA reaction product, 10 g, was weighed into each of five 60-mL bottles. The following amounts of glycerine, expressed as percent, were weighed, using an analytical balance, into the bottles: 0.36, 1.02, 2.60, 5.10, 11.11. Mixtures were then melted and stirred. Contact angles were measured, according to the procedure in the previous publication (11).

Soil Extraction. Granite Reef soil, 100 g, was treated with 30 mL of a 5% isopropanol solution of the partially hydrogenated tallow fatty acid-DETA reaction product and then air dried overnight and finally in a vacuum oven at 50°C for 1 hr to remove residual isopropanol. On the following day the treated soil was extracted with ethanol 8 hr in the Soxhlet apparatus. The extracted solvent was evaporated recovering 1 g residue. As a control experiment, untreated soil, 100 g, was also extracted 8 hr with ethanol,

recovering 0.2 g material. The dried extracted soil was placed in the chromatographic column and the infiltration test with 200 mL distilled water repeated.

Plant Growth Effect Test. Potting soil, 3.4 kg, was weighed into a 55 X 27.5 X 7.5 cm flat, treated with 1.2 L of a 5% solution of the partially hydrogenated tallow fatty acid-DETA diamide in isopropanol, and air dried for 2 days until the isopropanol had evaporated. Untreated potting soil, 3.4 kg, was weighed into another flat to be used as a control.

Soybeans

Fifty soybean seeds each were planted in the diamide-treated soil as well as in a flat with an untreated control soil. Each flat was watered weekly with 2 L tap water. Water absorption and plant growth were recorded.

Corn

Since the nitrogen requirement of corn plants is greater than the nitrogen content found in potting soil, additional nitrogen fertilizer, 15 g 20:20:20/2 L water, was added to the soil, prior to treatment with water repellent chemicals. Fifty corn kernels were planted in the treated soil and an untreated control flat. The flats were watered weekly as described above, and growth recorded. After several weeks the plants were harvested, weighed, and dried in a vacuum oven and weighed again.

Results and Discussion

This work describes the application to soil of compounds of a previous study (11) which dealt primarily with organic synthesis and physical properties of reaction products of pure fatty acids with DETA. In this study derivatives were prepared from various industrial fatty materials. In addition, water infiltration studies on sand, sandy soil, and clay soils were carried out on the previously prepared and new compounds. Finally, an investigation was initiated to determine the biological effects of one water-repelling chemical, the partially hydrogenated tallow-fatty acid-DETA reaction product, on seed germination and plant growth.

The DETA derivatives from industrial fatty materials for soils application were of special interest because of their ready availability, low cost, and greater solubility

than the DETA derivatives from the purified fatty acids. Diamides were prepared from tallow, tallow fatty acids, partially hydrogenated tallow fatty acids, hydrogenated tallow fatty acids, tall oil fatty acids, MO-5 acids (a mixture of oleic, isooleic, stearic, and elaidic acids), and isostearic acid (a mixture of branched chain isomeric acids).

Melting points and contact angle measurements of the fatty acid-DETA reaction products are recorded on Table I. The melting points of the pure saturated fatty acid-DETA derivatives were over 100°C and possessed low solubility in most organic solvents. The unsaturated fatty acid-diamides had much lower melting points. The industrial fatty-DETA derivatives with the exception of the product from hydrogenated tallow fatty acids melted at 60°C or below.

Contact Angle Measurements. It was planned to establish the hydrophilic or hydrophobic nature of the diamides by contact angle determination (14). The angles for the lauric diamides and higher saturated homologs were all above 90°. Thus, the contact angle measurements did not discriminate between members of a homologous series. The unsaturated fatty acid-DETA derivatives were predictably more hydrophilic. Among the industrial fatty acid-DETA derivatives, only three possessed contact angles over 90°. These were the DETA derivatives of partially and fully hydrogenated tallow fatty acids and the isostearic acid. Although a 50:50 mixture of DETA derivatives of isostearic and partially hydrogenated tallow fatty acids produced a compound with the desired melting point, the contact angle of this mixture fell to 73°. The data are reported in Table I.

Sand Penetration Tests. Since contact angle measurements appeared fairly insensitive to structure differences, a sand penetration test was devised. Water penetration rates through beds of treated sand were determined for the derivatives of the individual pure fatty acids, as well as for those from the industrial fatty materials as shown in the first column of Table II. Water passed quickly through the C₁₂ diamide-treated sand, whereas a period of 7 or more days was required for the C₁₄ and higher molecular weight-saturated diamides. While water penetrated the oleic diamide-coated sand within 5 min, 1-day was required for penetration of the elaidic diamide-coated sand, showing the superiority of the trans isomer. In the cis configuration, the molecule is bent back upon itself, resulting in properties

Table I. Physical Properties of Diethylenetriamine Reaction Products

R-COOH	Melting Point, C	Contact Angle (°)
C ₁₁ H ₂₃	110-111	99
C ₁₃ H ₂₇	112-113	99
C ₁₅ H ₃₁	116-117	96
C ₁₇ H ₃₅	118-119	98
Δ^9 C ₁₇ H ₃₃ , cis	52-53	50
Δ^9 C ₁₇ H ₃₃ , trans	91-92	62
Derivatives of Industrial Fatty Materials		
Tallow	50-60	37
Tallow Fatty Acid ^a	45-55	63
Tallow Fatty Acid ^b	55-65	97
Hyd. Tallow F.A.	90-95	94
Tall Oil F.A.	35-45	59
MO-5	30-40	56
Isostearic	30-40	91
Isostearic _c + Tallow Fatty Acid ^b (50:50)	40-45	73

^a = T-22 fatty acids, C₁₈ cis = 36%,
C₁₈ trans = 7%

^b = T-11 fatty acids C₁₈ cis = 6%, C₁₈ trans = 24%

Table II. Infiltration Properties of Diethylenetriamine Reaction Products

DETA-Fatty Acid Derivative from	Sand Penetration	Granite Reef Soil Infiltration	Walla Walla Soil Infiltration
C ₁₁ H ₂₃ COOH	1 hr	3 hr	5 hr
C ₁₃ H ₂₇ COOH	7 d	5 d	>2 wk
C ₁₅ H ₃₁ COOH	>7 d	5 d	>2 wk
C ₁₇ H ₃₅ COOH	>7 d	>2 wk	>2 wk
Δ ⁹ C ₁₇ H ₃₃ cis COOH	5 min	3 hr	8 hr
Δ ⁹ C ₁₇ H ₃₃ trans COOH	1 d	>2 wk	2 wk
Tallow	i ^c	4 hr	8 hr
Tallow Fatty Acid ^a	i	1 d	>2 wk
Tallow Fatty Acid ^b	i	1 wk	>2 wk
Hyd. Tallow F.A.	>7 d	>2 wk	>2 wk
Tall Oil F.A.	i	4 hr	8 hr
MO-5	i	2 hr	8 hr
Isostearic	i	2 hr	7 hr
Isostearic † Tallow F.A. ^b (50:50)	i	3 hr	2 wk
Control	i	4 hr	1 d

^a = T-22 fatty acids

^b = T-11 fatty acids

i^c = instantaneous

roughly analogous to those of a C₉ fatty acid derivative. Although the elaidic diamide derivative is more linear in configuration than the oleic diamide, the trans unsaturation disarranges the molecules, resulting in surface properties which are less hydrophobic compared to those of the saturated stearic acid derivative. These observations help explain the results obtained with the industrial fatty acid derivatives. Instantaneous penetration was observed for sand treated with the DETA derivatives of tallow, tallow fatty acids, tall oil fatty acids, and MO-5 acids as predicted by their low contact angles. All of these are high in oleic acid content. In contrast, sand treated with the completely hydrogenated tallow fatty acid-DETA diamide which had a high contact angle required more than 1 week for water penetration. In these two sets of examples, correlation as to degree of hydrophobicity was observed between the sand penetration tests and the contact angle measurement.

However, with the other derivatives there was disagreement. Water immediately penetrated sand coated with the DETA derivatives of partially hydrogenated tallow fatty acids and isostearic acid, despite their high contact angles of greater than 90°. Water quickly passed through sand treated with a 50:50 mixture of diamides of isostearic acid and partially hydrogenated tallow fatty acids. While these penetration results on standardized ASTM sand were interesting, they did not forecast the results found with sandy and clay soils.

Soil Column Tests. In the sand penetration test, a minimal amount of water was used. No consideration was given to the hydrostatic pressure which would occur in nature from a body of surface water. A new soil infiltration test was developed to take this into consideration. This test used a maximum amount of water (200 mL) on a minimum amount of treated soil (10 g) and was restricted only by the dimensions of the laboratory equipment. Our aim was to prepare an hydrophobe for soil which would support water over an extended period of time. Whereas water passed through soil treated with hydrophilic compounds within 8 hr, 2 weeks or more were required for penetration through an hydrophobe-treated soil. In the latter case the water level dropped 6 mm or less each day, showing that the cationic surfactant greatly hindered, but did not completely restrict the passage of water. The tests were usually terminated after 2 weeks, due to the large number of samples to be tested. The two soils were selected because of differences in

composition and properties. The results of the soil infiltration test are recorded in Table II.

Although the infiltration times differed slightly from each other, due to differences in soil structure, water passed quickly through soil treated with hydrophilic compounds, whereas a week or longer was required for passage through hydrophobic-treated soil. Water penetrated soil treated with the lauric acid diamide more rapidly than the controls, demonstrating the hydrophilic nature of the C₁₂ derivative. A much longer time period was required for penetration through soils, treated with the saturated C₁₄ and above diamides. Drastic differences were observed for the infiltration times of soils treated with the *cis* unsaturated oleic acid diamide (hr) compared to the *trans* unsaturated elaidic acid diamide (wk).

The industrial fatty acid-DETA derivatives were evaluated for application to soil. Water infiltrated soil coated with the DETA derivative of tallow more rapidly than the controls. This was due to the high unsaturation content and also in part to the glycerine retained in the product as discussed below. We were unable to find a solvent system which would readily separate the glycerine, formed from the triglyceride, from the DETA reaction product. If the glycerine were removed, the infiltration rates for the tallow-DETA derivative should be identical with the rates obtained for tallow fatty acid-DETA reaction product.

The soil treated with the tallow fatty acid-DETA reaction product retarded moisture infiltration on both soils. The partially hydrogenated and completely hydrogenated tallow fatty acid-DETA derivatives also displayed hydrophobic properties on both soils. Although the completely hydrogenated tallow fatty acid-DETA reaction product (m.p. 90°C) had optimum hydrophobic properties on all three soils, it was difficult to dissolve in most organic solvents. Even the partially hydrogenated tallow fatty acid-DETA reaction product, m.p. 45°-50°C, was not readily soluble. To overcome this difficulty, we examined the DETA derivatives of some other fatty materials, hoping to find an hydrophobe with a lower melting point.

Water infiltration tests were conducted on soils treated with the DETA derivatives of tall oil fatty acids, MO-5 acids, and isostearic acid, all of which melted below 45°. Water infiltrated sandy soil treated with these compounds within 4 hr and through clay containing soil within 8 hr, confirming their hydrophilic nature. The blending of these diamides into the tallow derivatives in order to lower melting points and enhance solubility causes

a serious loss of hydrophobicity in sandy soil. For example infiltration rates dropped from 1 week to 3 hr passing water through Granite Reef soil treated with a 50:50 mixture of DETA derivatives of isostearic acid and partially hydrogenated tallow fatty acids. The water infiltration rate on Walla Walla soil, treated with the 50:50 mixture, remained similar to that obtained with the partially hydrogenated tallow fatty acid-DETA derivative alone.

The soil properties observed with these chemicals suggest that the chemical structural requirements for an hydrophobic cationic surfactant appear to be:

- a. Molecular weight > 500.
- b. Prepared from saturated starting materials.
- c. Contain free amino groups to attach to soil particles.

Glycerine Effect on Hydrophobicity. The tallow-DETA reaction product, containing over 10% free glycerine, had a contact angle of 37° . Glycerine in measured amounts was added to the partially hydrogenated tallow fatty acid-DETA reaction product and contact angles measured (See Figure 1). The purpose was to determine how much glycerine a reaction product could tolerate and yet remain hydrophobic. The results show that glycerine amounts of as low as 1% render the reaction product hydrophilic and suggest that tallow fatty acids rather than tallow be used in the synthesis of DETA reaction products.

Retention on Soil. An experiment was conducted to demonstrate the retention of the cationic surfactant on the soil. Granite Reef soil, treated with the partially hydrogenated tallow fatty acid-DETA reaction product together with an untreated soil sample was extracted in the Soxhlet apparatus. The extracted soils were returned to the chromatographic column and the water infiltration test repeated. It has been reported previously (15) that short-chain alcohols form double layer complexes on the surface of soil particles, causing a modification of soil properties. Whereas water penetrated the untreated, unextracted Granite Reef soil control in 4 hr, 12 hr was now required for passage through the untreated, alcohol extracted soil. Water penetration through extracted treated soil was incomplete after 4 days, showing that the water repelling agent remained on the soil. Fripiat and coworkers (16) have reported that amines can protonate in soil and replace inorganic cations from the clay complex by ion exchange. Amines are adsorbed with their hydrocarbon chains perpendicular or parallel to the

clay surface, depending on the concentration (16). The surface of the soil particles has now become hydrophobic and delays the passage of water molecules.

The material (1 g) recovered by the alcoholic extraction of treated soil in the Soxhlet apparatus was identified by U.V. spectroscopy at 202 nm as being unreacted partially hydrogenated tallow fatty acid-DETA reaction product. The alcohol solubles from the untreated soil absorbed in the range of 230-220 nm with only a trace absorption at 202 nm. The 60% recovery suggests that the 5% concentration was too high and further work is required to determine the proper concentration.

Effects on Plant Growth. Experiments were initiated to determine the effect of a soil hydrophobe on seed germination. Potting soil was treated with the partially hydrogenated tallow fatty acid-DETA reaction product. Although no crust formed on the soil's surface after the addition, a coarser texture of the potting soil was observed. In reviewing plants which would germinate rapidly, soybeans were selected. After the seeds were planted in the treated soil, as well as an untreated control, the flats were watered weekly. We were surprised to see water roll off and down the sides of the treated flat. Whereas the control flat took up 1.7 kg of water, the treated soil flat gained only 110 g. The soybeans in the control flat germinated in 10 days and grew rapidly. After a period of 8 weeks, one seed germinated in the hydrophobe-treated soil (See Figure 2). This experiment was continued for another month, but no further plants appeared. The seeds were not able to germinate because the passage of water through the soil was blocked.

Corn was used to demonstrate the effects of soil hydrophobes on the cereal grasses. After adding nitrogen fertilizer, the potting soil was treated with the partially hydrogenated tallow fatty acid-DETA reaction product. As a result of this enrichment all seeds germinated in the treated soil and in the control. However, the corn plants grown in the treated soil soon developed a yellow cast and appeared stunted in growth. After 6 weeks the corn plants were harvested. The stalks planted in the treated soil weighed 54% of those grown in the control. The stalks were then dried in a vacuum oven to constant weight, and the plants from the hydrophobe-treated soil now weighed 47% of the control plants. These results show that the growth of plants was greatly impeded by the surfactant.

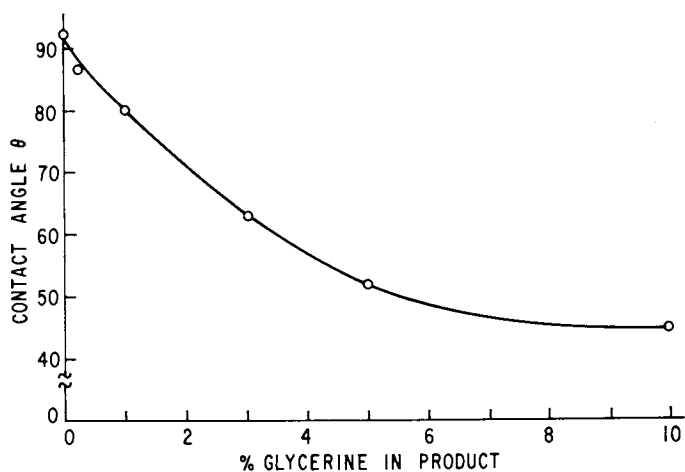


Figure 1. Effect of glycerine concentration on contact angle the partially hydrogenated tallow fatty acid-DETA reaction product.



Figure 2. Effect of soil hydrophobe on soybean germination.

Acknowledgments

D. Brower and M. P. Thompson carried out the plant experiments.

Literature Cited

1. Fink, D. H.; Cooley, K. R.; Frasier, G. W. J. Range Manage. 1973, 26, 396.
2. Myers, L. E.; Frasier, G. W. J. Irrig. Drain. Div. Amer. Soc. Civil Engin. Pro. 1969, 95, 43.
3. Fink, D. H.; Frasier, G. W. Soil Sci. Soc. Am. Publication #7, 1975, 173. ASCE 1969, 95, 43.
4. Giesecking, J. E. Soil Sci. 1939, 47, 14.
5. Law, J. P., Jr.; Kunze, G. W. Soil Sci. Soc. Am. Proc. 1966, 30, 321.
6. Greenland, D. J. Soc. Chem. Ind. Monograph 1970, 37.
7. Shapiro, S. H in "Fatty Acids and Their Industrial Application"; Pattison, E. S., Ed.; Marcel Dekker, Inc.: New York, NY, 1968; p. 98.
8. Fern, R. J.; Riebsomer, J. L. Chem. Rev. 1954, 54, 593.
9. Tornquist, J. Proc. of the 4th International Congress on Surface Active Substances, Vol. 1, Sect. A, Gordon and Breach Science Publishers, London, England, 1967, p. 387.
10. Ackley, R. R.; U.S. Patent 2,200,815, 1940.
11. Bistline, R. G., Jr.; Hampson, J. W.; Linfield, W. M. J. Am. Oil Chem. Soc. 1983, 60, 823.
12. Swern, D.; Scanlan, J. T. Biochem. Prep. 1953, 3, 118.
13. AOCs Test Method TF 1b-64 and TF 2b-64 "Quantitative Determination of Amines"; Am. Oil Chem. Soc.: Champaign, IL, 1979.
14. Rosen, M. J. in "Surfactants and Interfacial Phenomena"; John Wiley & Sons; New York, NY, 1978; p. 179.
15. German, W. L.; Harding, D. A. Clay Miner. 1971, 9, 167.
16. Fripiat, J. S.; Servias, A.; Leonard, A. Bull. Soc. Chim., France 1962; p. 635.

RECEIVED January 10, 1984

Binding of Alkylpyridinium Cations by Anionic Polysaccharides

A. MALOVIKOVA¹ and KATUMITU HAYAKAWA²

Department of Chemistry, Dalhousie University, Halifax, Nova Scotia, Canada B3H 4J3

JAN C. T. KWAK

Département de chimie, Université de Sherbrooke, Sherbrooke, Québec, Canada J1K 2R1

Solid state electrodes selective for alkylpyridinium cations are used to study the binding of these surfactants cations, with C₁₂, C₁₄ and C₁₆ alkyl chainlengths, to a number of anionic polyelectrolytes. The electrodes are shown to be effective from very low surfactant concentrations to the cmc, and can be used for accurate cmc determinations in solutions of high ionic strength. Binding isotherms of the alkylpyridinium cations with polyacrylate, alginate, pectate and pectinates are presented. All isotherms are highly cooperative. The surfactant chainlength dependence of the overall binding constant is identical to the case of micelle formation of the free surfactant, but for a given surfactant the overall binding constant depends strongly on the charge density of the polyion.

The binding of ionic surfactants by polyions of opposite charge distinguishes itself from the much more widely studied case of binding by neutral water soluble polymers mainly because binding occurs at much lower free surfactant concentrations (1,2). Thus, while the binding of ionic surfactants by neutral polymers is normally studied at concentrations close to or above the cmc of the surfactant, in the case of oppositely charged polyions and surfactant ions the first binding may take place at concentrations orders of magnitude below the cmc of the surfactant. It is therefore not surprising that a detailed study of this binding process had to await the development of suitable analytical methods, notably surfactant selective electrodes (2-10). The pioneering paper by Satake and Yang (2) demonstrates the strongly cooperative

¹Current address: Institute of Chemistry, Slovak Academy of Sciences, Bratislava, Czechoslovakia

²Current address: Department of Chemistry, Kagoshima University, Kagoshima, 890 Japan

character of the binding of decylsulfate anions by highly charged cationic polypeptides. These authors interpret their binding isotherms in terms of a nearest neighbour interaction model, with hydrophobic interactions between neighbouring bound surfactant ions accounting for the increase of the apparent binding constant with increased binding. They apply the theory of Zimm and Bragg, developed to describe the helix coil transition in polypeptides (11), to the case of surfactant binding by polymers, effectively fitting the observed binding isotherm to two parameters, i.e. K , the "intrinsic binding constant" between an isolated polymer binding site and a single surfactant ion, and u , a "cooperativity parameter" presumably determined by the hydrophobic interactions between neighbouring surfactants. The Satake-Yang treatment parallels the theory of Schwarz developed to describe the binding of anionic dyes to linear biopolymers (12), and in fact the binding of long chain surfactants may be a much better test of such a theory than the case of relatively bulky and stiff dye molecules.

Since the work of Satake and Yang, a number of other studies have appeared employing surfactant selective electrodes to study the binding of anionic surfactants by cationic polymers (13-15) or of cationic surfactants by anionic polymers (7,10,16-19), with most of these studies relying on the theories of Schwarz and Satake and Yang to describe the observed highly cooperative binding isotherms. Although in a number of cases special attention was given to conformational changes of the polymer induced by surfactant adsorption (2,7,20,21) it is of interest to note the difference between the models used to describe these data at very low surfactant and polymer concentrations, and the much more widely studied case of binding measurements close to or past the surfactant cmc (1,22-28). Thus, whereas the generally accepted model for micellar binding envisages a complex where the polymer envelops many distinct, micellar-like surfactant aggregates (24,26) in surfactant ion polyion binding studies at low surfactant concentrations it is generally assumed that the polyion maintains a well defined solution conformation, or the polyion conformation is not considered at all, with a description of the binding isotherm in terms of a nearest neighbour model. Such a description leaves open the question whether the hydrophobic part of the bound surfactant remains exposed to the aqueous phase, or whether after binding the surfactants aggregate into micelle-like groups, with the polymer surrounding the aggregates. It is important to note that the binding between oppositely charged surfactant ions and polyions initially takes place without phase separation, and is fully reversible. This distinguishes the binding measurements at low surfactant concentrations from the studies on precipitating systems with or without subsequent redissolution (1,24).

In previous studies we have described the binding of alkyl-trimethylammonium ions to a variety of polyanions (16-19). As has been observed by other authors, both the alkyl chainlength dependence and the ionic-strength dependence of the binding process

were found to be remarkably similar to the case of micelle formation, apparently independent of whether the polyion has a well-defined backbone configuration such as with DNA or pectic acid (18,19), or may be presumed to be extremely flexible, e.g. dex-transulfate or poly(styrenesulfonate) (16,17). On the other hand, the binding constants for a given alkylammonium cation are found to depend strongly on the polymer structure and charge density (19). In this paper we extend these measurements to the case of alkylpyridinium cations with dodecyl, tetradecyl, and hexadecyl alkyl groups (to be abbreviated as $C_{12}Py^+$, $C_{14}Py^+$ and $C_{16}Py^+$ respectively). As polyanions we choose two polysaccharides of well defined structure, i.e. alginic acid, a copolymer of mannuronic and guluronic acid, and pectic acid, a linear polymer of D-galacturonic acid (29). The influence of the charge density of the polyion is studied by comparing pectate with pectinates with degrees of esterification of the corresponding pectate varying from 20 to 70%. In addition, results are presented for binding to the sodium salt of poly(acrylic acid) (PAA). Polymer structures are shown in Figure 1.

Experimental

Surfactants. $C_{12}PyCl$ and $C_{16}PyBr$ were commercial products (Tokyo Kasei Kogyo Co., Ltd and Eastman Kodak Co., respectively). These products were purified by repeated recrystallization from acetone and treatment with active charcoal. $C_{14}PyBr$ was synthesized by reacting the corresponding alkylbromide (Eastman Kodak), purified by fractional distillation, with a slight excess of pyridine (30). The crude product was purified by extraction with diethylether, followed by up to 6 recrystallizations from acetone and treatment with active charcoal.

Polysaccharides. Na-alginate was isolated from *Laminaria Hyperborea*. The guluronic acid content was found to be 63.6%, corresponding to an M/G (mannuronic acid/guluronic acid) ratio of 0.57. The total carboxylate concentration was determined by ion exchange to the acid form followed by titration with NaOH. Pectins of various degrees of esterification, E, were prepared from a purified citrus pectin (Genu Pectin, Copenhagen, Denmark) by controlled alkaline deesterification (31). Degree of esterification, intrinsic viscosity $[\eta]$ and viscosity molecular weight were determined using standard procedures (31,32). The concentration of free carboxyl groups in the initial (stock) solutions of potassium pectate and sodium pectinate were determined by precipitation with Cu^{2+} (33,34).

Analytical grade NaCl, polyvinylchloride (Aldrich, high mol. wt.), bis(2-ethylhexyl)phthalate (GR, Aldrich), and tetrahydrofuran (AR, BDH Chemicals) were used without further purification. Polyacrylic acid, mol. wt. 250,000 (Aldrich) was titrated with NaOH to obtain a stock solution of NaPAA of known carboxylate concentration.

Potentiometry. Free surfactant concentrations were determined by means of solid state membrane electrodes responding to the alkylpyridinium cations. The electrodes were made as before (16-19) except that the carrier complex was prepared by reacting the required purified alkylpyridinium bromide with highly purified sodiumdodecylsulfate and repeated recrystallization from acetone of the resulting precipitate. Binding curves were determined by means of a titration technique, where surfactant solution is added to the polymer solution by means of a motorized piston buret. The polymer concentration is kept constant by adding an equal volume of polymer solution of double the initial concentration from a second piston buret (18). In a recent improvement of our experimental set-up, the electrometer output is now digitized and stored in a microcomputer which also checks for constancy of the e.m.f. and activates the piston burets. Thus complete binding curves can be determined unattended. In all measurements the temperature was constant at $30.0 \pm 0.1^\circ\text{C}$.

Results and Discussion

The surface tension of the pyridinium surfactants at 30°C as a function of concentration were measured by means of a Du Nouy ring tensiometer (Figure 2). No minima are apparent in the C_{14} and C_{16} curves, but a small minimum in the C_{12} curve indicates the presence of a minor impurity in the commercial C_{12}PyCl used, even after repeated recrystallizations. In spite of this, our result for the cmc, $1.40 (\pm 0.04) \times 10^{-2}$ m is in very reasonable agreement with literature data reported as 1.46×10^{-2} , 1.48×10^{-2} and 1.78×10^{-2} from conductance (35-37) and 1.62×10^{-2} from surface tension (37), all at 25°C . For C_{14}PyBr we find a cmc of $2.65 (\pm 0.05) \times 10^{-3}$ m, typical literature values are given as 2.57×10^{-3} m from surface tension (35) and 2.63×10^{-3} m from conductance (36). Finally, for C_{16}PyBr we obtain $6.2 (\pm 0.1) \times 10^{-4}$ m, where literature values vary rather widely, i.e. 5.8×10^{-4} (35,38) at 25°C and 7.05×10^{-4} at 30°C (36), both values from conductance, and 6.6×10^{-4} at 25°C from surface tension (39). Note that Anacker (40) has pointed out some difficulties in the determination of the cmc of C_{16}PyCl by conductance.

Typical electrode performances are shown in Figure 2 for C_{14} and C_{16} pyridinium cations in the presence of a large excess of NaCl. We note that the electrodes have an excellent selectivity for the surfactant cation. Response is Nernstian from below 10^{-6} m to the cmc for C_{16}Py^+ , and from about 3×10^{-6} m to the cmc for C_{14}Py^+ and C_{12}Py^+ (not shown). In fact, the electrodes provide for a convenient and accurate method to determine the cmc in particular of the higher chainlength cationic surfactants in solutions of high ionic strength, where other methods become increasingly more difficult (40). An example of the possible application of these electrodes in thermodynamic studies is shown in Figure 4, where the cmc as obtained from data such as in Figure 3 is plotted vs the total counterion concentration. When extrapolated to $m_{\text{NaCl}} =$

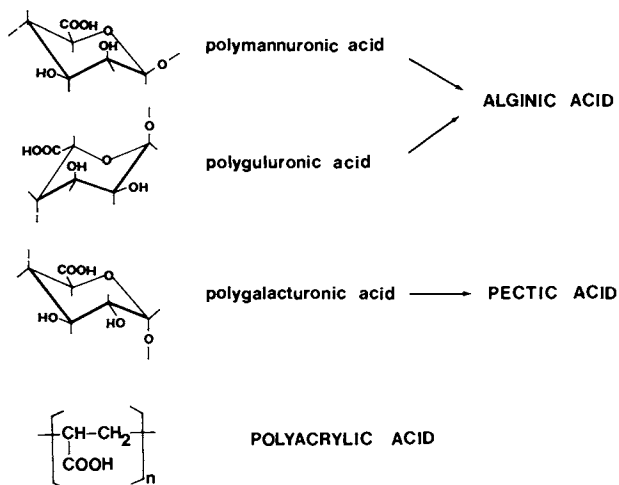


Figure 1. Polymer structures.

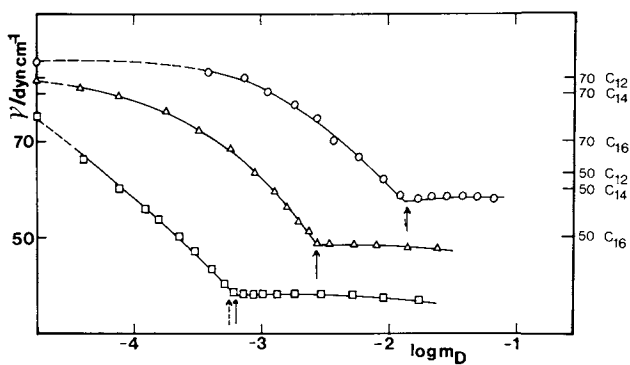


Figure 2. Surface tension of alkylpyridinium halides at 30°C.
 o $C_{12}\text{PyCl}$; Δ $C_{14}\text{PyBr}$; \square $C_{16}\text{PyBr}$.
 Note shifts in vertical scale for C_{12} and C_{14} .

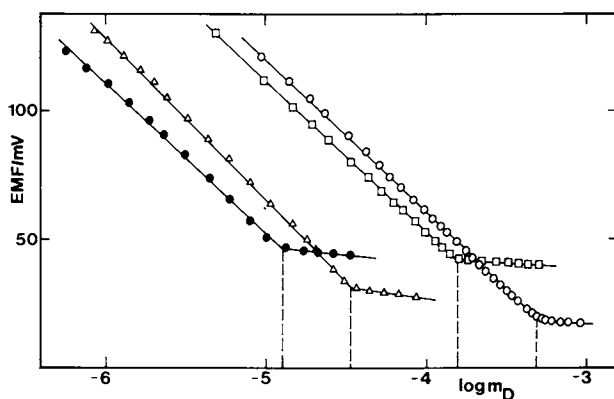


Figure 3. Electrode response for $C_{14}Py^+$ and $C_{16}Py^+$ with NaCl. $C_{14}Py^+$: \circ 0.1 m NaCl, \square 0.5 m NaCl; $C_{16}Py^+$: Δ 0.1 m NaCl, \bullet 0.5 m NaCl.

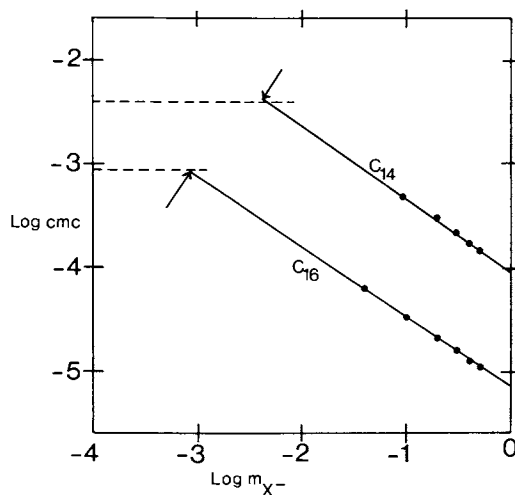


Figure 4. Log cmc vs total counterion concentration in solutions of $C_{14}PyBr$ and $C_{16}PyBr$ with added NaCl. Broken lines: cmc of corresponding chlorides (refs. 35,36). Arrows: extrapolated cmc's.

0, we obtain for pure C_{14} PyCl $\log \text{cmc} = -2.37 \pm 0.03$, and for C_{16} PyCl $\log \text{cmc} = -3.07 \pm 0.02$. Obviously better accuracy can be obtained in a more complete study with data at lower NaCl concentrations, but even these numbers are in reasonable agreement with literature data at 25°C for $\log \text{cmc}$ quoted as -2.40 (36) and -3.05 (35) for C_{14} PyCl and C_{16} PyCl respectively. Similarly, if we calculate the free energy of micellization, ΔG^0 from the intercept at $\log m_{\text{NaCl}} = 0$ we obtain -29.9 kJ/mole for C_{16}^m PyCl and -23.5 kJ/mole for C_{14} PyCl, i.e. a contribution per CH_2 group of 3.2 kJ/mole or 1.27 RT, and from the slope of the $\log \text{cmc}$ vs $\log m_{\text{NaCl}}$ curves we calculate an apparent degree of counterion dissociation of 0.30 ± 0.02 in both cases. These numbers are in good agreement with expected values (41), perhaps even surprisingly so given the high ionic strength of the systems from which these values have been calculated. For the moment they serve to underline the reliable performance of the electrodes in solutions of widely varying ionic strength, such as encountered in the present binding studies, and we leave the application of the e.m.f. method to cmc determinations especially of systems with low cmc and high concentration of various added electrolytes, including multivalent counterions, to the future.

In previous publications (10,16) we have described the procedure used to obtain the degree of binding, β , defined as

$$\beta = (m_D - m_D^f) / m_p \quad (1)$$

where m_D is the total surfactant concentration, m_D^f the free surfactant concentration and m_p the monomolar polyion concentration (i.e. moles $\text{COO}^-/\text{kg H}_2\text{O}$), from the e.m.f. data. All our data will be presented as "binding isotherms", where β is plotted vs $\log m_D^f$. As has been demonstrated before (19) the average linear charge separation on the polymer is the predominant factor in determining the m_D^f region where cooperative binding is observed. This charge separation on the polyion is often expressed in the form of a charge density parameter ξ ,

$$\xi = e^2 / \epsilon b k T \quad (2)$$

where e is the protonic charge, ϵ the dielectric constant, k the Boltzmann constant and T the temperature, and b is the average linear charge separation on the polymer, i.e. the average distance between charged groups on the fully extended polymer. Thus the charge density parameter ξ of polyacrylate has the value 2.83 typical for vinylic polymer chains. For pectate $\xi = 1.61$ if we assume that the 10% neutral sugars in this polymer are not randomly distributed. As is discussed in ref. 19, in the case of alginate there are good reasons to assume that the charge density parameter ξ is slightly larger than the value of 1.43 expected for a polyanuronic acid chain. Both the presence of guluronic acid blocks, and the larger flexibility of this polymer (42) would indicate a value in between 1.43 and 1.61 , the value for pectate (19). A typical example of the influence of the charge density is shown in

Figure 5, where we compare the binding of $C_{14}Py^+$ in the presence of 0.01 m NaCl to PAA, pectate and alginate. We note that the order of the overall binding constant K_u , defined by (2,11,12,16) varies

$$K_u = (m_D^f)^{-1}_{0.5} \quad (3)$$

in the order PAA \gg alginate $>$ pectate. This order of K_u is the same as was observed for alkyltrimethylammonium ions (19), but in the present case of alkylpyridinium ions the difference between alginate and pectate is slightly more pronounced. A number of other minor but typical characteristics can be observed in Figure 5. Binding to PAA reaches a second critical point around $\beta = 0.7$, again similar to the case of the corresponding trimethylammonium ions. All alkyl pyridinium binding curves give indications of a two-step binding process, as may be deduced from the behaviour of the binding isotherms below $\beta = 0.5$. The pectate binding curve seems to level off above $\beta = 1$, possibly indicating that the alkylpyridinium ion can bind to the approximately 10% neutral sugars present in pectate but not in alginate. All the pectate binding curves exhibit a significantly lower cooperativity, i.e. the rise in β with increasing m_D^f is less steep, than the corresponding alginate binding curve.

In Figure 6 we compare the binding of $C_{12}Py^+$ and $C_{14}Py^+$ to PAA to the case of the co-responding dodecyl- and tetradecyltrimethyl ammonium ions (DTA^+ and TTA^+) both in the presence of 0.01 m NaCl, and in Figure 7 a similar comparison is made for $C_{14}Py^+$ and $C_{16}Py^+$ binding to alginate and pectate. The remarkably consistent binding patterns of the various cations and polyions attest not only to the reproducibility of the results, but also to the highly specific character of the binding process. In the case of post-micellar binding the polymer concentration is an important parameter (24). In the present case the relation between the degree of binding, β , and the free surfactant concentration, m_D^f , is completely independent of the equivalent polymer concentration. For instance, curves in Figures 5-8 represent polymer monomolal concentrations of 10^{-4} , 5×10^{-4} , and 10^{-3} m, without any noticeable difference in the trends observed. Finally, in Figure 8 we show the influence of the polymer backbone, varying the degree of esterification of the carboxyl group in pectinates derived from the same polypectate. Relevant parameters characterizing the pectate and pectinates used are given in Table I (31,43). All binding isotherms in Figure 8 are for an equivalent polyion concentration (COO^- concentration) of 1×10^{-3} m, note that therefore the actual polymer concentration increases as the degree of esterification increases. The influence of the charge density is evident. In addition, the influence of the added NaCl concentration shows an interesting pattern: the difference between the m_D^f values at the half-bound point ($\beta = 0.5$) between $m_{NaCl} = 0.01$ and 0.02 is largest for pectate (and approximately as expected compared e.g. to the case of dextransulfate (16)) and becomes progressively smaller as the polyion charge density decreases.

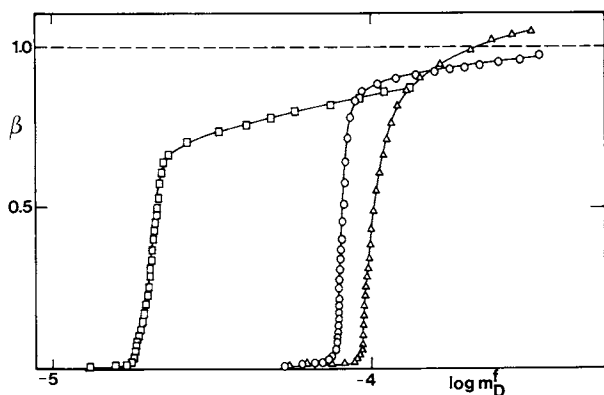


Figure 5. Binding isotherms for $C_{14}PyBr$. $m_{NaCl} = 0.01$ m. Polymers: \square NaPA (5×10^{-3} m); \circ Na-alginate, Δ K-pectate (1×10^{-3} m).

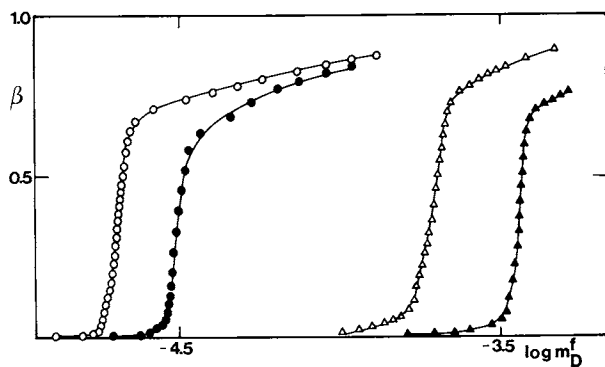


Figure 6. Binding isotherms with polyacrylate (5×10^{-4} m), $m_{NaCl} = 0.01$ m. Δ $C_{12}PyCl$, \circ $C_{14}PyBr$; \blacktriangle DTABr, \bullet TTABr (ref. 19).

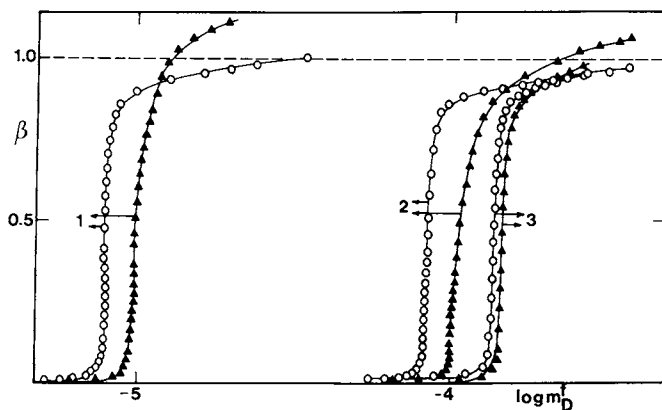


Figure 7. Polyuronide binding isotherms. $m_{\text{NaCl}} = 0.01$ m.
 o Na-alginate; \blacktriangle K-pectate. Curves 1: C_{16}PyBr
 (1×10^{-4} m uronide); 2: C_{14}PyBr , 3: C_{12}PyCl
 (1×10^{-3} m uronide).

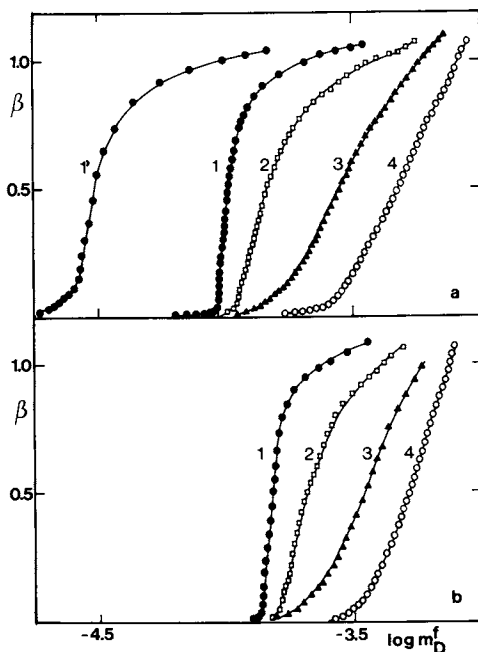


Figure 8. Pectate and pectinate binding isotherms, C_{14}PyBr ,
 $m_{\text{COO}^-} = 1 \times 10^{-3}$. esterification (E): 1 0%,
 2 20.6%, 3 46.1%, 4 70%. a: 0.01 m NaCl.
 b: 0.02 m NaCl. 1': 0%, salt free.

TABLE I. Characterization of Pectate and Pectinates

	Polyuronides %	E ¹ %	[η] ² m ³ kg ⁻¹	M _n ³	ξ
K-pectate	84.9	0	0.133	29,000	1.61
Na-pectinate (2)	86.1	20.6	0.211	41,000	1.28
Na-pectinate (3)	83.8	46.1	0.327	56,000	0.87
Na-pectinate (4)	88.9	70.0	0.092	22,000	0.48

1 Degree of esterification

2 Intrinsic viscosity

3 Molecular weight calculated from viscosity (ref. 43).

All binding parameters derived from fitting the binding isotherms to the equations of Schwarz or Satake and Yang (2,16,19) are collected in Table II. As has been stated before, the overall binding constant K_u can be determined accurately (estimated at $\pm 2\%$), but the determination of K and u separately is much more inaccurate. Generally we estimate the possible error in u at $\pm 20\%$. Even if the model considerations which equate u to a cooperativity parameter describing the aggregation of bound surfactant molecules, prove incorrect or inapplicable, from an experimental point of view u may be seen simply as a parameter indicating the slope of the binding isotherm in the cooperative region, i.e. higher u values mean steeper binding isotherms. What is most obvious from Table II is the identical surfactant chainlength dependence of the K_u values for all polymers, independent of the pyridinium or trimethylammonium head group of the surfactant and of the presence of added salt. The difference per CH_2 group in $\ln K_u$ for all cases presented in Table II averages 1.19_kT , very close to the value of 1.23_kT found for the case of DTA^+ and TTA^+ binding to DNA with or without added NaCl (18). It is hard to find any other explanation for this remarkable constancy than to assume that this factor reflects only the difference in hydrophobic interactions between the C_{12} , C_{14} , or C_{16} alkyl groups, and that the intrinsic binding between surfactant and polyion is unaffected by the surfactant hydrophobic chainlength. Of course the similarity between this hydrophobic effect in surfactant binding by polymers and micelle formation has been pointed out many times, but it is nevertheless satisfying to see this almost perfect correspondence between such widely varying systems.

Finally, we will consider the variation in K_u with surfactant head group, polymer structure and charge density, and added salt concentration. Generally, K_u decreases with increasing salt concentration, which is easily explained in terms of increased shielding of the polymer charges. It remains to be seen whether in fact this is a correct interpretation, it might for instance be argued that similar to the case of metal ion binding by polyelec-

TABLE II. Binding Constants Ku and Parameters u for Surfactant-Polyion Binding.

Polymer	m _{NaCl} (mol/kg)	C ₁₂ Py ⁺ log Ku u ¹	C ₁₄ Py ⁺ log Ku u ¹	C ₁₆ Py ⁺ log Ku u ¹	DTA ⁺² log Ku u ¹	TTA ⁺² log Ku u ¹
PAA	0				4.43	5.39
	0.01	3.69	4.67	250	3.43	4.48
Alginate	0	3.58		100	3.30	4.48
	0.01		4.08	2300		3.88
Pectate	0	3.42	4.52	770	3.35	4.46
	0.01		3.99	250		3.86
	0.02		3.82	320		
Pectinate	0.01		3.83	26		
(20.6% E)	0.02		3.68	50		
Pectinate	0.01		3.55	12		
(46.1% E)	0.02		3.45	26		
Pectinate	0.01		3.32	12		
(70% E)	0.02		3.28	26		

1 Estimated precision ± 20%
2 reference 19.

trolytes it is the entropy gain of the released counterions (i.e. Na^+) which should be considered (44,45). Both approaches would predict a decrease in K_u with increasing salt concentration for a given polyion-surfactant system, and both approaches would also predict a smaller dependence of K_u on the added salt concentration the smaller the polyion charge density. This last effect is sensitively demonstrated not only in our data for the pectinates, but also in the comparison between the salt dependence of K_u for dextran sulfate, polystyrene sulfate (16) and polyacrylate (Table II), all with charge density parameters of 2.8, and alginate and pectate.

The influence of the head group, i.e. pyridinium or trimethylammonium, on the overall binding constant K_u and the cooperativity parameter u is relatively small. It is perhaps surprising that in all cases K_u for the pyridinium salt is larger than for the trimethylammonium salt, as can be seen best e.g. by comparing C_{14}Py^+ and TTA^+ , just as the cmc for pyridinium salts is always lower than the cmc of the corresponding trimethylammonium salt. This may be caused by two factors. First of all, in the case of pyridinium salts there may be a contribution from the hydrophobic interactions between neighbouring bound headgroups (an effect which would not contribute to the free energy of micelle formation). Secondly, a steric hindrance effect may prevent the positive charge on the trimethylammonium head group from approaching close to the polyion charge.

In comparing binding data for the various polymers, it is clear that indeed the charge density is the dominant factor governing K_u . The inversion in K_u values observed between alginate and pectate should then be attributed to the larger flexibility of the alginate polyion (42), allowing it to bind and "envelop" the surfactant aggregates more efficiently. It is noteworthy that the K_u values for DTA^+ at 0.01 M NaCl with dextran sulfate and polyacrylate are virtually identical (16,19) but that in the case of polystyrenesulfonate K_u for DTA^+ is much larger, and u very much lower. These three polyions all have an identical charge density parameter of 2.8, and we conclude that only in the case of polystyrenesulfonate at least part of the surfactant alkyl group binds to the hydrophobic polymer backbone, and does not contribute to the cooperative binding between neighbouring surfactants. Thus it seems likely that, all other things being equal, more flexible polymers are more efficient in binding surfactants, as is particularly clear from the case of DNA (18). We have pointed out the similarity between polyion surfactant ion interaction and micelle formation of free surfactants. This similarity can be seen from e.g. the chainlength dependence of the overall binding constant as discussed above, or from a comparison of the thermodynamic parameters describing both processes (46). In the present context it now seems likely that this similarity extends to the actual aggregation process of the bound surfactants, with the polyion enveloping the micelle-like aggregates and neutralizing the charge of the

surfactant head groups. The remarkable fact remains that this charge neutralization allows aggregation to take place at free surfactant concentrations orders of magnitude below the cmc, dependent on the polyion charge density.

Acknowledgments

We are grateful to the Natural Sciences and Engineering Research Council of Canada and the Czechoslovak Academy of Sciences for the award of a scholarship under the auspices of the scientific exchanges agreement between the Council and the Academy, and the Killam Foundation for the award of a postdoctoral fellowship to one of the authors (A.M.). The authors are grateful to Drs. B. Larsen and O. Smidsrød, Institute of Marine Biochemistry, University of Trondheim, Norway for the donation of a fully characterized sample of Na-alginate, and to Dr. R. Kohn, Institute of Chemistry, Slovak Academy of Sciences, Bratislava, Czechoslovakia, for preparing and characterizing pectin samples with different degrees of esterification. This research is supported by the Natural Sciences and Engineering Research Council of Canada through grants to J.C.T.K.

Literature Cited

1. Goddard, D.E., Hannan, R.B. J. Colloid Interface Sci. 1976, 55, 73.
2. Satake, I., Yang, J.T. Biopolymers 1976, 15, 2263.
3. Gavach, C., Bertrand, C. Anal. Chim. Acta 1971, 55, 385.
4. Birch, B.J., Clarke, D.E. Anal. Chim. Acta 1973, 67, 387.
5. Cutler, S.G., Meares, P., Hall, D.G. J. Electroanal. Chem. 1977, 85, 145.
6. Yamauchi, A., Kunisaki, T., Minematsu, T., Tomokiyo, Y., Yamaguchi, T., Kimizuka, H. Bull. Chem. Soc. Jpn. 1978, 51, 2791.
7. Satake, I., Gondo, T., Kimizuka, H. Bull. Chem. Soc. Jpn. 1979, 52, 361.
8. Kale, K.M., Cussler, E.L., Evans, D.F. J. Phys. Chem. 1980, 84, 593.
9. Maeda, T., Ikeda, M., Shibaharu, M., Haruta, T., Satake, I. Bull. Chem. Soc. Jpn. 1981, 54, 94.
10. Hayakawa, K., Ayub, A.L., Kwak, J.C.T. Colloids Surf. 1982, 4, 389.
11. Zimm, B.H., Bragg, J.K. J. Chem. Phys. 1980, 84, 593.
12. Schwarz, G. Eur. J. Biochem. 1970, 12, 442.
13. Shirahama, K., Yuasa, H., Sugimoto, S. Bull. Chem. Soc. Jpn. 1981, 54, 375.
14. Fukushima, K., Murata, Y., Nishikido, N., Sugihara, G., Tanaka, M. Bull. Chem. Soc. Jpn. 1981, 54, 3122.
15. Fukushima, K., Murata, Y., Sugihara, G., Tanaka, M. Bull. Chem. Soc. Jpn. 1982, 55, 1376.

16. Hayakawa, K., Kwak, J.C.T. J. Phys. Chem. 1982, 86, 3866.
17. Hayakawa, K., Kwak, J.C.T. J. Phys. Chem. 1983, 87, 506.
18. Hayakawa, K., Santerre, J.P., Kwak, J.C.T. Biophys. Chem. 1983, 17, 175.
19. Hayakawa, K., Santerre, J.P., Kwak, J.C.T. Macromolecules 1983, 16, 1642.
20. Satake, I., Yang, J.T. Biopolymers 1975, 14, 1841.
21. Hayakawa, K., Ohara, K., Satake, I. Chem. Lett. (Jpn.) 1980, 647.
22. Robb, I.D. in "Surfactant Science Series", Vol. 11, E.H. Lucassen-Reynders, ed., Marcel Dekker, New York, 1981, p. 109.
23. Oteri, R., Dubin, P.L. Polymer Preprints 1982, 23, 45.
24. Dubin, P.L. Oteri, R. J. Coll. Interface Sci. 1983, 95, 453.
25. Murata, M., Arai, H. J. Coll. Interface Sci. 1973, 44, 475.
26. Gilanyi, T., Wolfram, E. Colloids Surf. 1981, 3, 181.
27. Nagarajan, R. Colloids Surf., in press.
28. Cabane, B., Colloids Surf., in press.
29. Kohn, R. Pure Appl. Chem. 1975, 42, 371.
30. Knight, A., Shaw, B.D. J. Chem. Soc. 682, 1938.
31. Kohn, R., Furda, I. Collect. Czech. Chem. Commun. 1967, 32, 1925.
32. Owens, H.S., Lotzkar, H., Schultze, T.H., Mackay, W.D., J. Amer. Chem. Soc. 1946, 68, 1628.
33. Tibensky, V., Rosik, J., Zitko, V. Nahrung 1963, 7, 321.
34. Kohn, R., Tibensky, V. Chem. Zvesti 1965, 19, 98.
35. Mukerjee, P., Mysels, K.J., "Critical Micelle Concentrations of Aqueous Solutions", NSRDS-NBS 36, USA, 1971.
36. Hoffman, H., Nagel, R., Platz, G., Ulbricht, W. Colloid Polymer Sci. 1976, 254, 812.
37. Rosen, M.J., Dahanayake, M., Cohen, A.W. Colloids Surf. 1982, 5, 159.
38. Evers, I.C., Kraus, C.A. J. Amer. Chem. Soc. 1948, 70, 3049.
39. Paluch, M. J. Coll. Interface Sci. 1978, 66, 582.
40. Anacker, E.W. J. Phys. Chem. 1959, 62, 41.
41. Anacker, E.W. in "Cationic Surfactants", Jungerman, E., Ed., Marcel Dekker, New York, 1970, p. 203.
42. Aspinall, G.O., "The Carbohydrates, Chemistry and Biochemistry", Academic Press; New York, 2nd ed., 1970, II, p. B515.
43. Kohn, R., Luknar, O. Collect. Czech. Chem. Commun. 1975, 40, 959.
44. Manning, G.S. Q. Rev. Biophys. 1978, 2, 179.
45. Mattai, J., Kwak, J.C.T. J. Phys. Chem. 1982, 86, 1026.
46. Santerre, J.P., Hayakawa, K., Kwak, J.C.T. Colloids Surf. in press.

RECEIVED March 6, 1984

Linear Sodium Alkylbenzene Sulfonate Homologs

Comparison of Detergency Performance with Experimental and Thermodynamic Wetting Theories

JAMES A. WINGRAVE¹

Conoco, Inc., Chemical Research Division, Ponca City, OK 74603

Pure homologs of linear alkylbenzene sulfonate sodium salts (LAS) were evaluated for detergency performance. The surface tensions of the wash liquors used for these detergencies were then measured and used in conjunction with a wetting model to calculate a theoretical detergency performance. The theoretical and experimental detergency results were compared. The molecular structure effects of the LAS homologs on detergency performance were calculated by incorporating into the detergency equation several molecular structure theories such as the cohesive energy ratio concept, molar-attraction constants, internal liquid pressure, and liquid thermal properties. The assets and deficiencies of these approaches are discussed.

The process of detergency involves the complete separation of two substances by means of a deterative bath. The success of such a process requires a knowledge of the chemistry between the two substances to be separated (henceforth referred to as soil and substrate). From this knowledge, a detergency bath can be designed with chemical characteristics necessary to separate the soil and substrate by overcoming the attractive forces between them. However, stating the principles of detergency and achieving them in practice are different; the latter being far more difficult, as noted by the voluminous literature on the subject (1-10). It will, therefore, be the purpose of this paper to develop a better understanding of how surfactant structure

¹Current address: E. I. du Pont de Nemours, Inc., Chambers Works, Deepwater, NJ 08023

effects detergency performance by using a homologous series of linear alkylbenzene sulfonate sodium salt (LAS) derivatives in the detergency bath.

The kinetic effects of detergency will not be explored in this study, but review articles on this topic can be found elsewhere (1-5). Instead, the agitation will be held constant (see Experimental Section) so that the equilibrium (or near equilibrium) processes can be observed. Equilibrium was achieved for similar soil/substrate systems within 5-10 minutes in previous studies (3).

For this study, the soil will be a mineral oil constituted as shown in Figure 1. The cloth used will be a cotton/polyester blend with a polyethylene glycol fabric finish. Since the soil will be a liquid, effective detergency will require a bath that can overcome the physical forces between the soil and fabric (i.e., the fabric finish). For physical forces, the problem becomes one of developing a model of the detergency system, then combining this model with wetting theory in order to produce a detergency equation for detergency performance.

Discussion

Soil-Fabric Morphology. In Figure 2, scanning electron micrographs of the fabric used in this study are shown. In the threads of the fabric are fibers which run very nearly parallel. When soiled with a liquid soil, a pendular drop of soil should form between contiguous fibers as shown in cross section in Figure 3. The bath/soil interface is shown planar and parallel with the plane passing through the fiber centers (Figure 4a). When one chooses a particular detergent bath/soil/fiber combination, the contact angle, ψ (measured through the soil phase), at the line where all three phases meet will strive to attain a specific value based on the properties of the three phases, as shown in Figure 4b. Therefore, the triple-phase line (TPL) will move to assume a value of ψ . This, in turn, will cause a curvature J in the soil/bath interface. This movement of the TPL is the process by which large soil drops can be formed on/in the fabric as ψ approaches values of 90° and greater, as shown in Figure 4c. This process is relatively rapid, occurring within 10 minutes for most systems, and is generally referred to as the roll-up mechanism of soil removal. From this description, it is obvious how agitation and buoyant effects of the soil could speed up this mechanism (in fact, roll up cannot occur at all unless buoyant or agitation forces act on the soil), but soil-removal rate is a kinetic question and will not be pursued further here.

Another soil-removal mechanism is also working, simultaneously, to remove soil albeit a much slower process (i.e., up to several hours). When the bath/soil interface becomes curved due to a change in ψ (see Figure 4d), its chemical potential is

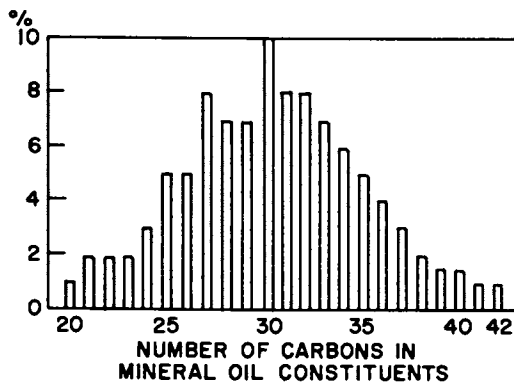


Figure 1. Constitution of the Mineral Oil Soil.

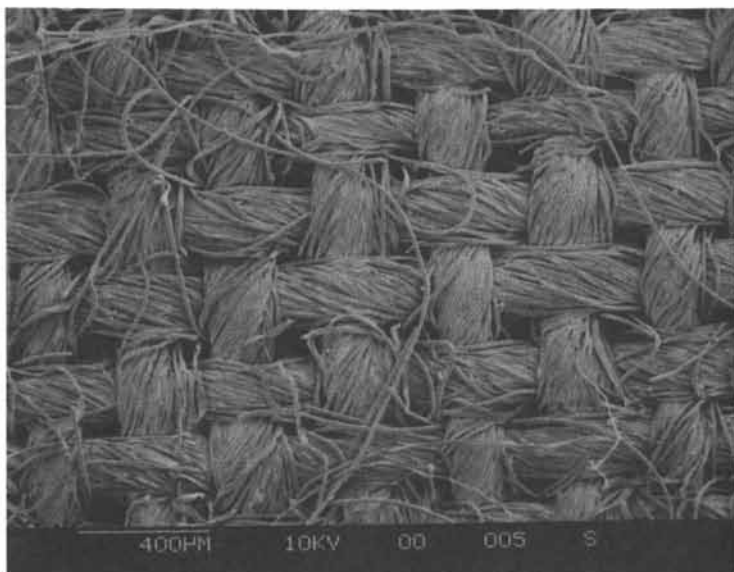
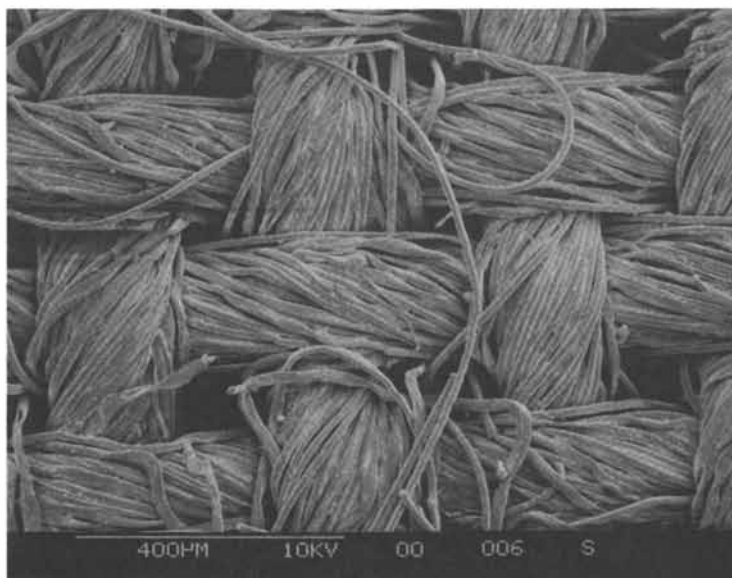


Figure 2. Scanning Electron Micrographs of Fabric Used for Detergency Studies.

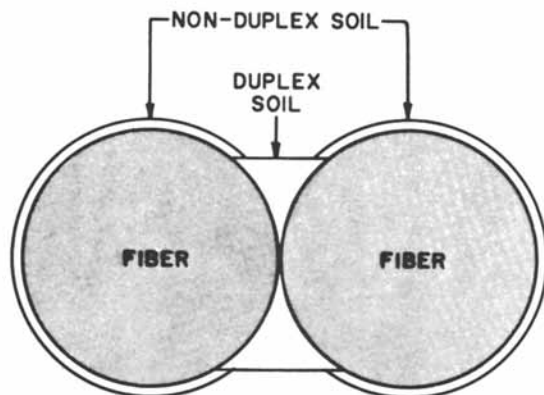


Figure 3. Cross-Sectional View of Soil Drop Between Contiguous Fibers.

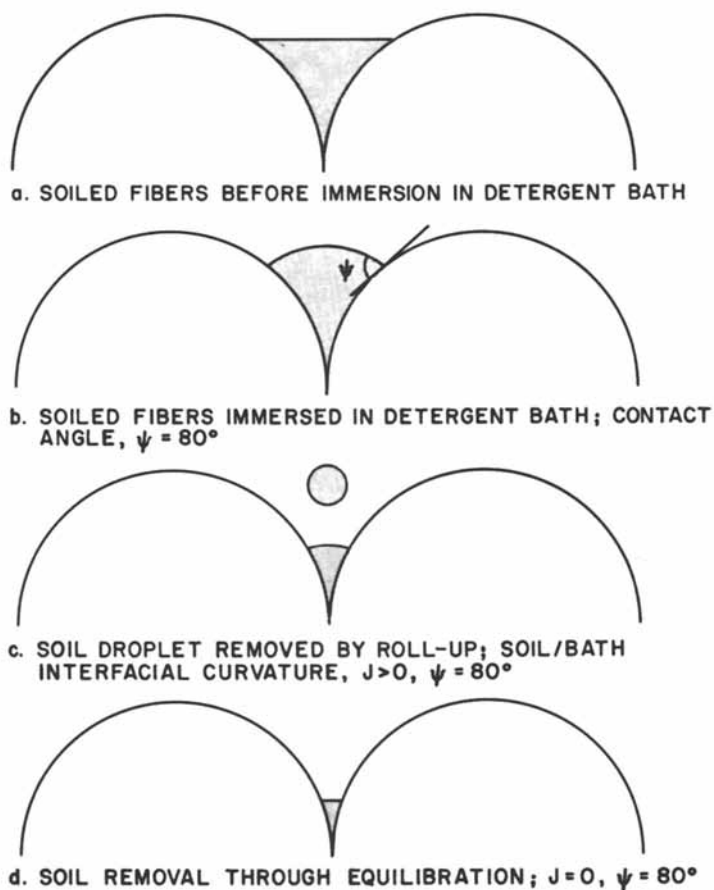


Figure 4. Mechanism for Soiled Fabric Fiber Detergency.

greater than a flat, bath/soil interface. The instantaneous curvature J will change through soil dissolution until it achieves a smaller curvature (flatter interface) J_e . The soil removed in this way will either solubilize in the bath, collect as small macroscopic oil droplets at the bath/air interface, or emulsify if agitation is present. Hence, in a detergency system that has attained equilibrium, soil lenses or small (nominally 1 mm diameter) soil droplets are commonly seen floating at the air/bath interface. Under these circumstances, the curvature is very small (nominally 1 mm diameter), and when applied to the scale of pendular oil droplets between fibers (nominally 1 to 10 μm diameter) the bath/soil interface will be flat for all practical purposes. Therefore, the model in Figure 3, showing a flat bath/soil interface, should be valid for all detergency systems where bulk soil is observed and fabric fibers are small (<100 nm diameter).

From this model, the volume of soil can be determined for the geometry shown in Figure 5 and the Appendix. The equation for this volume of a partially soil-filled pore with a contact angle ψ compared to the total pore volume, V_R , is (1)

$$V_R = \frac{2 \cos \psi (2 - \sin \psi) - (\pi - 2 \psi)}{(4 - \pi)} \quad (1)$$

Then since detergency is a soil-removal process, the relative detergency, D_R , can be written as a function of ψ only as

$$D_R = 1 - \frac{2 \cos \psi (2 - \sin \psi) - (\pi - 2 \psi)}{(4 - \pi)} \quad (2)$$

The quantity D_R ignores the adsorbed soil on the fiber surfaces. However, this can be shown (11) to be an insignificant amount of soil compared to the pore-held soil unless the fiber diameters were <0.1 μm . Hence Equation 2 should be quite satisfactory for almost all cloth in which fiber diameters are generally $\geq 1.0 \mu\text{m}$.

It is also noteworthy that the contact angle has been defined as being measured through the oil phase since that is the medium of interest. Furthermore, ψ varies directly with D_R by this definition (see Figure 6). Conventionally, contact angle is measured through the most dense medium (which would be the aqueous detergent bath) and given the symbol θ . Hence, the symbol ψ will be used in this work while it is clear that the two quantities are related as, $\psi = 180^\circ - \theta$.

With this geometric model for D_R as a function of ψ , it is now necessary to develop a method to evaluate ψ from wetting or surface chemistry parameters.

Evaluation of the Soil-Fiber Morphology Equation. The most direct method of evaluating Equation 2 for D_R is to measure the contact angle ψ for the fiber-soil-bath system of interest.

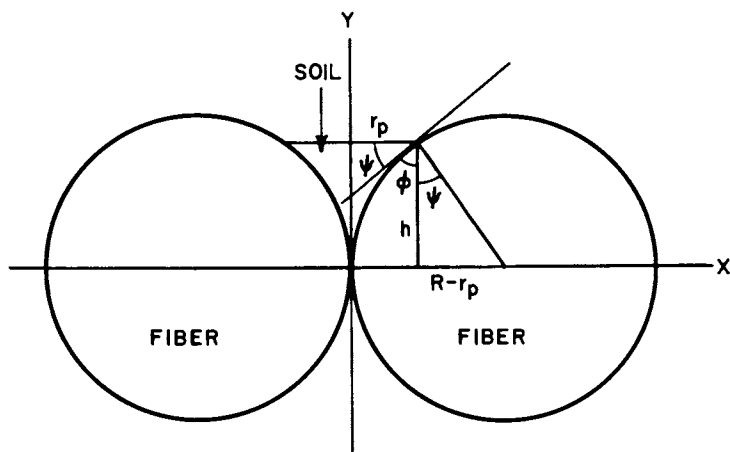


Figure 5. Cross-Sectional View of Soil/Fiber Geometry.

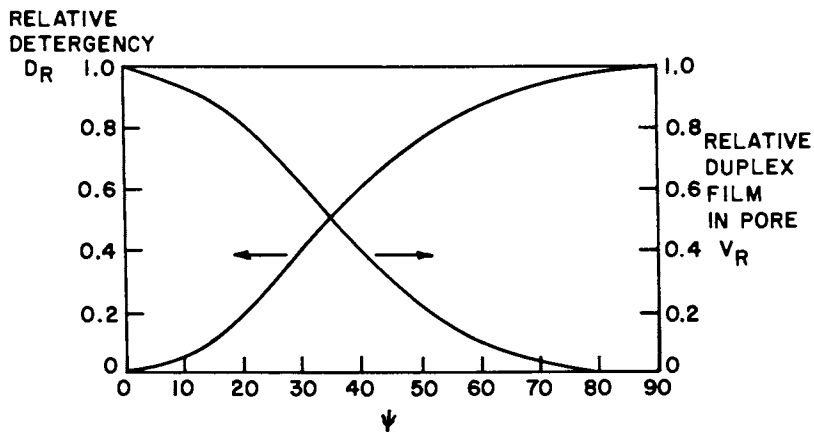


Figure 6. Dependence of Detergency on Soil-Fiber-Water Contact Angle.

American Chemical
Society Library

1155 16th St. N.W.

Washington, D.C. 20036
In Structure/Performance Relationships in Surfactants; Rosen, M.; ACS Symposium Series 20036; American Chemical Society: Washington, DC, 1984.

While direct, this method is the most difficult experimentally due to the diminutive nature of fiber diameters and the uncertainty involved with contact angle measurements and hysteresis. The value ψ can also be measured on flat sheets of the fiber material but due to fabric finishes and different surface properties incurred during manufacture, the surface energetics of the sheet and fiber may be very dissimilar. Therefore, the value of $\cos\psi$ was determined in the following manner from detergency data. The Kubelka-Munk Equation (12-13),

$$V_R(KM) = \frac{\alpha_{soil} - \alpha_{wash}}{\alpha_{soil} - \alpha_{clean}} \quad (3)$$

where $\alpha = \frac{K}{S} = \frac{(1-R_d)^2}{2R_d}$

R_d = reflectance (see Experimental Section for more details)

K = coefficient of reflectivity (12-13)

S = coefficient of light scattering (12-13)

α_{wash} = K/S for soiled cloth after washing

α_{soil} = K/S for soiled cloth

α_{clean} = K/S for unsoiled cloth

was combined with Equations 1 and 3

$$V_R(KM) = \frac{\alpha_{soil} - \alpha_{wash}}{\alpha_{soil} - \alpha_{clean}} = \frac{2 \cos \psi (2 - \sin \psi) - (\pi - 2 \psi)}{(4 - \pi)} \quad (4)$$

This yields an equation from which contact angle values, ψ , can be determined directly from reflectance readings (see Table 1).

Wettability Dependence of Detergency. The dependence of D_R on ψ was described above. The purpose of this section will be to develop an expression for ψ in terms of experimentally accessible interfacial tension quantities. To begin with, the TPL has a geometry as shown in Figure 7. For this system, the Young-Dupre' equation (14-16) can be written as

$$\gamma_{fw} = \gamma_{fs} + \gamma_{sw} \cos \psi \quad (5)$$

In a similar manner, an expression for the interfacial tension, γ_{fw} can be written using the geometric mean definition for work of adhesion, W_A (see Figure 8), and the Girifalco-Good interaction parameter (17-18), Φ as,

$$W_A = 2 \Phi_{fw}^* \sqrt{\gamma_{sw} \gamma_{fs}^*} \quad (6)$$

or

Table I. Kibulka-Munk Transformation of Detergency Reflectance Data to Wettability Data

Hardness (ppm)	LAS ^a	R _d	Detergency, DR (%)	cos ψ ^b
50	10	61.3	65.1	0.741
	11	63.7	70.7	0.702
	12	63.9	71.0	0.699
	13	64.9	73.2	0.682
	14	65.2	73.8	0.677
150	10	51.6	33.7	0.897
	11	58.1	56.4	0.793
	12	65.2	73.8	0.677
	13	65.8	75.0	0.677
	14	66.3	75.9	0.660
300	10	49.5	24.5	0.929
	11	62.2	67.2	0.727
	12	64.4	72.1	0.691
	13	61.6	65.7	0.737
	14	59.9	61.5	0.764

^aavalue refers to the number of carbon atoms in the linear alkyl chain of the linear alkylbenzene sulfonate sodium salt.

^bFrom Kibulka-Munk/detergency Equation 4.

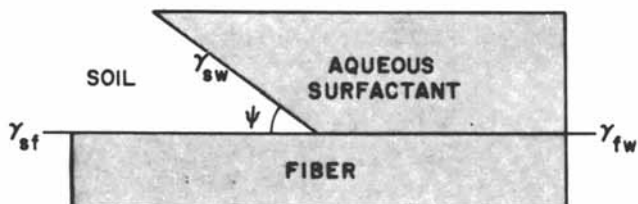


Figure 7. Triple-Phase Line Geometry for Soil/Fiber System.

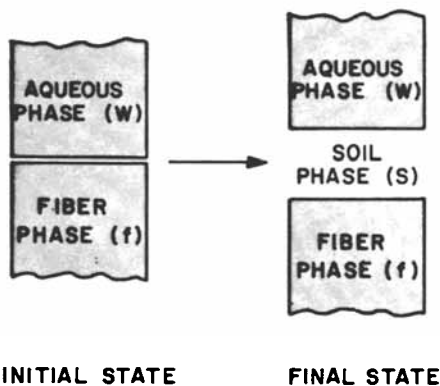


Figure 8.
Process for Defining the Work of Adhesion Between Two Dense Phases.

$$\gamma_{fw}^* = \gamma_{sw} + \gamma_{fs}^* - 2 \Phi_{fw}^* \sqrt{\gamma_{sw} \gamma_{fs}^*} \quad (7)$$

where the asterisk signifies that γ_{fs}^* is measured in the absence of the detergent bath and γ_{fw}^* in the absence of the soil.

Notice that the asterisk designation is not required when the third phase is air, or the vapor of one or more of the components already present in the system, since interfacial interactions are not significantly affected by phase dissolution and adsorption of air or a common vapor. Hence the asterisk designation was not required in Girifalco and Good's original work (17-18). In a similar fashion, the asterisk is not used with γ_{sw} since the solid is assumed insoluble in both the soil and bath.

When Equations 5 and 7 are combined and rearranged, a Girifalco-Good-type equation results as[†]

$$\cos \psi = 1 - 2 \Phi_{fw}^* \sqrt{\frac{\gamma_{fs}^*}{\gamma_{sw}}} + \frac{\pi_{fs} - \pi_{fw}}{\gamma_{sw}} \quad (8)$$

$$\text{where } \pi_{fs} = \gamma_{fs}^* - \gamma_{fs}$$

$$\pi_{fw} = \gamma_{fw}^* - \gamma_{fw}$$

If the substitution for Φ_{fw}^*

$$\Phi_{fw}^* = (\Phi_{fw}^* - 1) + 1 \quad (9)$$

is combined with Equation 8 and the resulting equation rearranged, then

$$\cos \psi = 1 - \frac{2 \sqrt{\gamma_{fs}^*}}{\sqrt{\gamma_{sw}}} + \frac{\pi_{fs} - \pi_{fw} + 2 (1 - \Phi_{fw}^*) \sqrt{\gamma_{sw} \gamma_{fs}^*}}{\gamma_{sw}} \quad (10)$$

Equation 10 is obviously a Girifalco-Good equation for a solid (f), liquid (s), liquid (w) system. If values of ψ and γ_{sw} are measured for a series of surfactant homolog solutions, a plot of $\cos \psi$ versus $1/\sqrt{\gamma_{sw}}$ will give a Girifalco-Good plot from which values of γ_{fs}^* and other surface energetic parameters can be determined under appropriate conditions. This evaluation will be the topic of the following sections.

Wettability Parameters From Detergency Data. If a series of surfactant homolog solutions is used to evaluate ψ and γ_{sw} for a given fiber and soil system, a Girifalco-Good plot can be constructed. Such data was gathered for LAS homologs at 50, 150, and 300 ppm hard ion concentration and plotted in Figure 9. From the form of Equation 10, it is clear that a plot of $\cos \psi$ versus $1/\sqrt{\gamma_{sw}}$ will give a linear plot which will fit a straight-line equation

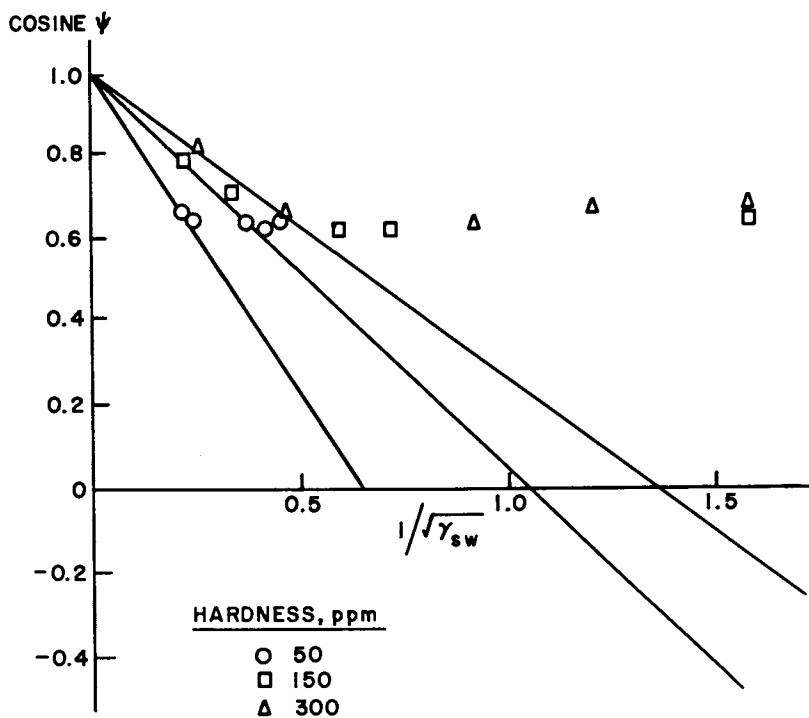


Figure 9.
Girifalco-Good Plot of Wettability Data From Detergency and Interfacial Tension Data.

$$\cos \psi = -\frac{a}{\sqrt{\gamma_{sw}}} + 1 + \frac{b}{\gamma_{sw}} \quad (11)$$

where $a = 2\sqrt{\gamma_{fs}^*}$

$$b = \pi_{fs} - \pi_{fw} + 2(1 - \phi_{fw}^*)\sqrt{\gamma_{sw}\gamma_{fs}^*}$$

From the form of Equation 11, it is clear that the slope, a , will be independent of the aqueous surfactant solution. However, b in the intercept, $1 + (b/\gamma_{sw})$, will not be zero; in fact, it will not even be independent of the aqueous surfactant solution. Therefore, the conventional methods of Girifalco-Good plot analysis with an intercept of unity will not work for the detergency systems of interest in this work. The impediment to the Girifalco-Good analysis method is obvious from Figure 9, where no set of data points (3 or more) lies on a line passing through the coordinates $\cos \psi = 1$, $0 = 1/\gamma_{sw}$. The evaluation of the surface chemical properties will require a different evaluation method.

Wetting Parameters in the Detergency Equation. The detergency system has three interfaces which have three interfacial tensions at equilibrium with all three phases: γ_{sw} , γ_{fs} , and γ_{fw} . When only two phases are in equilibrium, three other surface tensions are possible: γ_{sw}^* , γ_{fs}^* , and γ_{fw}^* (however, when the fiber is an insoluble solid, $\gamma_{sw} = \gamma_{sw}^*$, and so only γ_{sw} will be referenced). Corresponding to these interfaces are Girifalco-Good interaction parameters: ϕ_{sw}^* , ϕ_{fs}^* , and ϕ_{fw}^* . The final parameter type in a detergency system is film pressure of the two liquids on the solid fiber: π_{fs} and π_{fw} .

These ten interfacial parameters give a very complete description of the energetics of a detergency system. Further surface tension variables for a fluid-air or solid-air interface will also be used to evaluate these ten interfacial parameters. The remainder of this section will explore their evaluation.

To begin with, as many of the parameters as possible were experimentally measured. These values are given in Table 2. The contact angle ψ was determined from detergency results as described earlier.

The values of γ_s , γ_w , and γ_{sw} were measured by spinning drop interfacial tensiometry (SDIT) as described in the Experimental Section. The values of γ_f^* and γ_{fs}^* were obtained by the SDIT method using a polyethylene glycol (PEG), Jeffox PEG-300

† Note that the $\cos \psi = -\cos \theta$, hence, Equation 6 differs from References 14-16 due to the definition of the contact angle.

Table II

Hard- ness (ppm)	HF LAS Homo-	MEASURED VALUES ^a				
	log	$\cos \psi$	γ_w	γ_{sw}	ϕ_{sw}	ϕ_{fw}^*
50	10	0.741	46.7	20.1	0.756	0.978
	11	0.702	41.1	15.3	0.794	0.992
	12	0.699	30.2	7.24	0.879	1.007
	13	0.682	30.7	5.57	0.908	0.996
	14	0.677	30.2	4.04	0.932	0.985
150	10	0.897	41.7	17.6	0.764	0.984
	11	0.793	33.0	8.2	0.870	1.003
	12	0.667	26.7	2.8	0.951	0.977
	13	0.667	25.9	1.9	0.968	0.964
	14	0.660	25.8	0.4	0.995	0.911
300	10	0.929	38.3	13.3	0.811	0.997
	11	0.727	30.3	4.5	0.925	0.989
	12	0.671	26.0	1.2	0.981	0.945
	13	0.737	27.5	0.7	0.989	0.923
	14	0.764	26.0	0.4	0.994	0.911

^aOther measured values:

$$\gamma_s^* = 29.6 \text{ dynes/cm.}$$

$$\gamma_f^* = 39.7 \text{ dynes/cm.}$$

$$\gamma_{fs}^* = 10.5 \text{ dynes/cm.}$$

^bOther calculated values:

$$\phi_{fs}^* = 0.858.$$

CALCULATED VALUES ^b					
γ_{fw}^*	γ_{fw}	π_{fw}	γ_{fs}	π_{fs}	b
2.19	16.1	-13.9	1.20	9.3	-23.8
0.65	12.0	-11.3	1.30	9.2	-20.8
0.19	5.95	-5.76	0.887	9.6	-15.3
0.83	4.74	-3.91	0.943	9.6	-13.52
1.71	3.65	-1.94	0.910	9.6	-11.72
1.36	16.0	-14.64	0.180	10.3	-25.4
0.08	6.96	-6.88	0.455	10.05	-16.9
2.70	2.74	-0.04	0.843	9.7	-9.94
3.79	2.17	1.62	0.901	9.6	-8.30
7.16	1.47	5.69	1.203	9.3	-3.96
0.23	12.4	-12.2	0.072	10.4	-22.7
1.41	3.94	-2.53	0.665	9.8	-12.5
4.99	1.63	3.36	0.802	9.7	-6.73
6.19	1.089	5.10	0.573	9.9	-5.24
7.17	0.782	6.39	0.477	10.0	-4.00

(Jefferson Chemical Company, Austin, Texas), for the fiber surface analog. This substitution was made since the fabric used in this study had a PEG fabric finish. This fabric finish differed from the Jeffox PEG-300 only in the fact that the former was higher molecular weight and therefore solid, while the latter was a liquid and amenable to SDIT measurement of γ_f^* and γ_{fs}^* . With these values, the remaining eight surface parameters can be calculated.

The Girifalco-Good equation for the soil-water interfacial tension

$$\gamma_{sw} = \gamma_s^* + \gamma_w^* - 2 \Phi_{sw}^* \sqrt{\gamma_s^* \gamma_w^*} \quad (12)$$

can be rearranged to calculate Φ_{sw}^* as

$$\Phi_{sw}^* = \frac{\gamma_s^* + \gamma_w^* - \gamma_{sw}^*}{2 \sqrt{\gamma_s^* \gamma_w^*}} \quad (13)$$

where $\Phi_{sw}^* = \Phi_{sw}$, as was the case for sw interfacial tensions.

For the quantity γ_{fs} , one can combine the Young-Dupre' equation

$$\gamma_{fw} = \gamma_{fs} + \gamma_{sw} \cos \psi \quad (14)$$

with the Girifalco-Good equation

$$\gamma_{sw} = \gamma_{fs} + \gamma_{fw} - 2 \Phi_{sw} \sqrt{\gamma_{fs} \gamma_{fw}} \quad (15)$$

to yield the quadratic equation for γ_{fs} as

$$\gamma_{fs}^2 - \left[\frac{(1 - \Phi_{sw}^2) \gamma_{sw} \cos \psi}{1 - \Phi_{sw}^2} \right] \gamma_{fs} + \frac{\gamma_{sw}^2 (1 - \cos \psi)}{4 (1 - \Phi_{sw}^2)} = 0 \quad (16)$$

which can be solved and simplified to yield

$$\gamma_{fs} = \frac{\gamma_{sw}}{2 (1 - \Phi_{sw}^2)} \left\{ \left[1 - (1 - \Phi_{sw}^2) \cos \psi \right] + \sqrt{\left[1 - (1 - \Phi_{sw}^2) \cos \psi \right]^2 - (1 - \cos \psi)^2} \right\} \quad (17)$$

Using the value of γ_{fs} , the quantity γ_{fw} can be calculated from the Young-Dupre' Equation 14.

The quantity γ_{fw}^* can be calculated by the simultaneous solution of two Girifalco-Good equations for γ_{fw}^* :

$$\gamma_{fw}^* = \gamma_f^* + \gamma_w^* - 2 \Phi_{fw}^* \sqrt{\gamma_f^* \gamma_w^*} \quad (18)$$

and

$$\gamma_{fw}^* = \gamma_{sw} + \gamma_{fs}^* - 2 \Phi_{fw}^* \sqrt{\gamma_{sw} \gamma_{fs}^*} \quad (7)$$

to yield

$$\gamma_{fw}^* = \frac{(\gamma_{sw} + \gamma_{fs}^*) \sqrt{\gamma_f^* \gamma_w^*} - (\gamma_f^* + \gamma_w^*) \sqrt{\gamma_{sw} \gamma_{fs}^*}}{\sqrt{\gamma_f^* \gamma_w^*} - \sqrt{\gamma_{sw} \gamma_{fs}^*}} \quad (19)$$

Equation 7 can then be rearranged to allow calculation of Φ_{fw}^* as

$$\Phi_{fw}^* = \frac{\gamma_{sw} + \gamma_{fs}^* - \gamma_{fw}^*}{2 \sqrt{\gamma_{sw} \gamma_{fs}^*}} \quad (20)$$

The last quantity to be calculated is Φ_{fs}^* , which can be determined from the Girifalco-Good equation for γ_{fs}^* as

$$\Phi_{fs}^* = \frac{\gamma_f^* + \gamma_s^* - \gamma_{fs}^*}{2 \sqrt{\gamma_f^* \gamma_s^*}} \quad (21)$$

Equations 12 through 21 were used to calculate the interfacial parameters for the detergency system consisting of PEG-finished polyester/cotton cloth, mineral oil soil, and detergent baths consisting of varying homolog solutions of LAS homologs from 10- to 14-carbon-atom alkyl chain length. The calculated and experimentally determined results are listed in Table 2. These results will be the topic of the following section.

Interfacial Parameters in the Detersive System. Three phases are present in the detergency system in this study: a PEG (fiber), a hydrocarbon (soil), and an aqueous surfactant (bath) phase. These three phases meet to form three binary interfaces, whose interfacial energetic properties vary as a function of LAS homolog molecular weight.

The interfacial tension data listed in Table 2 show variations with LAS homolog molecular weight that can be ascribed to the Ferguson effect (19). This is best demonstrated at 50 ppm hardness for γ_{fw}^* , where the 12-carbon homolog gives the minimum interfacial tension. The lower and higher homologs give greater interfacial tensions (i.e., have less interfacial affinity) as a result of being too water-soluble and insoluble, respectively. Other surface and interfacial tensions, such as γ_w and γ_{sw} , show only a decrease in value with increasing LAS homolog carbon chain number. However, if tension values on LAS carbon chain homologs >14 were measured, increasing tension values with carbon chain would eventually be observed.

The film pressure values for the detergency system are also listed in Table 2. These quantities represent the difference in interfacial tension between two pure phases and the interfacial tension of the same two phases which are at saturation equilibrium with the third phase. Since the PEG fiber surface was assumed insoluble in either the bath or soil, $\pi_{sw} = 0$.

The value of π_{fs} is seen to be nearly constant, indicating that the adsorption of the bath (water, surfactant, and hardness) at the fs interface is negligible. The π_{fw} value is, however, quite interesting in that it shows dramatic variations with homolog and hardness changes from negative to positive in magnitude. From the data, it can be seen that with the introduction of soil into the fw interfacial system, the value of γ_{fw} increases. While the mechanism for this behavior was not determined in this study, it would seem most likely that this behavior occurs as a result of surfactant leaving the fw interface to either emulsify or solubilize into the soil phase. Since the free energy process that corresponds to the π_{fw} value could only be spontaneous if π_{fw} was positive, another compensating process in the bath phase which had a greater free energy change, such as soil emulsification or surfactant-in-soil solubilization, must occur simultaneously.

Molecular Structure Effects and Detergency. The correlation of surfactant structure with interfacial and colloid properties is a poorly understood science. Much study in this area has been thermodynamic which has been a useful endeavor but which nevertheless fails to provide specific molecular structure/physical property correlations. The following study has also been largely thermodynamic to this point; however, since the data has been collected on pure LAS homologs, it provides an opportunity to apply some of the quasi-thermodynamic treatments that have been proffered in the literature to date.

The first of these to be discussed will be the Cohesive Energy Ratio, R concept (20). Using the concept of cohesive energy between molecules, Winsor recognized four structures. These are present in an immiscible two-phase system (O and W denoting oil and water, respectively) containing a third-surfactant component with partial solubility in both bulk phases. Each surfactant molecule has a hydrophilic (denoted by H) and a lipophilic (denoted by L) section. Conceptually then Winsor views all the possible molecular interactions in such a system in terms of their cohesive energy (denoted by C). For such a system, there are then 10 possible cohesive molecular interactions (i.e., 10 unique combinations of the letters O, W, H, and L). In the ideal case, the lipophile-oil and the hydrophile-water interaction will be the predominant interactions. The relative magnitude (R) of these two interactions

then defines the location of the surfactants in the oil-water interface, and the nature of the emulsion formed, if any, as

$$R = \frac{C_{LO}}{C_{HW}} \quad \begin{cases} R > 1, \text{ W/O emulsion} \\ R = 1, \text{ planar interface} \\ R < 1, \text{ O/W emulsion} \end{cases} \quad (22)$$

the R system corresponds to the HLB scale (20-22) where

$$\begin{aligned} R > 1 &\rightarrow \text{HLB} < 10 \\ R = 1 &\rightarrow \text{HLB} = 10 \\ R < 1 &\rightarrow \text{HLB} > 10 \end{aligned} \quad (23)$$

The main advantage to the Winsor system is its heuristic feature of treating all cohesive interactions in a two-phase surfactant system. However, to date only the simple form of Equation 22 has been exploited quantitatively (21, 23) as

$$R = \frac{\bar{V}_L \delta_L}{\bar{V}_H \delta_H} = \frac{\bar{V}_O \delta_O}{\bar{V}_W \delta_W} \quad (24)$$

To incorporate the surfactant structure concept, it is now convenient to introduce the group additive concept for cohesive energy densities (CED) introduced by Burrell and others (24, 25). Molecular segments are given a molar-attraction constant G. The CED is then determined for the *i*th compound as

$$\delta_i = \frac{\sum G}{V_i} \quad (25)$$

where the sum of all group molar-attraction constants in the molecule of interest is represented as $\sum G$.

To facilitate the use of CED calculations for Equation 24, a semiquantitative relationship developed by Beerbower and others (26-29) relates the surface tension of a phase to its CED as

$$\delta^2 = 16 \frac{\gamma}{\bar{V}^{1/3}} \quad (26)$$

A final quasi-thermodynamic approach to molecular structure effects has been proposed by Good et al. (17-18) which relates molar volumes and the Girifalco-Good interaction parameter, Φ , as

$$\Phi_{sw} = \frac{A_{sw}}{(A_{ss} A_{ww})^{1/2}} \cdot \frac{4(\bar{V}_s \bar{V}_w)^{1/3}}{(\bar{V}_s^{1/3} + \bar{V}_w^{1/3})^2} \cdot \frac{4(\bar{V}_s \bar{V}_w)^{1/3}}{(\bar{V}_s^{1/3} + \bar{V}_w^{1/3})^2} \quad (27)$$

where A = attractive coefficient in the Lennard-Jones 6-12 potential equation.

\bar{V}_i = molar volume of i th phase.

The values of A are not readily available for the phases in this study, so the commonly made approximation (17) of setting the ratio of A values to 1 will be made.

With these concepts, expressed in Equations 24 to 26, three types of questions can now be given semiquantitative answers: (1) CED values can be determined from surface tension measurements, (2) the effects of particular molecular components of surfactant molecules on surface tension and CED can be addressed, and (3) the emulsion type and stability can be evaluated based on either molecular structure surface tension and/or CED.

In Table 3 are the values of surface tension for the aqueous LAS homolog solutions. Values of molar volume used are those for the pure LAS homolog independent of water. The justification for this comes from the Winsor R model (20, 21) and work by Scriven and Davis (30) who showed that accurate CED values can be obtained from a statistical mechanical treatment of an interface using only 2 or 3 atomic or molecular layers of that interface. For a surfactant solution, the surfactant will predominate in the interface, hence the choice of pure LAS for the solution molar volumes.

Using the Beerbower Equation 26, values of the CED were calculated and listed in Table 3. At all hardnesses, the 10 and 11 carbon LAS homologs have significantly larger CED values. This is probably an artifact as a result of all solutions being .024 weight/weight percent. Because the two lower homologs have CMC values above this concentration and *vice versa* for the higher homologs, the δ values for the 10 and 11 carbon homologs violate the premise of a surfactant-saturated interface. Therefore, the δ values for the two lowest homologs are tenuous because, among other things, the value of \bar{V} used in the Beerbower equation would be uncertain.

In the last columns of Table 3 are the calculated and experimental values of Φ_{sw} . Comparison of these values shows the calculation to do a poor job of predicting the experimental Φ_{sw} values. This discrepancy could result from many sources. An obvious source of error could be the approximation of setting the A ratio to 1, thereby neglecting differences in types of interactions between the s and w phases across the sw interface. Another possible cause for the poor predictive power of Equation 27 could be the fact that the value of \bar{V}_w used in that equation was for the LAS homolog molecule, while the phase is actually an aqueous LAS solution. As discussed earlier, this approximation for surfactant solutions is probably good when the interface is saturated with surfactant molecules but should include the molar volume of water molecules as the mole fraction of adsorbed surfactant decreases. Since the lower LAS homologs

Table III. Quasi-Thermodynamic Analysis of Detergency Data For Molecular Structure Effects on Detergency

Hard-ness (ppm)	LAS Homolog	Cube Root Molar Volume (mole/cm ³) ^{1/3}	Surface Tension at .024% Solutions (dyne/cm)	CED for LAS traction (Hildebrand-Sulfone brands)	Molar Attraction Constant for Sulfonate	Winsor R	Experimental Detergency DR (%)	Calculated
50	10	6.79	46.7	10.5	1242	1.92	65	0.76
	11	6.89	41.1	9.8	1027	1.96	71	0.79
	12	6.99	30.2	8.3	524	2.22	71	0.88
	13	7.08	30.7	8.3	502	2.14	73	0.91
	14	7.17	30.2	8.2	446	2.08	74	0.93
150	10	6.79	41.7	9.9	1054	2.03	34	0.76
	11	6.89	33.0	8.8	700	2.19	56	0.87
	12	6.99	26.9	7.8	353	2.37	74	0.95
	13	7.08	25.9	7.7	289	2.30	75	0.97
	14	7.17	25.8	7.6	224	2.25	76	1.00
300	10	6.79	38.3	9.5	929	2.12	25	0.81
	11	6.89	30.7	8.4	569	2.29	67	0.93
	12	6.99	26.0	7.7	319	2.39	72	0.98
	13	7.08	27.5	7.9	360	2.25	66	0.99
	14	7.17	26.0	7.6	224	2.25	62	0.99
Mineral oil soil		9.65	29.6	7.01				
PEG cloth finish		3.42		11.1 ^a				

^aBased on tetraethylene glycol, Reference 33.

are below their CMC values, as evidenced by γ_w and γ_{sw} values, thereby having a greater mole fraction of adsorbed water, it seems reasonable that molar volumes for the lower LAS Homologs should be lower than those shown in Table 3. Directionally, this would make calculated values of ϕ_{sw} lower for the lower LAS homologs, which would improve agreement between experimental and theoretical values.

Another aspect of this quasi-thermodynamic approach is to use Equation 25, along with G values from Table 4, to calculate the molar-attraction constant for the sodium sulfonate molecular group or

$$G_{sulf} = \delta_i \cdot \bar{V} - 1114 - 133 (n-3) \quad (28)$$

where n = number of carbons in alkyl chain of LAS molecule.

δ_i = cohesive energy density of the i th LAS homolog solution.

Using Equation 28, the values of G_{sulf} determined in this manner are listed in Table 3. The most obvious feature of the G_{sulf} values is that the 10 and 11 homologs give much higher values. However, this apparent deviation is a result of γ_w values being measured on less than saturated air/aqueous interfaces (below the CMC for that surfactant). Hence these values should be expected but are probably artifacts.

For the higher homologs (i.e., 12 to 14 LAS), the values of G_{sulf} are more nearly, but not completely, constant. They vary first due to hardness. This reflects on the fact that G_{sulf} values of γ_w at 50 ppm are higher than at 150 and 300 ppm. At the higher hardnesses, the sulfonate group repulsion for the adsorbed LAS molecules is at a minimum in the presence of excess divalent cation (i.e., hardness). This results in better LAS packing in the interface, lower surface tensions, and lower CED values which finally culminates in a lower G_{sulf} . It should be pointed out that this difference between G_{sulf} values at 50 ppm hardness and those at 150 and 300 ppm hardness is a result of the \bar{V} values used in its calculation. The value of \bar{V} was arrived at by dividing the specific density of pure LAS by its molecular weight. The adsorbed molecules only approach this molar volume such that if the actual \bar{V} of the interfacial adsorbed density of the LAS molecules were known and could be used to calculate G_{sulf} , its value at all hardness levels should be more nearly constant.

Another trend for the G_{sulf} values is also seen within each hardness group in which this constant decreases for the 12 to 14 homologs. There is no simple explanation for this trend except to say that additivity theories like Equation 25 are not absolutely precise. Therefore, an average value of G_{sulf} for the 12 to 14 homologs at 150 and 300 ppm will be taken as the G_{sulf}

value and a 95 percent confidence interval for these six data (given as \pm) are listed in Table 4. While an uncertainty of 120 units in G_{sulf} may seem large compared to its value of 295, for most δ calculations by the molar-attraction constant method, the value of ΣG in Equation 25 will be $> 2,000$ for most molecules of interest. Therefore, the relative uncertainty will be < 10 percent, which is about the best precision one can expect from this method for calculating δ anyway, especially for polar moieties.

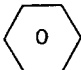
A third molecular structure/physical property correlation that can be made is to calculate the Winsor R for the homolog solutions by Equation 24. The resulting values are listed in Table 3. The R values are all clustered around the value of 2. This would suggest the surfactant would tend to form water-in-oil emulsions. From a detergency perspective, this data indicates that solubilization of oil in water is not the deterative mechanism. A final observation on this data is that R does not correlate well with detergency performance, as shown in the correlation plot of Figure 10. The quantity R is not a single valued function of detergency as can be seen in Figure 10. The reason for this is difficult to ascertain since the calculation scheme for R used in this study is so approximate. Nevertheless, the value of ca. 2 is a valid observation. Therefore, as noted above, oil-in-water emulsions, or detergency by the solubilization mechanism, is not the apparent mechanism suggested by these data for the systems studied.

Summary

A model for detergency performance was developed based on SEM photographs of cloth and fiber bundles within a cloth. The detergency or relative soil removal for this model was shown to be entirely dependent on the contact angle at the soil/fiber/detergent bath triple-phase line. A wetting equation was then derived so that the soil removal performance could be directly related to the wetting characteristics of the soil, fiber, and detergent bath interfacial properties through the contact angle. The detergency performance equation was then applied to experimental detergency data, so that the wetting characteristics of the pure LAS homolog solutions could be examined and molecular structure effects could be investigated. This segment of the work showed that detergency performance was dependent exclusively on the soil/bath interfacial tension so long as only the molecular weight of the LAS homolog changed. This result is consistent with other studies involving the effects of interfacial tension on detergency performance (31, 32).

Other LAS homolog structural effects on wettability and soil removal were found when the data were analyzed using the cohesive energy ratio, R, the regular solution theories of the

Table IV. Molar-Attraction Group Constants
For Cohesive Energy Density Determination

REFERENCES 23, 24		CALCULATED	
Group	G	Group	G
--CH ₃	214	-SO ₃ N _a	295 ± 120
--CH ₂ --	133		
--CH	28		
--  --	658		

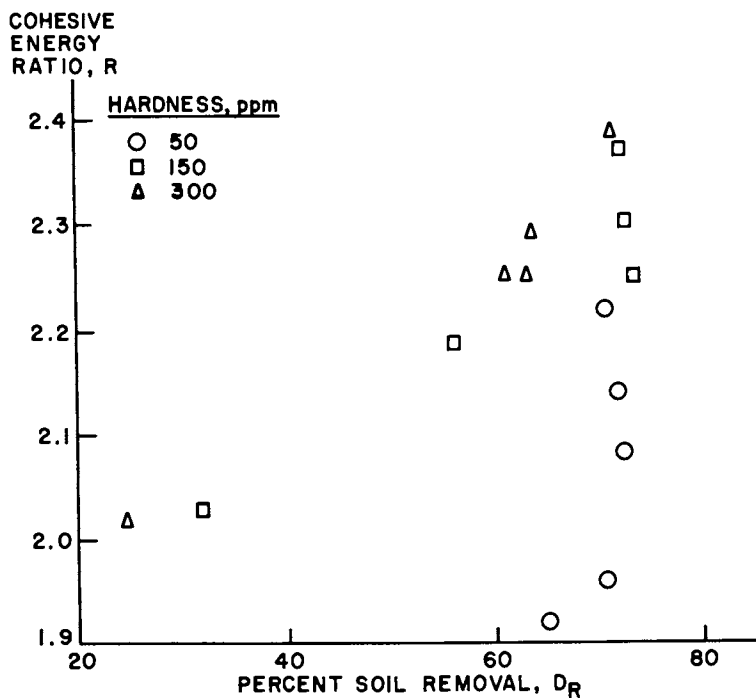


Figure 10.
Correlation Plot of Cohesive Energy Ratio for LAS Homolog
Detergency of Mineral and the Experimental Soil Removal.

Beerbower equation and the additivity concepts of molar-attraction constants for determining the cohesive energy density. From these treatments, it was possible to calculate a molar-attraction group constant for the sodium sulfonate group of 120 (in Hildebrand units).

Experimental

The soil used in this study was a mineral oil (see Figure 1) manufactured by Squibb, which had a trace amount of an oil-soluble red dye added for visual acuity. The linear alkylbenzene sulfonate sodium salts (LAS) were homologically pure samples, each with a different linear alkyl carbon chain of 10, 11, 12, 13, or 14 carbon atoms. Each of the LAS samples was a mixture of isomers with phenyl attachment ranging in nearly equal amounts from 2 through 5, 6, or 7 (depending on the alkyl chain length). These LAS samples were made with an HF catalyst.

Inorganic ingredients were used as received from their supplier and included; sodium tripolyphosphate or STPP (FMC Corporation) and RU silicate or $\text{SiO}_2/\text{Na}_2\text{O}$ (the P.Q. Corporation).

The detergency testing was done using a Tergotometer (U.S. Testing Company, Inc.). Synthetic hard water was prepared by adding varying amounts of a concentrated solution of calcium and magnesium chlorides in a 4:1 cation mole ratio, respectively, to the detergency bath. The Tergotometer was run for 10 minutes at 100°F and 100 rpm with one liter of a 0.15 percent detergent formulation in each pot followed by a 5-minute, 100-rpm rinse with 1 liter of deionized water. The formulation was 16 percent LAS, 30 percent STPP, and 10 percent $\text{SiO}_2/\text{Na}_2\text{O}$. The cloths were a 35/65 blend of cotton/Dacron with a polyethylene glycol permanent press finish (Testfabrics, Inc., Cloth No. S/7406) that had been sized. The cloths were soiled in a Benz soiling unit (Ernst Benz AG) type KLFM "K" and KTF/M. The reflectance readings on clean, soiled, and washed cloths were performed on a Gardner Colorimeter (Gardner Laboratory, Inc.) using the Y axis of the YXZ scale. The cloth readings were made on individual cloths using a backing plate then corrected graphically for the backing plate effect.

Surface and interfacial tension measurements were made at 40°C with a Model 300 Spinning Drop Tensiometer obtained from the University of Texas at Austin, Chemistry Department.

Acknowledgments

The author would like to thank Ms. M. Debra Davis for making the surface and interface tension measurements and Dr. K. Lee Matheson for the detergency data. In addition, the author

wishes to thank Conoco Inc. for permission to publish this study.

Literature Cited

1. W. G. Cutler and R. C. Davis, "Detergency," Parts I, II, and III, Marcel Dekker, Inc., New York, 1972 through 1981.
2. E. Kissa, Textile Res. J., 41, 760 (1971).
3. E. Kissa, Textile Res. J., 45, 736 (1975); Pure and Appl. Chem., 53(11), 2255-68 (1981).
4. A. F-C Chan, "Solubilization Kinetics in Detergency," Diss. Abstr. Int. B, 38(4), 1,808 (1977).
5. O. C. Bacon and J. E. Smith, Ind. Eng. Chem., 40, 2,361-2,370 (1948).
6. W. J. Popiel, "Introduction to Colloid Science," Exposition Press, Hicksville, New York, pp. 37-46 (1978).
7. J. Chem., J. Chem. Ed., 56(9), 610-611 (1979).
8. A. M. Schwartz, "Surf. and Colloid Sci.," Vol. 11, Plenum Press, New York, p. 307 (1979).
9. A. W. Adamson, "Physical Chem. of Surfaces," 3d ed., Wiley, New York, pp. 474-484 (1976).
10. H. Renmuth, "Haus der Technik Vor. Essen No. 68," pp. 7-24 (1965, published 1966).
11. J. A. Wingrave, presented at the 57th National Colloid and Interface Science Symposium, University of Toronto, Toronto, Canada, June 12-15, 1983.
12. P. Kubelka and F. Munk, Z. Tech. Physik, 12, 593 (1931).
13. Cutler and Davis, *ibid.*, pp. 386-92.
14. A. W. Adamson, *ibid.*, pp. 339-42.
15. T. Young, "Miscellaneous Works," Vol. I, G. Peacock, ed., Murray, London, 1855, p. 418.
16. A. Dupre, "Theorie Mecanique de la Chaleur," Paris, 1869, p. 368.
17. L. A. Girifalco and R. J. Good, J. Phys. Chem., 61, 904-9 (1957).
18. R. J. Good and E. Elbing, Ind. Eng. Chem., 62(3), 54-78 (1970).
19. J. Ferguson, Proc. Roy. Soc. (London), 127B, 387 (1939).
20. P. Winsor, "Solvent Properties of Amphiphilic Compounds," Butterworth Sci. Publ., London, 1954.
21. A. Beerbower and M. W. Hill, Detergents and Emulsifiers, 223-36 (1971).
22. W. C. Griffin, J. Soc. Cosmet. Chem., 5, 249 (1954).
23. A. Beerbower and J. Nixon, Div. Petr. Chem. Preprints, ACS, 14(1), 62-71 (1969).
24. H. Burrell, Official Digest of the Federation of Societies for Paint Technology, 27, 726 (1955); 29, 1069 (1957); 29, 1159 (1957).
25. P. A. Small, J. Appl. Chem., 3, 71 (1953).

26. A. Beerbower, J. Colloid Interface Sci., **35(1)**, 126-32 (1971).
27. J. H. Hildebrand and R. L. Scott, "Solubility of Nonelectrolytes," 3d ed., Reinhold, N.Y. (1950).
28. A.F.M. Barton, Chem. Rev., **75(6)**, 731-53 (1975).
29. C. Hansen and A. Beerbower in "Kirk-Othmer Encyclopedia of Chemical Technology," Supl. Vol., 2nd ed., A. Standen (ed.), p. 889 (1971).
30. L. E. Scriven and H. T. Davis, J. Phys. Chem., **80(25)**, 2805-6 (1976).
31. M. P. Aronson, M. L. Gum, and E. D. Goddard, J. Am. Oil Chem. Soc., **60(7)**, 1333-9 (1983).
32. K. W. Dillan, E. D. Goddard, and D. A. McKenzie, J. Am. Oil Chem. Soc., **57**, 230 (1980).
33. "The Handbook of Chemistry and Physics; 49th Ed.", R. C. Weast, Ed., CRC Co., Cleveland, Ohio, p. C-562 (1968).

Appendix
Pore Volume Between Fibers

The pore volume, shown as a cross section of two parallel fibers of length, L, and radius, R, has a half-surface dimension, r_p , and meets the fiber surface with an angle, ψ (see Figure 5). The volume of such a pore, V_D , will be

$$V_D = 2L \left[hr_p - \int_{R-r_p}^R Y dX \right] \quad (29)$$

Then since

$$Y = \sqrt{R^2 - X^2} \quad (30)$$

Equations 29 and 30 combine to yield

$$V_D = 2L \left[hr_p - \int_{R-r_p}^R \sqrt{R^2 - X^2} dX \right] \quad (31)$$

which can be integrated to yield

$$V_D = 2Lhr_p + 2L \left(\frac{X}{2} \sqrt{R^2 - X^2} + \frac{R^2}{2} \sin^{-1} \frac{X}{R} \right) \Bigg|_R^{R-r_p} \quad (32)$$

or

$$V_D = 2Lhr_p + L \left[(R - r_p) \sqrt{R^2 - (R - r_p)^2} + R^2 \sin^{-1} \left(\frac{R - r_p}{R} \right) - R^2 \frac{\pi}{2} \right] \quad (33)$$

Then noting

$$h = R \cos \psi \quad (34)$$

$$R - r_p = R \sin \psi \quad (35)$$

$$r_p = R(1 - \sin \psi) \quad (36)$$

Equations 33 through 36 can be combined and simplified to yield the desired expression of V_D as

$$V_D = LR^2 \cos \psi (2 - \sin \psi) - LR^2 \frac{\pi}{2} - \psi \quad (37)$$

The total pore volume, V_T , can be determined from Equation 37 when $\psi = 0$ as,

$$V_T = LR^2 \left(2 - \frac{\pi}{2} \right) \quad (38)$$

If a cloth is soil-saturated, then the relative soil removal of the duplex cloth-held soil, V_R , will be,

$$V_R = \frac{V_D}{V_T} \quad (39)$$

or combining Equations 37 and 39 yields,

$$V_R = \frac{2 \cos \psi (2 - \sin \psi) - (\pi - 2\psi)}{4 - \pi} \quad (40)$$

RECEIVED January 20, 1984

Relationship Between Surfactant Structure and Adsorption

P. SOMASUNDARAN, R. MIDDLETON, and K. V. VISWANATHAN

School of Engineering and Applied Science, Columbia University, New York, NY 10027

Adsorption of a surfactant on solids is dependent, among other things, on the structure of both the hydrophobic and hydrophilic portions of it. There are a number of mechanisms proposed for surfactant adsorption and an understanding of the effects of the structure of the surfactant can help in elucidating the role of these mechanisms. In this study, the effect on adsorption on alumina of some structure variations of sulfonates (chain length and the branching and the presence of ethoxyl, phenyl, disulfonate and dialkyl groups) is examined above and below CMC as a function of surfactant concentration, pH and salinity. Co-operative action between an ionic alkylsulfonate and a nonionic ethoxylated alcohol is also studied.

Surfactant adsorption on solids from aqueous solutions plays a major role in a number of interfacial processes such as enhanced oil recovery, flotation and detergency. The adsorption mechanism in these cases is dependent upon the properties of the solid, solvent as well as the surfactant. While considerable information is available on the effect of solid properties such as surface charge and solubility, solvent properties such as pH and ionic strength (1,2,3), the role of possible structural variations of the surfactant in determining adsorption is not yet fully understood.

Adsorption is governed by a number of forces: covalent bond formation or electrostatic attraction or hydrogen bond formation between the adsorbate and the adsorbent, electrostatic repulsion among the adsorbate species, lateral associative interaction among adsorbed species, solvation of adsorbate or adsorbent surface species. Structural modifications can affect one or more of the above interactions that might be predominant in different concentration regions, and it is the cumulative effect of all of these modifications on all interactions in various concentration regimes that will determine the overall adsorption behavior of a surfactant (4,5). Thus while in practice chain length or branching will affect only the lateral interactions in the hemi-micellar region,

0097-6156/84/0253-0269\$06.50/0

© 1984 American Chemical Society

presence of multifunctional groups (such as disulfonates with an ether linkage) can affect both electrostatic and lateral association interactions. Coadsorption between different surfactant species also can be expected to be influenced significantly by such structural variations.

In this paper the adsorption characteristics of a series of structurally modified surfactants will be analyzed. Figure 1 summarizes this series showing the following structural variations: aryl addition, chain length variation, branching, xylene alkyl addition, ether linkage and ethylene oxide addition, with alumina as the adsorbent. By understanding the effect of structural variations upon the adsorption mechanism a guideline may be established by which a surfactant may be tailored with specific structural modifications for certain situations.

Experimental

Surfactants. n-sodium dodecylsulfonate specified to be 99.4% pure was purchased from Aldrich Chemicals.

n-sodium octyl, decyl, dodecyl and tetradecylbenzene sulfonates were synthesized and purified in our laboratory. Characterization of these chemicals using p-NMR, C-13 NMR, mass spectrometry and ALC showed these compounds to be isomerically pure. Branched hexadecyl benzene sulfonate was obtained from Conoco and used as received after characterization.

Alkyl aryl orthoxylene sulfonates were also investigated. The first being a linear nonyl orthoxylene sulfonate and the second being a branched dodecyl one. Both were supplied by the Exxon Corporation and contain known amounts of unsulfonated hydrocarbons (14% and 25.2% respectively).

The disulfonate, Dowfax 3B2, used was a didecylphenoxy-disulfonate containing 10% monosulfonated impurities. HPLC analysis showed this surfactant to be a mixture of several compounds.

Triton X-200 was used to study the effects of ethoxylation on the sulfonates. Nonionic ethoxylated surfactants were investigated using Synfac 8216 obtained from the Milliken Corporation. This was stated to be 100% active with a molecular weight of 1100-1200. HPLC showed this surfactant to be a mixture of several components.

Mineral. Alumina used in this study was a high purity α -Linde sample purchased from the Union Carbide Corporation. BET surface area was determined to be 15.0 m²/g.

Procedure. A gram of the mineral was preconditioned for 90 minutes with 5cc of a 0.2 kmol/m³ sodium chloride solution at 75°C on a wrist action shaker. Then a 5cc solution of known surfactant concentration is added and allowed to shake for four hours. Four hours mixing was found to be sufficient to reach equilibrium from adsorption test conducted as a function of mixing time. The

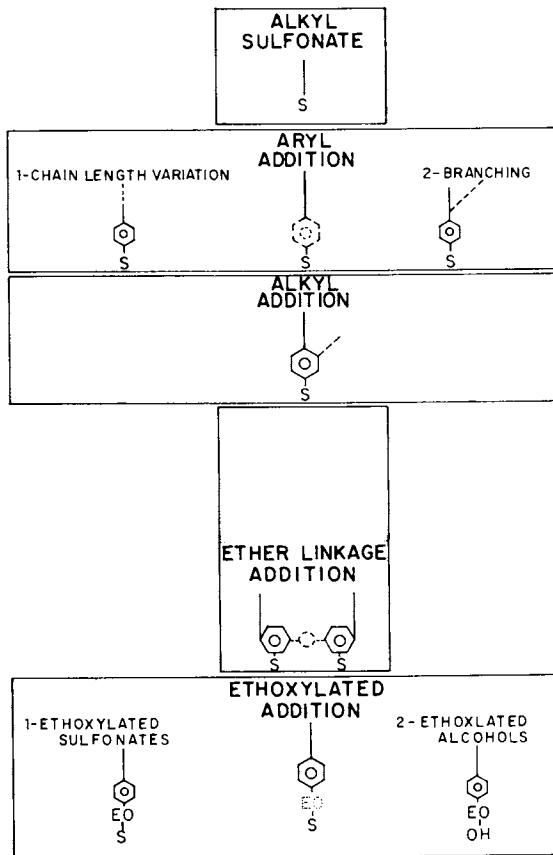


Figure 1. General overview.

supernatant was obtained using a thermostated centrifuge at 4500 rpm. Analyzation of surfactant concentration was completed using a two-phase titration technique and U.V. spectroscopy.

Results and Discussion

The adsorption isotherm obtained for dodecylsulfonate (DDS) on alumina is given in Figure 2. This isotherm is similar to that obtained in the past for sulfonate/alumina systems (4). This isotherm behaves in an s-shaped manner (6) revealing its four characteristic regions of adsorption: 1) Electrostatic interaction 2) Lateral association (hemimicellization), 3) Electrostatic hindrance and 4) micellization.

In Region 1, under low surfactant concentration conditions, adsorption occurs mainly due to the electrostatic attraction between the surfactant ion and the charged sites on the solid surface (3). The beginning of Region 2 is characterized by the onset of lateral association among the adsorbed surfactant species (4). This process is analogous to micellization but takes place at a lower surfactant concentration assisted by the electrostatic attractive forces between the hemi-micelle and the charged solid (7, 4). While sufficient surfactant ions have been adsorbed to neutralize the surface charge of the mineral, further adsorption progresses owing to continued hemimicellization. Charge reversal occurs and adsorption in this concentration region is hindered by the increasing electrostatic repulsion between the now similarly charged solid and surfactant species (Region 3) (4). Region 3 ends and a new region begins with the onset of micellization (8). In the micellar region, adsorption is nearly constant due to the absence of a marked increase in activity of the surfactant species in this region with an increase in its concentration (8). In this region apparent "adsorption" can, however, undergo drastic changes owing, among other things, to precipitation or micellar redissolution of the surface precipitate (5, 9), resulting in adsorption maxima and minima. While adsorption in the hemimicellar region, like that in the micellar region, is dependent on the hydrophobic properties of the surfactant, adsorption in the electrostatic region and alterations in adsorption owing to precipitation, redissolution and reprecipitation will depend upon solution properties such as pH, salinity and hardness. Thus factors to be considered while examining the effect of surfactant structure will include changes in the electrostatic attraction and repulsion of the adsorbate and adsorbent, solvent power of the medium for the surfactant and its precipitates, and lateral association as well as electrostatic repulsive interactions among the adsorbed species.

Aryl Addition. Surfactants having an aryl group added between the sulfonate and alkyl chain are studied using the standard adsorption procedure, and compared with an alkyl sulfonate. Figure

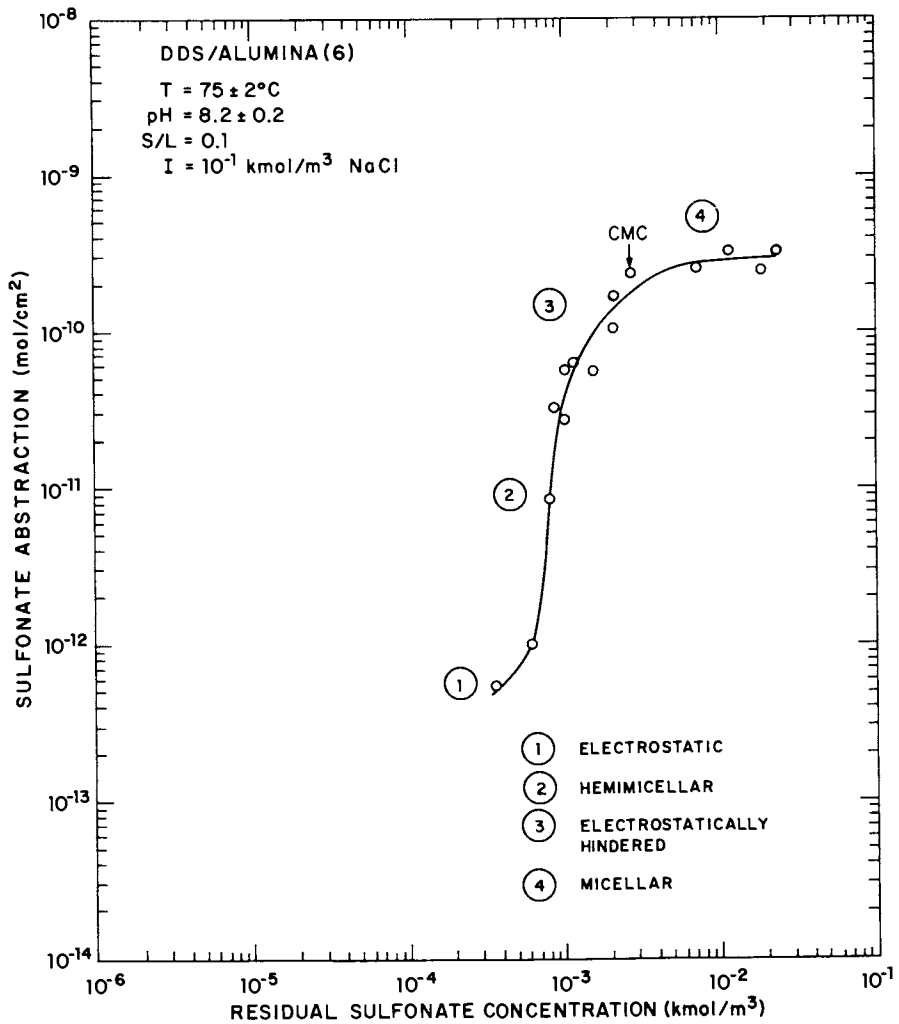


Figure 2. Alkyl sulfonate adsorption.

3 shows the adsorption isotherms of DDS, OBS and DDBS. Under the assumption that one benzene ring equals 3.5 alkyl units (10), the equivalent alkyl chain length of OBS and DDBS can be calculated: 11.5 and 13.5 respectively. DDS and OBS, both having similar equivalent alkyl chain lengths (.5 alkyl difference), do behave with similar adsorption characteristics. Comparison of DDS and DDBS shows the large increase in adsorption associated with the aryl addition.

Chain Length Variation. Adsorption isotherms obtained for alkylbenzene sulfonates of varying chain length are given in Figure 4. Adsorption clearly increases as the chain length of the alkyl group is increased from 8 to 14. This is found to be the case even in Region 1 where adsorption has been proposed to take place owing to electrostatic attraction only. Since in all cases, the charge of the sulfonate species is 1, adsorption in the electrostatic region should have been invariant with chain length. The fact that it is, to the contrary, dependent on the chain length suggests the possible influence of the reduced dielectric constant in the interfacial region(11). Transfer of the monomer chain into a less dielectric region should result in a lowering of free energy, with the reduction being larger for the longer chains. Adsorption of the long chain sulfonates in Region 1 should therefore be considered to be the result of electrostatic attraction as well as increased solvent power of the interfacial water. Increase in adsorption seen in the lower three regions (Figure 4) can be attributed to the increase in hydrophobicity with chain length resulting in stronger hemi-micellization as well as monomer transfer. The shift in the micellar regions of the AAS isotherms is in effect a measure of the increased hemimicellization versus micellization as the chain length is increased (12). When the hemi-micellization is essentially complete at the end of Region 3, the end methylene group of the peripheral chains in each hemimicelle is still exposed to bulk water; however, the fraction of exposed groups per chain will decrease with increase in chain length. Any such change in the case of micellization could be expected to be of a lower magnitude. Thus the higher adsorption of longer chains achieved at the beginning of the Region 4 can conceivably be the result of the greater energy of hemimicellization energy in relation to that of micellization.

Effect of Branching. The effect of branching was investigated by comparing the adsorption of various hexadecylbenzene sulfonates (Figure 5). The first had the benzene group occupying the number 2 position upon the alkyl chain and the second had it at the 8 position. Adsorption of the 2 ϕ HDBS is significantly higher than that of the 8 ϕ HDBS. In the low concentration region the former appears to adsorb almost an order of magnitude more than the latter; it is however to be noted that adsorption in this region borders upon the experimental limitations; even in the micellar region, adsorption of it is higher. 2 ϕ HDBS which is least branched

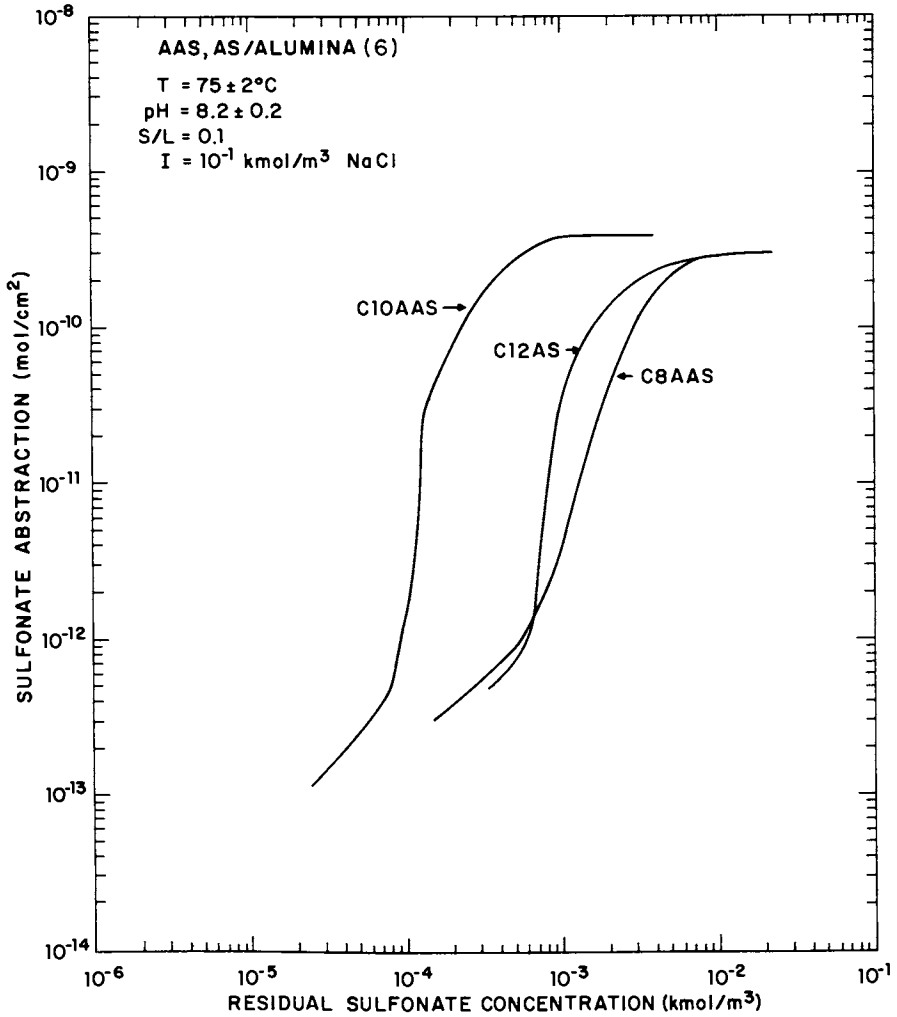


Figure 3. Structural comparison: AAS vs. AS.

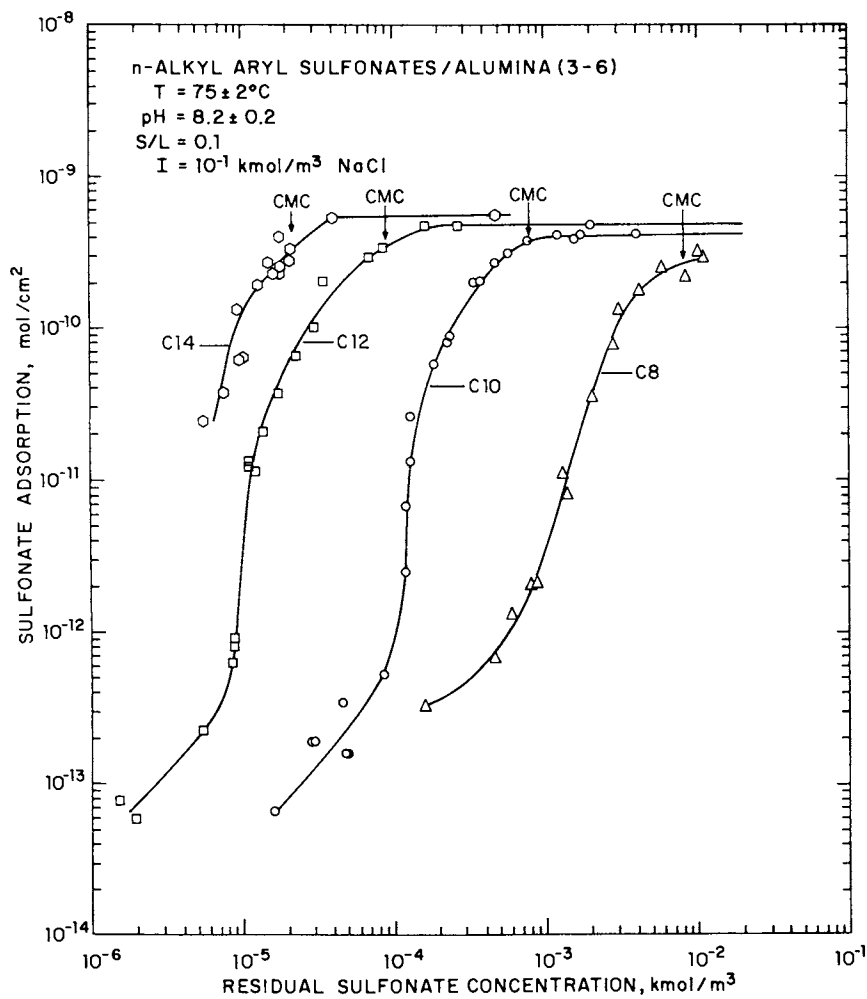


Figure 4. Effect of chain length.

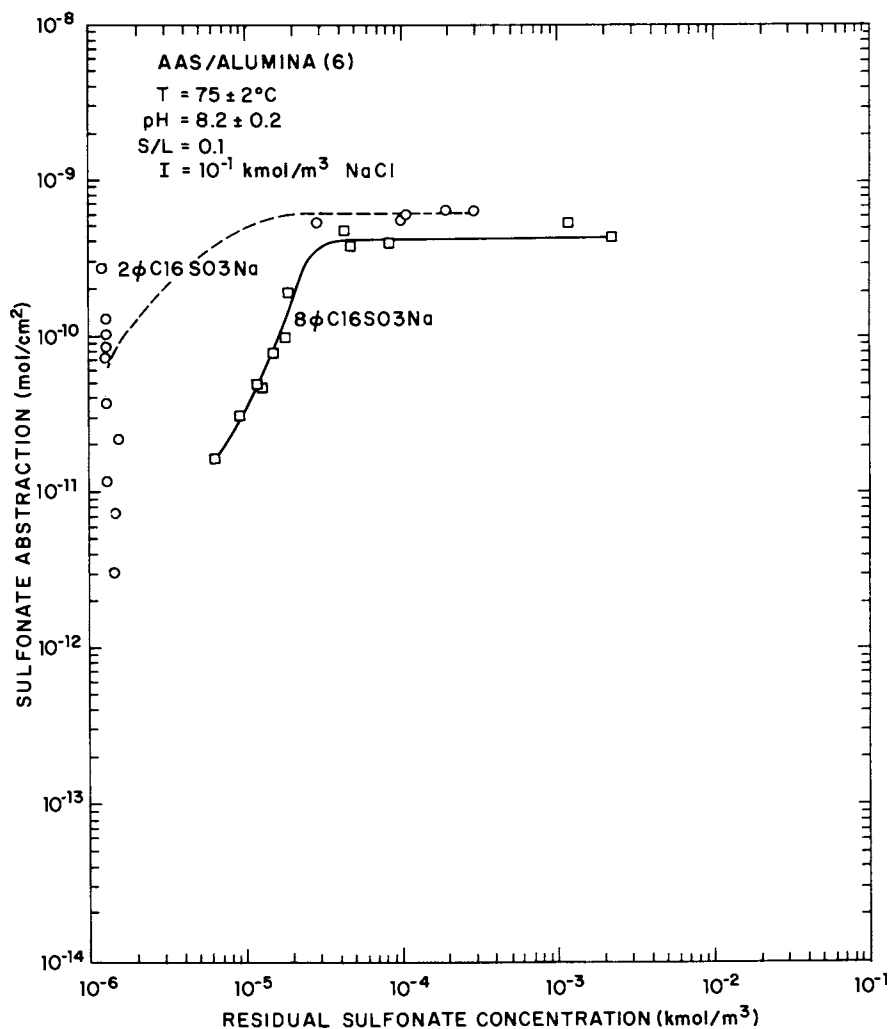


Figure 5. Effect of branching.

is considered to have a larger effective alkyl chain than the 8 ϕ HDBS (13), since the CMC of the former is considerably lower than that of the latter. It must, however, be pointed out that while formation of a spherical micelle might be more easily accomplished with the 2 ϕ HDBS than with the 8 ϕ HDBS, it is not fully evident as to why a planar hemi-micelle should be more easily achieved with the 2 ϕ HDBS.

Comparison of these adsorption isotherms with those obtained for the linear alkyl aryl sulfonates (Figure 6) reveals the behavior of the 2 ϕ HDBS to be close to that which would be expected for a 1 ϕ HDBS and that of the 8 ϕ HDBS to be equivalent to that of a tridecyl benzene sulfonate. Development of a quantitative model that can account for the effect of the position of the benzene group on the chain warrants additional data for a variety of surfactants with branched chains.

Alkyl Addition on the Aromatic Ring. The two surfactants chosen to be representative of this section were alkylaryl sulfonates having an additional alkyl group substituted in the aromatic ring. These compounds were commercially named alkylaryl-orthoxylylene sulfonates and referred to as such. The adsorption behavior of the following xylene sulfonates was examined: linear nonylorthoxylylene sulfonate and branched dodecylorthoxylylene sulfonate. Such orthoxylylene sulfonates have been reported to be very effective in reducing interfacial tensions; however, adsorption characteristics of these compounds are not clearly known. Results obtained for the two alkylorthoxylylene sulfonates are given in Figure 7. Since the position of the aryl group in the dodecyl chain was unknown for the branched orthoxylylene sulfonate, an estimate of the relative hydrophobicity of the two compounds was obtained using HPLC. Two peaks were analyzed for both of the compounds giving retention times of 2.4 and 3.0 minutes for NXS and 2.8 and 3.74 minutes for DDXS. Therefore, DDXS, even though branched can be considered to possess an effective chain length longer than that of NXS; the larger adsorption of the former is in accord with the results of the above HPLC analysis. The above samples of the commercial xylene sulfonates were, however, reported to contain significant amounts of unsulfonated hydrocarbons (oil), NXS containing 14% and DDXS containing 25.2%. As oil is known to produce marked effects on adsorption, it becomes necessary to determine the adsorption behavior of the deoiled samples of the above sulfonates in order to more precisely identify the properties of xylene sulfonates. The adsorption isotherms of the deoiled xylene sulfonates are given in Figure 8 along with those of OBS and DBS for comparative purposes.

Firstly, deoiling is seen to produce lower adsorption; secondly, the isotherms for these deoiled sulfonates also show lower adsorption levels when compared with the straight chain alkylaryl sulfonates. In Figure 8, the nonylxylene sulfonate acts

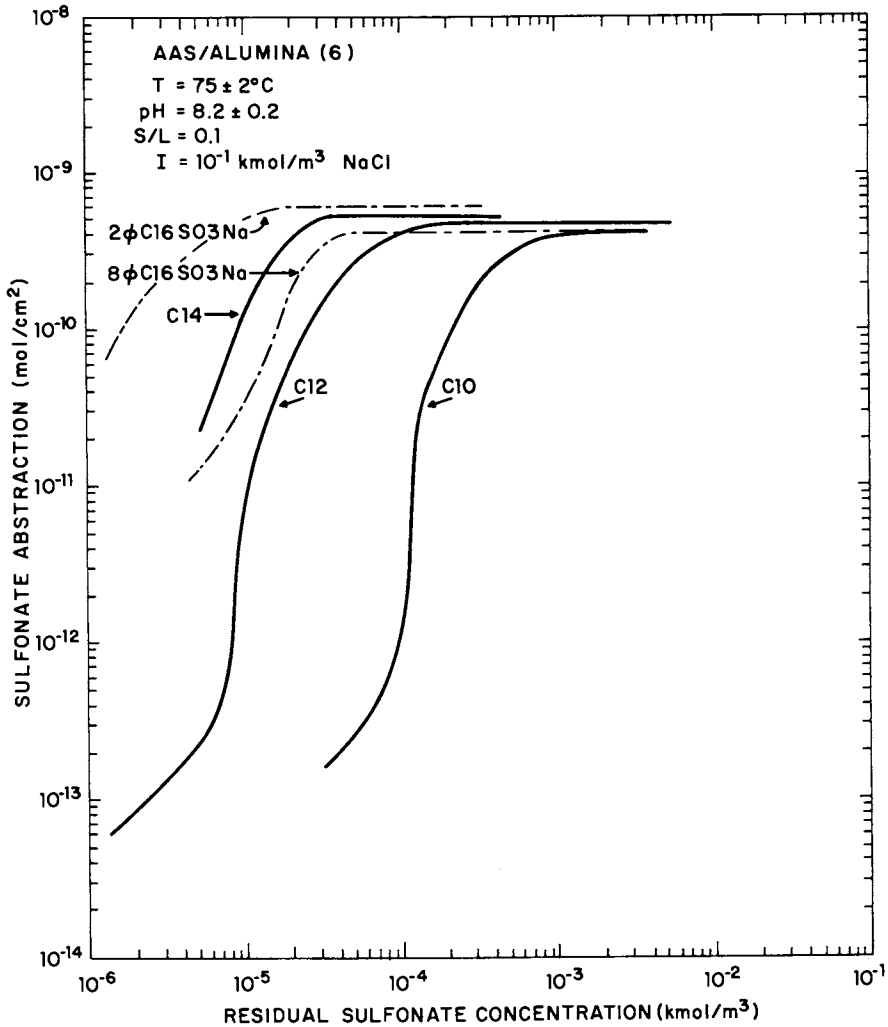


Figure 6. Structural comparison: branched vs. linear AAS.

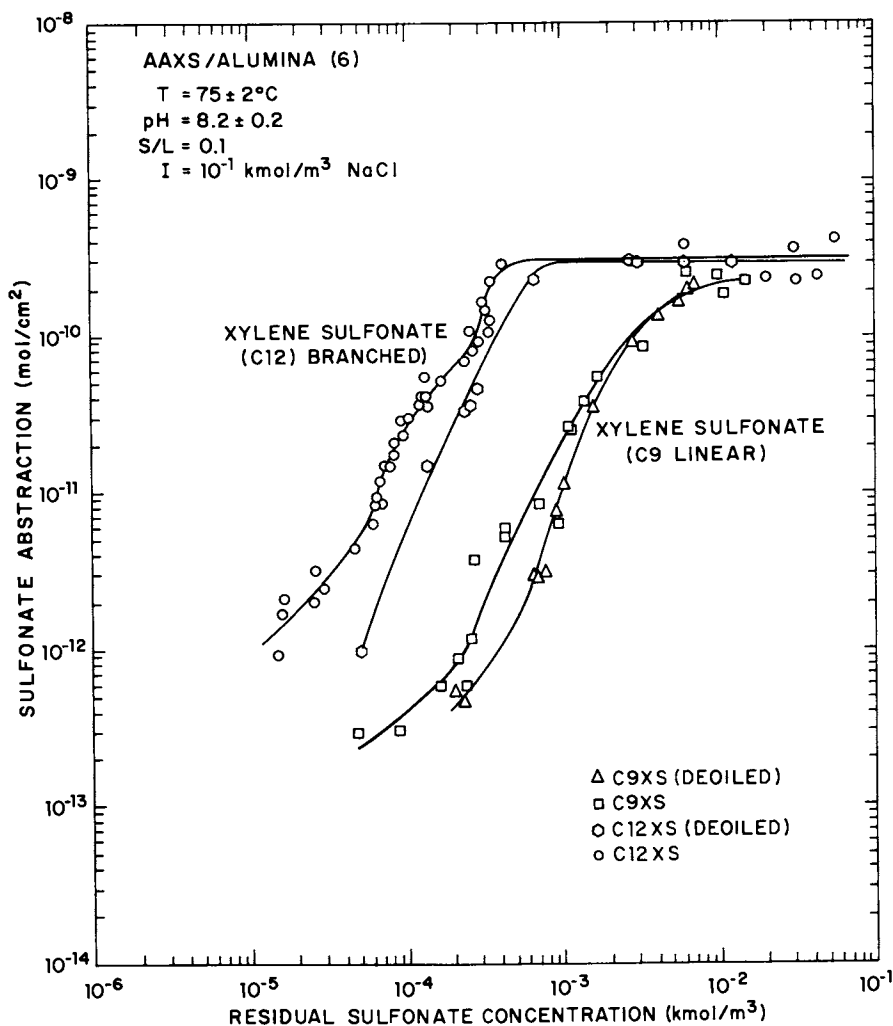


Figure 7. Alkylarylorthoxylene sulfonate adsorption.

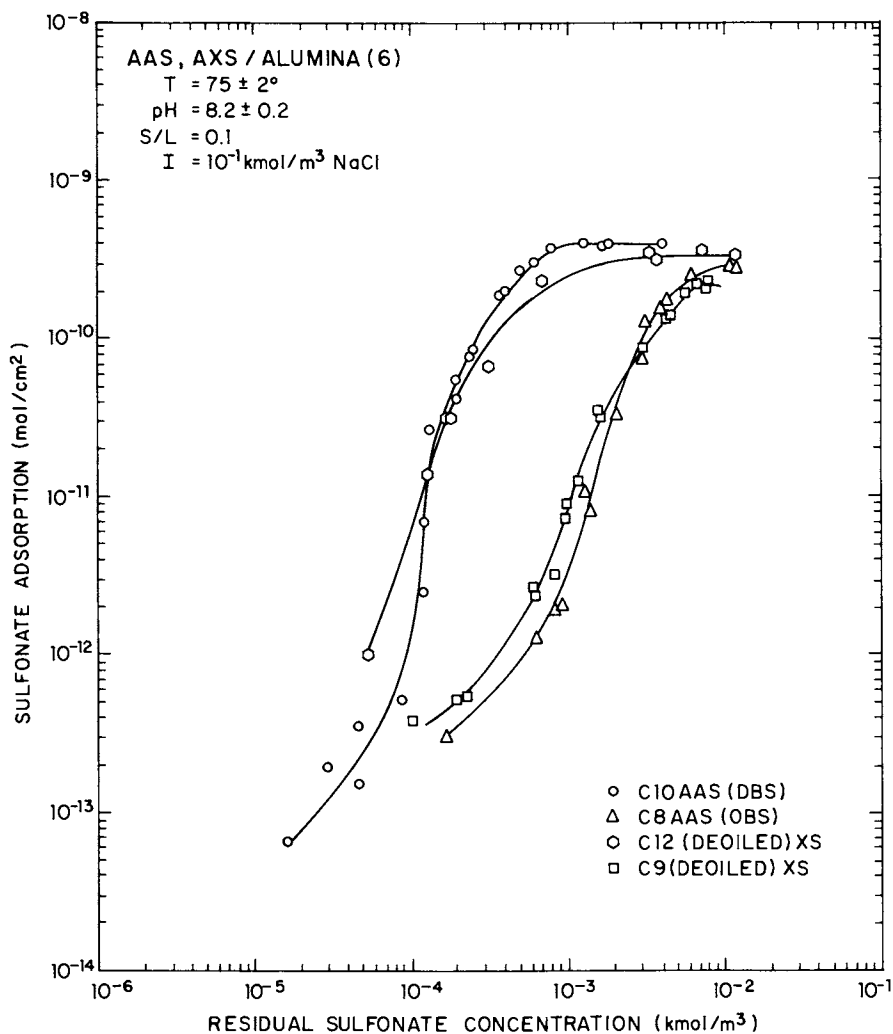


Figure 8. Structural comparison: xylene sulfonate (deoiled) vs. AAS.

equivalently with the OBS and the branched dodecylxylene sulfonate approximates the behavior of DBS. Thirdly the slope of the hemimicellar region did decrease without any measurable effect in the micellar region itself. Evidently the presence of the alkyl group on the benzene ring creates some steric hindrance in the two-dimensional packing of the surfactant species into the hemimicelles. The factors responsible for these different effects of the xylene sulfonates in different regions could similarly yield different interfacial effects (interfacial tension vs. adsorption) and a full understanding of the mechanisms responsible for it should prove useful.

Ether Linkage (Disulfonate). The disulfonate used here is essentially two decylbenzene sulfonates connected through an oxygen (14). The isotherm obtained with the dodecylphenoxy sulfonate is compared in Figure 9 with that for the decylbenzene sulfonate. The disulfonates isotherm is characterized by the absence of multiple regions obtained in all other cases. Adsorption in the "Electrostatic region" is comparable, but at higher concentrations, adsorption of the disulfonate is markedly lower than that of the DBS. Importantly, there is an absence of the sharp rise in adsorption (attributed to hemimicellization). Evidently, the disulfonate with the oxygen linkage in between the two AAS prevents the alkyl chains from packing tightly to form the two-dimensional aggregate. Also, a molecular model of the compound suggests the possibility of coiling of the two alkyl chains, even in the bulk, minimizing the driving force for aggregation on the surface (Figure 10). Adsorption under these conditions should be considered to be the result of electrostatic attraction only. The fact that the disulfonates adsorption was greater than the monosulfonates in the electrostatic attraction region helps prove these assumptions. Also, a value of 1.1 was obtained for the slope of the isotherm ($3 \times 10^{-6} - 2 \times 10^{-3}$ kmol/m³ range) further supports this consideration.

Ethylene Oxide Addition. Anionic and nonionic alkylaryl compounds containing amount of thylene oxide were used in this study. Addition of ethylene oxide groups is known to impart salt tolerance to the surfactant and therefore these compounds are of particular interest for micellar flooding purposes.

The anionic alkylarylpolyether sulfonate used in this study was Triton X-200. The chemical composition of this compound is such that the sulfonate is connected to a small alkyl group which in turn is connected to the ethylene oxide group. Then comes the aryl and alkyl groups. Due to the alkyl sulfonate link comparison with an alkyl sulfonate might prove more helpful than comparisons made with alkylaryl sulfonates. The isotherm obtained for Triton X-200 is similar in shape to that of the alkyl sulfonate, of equivalent chain length (Figure 11), with the electrostatic, hemimicellar, electrostatic hindered and micellar regions all being comparable. When a 10^{-2} kmol/m³ solution of

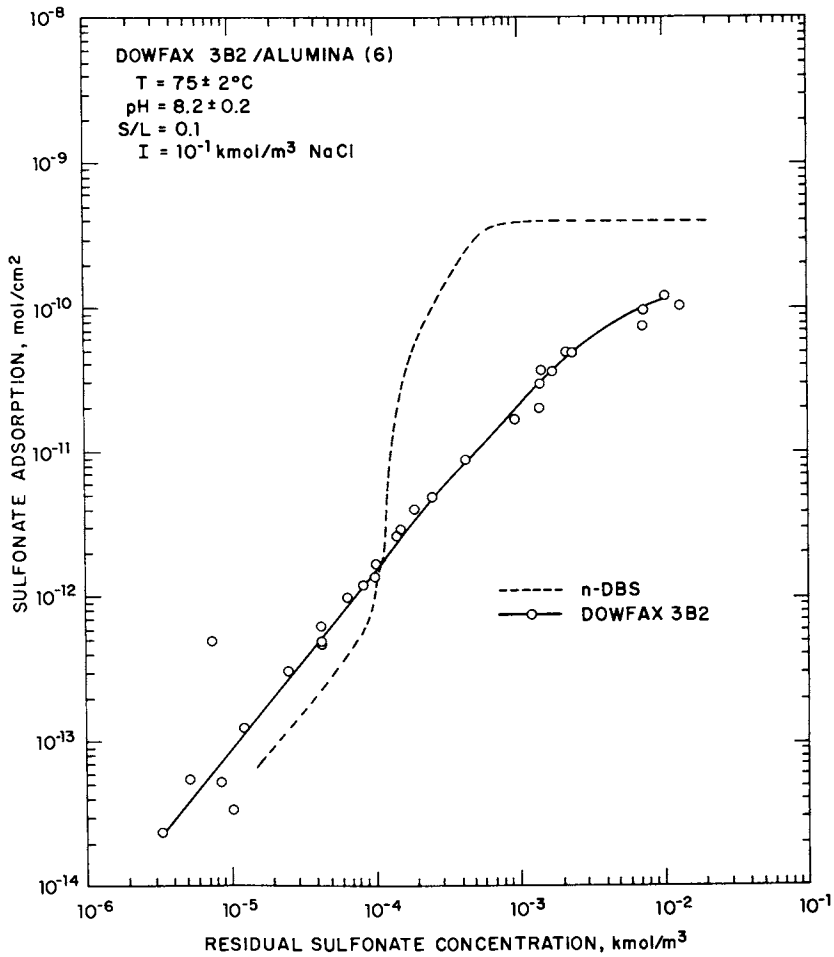


Figure 9. Structural comparison: disulfonate vs. AAS.

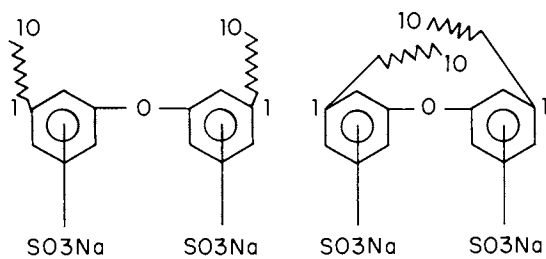


Figure 10. Disulfonate adsorption model.

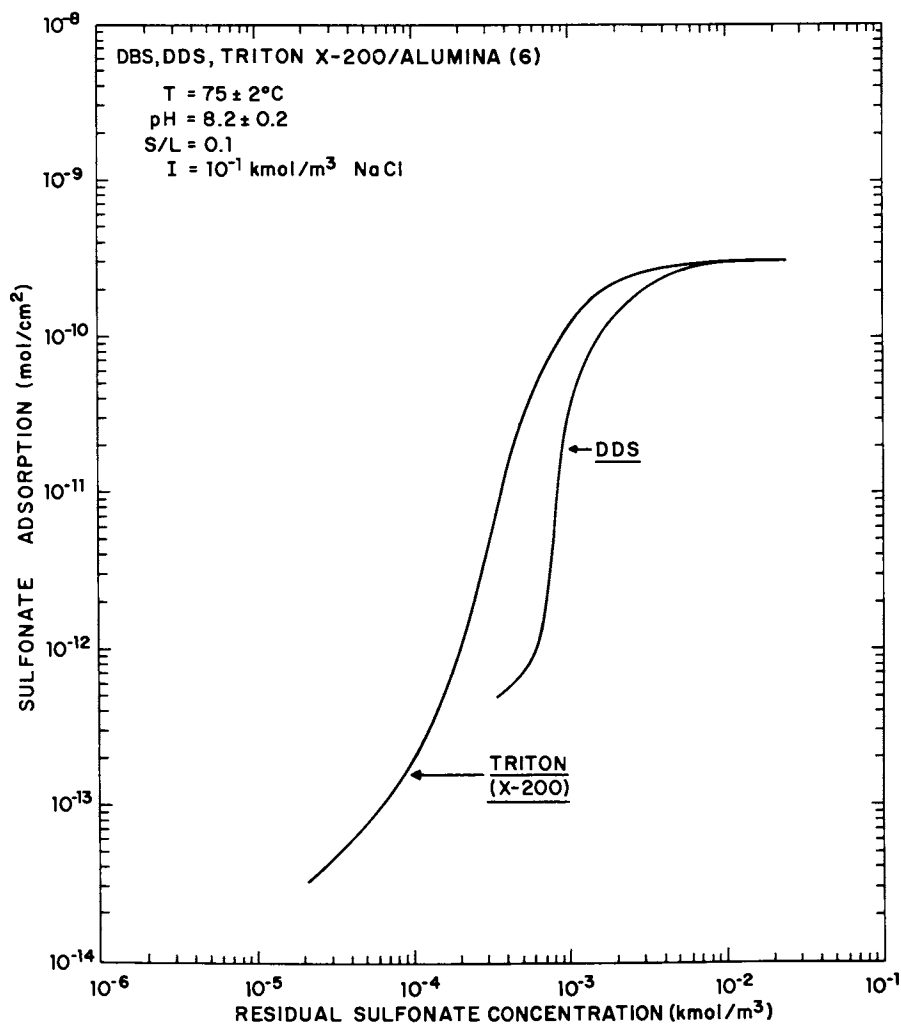


Figure 11. Structural comparison: ethoxylated sulfonate vs. AS.

calcium chloride was added to each of these systems the alkyl sulfonate precipitated while the Triton X-200 adsorption values remained relatively unchanged proving the salt tolerance of the ethylene oxide groups.

The nonionic surfactant used is Synfac 8216, an alkylaryl-ethoxylated alcohol. This compound did not adsorb by itself on alumina at a concentration of 4.3×10^{-4} kmol/m³ even after a salt level of 30% at 27°C. At 75°C measurements were conducted in up to 5% NaCl and no significant adsorption was obtained. Synfac did however, undergo significant adsorption in the presence of dodecylsulfonate with maximum adsorption under the tested conditions at 1.5×10^{-3} kmol/m³ DDS (see Figure 12). The adsorption of sulfonate was also enhanced by the addition of Synfac except in the micellar region (Figure 13). Synergetic interaction between Synfac and dodecylsulfonate suggests chain-chain interaction between the chains of the two reagents. Co-adsorption of nonionics can enhance hemi-micellization of ionic surfactants on account of the reduced lateral electrostatic repulsion between the ionic heads and thereby also increase the overall adsorption of both the compounds. Indeed, if most or all of the adsorption sites are occupied, the two species will have to share the sites, and under these conditions the individual adsorption of both the compounds will undergo a decrease unless multilayer adsorption can take place. It is clear from the results given in Figures 12 and 13 that interactions between various surfactants and co-surfactants can play a major role in determining the adsorption in the system depending particularly on their chemical structure.

Conclusions

Structural variations of sulfonate surfactants in terms of chain length and branching, incorporation of phenyl, ethoxyl and multiple functional groups are found to produce specific effects in various adsorption regimes (electrostatic, hemimicellar, electrostatic hindered and micellar regions):

- a) Incorporation of the phenyl group between the α -CH₂ and the sulfonate of the octyl and decyl sulfonate increased the effective chain length by 3 to 4 CH₂ groups with respect to its adsorption on alumina;
- b) Increase in the chain length of the alkyl groups increased the adsorption in all the regions except the micellar region. These effects suggest the role of hemi-micellization as well as the enhanced solvent power of the interfacial region for the longer chains;
- c) The position of the branching of the sulfonate has a measurable effect on adsorption. The nature of the effect of the positioning on adsorption, particularly in hemi-micellar region, is suggestive of the type of packing of the surfactant species in the two-dimensional aggregates;
- d) Presence of alkyl substitutions on the aromatic ring

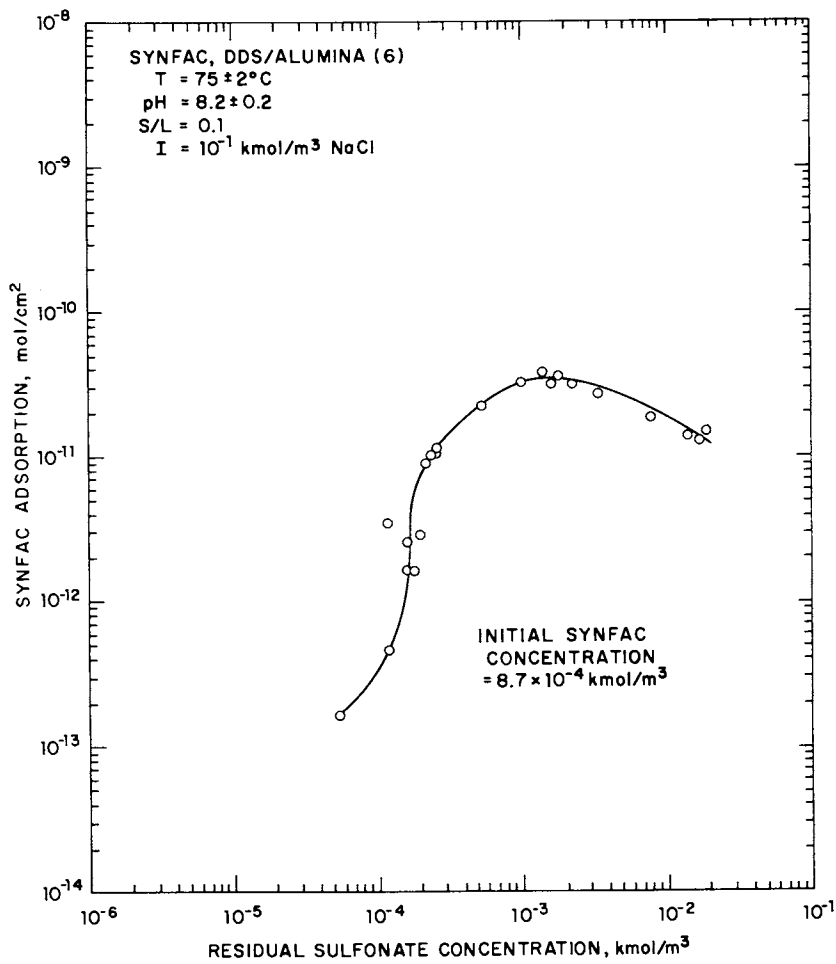


Figure 12. Ethoxylated alcohol coadsorption.

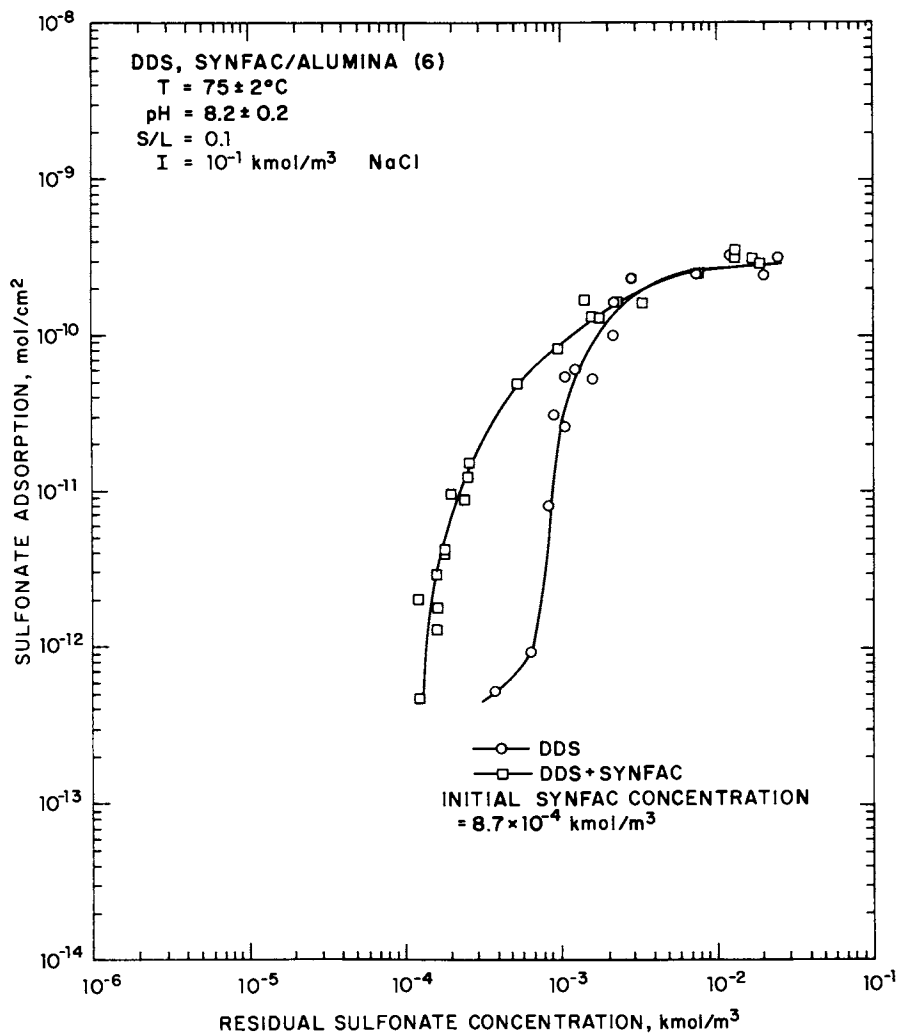


Figure 13. Effect of ethoxylated alcohol upon AS adsorption.

of the alkylaryl sulfonate decreased the adsorption. Furthermore, the hemi-micellization effect was also reduced apparently due to the steric hindrance produced by the xylene group.

e) Adsorption of the disulfonate, while comparable in the electrostatic region, was markedly lower at higher concentrations than that of the monosulfonate. Non-appearance of the sharp transition observed normally between Regions 1 and 2 suggests absence of hemi-micellization in the present case due to the head group bulkiness introduced by the ether linkage connecting the two sulfonates;

f) Adsorption characteristics of an anionic and a nonionic surfactant containing ethylene oxide groups were also studied. Even though salt (Ca) tolerance of the alkylaryl polyether sulfonate was markedly higher than that of the alkyl sulfonate of similar chain length, their adsorptions were not significantly different. The nonionic polyether alcohol, on the other hand, did not adsorb on alumina under the conditions studied. However, its adsorption was significant when the alkyl sulfonate was present in the system. This co-adsorption was also found to enhance the adsorption of the sulfonate.

The important role of the structure of the surfactants in determining adsorption is evident. Some of the surfactants discussed above can produce low interfacial tension and some others have excellent salt tolerance. A knowledge of the structure of such surfactants in adsorption can be helpful in developing surfactants that will meet different requirements simultaneously for special applications such as in enhanced oil recovery.

Acknowledgments

Support of the Department of Energy, National Science Foundation (CPE-82-01216), Amoco Production, Chevron Oil Field Research, Exxon Research and Engineering, Gulf Research and Development, Marathon Oil, Shell Development, Standard Oil of Ohio, Texaco, and Union Oil, is gratefully acknowledged.

Literature Cited

1. P. Somasundaran and K.P. Ananthapadmanabhan, "Physico Chemical Aspects of Adsorption on Surface Active Agents on Minerals", *Croatica Chemica Acta*, 52, 1979, p. 67-86.
2. E.D. Goddard and P. Somasundaran, "Adsorption of Surfactants on Solids", *Croatica Chemica Acta*, 48, 1976, p. 451-61.
3. H.S. Hanna and P. Somasundaran, "Physico-Chemical Aspects of Adsorption at Solid/Liquid Interfaces, Part II. Berea Sandstone/Mahogany Sulfonate System", in Improved Oil Recovery by Surfactants and Polymer Flooding, D.O. Shah and R.S. Schechter, eds., Academic Press, 1977, p. 253-274.

4. P. Somasundaran and D.W. Fuerstenau, "Mechanism of Alkyl Sulfonate Adsorption at the Alumina-Water Interface", *J. Phys. Chem.*, **70**, 1966, p. 90-96.
5. P. Somasundaran, M. Celik, and A. Goyal, "Precipitation and Redissolution of Sulfates and Their Role in Adsorption on Minerals", in Surface Phenomena in Enhanced Oil Recovery, D.O. Shah, ed., Plenum, 1981, p. 641.
6. M. Nakagaki, T. Hamda, and Shimabapashi, in *J. Colloid and Interface Science*, 1973, Vol. 43, p. 521-9.
7. C. Giles, T. MacEwan, H. Nakhwa, and D. Smith, *J. ACS*, **3973**, 1969.
8. B. Tamamushi, Colloidal Surfactants, Academic Press, New York, 1963, p. 125.
9. M. Celik, A. Goyal, E. Manev, and P. Somasundaran, "The Role of Surfactant Precipitation and Redissolution in the Adsorption of Sulfonates on Minerals", *S. of Petroleum Eng.*, SPE 8263, 1979.
10. K. Shinoda, Colloidal Surfactants, Academic Press, New York, 1963.
11. P. Somasundaran, "The Relationship Between Adsorption at Different Interfaces and Flotation Behavior", *Trans. AIME*, **241**, 1968, p. 105-108.
12. G. Parks, "Adsorption in the Marine Environment" in Chemical Oceanography, 2nd Ed., Riley and Shirrow, Academic Press, 1974.
13. S. Dick, D.W. Fuerstenau, and T. Healy, *J. Colloid and Interface Science*, **37**, 1971.
14. R. Marriot, C. Kao, and F. Kristal, *SPE J.*, 1982, p. 993-997.

RECEIVED March 6, 1984

The Effect of Preadsorbed Polymers on Adsorption of Sodium Dodecylsulfonate on Hematite

J. E. GEBHARDT¹ and D. W. FUERSTENAU

Department of Materials Science and Mineral Engineering, University of California, Berkeley, CA 94720

The presence of pre-adsorbed polyacrylic acid significantly reduces the adsorption of sodium dodecylsulfonate on hematite from dilute acidic solutions. Nonionic polyacrylamide was found to have a much lesser effect on the adsorption of sulfonate. The isotherm for sulfonate adsorption in absence of polymer on positively charged hematite exhibits the typical three regions characteristic of physical adsorption in aqueous surfactant systems. Adsorption behavior of the sulfonate and polymer is related to electrokinetic potentials in this system. Contact angle measurements on a hematite disk in sulfonate solutions revealed that pre-adsorption of polymer resulted in reduced surface hydrophobicity.

Technological problems caused by fine particulates occur in many industrial situations including mineral processing circuits. The processing of fine particle suspensions has been the topic of several technical conferences in recent years (1-2). One method exhibiting significant potential for recovering valuable minerals from fine-particle suspensions is selective flocculation. This involves the use of a polymer or long-chained organic molecule to selectively aggregate particles of one of the minerals prior to a separation stage. Depending on the process and mineral composition, either the valuable or gangue mineral may be flocculated. To obtain a suitable concentrate, the flocculated particles must be separated from the suspension. The usual method is sedimentation of the flocs combined with elutriation of the dispersed particles. Flotation of the flocculated particles is a possible method to achieve that separation. The effect of polymers used as flocculants on the flotation of a few minerals has received

¹Current address: U.S. Bureau of Mines, Avondale Metallurgy Research Center, 4900 LaSalle Road, Avondale, MD 20782

0097-6156/84/0253-0291\$06.00/0
© 1984 American Chemical Society

limited investigation (3-5), and details on the mechanism of polymer and flotation collector coadsorption and relation to flotation are lacking. This paper reports the results of an investigation undertaken to delineate the role of polymer and collector interactions with fine particles and their relation to resultant surface wettability. In particular, the adsorption of an anionic surfactant on a surface with previously adsorbed non-ionic or anionic polymer is examined.

Experimental Methods and Materials

Materials. Synthetic hematite was obtained from J. T. Baker Chemical Company, Phillipsburg, NJ. Particle size analysis using a HIAC instrument (Montclair, CA) indicated the particles to be 80 percent (number) finer than 2 microns. Using nitrogen as the adsorbate, the B.E.T. specific surface area was found to be 9 square meters per gram. The point of zero charge, as obtained from electrophoretic measurements in the presence of indifferent electrolytes, occurred at pH 8.3.

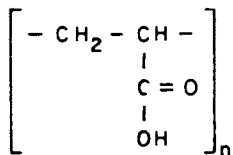
Polyacrylic acid (PAA) was obtained from Scientific Polymers, Inc., Ontario, NY, as a secondary standard with a mass-averaged molecular weight of two million. The polyacrylamide (PAM) used was Separan MGL obtained from Dow Chemical Company, Midland, MI. Its reported molecular weight was in the range of 500,000 to 5,000,000. The monomer structures of PAA and PAM are illustrated in Figure 1.

Sodium dodecylsulfonate (SDS) was prepared from dodecyl alcohol by Ben Den Chemical Company, Naperville, IL. The material was recrystallized by dissolution in hot ethanol solution, filtering and cooling to crystallize the SDS. The precipitate was filtered, washed with cold ethanol, and dried in a dessicator under vacuum. Analytical-grade HCl and NaOH were used for pH adjustment and NaCl for controlling ionic strength.

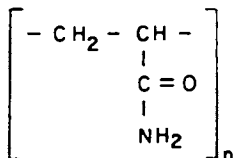
Adsorption Methods. Five grams of hematite were first conditioned in 0.001 M NaCl at pH 4.1. After the SDS had been added to the slurry and the pH adjusted as required, the samples were conditioned on a rotating shaker for two hours. The solutions were then centrifuged, and the supernatant liquid analyzed for its SDS content. The amount of SDS adsorbed was calculated as the difference between the initial amount added and the residual amount measured. Experimental results showed that two hours was sufficient time for equilibrium to be reached. Somasundaran (6) observed similar equilibrium adsorption times for sulfonate adsorption on aluminum oxide.

For adsorption on flocculated particles, the polymer was added in a drop-by-drop-wise manner from a burette containing a 50 cc solution to a 50 cc solution containing the solids. Flocculation was performed in an unbaffled vessel, 58 mm in diameter. Agitation was achieved with a 3-bladed propeller, 35 mm in

POLYACRYLIC ACID (PAA)



POLYACRYLAMIDE (PAM)



SODIUM DODECYLSULFONATE (SDS)

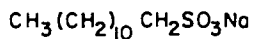


Figure 1. Chemical structure of polyacrylic acid and polyacrylamide monomers and sodium dodecylsulfonate.

diameter, which was located approximately 10 mm from the bottom of the vessel. Each blade was 13 mm across having a pitch of about 30 degrees. After agitating the slurry for 10 minutes at 600 rpm, the solution was decanted and the residual polymer determined. Polymer adsorption was rapid, and the method of polymer addition to these well-mixed suspensions was found to yield reproducible results. The flocs were transferred to 70-cc glass sample bottles to which SDS was added. The pH was adjusted as required, and the samples were conditioned on a rotating shaker (approximately 60 rpm) for two hours. Two hours was observed to be adequate for constant adsorption values to be reached in the case of particles that had been previously flocculated with polymer.

Electrokinetic Measurements. Electrophoretic mobilities were measured with a flat-cell apparatus manufactured by Rank Brothers, Cambridge, England. In addition, several mobility values were checked for accuracy with a Zeta Meter, New York. Mobilities were determined with a small volume of the suspension (approximately 25 cc) that had been prepared for the adsorption experiments. The pH of the solution was measured prior to determining the electrophoretic mobilities, which involved measuring the velocities of five to ten particles in each direction. An average value of the mobilities was recorded. Samples containing the flocculated particles were dipped into an ultrasonic bath for approximately one second prior to making the pH and mobility measurements.

Contact Angle Measurements. Contact angles were measured on a mounted disk of synthetic hematite. The disk was prepared by cold pressing hematite powder in a steel die and sintering it at 1,000 degrees Celsius for 8 hours in air. X-ray diffraction patterns indicated that the sample was still α -hematite. The angle formed by a bubble attached to the disk was measured using a goniometer. To form a bubble, a J-shaped glass capillary was placed under the disk, which had been positioned surface-side down in the solution. Advancing and receding angles were obtained by manipulating air in and out of the capillary tube. "Equilibrium" angles were determined by detaching the bubble from the capillary. The disk was cleaned between each measurement by several turns on a polishing wheel.

Surface Tension Measurements. The surface tension of surfactant solution was measured by the capillary rise method with a glass capillary tube, 18.66 cm in length and 0.0531 cm internal diameter. This was obtained by filling the capillary with a column of mercury and weighing the capillary with and without the mercury. The density of mercury was taken to be 13.5939 grams per cubic centimeter at 20 degrees Centigrade (7). The height of capillary rise was measured with a cathetometer manufactured by

Gaertner Scientific Corp., Chicago, IL, in a temperature-controlled room at 21 degrees Centigrade.

Analytical Methods. It was found that the concentration of both polymers could be analyzed by determining the total carbon in solution with a carbon dioxide coulometer, Coulometrics, Inc., Wheat Ridge, CO. The accuracy of this method is not good in the low polymer concentration range, that is less than 10-15 ppm. For higher accuracy in the low polymer concentration range, two different methods were used. In the case of PAA, potentiometric titrations of solutions of PAA were performed with 0.01 N NaOH using a Brinkman model, Westbury, NY, automated titrator. Blank tests indicated no interfering species. Known amounts of PAA were used to prepare a calibration curve immediately after titration of the samples containing unknown amounts of polymer. The starting point of the titration was pH 4.0, and the end point was reached near pH 8. Total volumes of 75 or 100 cc were used for the titrations, and the ionic strength was controlled at 0.01 M NaCl.

For the determination of PAM, UV adsorbance at 189 nm was measured for various PAM concentrations. The nephelometric technique of Attia and Rubio (8) as modified by Pradip (9) was used to check the calibration curve obtained by the UV method.

The amount of SDS in solution was determined by the method of Jones (10) modified in a manner similar to that of Somasundaran (6). Methylene blue chloride was added to a solution containing SDS. The resulting blue complex was extracted into an organic phase, and the absorbance in the visible range was measured. One-half cc of a one percent (by weight) methylene blue chloride solution was added to a 4.5 cc sample of solution containing 5-20 micrograms of SDS. Five cc of chloroform was then added and the solutions shaken by hand for 30 seconds. For the flocculated system, the polymer content was determined first and sufficient amounts of polymer were added prior to SDS determination to maintain the polymer level constant at 200 ppm. A calibration curve was made using absorbance at 652 nm as a function of SDS concentration.

Results and Discussion

Polymer/Surfactant Interactions. Interaction between polymers and surfactants was recently reviewed by Robb (11) and surfactant association with proteins by Steinhardt and Reynolds (12). Polymer/surfactant interactions are highly dependent on the chemical nature of the polymer and the surfactant. In general, surfactants tend to associate with uncharged polymers in aggregates rather than individual surfactant molecules interacting with the macro-molecule. The ability of surfactants to form micelles is thought to be an important factor in the role of surfactant behavior in interactions with polymers. Individual surfactant

molecules can interact directly with polyelectrolytes or polymers capable of some degree of ionization, such as proteins, while association between polymers and surfactant aggregates follows at higher surfactant concentrations. Electrostatic forces are primarily responsible for the different interaction behavior of surfactants with the charged and uncharged polymers.

The measurement of the surface tension of SDS solutions at constant polymer additions was performed to investigate any possible interactions between SDS and the polymers used in these experiments. The results, shown in Figure 2, indicate no interaction between SDS and either PAA or PAM. Interactions between similarly charged surfactant and polyelectrolyte are not common as electrical effects frequently dominate to prevent any hydrophobic or hydrogen bonding interaction. The hydrophilic nature of the amide dipole of polyacrylamides has been suggested (11) as a possible factor in preventing interaction with sodium dodecylsulfate.

Adsorption of SDS on Hematite. Adsorption of SDS on hematite at pH 4.1 is illustrated in Figure 3 as the zero polymer (top line-filled circles) addition. The results indicate three distinct regions of adsorption and in this respect agree well with previous investigations (13, 14) of systems involving adsorption of an anionic surfactant from an aqueous solution of constant ionic strength onto a positively charged oxide surface. Fuerstenau and Raghavan (15) have summarized the proposed mechanism of adsorption by describing the three regions of differing slope. In brief, at low SDS equilibrium concentration the adsorption process is described as being an electrostatic exchange of surfactant ions for counter ions in the double layer. The increased slope of the next region is attributed to the onset of hemi-micelle formation. At high SDS equilibrium concentration, the zeta potential is of similar sign as the surfactant and electrostatic interactions oppose specific interactions resulting in a reduced slope of the adsorption isotherm.

Adsorption on Hematite With Pre-Adsorbed PAA. The adsorption of SDS on hematite particles which were previously flocculated by the addition of PAA is illustrated in Figure 3. The adsorption of SDS decreases as increasing amounts of PAA occupy surface sites. The adsorption of PAA on hematite, which had been investigated previously (16), is given in Figure 4 as a function of equilibrium PAA concentration for various pH values. These results show that the adsorption of PAA is characterized by high adsorption densities at low equilibrium concentrations. The plateau or surface saturation value for pH 4.1 would be approximately 0.41-0.42 mg PAA per square meter. This corresponds approximately to the highest PAA addition shown in Figure 3, 0.44 mg PAA per square meter, where it was determined that 0.41 mg PAA

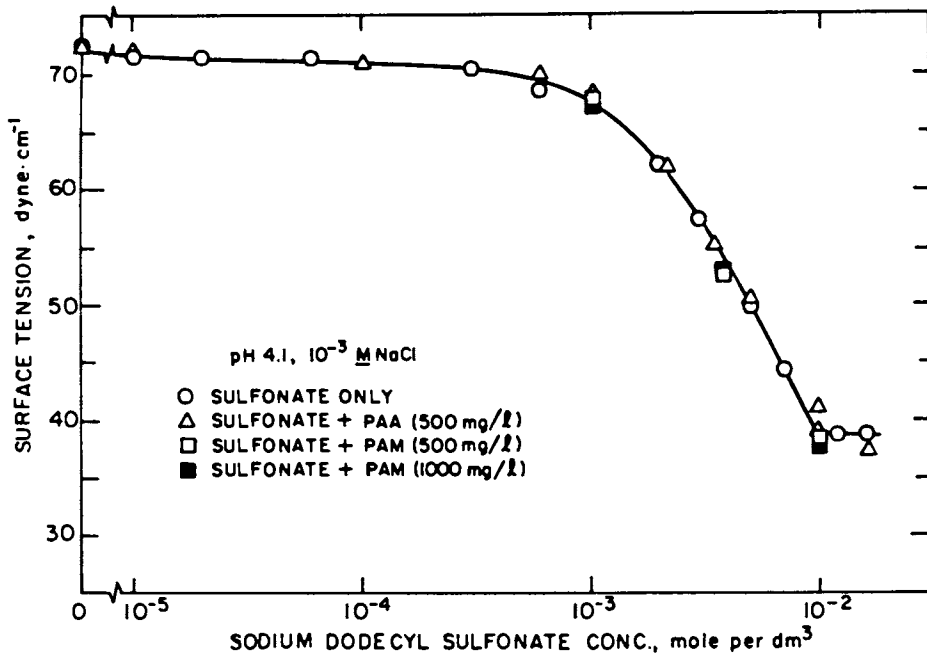


Figure 2. Surface tensions of sodium dodecylsulfonate solutions with and without polymer addition as measured by the capillary rise method.

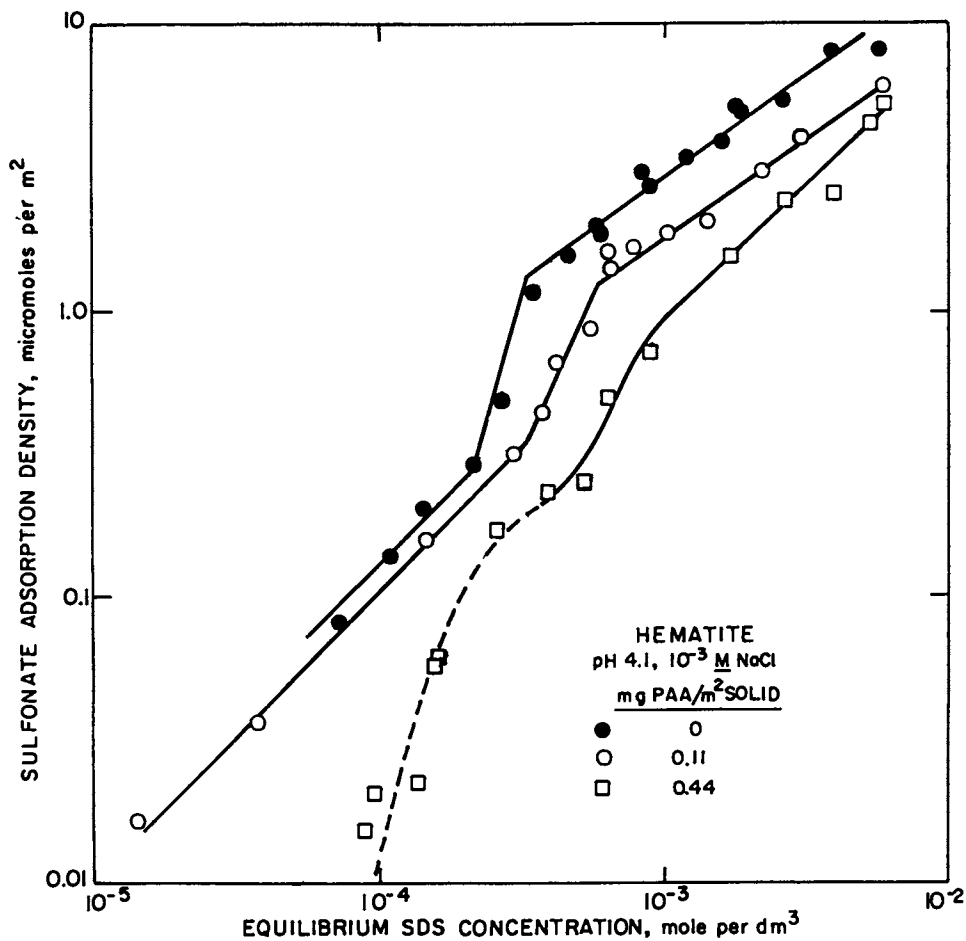


Figure 3. Equilibrium adsorption densities of sodium dodecylsulfate on hematite at pH 4.1 and 0.001 M NaCl in the presence and absence of pre-adsorbed polyacrylic acid.

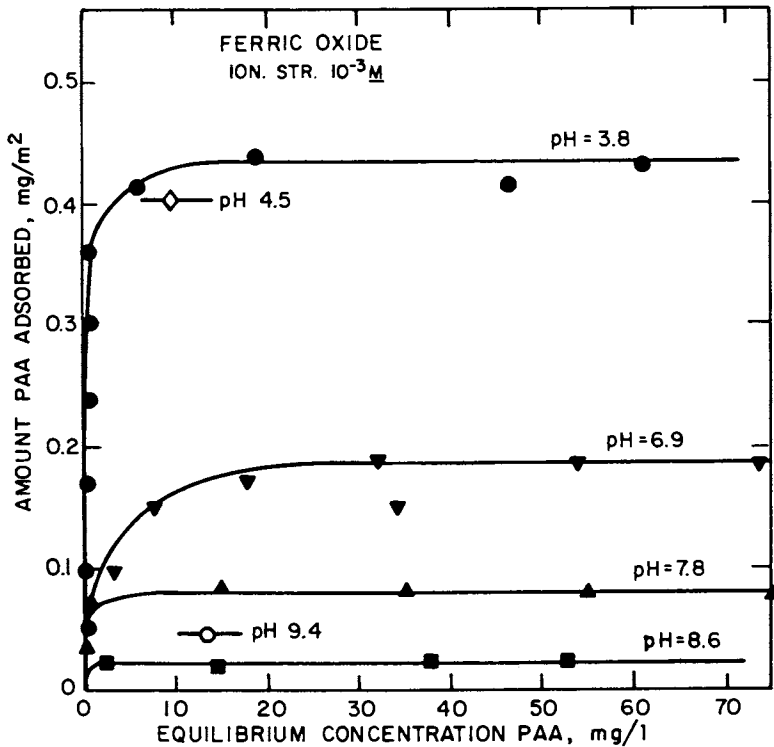


Figure 4. Equilibrium adsorption densities of polyacrylic acid on hematite at various pH values. Reproduced with permission from Ref. 22. Copyright 1983, Colloids and Surfaces.

per square meter had been adsorbed. No residual polymer was measured in solution for the 0.11 mg PAA addition.

In general, the adsorption of a surfactant on particles with previously adsorbed polymer can be influenced by (i) a reduction of surface area available for adsorption as a result of the presence of adsorbed polymer, (ii) possible interactions between polymer and surfactant in the bulk solution or in the interfacial region (that is, surfactant with loops, tails or trains of adsorbed polymer molecules), (iii) the steric effect of adsorbed polymer, preventing approach of surfactant molecules for adsorption at the surface, or (iv) possible electrostatic effects if polymer and/or surfactant are charged species.

Since there was no evidence of surfactant/polymer interactions, the two most important factors affecting SDS adsorption on PAA-flocculated hematite particles are believed to be electrostatic effects and a reduction in the number of surface adsorption sites due to adsorbed polymer segments. Polyelectrolyte adsorption on oppositely charged surfaces can involve strong attractive forces (as evidenced by the high affinity isotherm) and is expected to result in a somewhat flat surface configuration (17). Using the surface saturation value of 0.41 mg PAA per square meter and assuming a 25 square angstrom PAA monomer segment size, 87 pct of the total surface area would be occupied by polymer segments if the segments were free to make contact individually. In actuality, polymer segments are not free to make individual contact with the surface because of the nature of the molecular chain structure. However, the adsorbed amounts shown in the adsorption isotherms of SDS on PAA-flocculated hematite indicate that the polymer chains may have a significant number of segments in contact with the surface, thereby reducing the number of sites available for SDS adsorption.

The effect of polymer charge on the zeta potential is given in Figure 5 where the electrophoretic mobility of hematite particles flocculated with PAA and conditioned in SDS is indicated as a function of SDS adsorption density. The electrophoretic mobilities of hematite particles without polymer in the presence of SDS are also shown in Figure 5 (filled circles). In the presence of the anionic surfactant, the electrophoretic mobility decreases with increasing SDS adsorption density, reverses in sign and becomes negative in value at high SDS adsorption densities. This behavior is typical for anionic surfactant interaction with an oppositely charged surface and has been observed by other researchers (18). At pH 4.1 in the absence of surfactant (and polymer), hematite particles are positively charged and have a mobility of 3.9 electrophoretic mobility units.

For the addition of 0.11 mg PAA per square meter hematite, the mobility decreased at SDS adsorption densities less than 0.3 micromoles per square meter but remained positive in value. Above this adsorption density, negative mobilities were recorded. At PAA additions of 0.22 and 0.44 mg per square meter hematite,

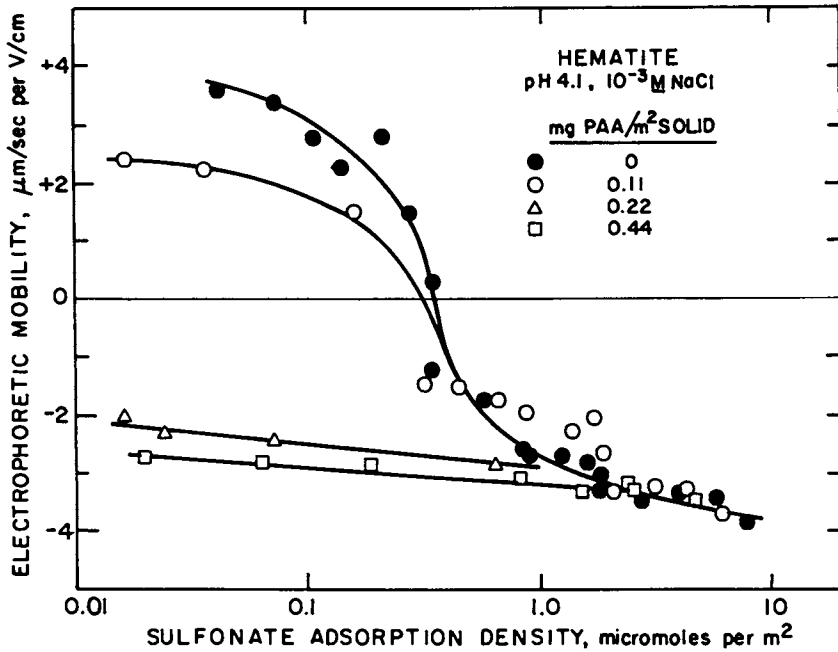


Figure 5. Electrophoretic mobility of hematite at pH 4.1 and 0.001 M NaCl as a function of sulfonate adsorption density in the absence and presence of pre-adsorbed polyacrylic acid.

mobility values were negative for all SDS concentrations and became slightly more negative with increasing surfactant adsorption. The presence of PAA has a dramatic effect on the mobility values, although surfactant adsorption also contributed to changes in the mobility, especially at PAA additions less than 0.22 mg per square meter. Above SDS adsorption densities of 1-2 micromoles per square meter, the mobilities observed in all the experiments were the same in the absence or presence of pre-adsorbed polymer.

The surface charge of the hematite used here was measured by titration (16) and found to be approximately 18 microcoulombs per square meter, equivalent to a charge of 5.40×10^8 esu per square meter of hematite. Assuming one equivalent per monomer segment, the total charge of PAA would be 4.02×10^9 esu per mg PAA for the totally ionized polymer. Approximately 0.11 mg PAA (if totally ionized) would be almost sufficient to neutralize the charge of one square meter of hematite. The transition of positive mobility to negative mobility occurs between 0.11 and 0.22 mg PAA per square meter hematite, in accordance with the amount of polymer charge required to neutralize the solid surface charge.

Adsorption on Hematite With Pre-Adsorbed PAM. Adsorption of SDS on hematite flocculated with PAM was investigated with 0.44 mg PAM per square meter hematite. SDS adsorption density as a function of equilibrium SDS concentration is shown in Figure 6 for the same conditions as used in the PAA/SDS system. In the low SDS concentration range (that is, less than 0.0003 M SDS), adsorption of SDS was unaffected by the presence of PAM. At equilibrium concentrations greater than 0.0003 M SDS, adsorption of SDS on the flocculated particles was reduced from that on the unflocculated particles. Adsorption of PAM on hematite as a function of PAM solution concentration is shown in Figure 7. Adsorption of PAM does not exhibit the strong affinity observed for PAA, although the plateau or saturation value is similar and slightly higher for PAM. These results suggest that PAM adsorption may occur in a more loosely packed surface configuration.

Some polymer molecules can be regarded to maintain their approximate solution conformation upon adsorption (19). Adsorption of a nonionic polymer would lead to a coiled adsorbed polymer configuration with a small number of polymer segments in actual contact with the surface. The number of surface sites available for surfactant adsorption would remain quite large.

At equilibrium surfactant concentrations of less than 0.0003 M SDS where the hematite surface is still positively charged, adsorption of surfactant follows its normal pattern due to the electrostatic forces which provide the driving force for adsorption. Sufficient effective surface area must be available for this level of SDS adsorption density. As surfactant adsorption

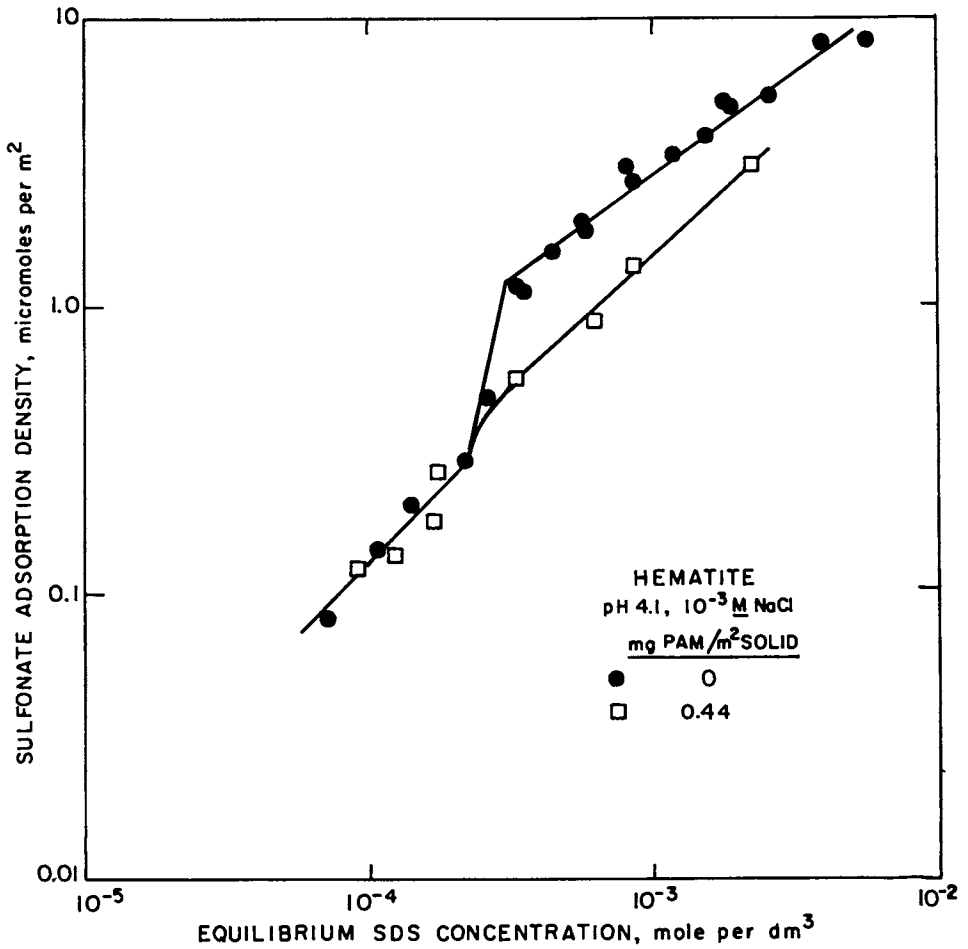


Figure 6. Equilibrium adsorption densities of sodium dodecylsulfonate on hematite at pH 4.1 and 0.001 M NaCl in the presence and absence of pre-adsorbed polyacrylamide.

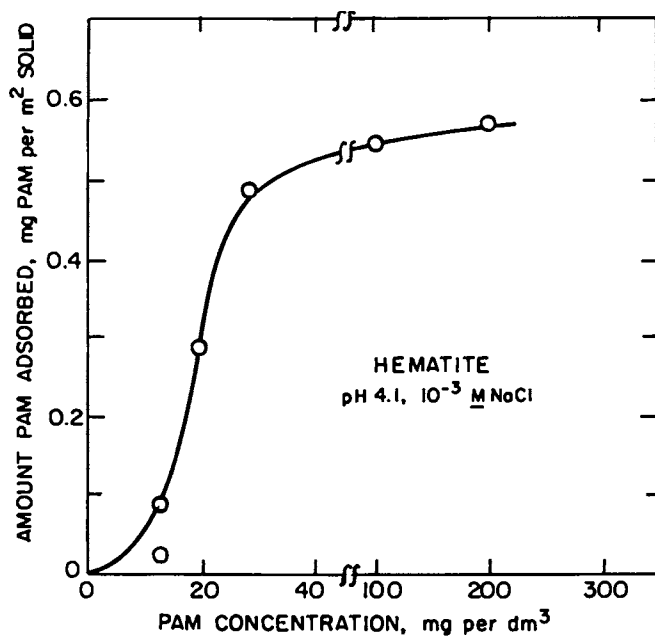


Figure 7. Equilibrium adsorption densities of polyacrylamide on hematite at pH 4.1 and 0.001 M NaCl.

increases with increasing SDS concentration, the surface charge is reversed (see Figure 8), and additional surfactant adsorption is reduced due to electrical forces and also to a reduction of available surface area due to adsorbed PAM segments. No significant change in slope is observed, and it is possible that the presence of adsorbed polymer prevents or reduces the effect of hemi-micelle formation.

The number of polymer segments in contact with the surface can be estimated from Figure 6 at high SDS concentrations. It is assumed that reduction in sulfonate adsorption, for the nonionic polymer case, is due only to the presence of adsorbed polymer segments. The amount of reduction in SDS adsorption at high SDS concentrations is taken (from Figure 6) to be an average of 50 percent, that is the effective area available for SDS adsorption is reduced by 50 percent. Using a monomer size of 25 square angstroms, a total of 10.7 mg of PAM would be required to occupy the area reduced which in this case is 22.5 square meters (total sample surface area was 45 square meters). Since the uptake of PAM was an average of 18 mg PAM, it is estimated that, at the most, approximately 50 to 60 percent of the PAM segments are in contact with the surface.

Surface Wettability. Contact angles on hematite at pH 4.1 were measured as a function of PAA and PAM concentration at constant surfactant concentration of 0.001 M SDS. The results are given in Figures 9 and 10 for PAA and PAM, respectively. The hematite disk was conditioned for 15 minutes in a solution containing the polymer and then transferred to the SDS solution for contact angle measurement. The angles were measured after 15 minutes conditioning with SDS and were not observed to vary with longer conditioning times. With no polymer present, the bubble contact angle was high, indicative of a hydrophobic surface. It is evident that adsorbed polymer caused a dramatic decrease in the contact angle. No bubble contact, for the equilibrium angle, could be achieved above polymer solution concentrations of 2 ppm for either PAA or PAM. Both polymers, being hydrophilic in character, prevent bubble attachment when a sufficient amount of polymer has been adsorbed. These results parallel findings by Somasundaran and coworkers (20, 21) that adsorption of a large hydrophilic molecule masks any effect that adsorbed surfactant molecules may have on the surface wettability.

Additional contact angles were measured at 0.001 M SDS concentration. The hematite disk was conditioned in the SDS solution before adding polymer to the solution. The contact angle was measured after adding sufficient quantities of polymer for concentrations of 1, 3, and 5 ppm. For both PAA and PAM, the contact angle remained constant and identical to the value obtained in the absence of polymer. No polymer was able to adsorb on the surfactant-coated disk. It can be concluded that whichever species, surfactant or polymer, adsorbed first was not

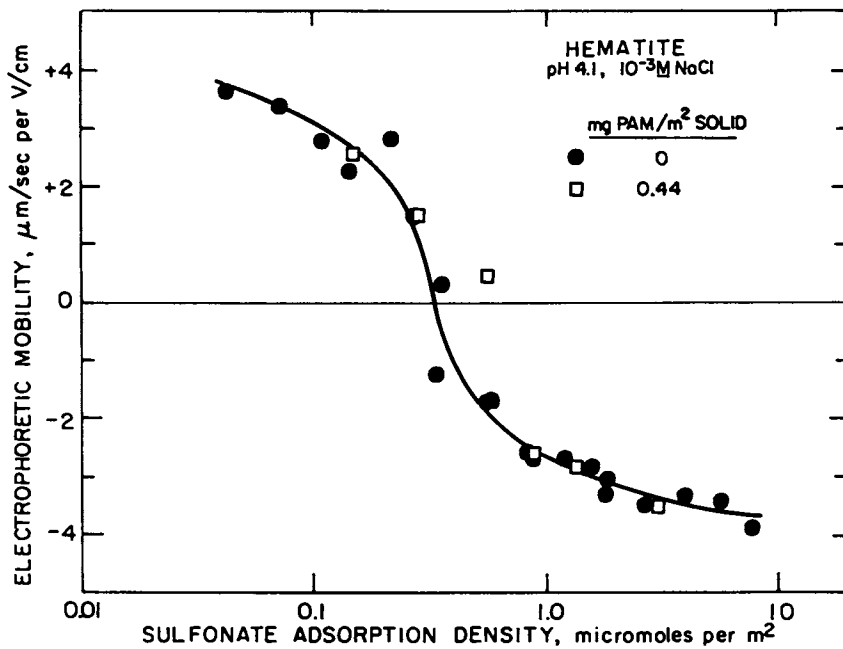


Figure 8. Electrophoretic mobility of hematite at pH 4.1 and 0.001 M NaCl as a function of sulfonate adsorption density in the absence and presence of pre-adsorbed polyacrylamide.

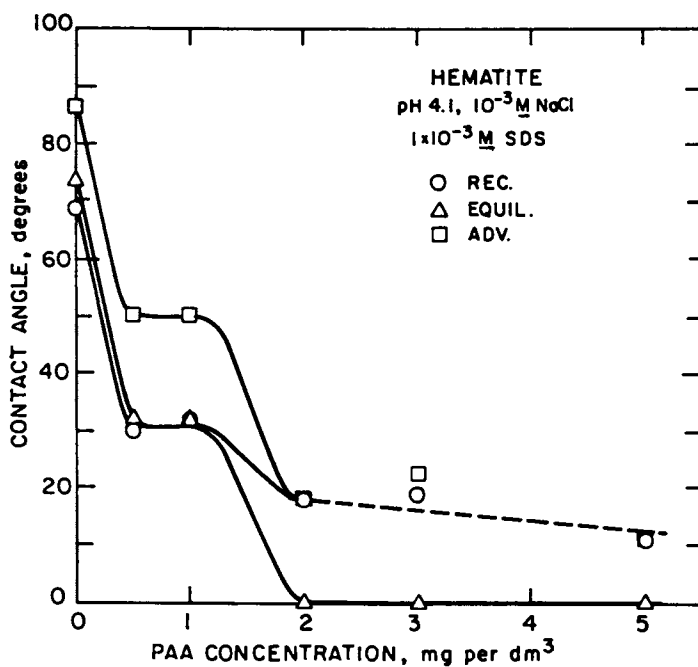


Figure 9. Contact angles on a hematite disk at 0.001 M SDS, pH 4.1, and 0.001 M NaCl as a function of the polyacrylic acid concentration in which the hematite disk had been preconditioned.

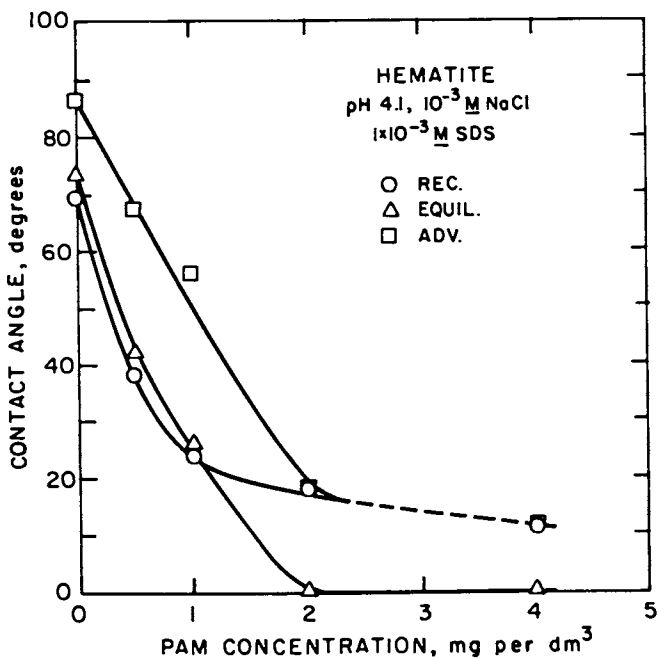


Figure 10. Contact angles on a hematite disk at 0.001 SDS pH 4.1, and 0.001 M NaCl as a function of the polyacrylamide concentration in which the hematite disk had been preconditioned.

replaceable by the other, at least under these particular conditions.

Summary

The adsorption behavior of surfactant onto particles in the absence and presence of pre-adsorbed polymer was determined. Electrokinetic studies of the system were made. Contact angle measurements yielded information on the level of hydrophobicity achieved at various additions of polymer and collector.

The results are summarized as follows:

1. Surface tension measurements indicated no bulk interaction between the anionic surfactant and the anionic or nonionic polymer.
2. The adsorption of an anionic surfactant on a positively charged oxide surface is significantly reduced by the presence of a pre-adsorbed anionic polymer.
3. The presence of a pre-adsorbed nonionic polymer has almost negligible effects on surfactant adsorption except at high surfactant concentrations where surfactant adsorption is reduced.
4. Electrokinetic studies revealed that the mobilities of particles with pre-adsorbed anionic polymer in the presence of surfactant were controlled by the charge associated with the polymer, while the mobilities were unaffected by the presence of pre-adsorbed nonionic polymer.
5. Contact angle measurements indicated that conditioning with increasing amount of polymer before conditioning with surfactant resulted in reduced surface hydrophobicity. Pre-conditioning with surfactant resulted in a hydrophobic surface which was not affected by subsequent polymer additions.

Acknowledgments

The authors wish to acknowledge support of this research by the National Science Foundation and the Department of the Interior for a Grant to the California MMRRI, University of California.

Literature Cited

1. "Fine Particles Processing"; Somasundaran, P., Ed.; Society of Mining Eng. of AIME: New York, 1980; 1865 pp.
2. "Beneficiation of Minerals Fines"; Somasundaran, P.; Arbiter, N., Eds.; American Institute of Mining & Metallurgical Engineers: New York, 1979; 406 pp.
3. Usoni, L.; Rinelli, G.; Ghigi, G. Proc. 8th International Mineral Processing Congress 1968, 14 pp.
4. Osborne, D. G. Trans. Instn. Min. Metal. 1978, 87, C189-C193.

5. Balajee, S. R.; Iwasaki, I., Trans. A.I.M.E., 244, 401-406; 407-411 (1969).
6. Somasundaran, P., Ph.D. Thesis, University of California, Berkeley, 1961.
7. "CRC Handbook of Chemistry and Physics"; 60th Edition, 1981.
8. Attia, Y. A.; Rubio, J. Br. Polymer J. 1975, 7, 135-138.
9. Pradip, M. S. Thesis, University of California, Berkeley, 1977.
10. Jones, J. H. J. Assoc. Official Agricultural Chem. 1945, 28, 398-409.
11. Robb, I. D. in "Anionic Surfactants: Physical Chemistry of Surfactant Action"; Luscassen-Reynders, E. H., Ed.; Marcel Dekker, Inc.: New York, 1981; Chap. 3, pp. 109-142.
12. Steinhardt, J.; Reynolds, J. A. "Multiple Equilibria in Proteins" Academic Press: New York, 1969; 234 pp.
13. Wakamatsu, T.; Fuerstenau, D. W., in ADVANCES IN CHEMISTRY SERIES Vol. 79, Gould, R. F., Ed.; 1968, pp. 161-172.
14. Somasundaran, P.; Fuerstenau, D. W. J. Phys. Chem. 1966, 70, 90-96.
15. Fuerstenau, D. W.; Raghavan, S. "Flotation: A.M. Gaudin Memorial Volume"; Fuerstenau, M. C., Ed.; American Institute of Mining, Metallurgical, and Petroleum Engineers, Inc.: New York, 1976: Vol. 1, pp. 21-65.
16. Gebhardt, J. E., M.S. Thesis, University of California, Berkeley, 1979.
17. Eirich, F. R. J. Colloid Interface Sci. 1977, 58, 423-435.
18. Hunter, R. J. "Zeta Potential in Colloid Science"; Academic Press: New York, 1981.
19. Rowland, F.; Bulas, R.; Rothstein, E.; Eirich, F. R. in "Chemistry and Physics of Interfaces"; Ross, S., Ed.; American Chemical Society: Washington, D.C., 1965.
20. Somasundaran, P. J. Colloid Interface Sci. 1969, 31, 557-565.
21. Somasundaran, P.; Lee, L. T. Separation Sci. & Tech. 1981, 16, 1475-1490.
22. Gebhardt, J. E.; Fuerstenau, D. W. Colloids and Surfaces 1983, 7, 221-231.

RECEIVED February 3, 1984

Adsorption and Electrokinetic Effects of Amino Acids on Rutile and Hydroxyapatite

D. W. FUERSTENAU, S. CHANDER¹, J. LIN², and G. D. PARFITT³

Department of Materials Science and Mineral Engineering, University of California, Berkeley, CA 94720

The mechanism of interaction of amino acids at solid/ aqueous solution interfaces has been investigated through adsorption and electrokinetic measurements. Isotherms for the adsorption of glutamic acid, proline and lysine from aqueous solutions at the surface of rutile are quite different from those on hydroxyapatite. To delineate the role of the electrical double layer in adsorption behavior, electrophoretic mobilities were measured as a function of pH and amino acid concentrations. Mechanisms for interaction of these surfactants with rutile and hydroxyapatite are proposed, taking into consideration the structure of the amino acid ions, solution chemistry and the electrical aspects of adsorption.

Interest in the nature of interactions between shortchain organic surfactants and large molecular weight macromolecules and ions with hydroxyapatite extends to several fields. In the area of caries prevention and control, surfactant adsorption plays an important role in the initial states of plaque formation (1-5) and in the adhesion of tooth restorative materials (6). Interaction of hydroxyapatite with polypeptides in human urine is important in human biology as hydroxyapatite has been found as a major or minor component in a majority of kidney stones (7). Hydroxyapatite is used in column chromatography as a material for separating proteins (8-9). The flotation separation of apatite from

¹Current address: Mineral Processing Section, Department of Mineral Engineering, The Pennsylvania State University, University Park, PA 16802

²Current address: Research Laboratory, IBM, San Jose, CA 95113

³Current address: Department of Chemical Engineering, Carnegie-Mellon University, Pittsburgh, PA 15213

gangue minerals as an important industrial operation in which surfactants are used to effect the separation (10). Dewatering of the colloidal phosphatic slimes that are generated in large quantities in the processing of phosphate rock is a major industrial problem which has been studied by a number of researchers in recent years (11).

Only a few systematic studies have been carried out on the mechanism of interaction of organic surfactants and macromolecules. Mishra et al. (12) studied the effect of sulfonates (dodecyl), carboxylic acids (oleic and tridecanoic), and amines (dodecyl and dodecyltrimethyl) on the electrophoretic mobility of hydroxyapatite. Vogel et al. (13) studied the release of phosphate and calcium ions during the adsorption of benzene polycarboxylic acids onto apatite. Juriaanse et al. (14) also observed a similar release of calcium and phosphate ions during the adsorption of polypeptides on dental enamel. Adsorption of polyphosphonate on hydroxyapatite and the associated release of phosphate ions was investigated by Rawls et al. (15). They found that phosphate ions were released into solution in amounts exceeding the quantity of phosphonate adsorbed.

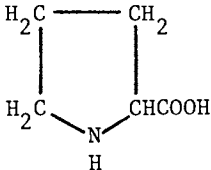
The present investigation was undertaken to study the mechanism of adsorption of selected amino acids in order to understand their interfacial behavior at the hydroxyapatite surface. The presence of two or more functional groups in amino acids give rise to surface properties which are quite different from the interfacial properties for the adsorption of simple surfactants, that is, those containing only one charged group. The adsorption behavior of hydroxyapatite is further complicated because of its partial solubility. Accordingly, the interfacial properties were also determined for TiO_2 and compared with those of hydroxyapatite.

Properties of Amino Acids

Amino acids are characterized by the presence of adjacent carboxylic ($-CO_2H$) and amino ($-NH$) functional groups. The equilibrium constant for protonation or dissociation of these groups is a function of their position in the amino acid molecule. Therefore, widely differing acid-base properties of amino acids occur, depending upon the number of functional groups and their relative position in the molecule. The dissociation constants for various amino acids used in this investigation are given in Table I.

The first dissociation constant for the $-CO_2H$ group is the more acidic group with a pK of 1.8 to 2.4. This group in amino acids is substantially more acidic than acetic acid, which has a $pK_a = 4.76$ due to the large inductive effect of the adjacent $-NH_3^+$ group. The pK for the protonation of the amino group has a value of 9.0 to 10.0 which is slightly lower than that for the conjugate acid of methylamine with a pK of 10.4. Thus, the amino acids have a positively charged $-NH_3^+$ group acidic pH 's ($pH < 2$) a positive $-NH_3^+$ and a negative $-CO_2^-$ group at neutral pH 's ($3 < pH < 9$) and

Table I. Stability Constants of Amino Acids

Amino Acid	Formula	pK_1	pK_2	pK_3
Glutamic acid	$\begin{array}{c} \text{NH}_2 \\ \\ \text{HOOC}(\text{CH}_2)_2\text{CHCOOH} \end{array}$	2.13	4.32	9.95
Lysine	$\begin{array}{c} \text{NH}_2 \\ \\ \text{H}_2\text{N}(\text{CH}_2)_4\text{CHCOOH} \end{array}$	2.16	9.20	10.80
Proline		1.95	10.64	

a negative $-\text{CO}_2^-$ group in alkaline pH's ($\text{pH} > 10$). In addition, one must consider dissociation of other functional groups present as part of the amino acid. For example, glutamic acid contains another $-\text{CO}_2^-$ which has a pK (dissociation constant) of 4.32, and lysine has another amine group with the pK of its conjugate acid being 10.80. Proline, because of its nitrogen being part of the cyclic ring, has pK's of 1.95 and 10.64. The charge on various functional groups as a function of pH is schematically illustrated in Table II. It is evident that an amino acid molecule may have strongly charged positive and negative sites even though the molecule has an overall charge neutrality. The present study shows that this zwitterionic character of amino acids plays an important role in the adsorption process.

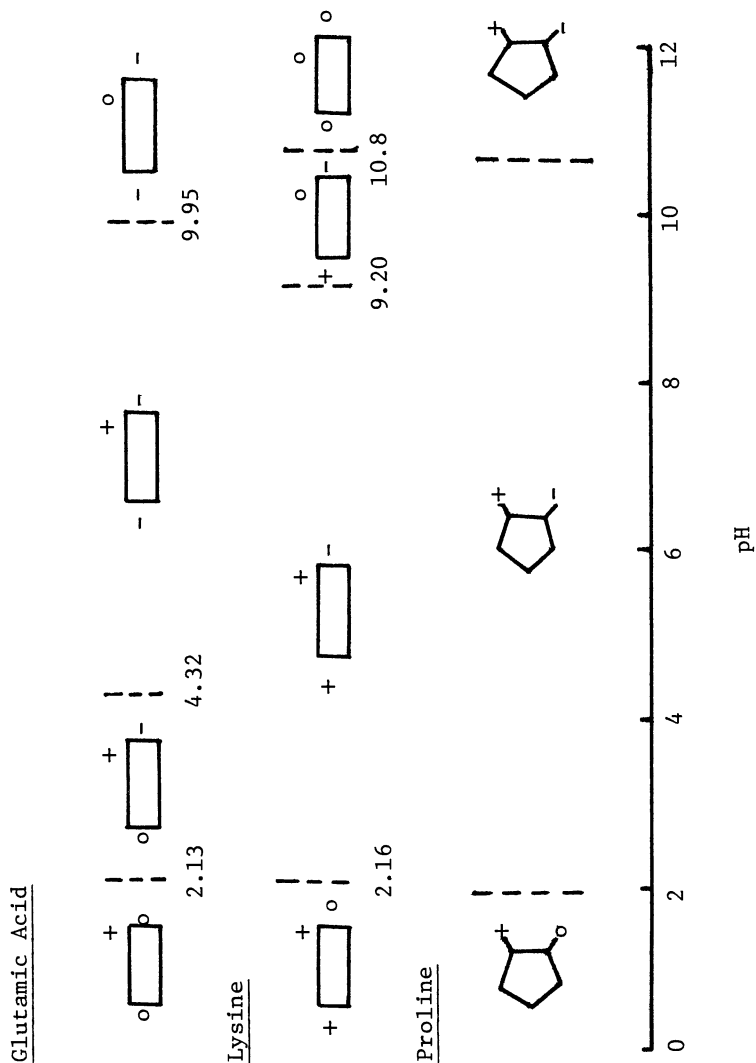
Experimental Methods and Materials

Synthetic hydroxyapatite prepared by mixing stoichiometric amounts of aqueous solutions of calcium nitrate and ammonium phosphate was used in this study. The pH of the boiling suspension was maintained at about 10 by flowing a mixture of NH_3 and N_2 throughout the precipitation process. The precipitate was repeatedly washed until the conductivity of the supernatant liquid was observed to be constant. The washed sample was freeze-dried and analyzed. An elemental analysis of the batch preparation showed the Ca/P molar to be ratio 1.64, with the predominant impurity being Si (0.12% SiO_2). The sample had a BET surface area of $19.6 \text{ m}^2/\text{g}$ and a density of $2.96 \text{ g}/\text{cm}^3$. The x-ray diffraction pattern was sharp and characteristic of synthetic hydroxyapatite. "Analytical grade" reagents and CO_2 -free double-distilled water were used throughout the investigation. The hydroxyapatite suspensions for the adsorption studies were prepared by adding 0.25 g hydroxyapatite to 25 ml of 10^{-2} M KNO_3 solution (unless otherwise indicated) and the requisite amount of the amino acid. After equilibration for one hour, the solids were separated in a centrifuge and the liquid was analyzed for its equilibrium amino acid concentration by the minhydrin method. The suspension was maintained at $37 \pm 0.5^\circ\text{C}$ throughout the adsorption equilibration period. Electrophoretic mobilities were measured with a Zeta-Meter electrophoresis apparatus. Lower concentrations of KNO_3 (generally $2 \times 10^{-3} \text{ M}$) were used in these tests to avoid excessive compression of the electrical double layer and to maintain thermal stability of the suspension in an electrical field.

Results and Discussions

Adsorption and Electrokinetic Behavior of Rutile. Isotherms for the adsorption of lysine, proline and glutamic acid on rutile (TiO_2) are given in Figure 1. There is no simple relationship between the adsorption density and the equilibrium concentration. The adsorption does not obey the Langmuir, Freundlich or Stern-Grahame relationships. The leveling-off of the adsorption

Table II. Schematic Illustration of Charges on Functional Groups in Amino Acids



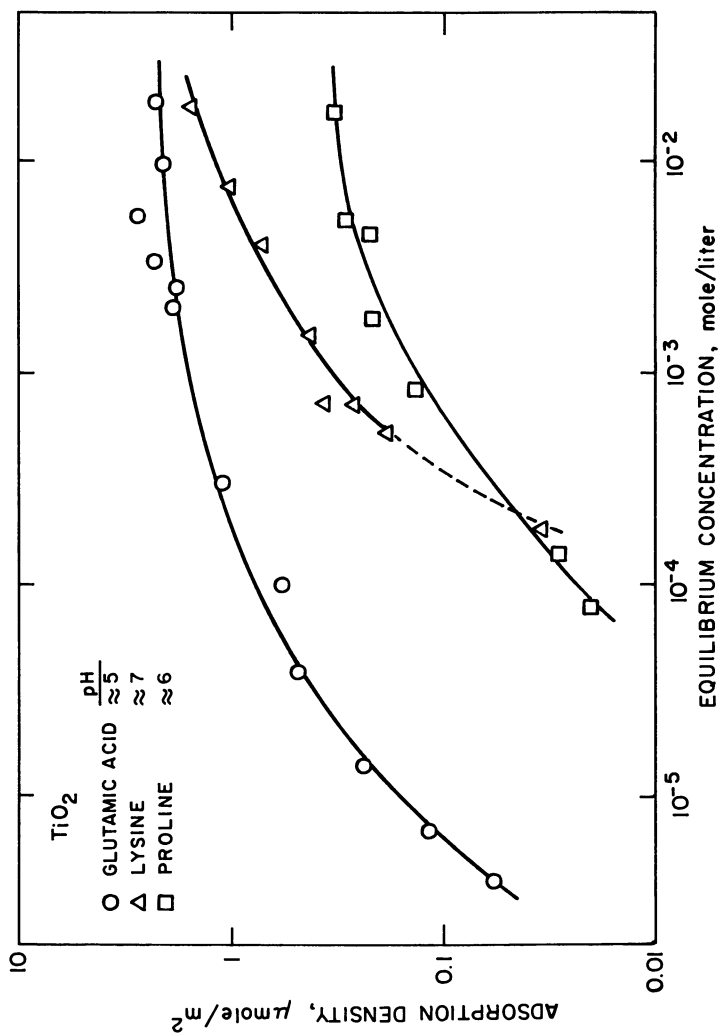


Figure 1. The isotherms for adsorption of glutamic acid, lysine and proline on rutile.

isotherms at high concentrations shows an apparent decrease in the free energy of adsorption with increase in concentration. This decrease in overall adsorption energy may be attributed to repulsion between the adsorbed molecules. Figure 2 further illustrates the electrostatic nature of interactions between the rutile surface and the amino acids. At pH's below the PZC of rutile (pH 6.7) the solid is positively charged and it is negatively charged at higher pH's. Glutamic acid which has two negative charges between pH 4.3 and 10.0 adsorbs mainly at the positive surface. Adsorption through the amine group on the negative surface is much weaker, perhaps because of the repulsion between the two negatively charged carboxylate groups and the negative surface. Lysine adsorbs only through electrostatic interactions also, and there is no indication of adsorption through carboxylic groups. Proline exhibits a very complex behavior, however. Although the uptake of proline can be considered to involve specific adsorption, the results can be interpreted by an electrostatic model if reorientation of the surfactant molecules is taken into consideration. As compared to glutamic acid and lysine, proline molecules contain only two functional groups. At a positive surface the adsorption could occur through the carboxylate group, whereas at a negative surface the molecule adsorbs through the amine group. Stronger repulsion between the identically charged groups in the adsorbing molecule and the surface is perhaps the reason for the relatively lower adsorption density of proline compared to glutamic acid.

The electrophoretic behavior of TiO_2 in glutamic acid, lysine and proline solutions are given in Figures 3, 4 and 5, respectively. Below the PZC of TiO_2 (pH < 6.7) adsorption of glutamic acid makes the electrophoretic mobility more negative as anticipated. At pH's greater than the PZC (pH > 6.7) a weak adsorption through amine groups makes the electrophoretic mobility even more negative because for each of the glutamic acid molecule adsorbed, two carboxylate groups are attached to the surface. At pH's near 10 or higher, the adsorption of amine groups ceases because they hydrolyze to the neutral form. Therefore all electrophoretic mobility curves merge at pH 10.

Lysine does not exhibit any significant influence on the electrophoretic mobility at pH values below the PZC of TiO_2 . At higher pH's, the electrophoretic mobility slightly increases because two amine groups are adsorbed for each adsorbed molecule. Proline makes the electrophoretic mobility slightly more negative in the intermediate pH range. Apparently, carboxylate ions in the adsorbing molecules are oriented in an outward direction such that they make the electrophoretic mobility more negative even though the proline molecule is overall neutral.

Adsorption and Electrokinetic Behavior of Hydroxyapatite. The adsorption densities of glutamic acid and lysine on hydroxyapatite are shown in Figures 6 and 7. The change in slope of the adsorption isotherm at 10^{-3} M glutamic acid is considered to be due to a

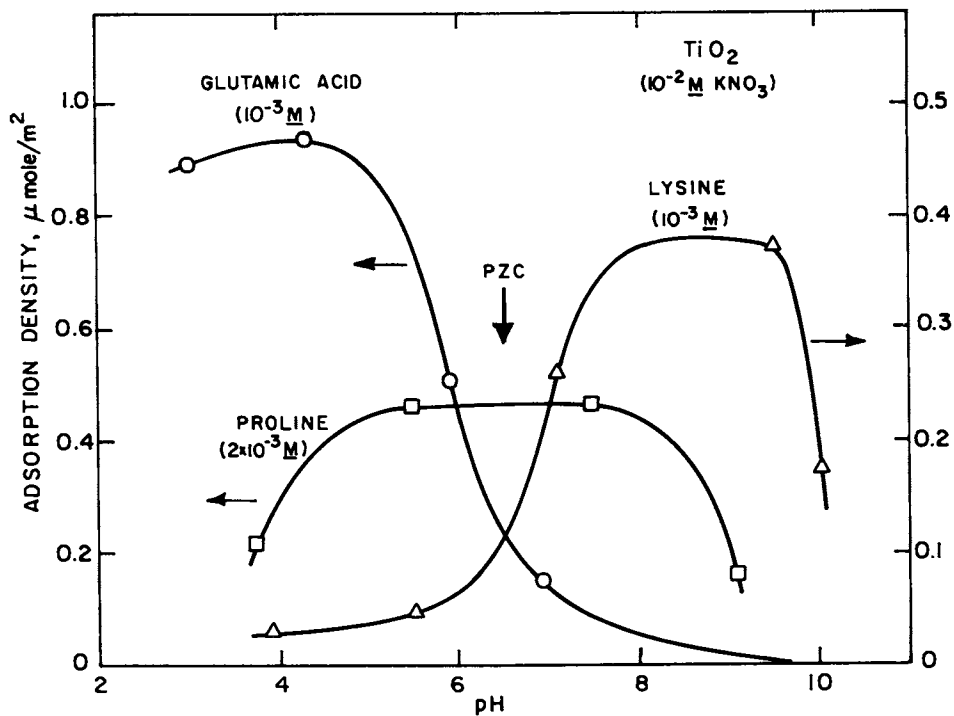


Figure 2. The effect of pH on the adsorption of glutamic acid, lysine and proline on rutile.

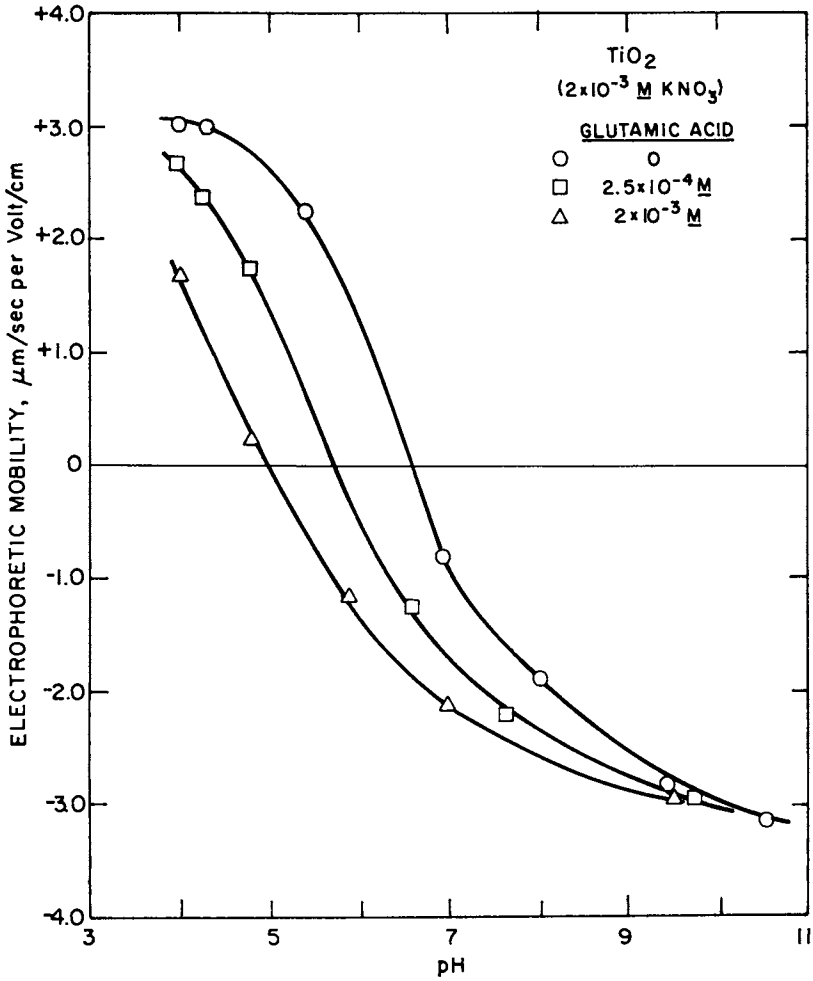


Figure 3. The effect of glutamic acid on the electrophoretic mobility of rutile.

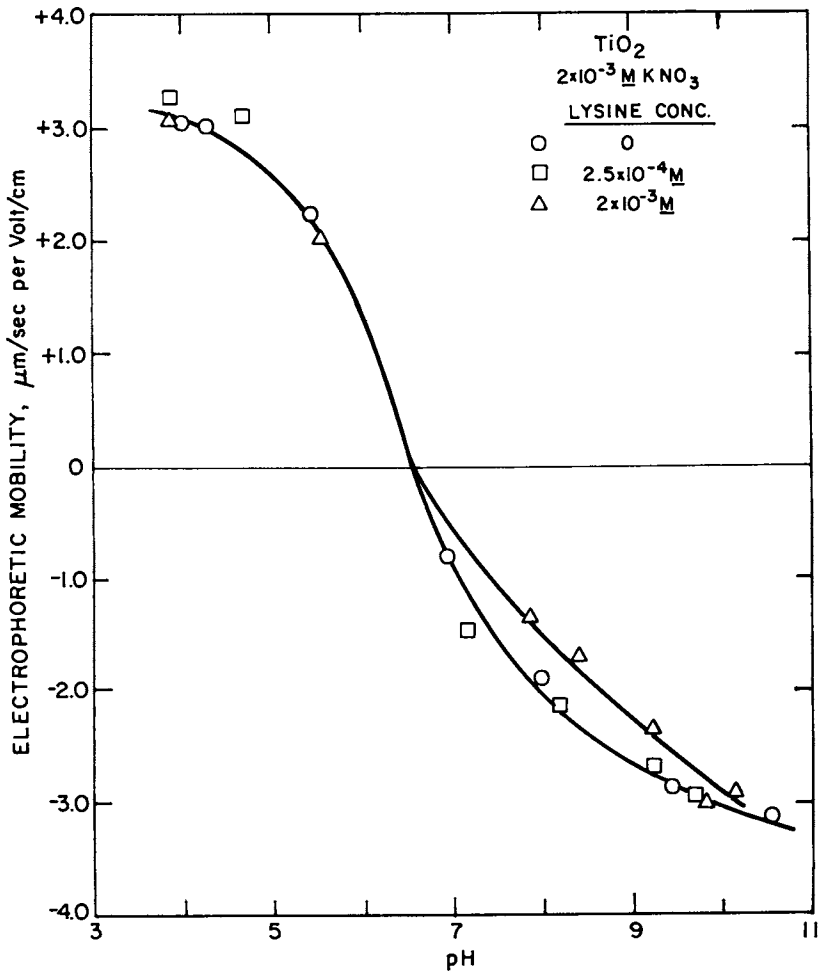


Figure 4. The effect of lysine on the electrophoretic mobility of rutile.

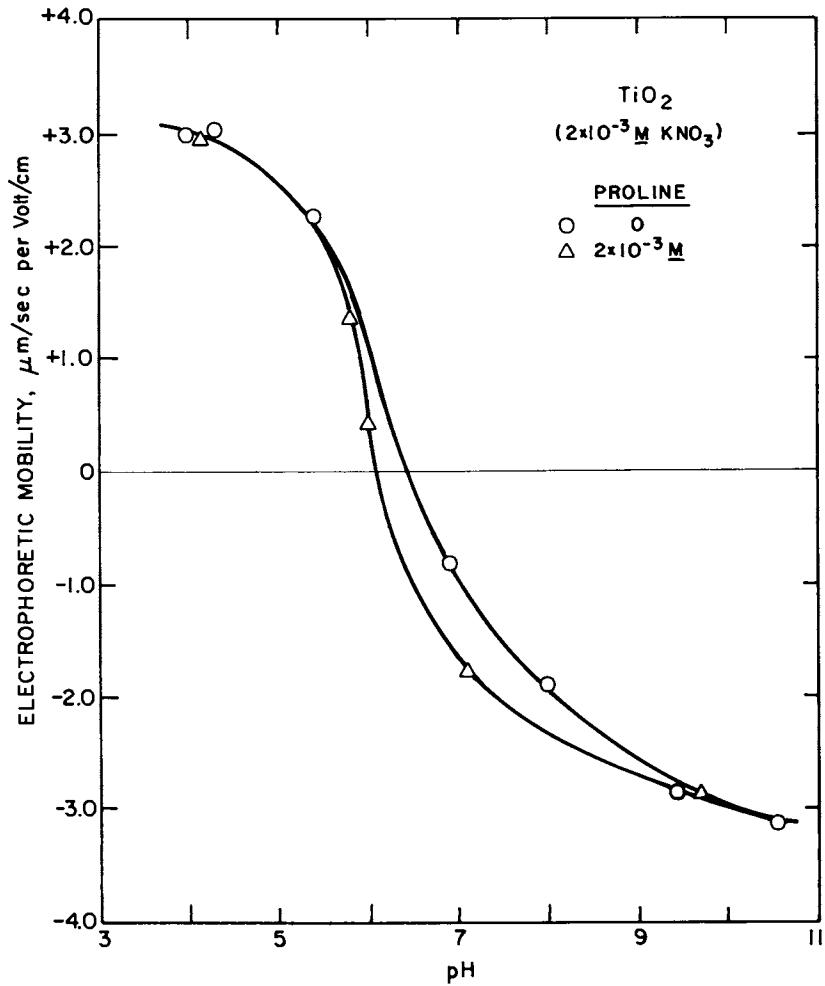


Figure 5. The effect of proline on the electrophoretic mobility of rutile.

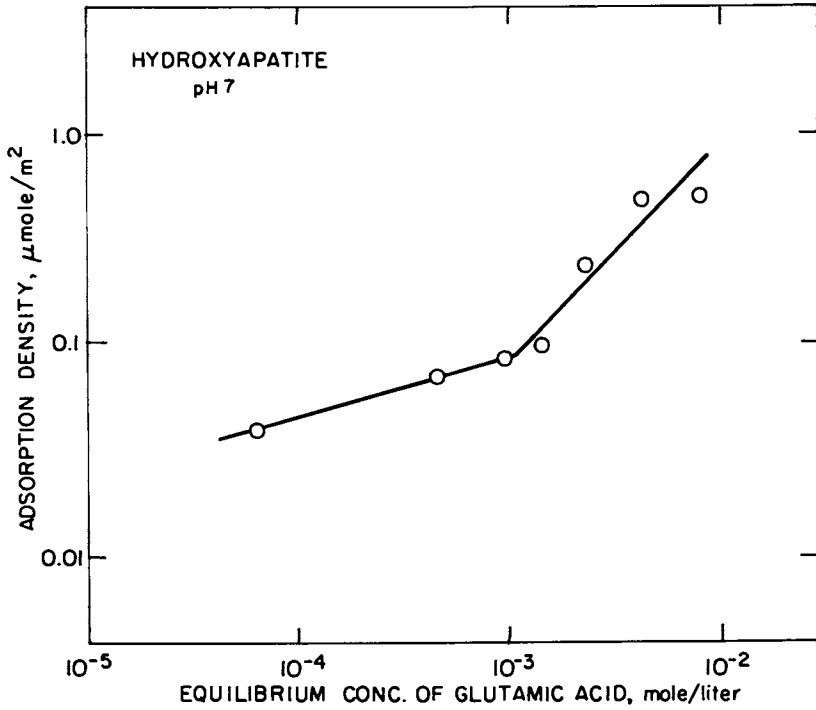


Figure 6. The isotherm for adsorption of glutamic acid on hydroxyapatite.

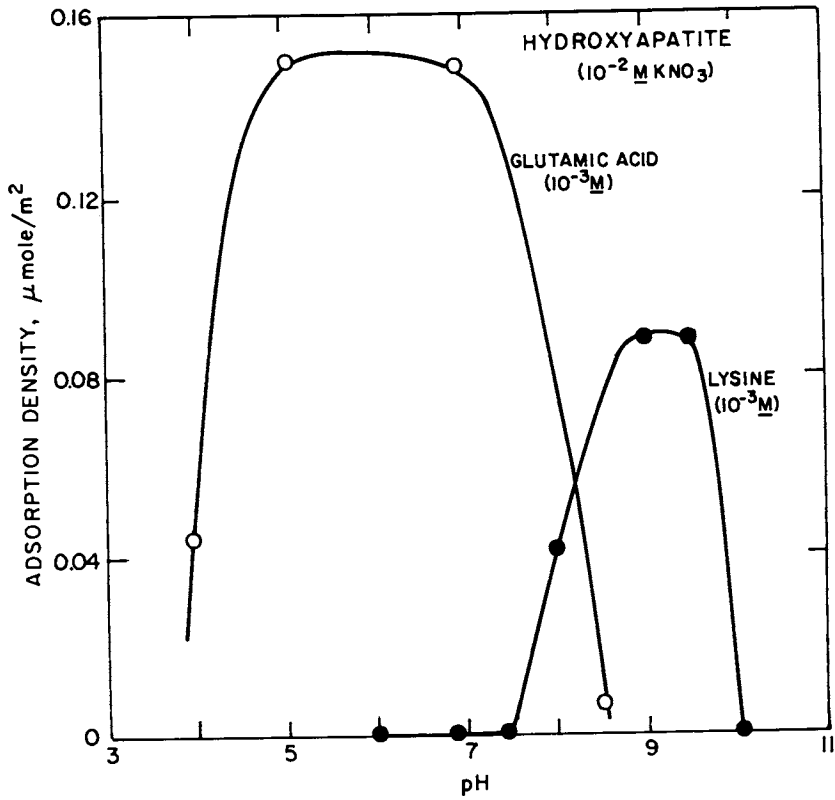


Figure 7. The effect of pH on the adsorption of glutamic acid and lysine on hydroxyapatite.

change in the adsorption mechanism. At low concentrations, we propose that the glutamic acid adsorbs whereas at high concentration the system undergoes chemical reaction involving the calcium ions at the surface. This hypothesis may explain the complex electrokinetic behavior of hydroxyapatite shown in Figure 8. At low concentration of glutamic acid, the electrophoretic mobility becomes more negative as would be expected if glutamic acid adsorbs. At higher concentrations, a chemical reaction occurs with the surface becoming positively charged, apparently because of a high concentration of coadsorbed calcium ions. Further studies are required to completely understand this highly complex system.

The adsorption of both glutamic acid and lysine is almost an order of magnitude smaller on hydroxyapatite than it is on TiO_2 (compare Figures 2 and 7). Glutamic acid adsorbs even at pH 7, suggesting that the adsorption can occur in different orientations of the glutamic acid ion. Lysine adsorbs only at a negative surface through the amine groups and adsorption ceases at pH 10 because the amine groups hydrolyze. The influence of lysine on the electrophoretic mobility of hydroxyapatite is presented in Figure 9. The mobility becomes positive because of the presence of two positively charged amine groups for each adsorbing ion.

Concluding Discussion

The adsorption of amino acids on rutile and hydroxyapatite exhibits some characteristics of specific adsorption. The results can be interpreted in terms of electrostatic models of adsorption, however, if reorientation of adsorbed molecules is taken into consideration. The electrokinetic behavior of hydroxyapatite in glutamic acid is complicated because of a chemical reaction, possibly involving calcium ions. The study shows that it is necessary to take into consideration the orientation of adsorbed molecules, particularly for zwitterionic surfactants.

Acknowledgments

The authors wish to acknowledge the National Science Foundation and the National Institute of Health, Grant NIH R01 DE 03708-06 for the support of this research.

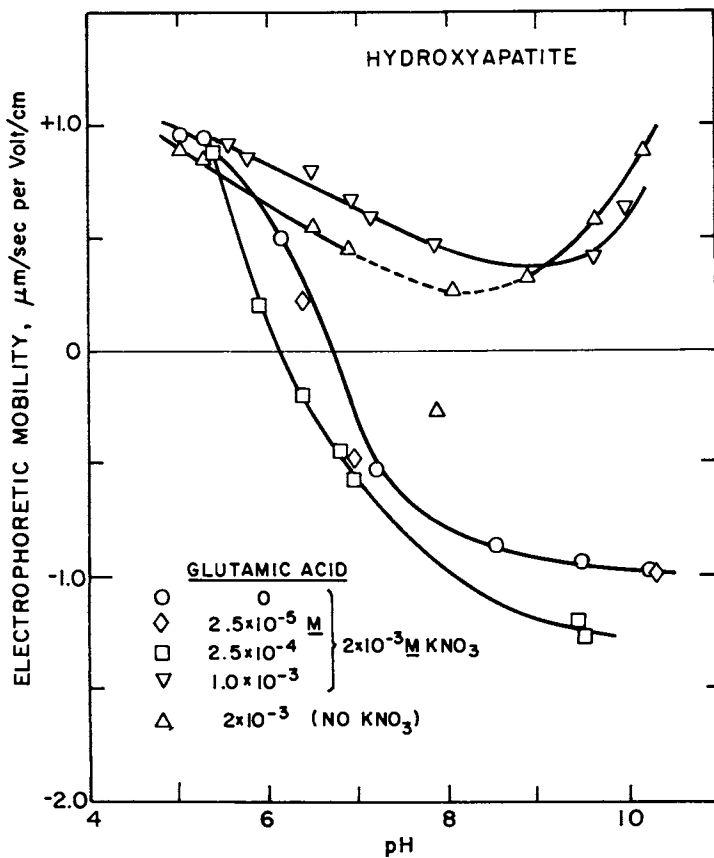


Figure 8. The effect of glutamic acid on the electrophoretic mobility of hydroxyapatite.

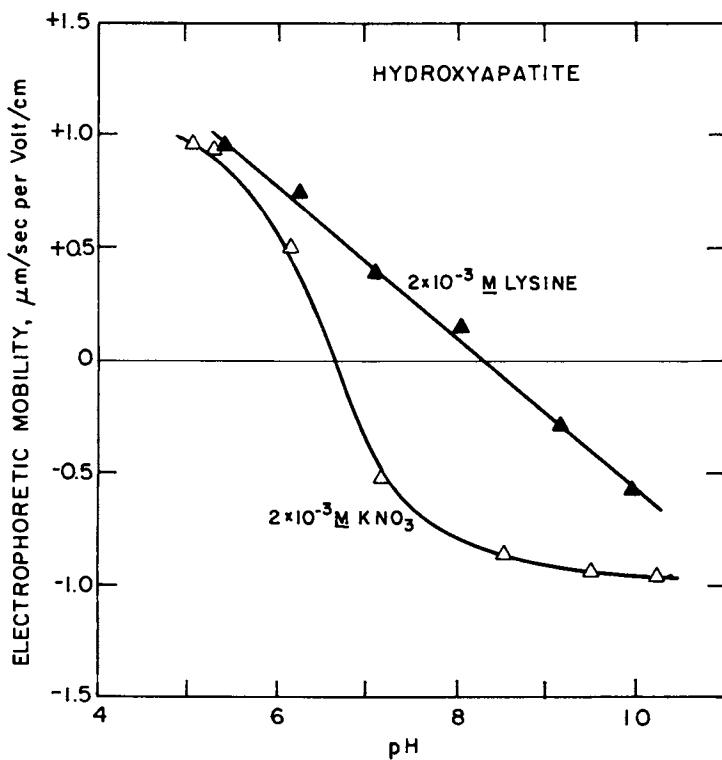


Figure 9. The effect of lysine on the electrophoretic mobility of hydroxyapatite.

Literature Cited

1. Hay, D. I. Arch. Oral Biol. 1967, 12, 937.
2. Francis, M. D. Calif. Tissue Res. 1969, 3, 151.
3. Anbar, M.; St. John, G. A.; Elward, T. E. J. Dental Res. 1974, 53, 1240.
4. Quintana, R. P. in "Applied Chemistry at Protein Interface"; Baier, R. E., Ed.; ACS SYMPOSIUM SERIES No. 145, American Chemical Society: Washington, D. C., 1975; p. 290.
5. Bartels, T.; Schudhof, J.; Arends, J. J. Dentistry 1979, 7, 221.
6. Farley, E. P.; Jones, R. L.; Anbar, M. J. Dental Res. 1977, 56, 943.
7. Malek, R. S.; Boyce, W. H. J. Urol. 1977, 117, 336.
8. Bernardi, G.; Kawasaki, T. Biochem. Biophys. Acta 1968, 160, 301.
9. Bernardi, G. in "Methods in Enzymology"; Hirs, Ch. W.; Timasheff, S. N., Eds.; Academic: New York, 1972; Vol. 27, p. 471.
10. Smith, P. R., Jr., in "Flotation, A. M. Gaudin Memorial Volume"; Fuerstenau, M. C., Ed.; AIME: New York, 1976; Vol. 2, p. 1265.
11. Nagraj, D. R.; McAllister, L.; Somasundaran, P. Int. J. Mineral Processing 1977, 4, 111.
12. Mishra, R. K.; Chander, S.; Fuerstenau, D. W. Colloids and Surfaces 1980, 1, 105.
13. Vogel, J. C.; Frank, R. M. J. Colloid Interface Sci. 1981, 83, 26.
14. Juriaanse, A. C.; Arends, J.; Tenbasch, J. J. J. Colloid Interface Sci. 1980, 76, 212.
15. Rawls, H. R.; Bartels, T.; Arends, J. J. Colloid Interface Sci. 1982, 87, 339.

RECEIVED January 20, 1984

Interfacial Tension of Aqueous Surfactant Solutions by the Pendant Drop Method

K. S. BIRDI and E. STENBY

Fysisk-Kemisk Institut, Technical University of Denmark, DK-2800 Lyngby, Denmark

The low interfacial tensions between two liquids have been measured for different systems by using the pendant drop method. In the case of the quaternary system: $C_{12}H_{25}SO_4Na+H_2O+n\text{-Butanol}+Toluene$, the interfacial data as measured by pendant drop method are compared with reported literature data, using other methods (with varying NaCl concentration). In order to understand the role of co-surfactant, ternary systems were also investigated. The pendant drop method was also used for measuring the interfacial tension between surfactant- H_2O/n -alcohol (with number of carbon atoms in alcohol varying from 4-10). The interfacial tension variation was dependent on both the surfactant and alcohol.

In the current literature one finds that the knowledge of interfacial tension, γ_{ij} , at liquid_i-liquid_j is of much importance in many different systems, e.g. emulsions, microemulsions, enhanced oil recovery etc.

If one considers a system consisting of: water (with or without added electrolyte) + oil + surfactant (with or without a co-surfactant) at equilibrium, there will most likely be present more than two phases (due to the formation of emulsion or microemulsion). The determination of the interfacial tension, γ_{ij} , between the two liquid phases is, therefore, of much importance, in order to understand the forces which stabilize these emulsions or microemulsions. The interfacial tension can be measured by using a variety of methods, as described in detail in surface chemistry text-books (1-3). If the magnitude of γ_{ij} is of the order of few mN/m (=dyne/cm), then the methods generally used are: Wilhelmy plate method or the drop volume (or weight) method (1-4). However, in certain systems ultra-low (or low) interfacial tensions have been reported. Since these low values are reported to be essential in order to mo-

0097-6156/84/0253-0329\$06.00/0
© 1984 American Chemical Society

bilize the residual oil, these studies are of much importance in the enhanced oil recovery processes (5,6,7). In the current literature, almost all the low or ultra-low γ_{ij} values have been measured by using the "spinning drop" method (8-10). The purpose of this study is to report comparative data of a system (11,12), *i.e.* NaDDS ($C_{12}H_{25}SO_4Na$)+ H_2O + n -Butanol+Toluene, by using the pendant drop method. Further, the pendant drop method is used to determine the γ_{ij} of various ternary systems. The general application feasibility of the pendant drop method is described. As regards these various methods used for measuring the magnitudes of γ_{ij} at two liquid interfaces, we must mention that the only low γ_{ij} value of a known system is for the interface, n -Butanol/ H_2O ($\gamma_{ij}=1.8$ mN/m at 20 °C) (1,13). In other words, whether one uses the spinning drop method or the pendant drop method (or any other), one will have to extrapolate from 1.8 mN/m to very low values of γ_{ij} (about 10^{-6} mN/m as reported from spinning drop method). This general procedure of extrapolation by few decades prompted us to reinvestigate some ternary and quaternary systems by using the pendant drop method.

Theory

The detailed theoretical derivations for the determination of the interfacial tension by the pendant drop are given in different literature reports (1-3,14-19). The profile of any liquid drop, Figure 1, of a given volume hanging from the smooth horizontal circular syringe is an unique function of the tube radius, interfacial tension (surface tension), density difference between the liquid in the syringe and the surrounding (air or another liquid) and the gravitational acceleration. As is well known, when one creates such a drop, it increases to a certain height (volume or weight) until it detaches itself. It is known that all such drops are in stable equilibrium, so that the drop falls when its theoretical maximum weight (volume) is attained.

If we consider the pendant drop as shown in Figure 1, we can write from the Laplace equation (20) for the point P in terms of the pressure differences across the interface at a reference point B:

$$(P_{B,i} - g\rho_i Z) - (P_{B,j} - g\rho_j Z) = \gamma_{ij} (1/R_{i,P} + 1/R_{j,P}) \quad (1)$$

where $P_{B,i}$ and $P_{B,j}$ are the pressures on the concave and the convex side of the surface at point B, respectively; γ_{ij} is the interfacial tension, $R_{i,P}$ and $R_{j,P}$ are the two principal radii of curvature of the surface at any reference point P in the coordinate system, where point B is chosen as the origin.

From geometry we find that at point B: $R_{B,i} = R_{B,j} = R_o$, and $(P_{B,i} - P_{B,j}) = 2\gamma_{ij}/R_o$.

From Equation 1 and these relations we get:

$$\gamma_{ij}(1/R_{1,P} + 1/R_{2,P}) = 2\gamma_{ij}/R_o + (gz\Delta\rho) \quad (2)$$

where $\Delta\rho = \rho_j - \rho_i$.

This equation is exact, and therefore the determination of the principal radii of curvature at two points on the interface enables one to estimate γ_{ij} and R_o . However, it is also clear that the photographic image if analyzed, as such, is not accurate enough to give a satisfactory accuracy.

Another procedure is to rewrite the relation in Equation 2 in terms of quantities which can be accurately measured from a photographic image (1,2,20). At point P we can let the radius of curvature be $R_{1,P}$ of curve V_1 , Figure 1. The curve V_2 , which is perpendicular to V_1 , and passes through P, will be such that OP is normal to both curves at P. Further, since OP is on the axis of revolution, P remains on curve V_1 when OP rotates about the axis BO. This gives the relation: $OP = X/\sin\phi$, which is the other radius of curvature of the interface at point P = R_{2P} . We can now rewrite Equation 2 as:

$$\gamma_{ij}(1/R_{1,P} + \sin\phi/X) = 2\beta Z/R_o \quad (3)$$

where $\beta = -\Delta\rho g R_o^2 / \gamma_{ij}$.

The standard relation which gives the radius of curvature of a curve in the X-Z plane (1) is as follows:

$$R_{1,P} = (1 + (dZ/dX)^2)^{3/2} / (d^2Z/dX^2) \quad (4)$$

Since $\tan\phi = dZ/dX$, and $\sin\phi = \tan\phi / (1 + \tan^2\phi)^{1/2}$, we can obtain:

$$d^2Z/dX^2 + (dZ/dX)/X(1 + (dZ/dX)^2) = (2/R_o - \beta Z/R_o^2)(1 + (dZ/dX)^2)^{3/2} \quad (5)$$

These derivations have been described in detail (15). However, the relationship in Equation 5 was found to be very unsuitable for the determination of γ_{ij} , since the curvatures are not easily evaluated from the photographic images. Especially, the older studies were unsatisfactory, arising from the inadequate optical and photographic techniques. In a later analysis an empirical procedure was described (21) which defined a function, S, which determines the drop shape as:

$$S = d_e/d_s \quad (6)$$

where d_e is the maximum (equatorial) diameter of the pendant drop, and d_s is the diameter of the drop at a selected plane at a distance d_e from the apex of the drop, Figure 2. As depicted in Figure 1, the distance O-E and OZ are different, which arises from the gravity forces. This observation (21) was described by another quantity in terms of d_e and R_o :

Figure 1: The Profile of a Pendant Drop.

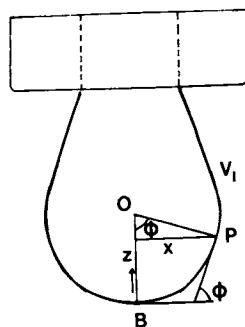
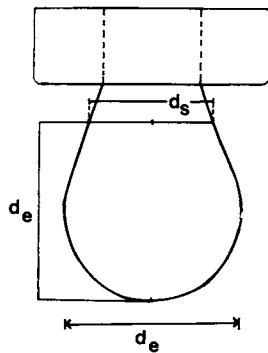


Figure 2: The selected planes of pendant drop.



$$H = -\beta(d_e/R_o)^2 \quad (7)$$

Further, rewriting Equation 7 by eliminating β we get:

$$\gamma_{ij} = \Delta\rho \cdot g \cdot (d_e^2/H) \quad (8)$$

This requires the knowledge of d_e , d_s , $\Delta\rho$, and $(1/H)$. In literature, tables are found which give $(1/H)$ as a function of S (19). However, for general accuracy (less than 10 %), the following relationship is found to be satisfactory (22):

$$(1/H) = 0.31270 (S)^{-2.6444} \quad (9)$$

Experimental and Methods

All chemicals used were of very high purity grade (>99 %). The quaternary systems were mixed and allowed to reach equilibrium over a week at constant temperature, with occasional stirring. The oil phase (top phase) was placed in the measuring cell of the pendant drop apparatus. The bottom (aqueous) phase was filled in the syringe for the measurement.

In the ternary systems, the aqueous phase was filled in the syringe and the drop was formed, with over 10 minutes interval, in the oil (toluene or n-heptane or the n-alcohols) phase.

$C_{12}H_{25}SO_4Na$ (NaDDS) from B.D.H. or Serva (Germany); Na-deoxycholate (NaDOC) from Sigma; Cetyl trimethylammonium bromide (CTAB) from Schuchardt, were used as supplied by the respective manufacturer (over 99 % purity). Distilled water was used after treatment with the Millipore Q filter.

Apparatus

The apparatus consists of a light source which is placed next to a cell with thermostat. The oil phase is contained in the cell while the aqueous phase is filled in a syringe (with thermostat jacket) with diameters as:

outside, 0.45 or 0.2 mm; inside, 0.2 or 0.10 mm, respectively.

The drop formed is photographed by a suitable camera (Linhof, W.Germany) with a magnification of about 20 times. This magnification is sufficient for the range of γ_{ij} measured, since the diameters were measured by using a suitable microscope (with an accuracy of ± 0.01 mm). The whole setup was mounted on a vibration-free optical bench.

Results

System A: NaDDS + H₂O + n-Butanol + Toluene

The phase diagram of the system NaDDS+H₂O+n-Butanol+Toluene has

been extensively described in the literature (11,12). Further, the interfacial tensions of this system when it separates into two or three phases has been reported, depending on the concentration of the added electrolyte, NaCl, Tables I and II. (12)

Table I. Composition of the system (12)

	weight	mol
Salt water	48 %	2.7 (H ₂ O)
Toluene	46 %	0.5
NaDDS	2 %	0.042
n-Butanol	4 %	0.051
Total	100 g	3.29 mol/100 g mixture

Table II. Number and Composition of the Phases in Equilibrium as a function of salinity (11,12, this study) at 20 °C

2-Phases	3-Phases	2-Phases
Oil rich phase	Oil rich phase	Water in oil microemulsion
Oil in water	Microemulsion (inversion zone)	
Microemulsion	Aqueous Phase	Aqueous phase
0 % NaCl	6	8 10

In this system, in the aqueous phase, the micellar system, NaDDS, on addition of butanol would change in free energy due to mixed micelle formation (i.e. NaDDS+n-Butanol), as we showed in an earlier study (23). The change in free energy is also observed from the fact that both the critical micelle concentration (c.m.c.) and the Krafft point of NaDDS solution change on addition of n-Butanol (23, 24). The addition of electrolyte, NaCl, to this system (11,12, present study) gives rise to the formation of three-phases, when the salinity is between 5.8 % to 7.8 %. On the other hand, the system consists of two-phases from 0 - 5.8 % and 7.8 to 10 % NaCl, at 20 °C (experiments at 25 °C gave the same results; unpublished) Table II.

Further, it is well known that the addition of electrolytes to ionic surfactant aqueous solutions increase the Krafft point (24, 25). This indicates that as one increases the NaCl concentration, the Krafft point is most likely higher than the experimental tem-

perature, 20 °C, in this case. However, the meaning of Krafft point is ambiguous at lower NaCl concentrations where both butanol and some toluene (solubilized in NaDDS micelles) are present in the aqueous phase.

From these observations we will argue that the transition from the three-phase to the two-phase region with increasing NaCl takes place where the Krafft point is most likely higher than the experimental temperature (24).

The interfacial tensions, γ_{om} and γ_{mw} , where oil (top), middle and bottom (water) phases are designated as o, m, and w, respectively, are given in Figure 3. It is seen that the magnitude of γ_{ow} decreases on addition of NaCl all the way down to where the system separates into three-phases, about 5.8 % NaCl (about 1.0 M/L in aqueous phase).

The pendant drop interfacial tensions, γ_{ow} , are given in Figure 3 together with the literature data. It is seen that the two sets of data agree with each other for γ_{ow} to as low as 0.02 mN/m. In the three-phase region, where ultra-low γ_{ij} values have been reported by the spinning drop and other methods, the pendant drop could not provide any useful data when using a syringe of the diameter of 0.2 mm. However, investigations are in progress where much thinner syringes will be used. Theoretically one should not expect any reason why the pendant drop theory should not be valid for very small drops (19). This is the first time in the current literature that pendant drop has been used to investigate the phase behaviour of multicomponent systems. The magnitude of γ_{ow} in the absence of NaCl is 1.3 mN/m, which compares with the value of 1.8 mN/m for n-butanol-H₂O interface. In order to understand the effect of NaCl, we further investigated the interfacial tensions of other systems where n-butanol was absent.

System B: Aqueous Phase: (Surfactant + H₂O with or without n-Butanol)
Oil Phase : Toluene or n-Heptane

The purpose of this series was to determine the variation of γ_{ow} at the aqueous phase (with the addition of NaCl to the surfactant (with or without butanol)), and the oil phase (n-heptane or toluene) interface. The data in Figure 4 (a,b) show clearly that NaDOC gives a higher γ_{ow} in both systems, in comparison with NaDDS. The general effect, *i.e.* decrease in magnitude of γ_{ow} , on addition of NaCl is the same in all the systems.

The addition of 8 % butanol reduces the interfacial tensions by about 2 mN/m in all the systems. The systems show divergent curves as regards the effect of added NaCl in these systems.

In comparison with System A, we thus find that different surfactants would give divergent phase behaviour, due to the dependence of γ_{ow} on surfactant characteristics. Further, the addition of n-butanol gives rise to a lowering of γ_{ow} by about 2 mN/m (Fi-

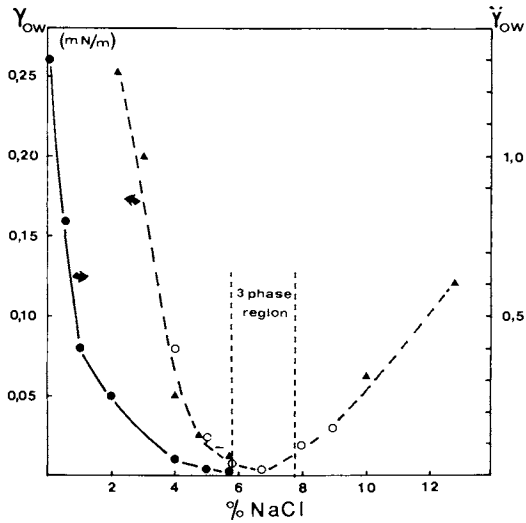


Figure 3: Variation of γ_{ow} for the system:
 NaDDS + H₂O + n-Butanol + Toluene by Pendant Drop (,)
 and other (O; Ref. 12) methods.
 γ_{ow} is the interfacial tension between oil (top) and
 bottom (water) phase.

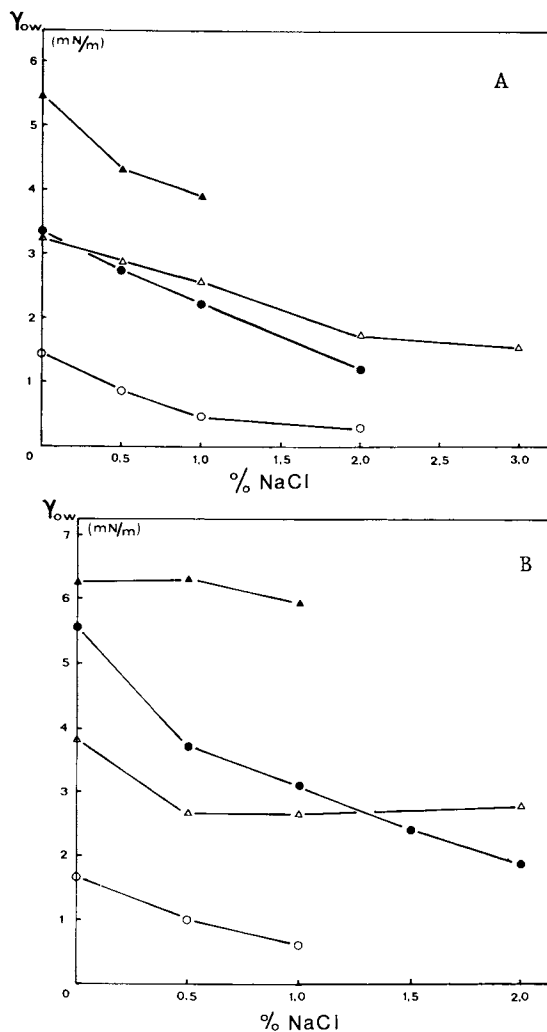


Figure 4. Variation of γ_{ow} of the systems. A, aqueous phase: surfactant + H₂O; oil phase: toluene; with pendant drop method (24 °C). Concentration of detergent = 20 g/L. NaDOC (▲); NaDOC + 8% n-butanol (△); NaDDS (●); NaDDS + 8% n-butanol (○). B, aqueous phase: surfactant + H₂O; oil phase: n-heptane; by pendant drop method (25 °C). Key same as for 4A.

gure 4 (a,b)). This is important difference, since the role of co-surfactant, i.e. n-butanol, is obviously related to this observation.

System C: Aqueous Phase: Surfactant + H₂O

Oil Phase : n-Alcohol

The purpose of this series of measurements was to study the interfacial tension, γ_{wa} between phases:

Aqueous phase: Surfactant + H₂O:Oil phase: n-alcohol (after the phases were allowed to reach equilibrium), as a function of surfactant and number of carbon atoms, n_C , in the alcohol. The different surfactants used were: NaDDS, NaDOC (Na-deoxycholate) and CTAB (cetyl trimethyl ammonium bromide). The data in Figure 5 show that the magnitude of γ_{wa} for CTAB is larger than that of the system with NaDDS or NaDOC. Further, all systems show a "liquid-crystalline" structure formation when n-decanol is the second phase (n-dodecanol gives the same results (Birdi, unpublished)). These results show that the "liquid-crystal" formation is not dependent on the surfactant, but mostly on the characteristics of alcohol. Similar structure formations have been reported by other investigators (25) from spinning drop studies of quaternary systems. This observation is very significant, since in the development of equations under theoretical section, the two-phases were assumed to be liquids. However, if one of the phases is transformed into a liquid-crystalline state, the equations used would need modifications. The same will be true for the application of spinning drop analyses. However, no such modifications have been reported in literature, and this will be pursued as more data becomes available in the authors laboratory.

Discussion

These studies, carried out by measuring interfacial tensions, γ_{ow} , between aqueous and oil phases, by using the pendant drop method, show that this method is very useful for ternary and quaternary systems. In one system (A), e.g. NaDDS + H₂O + n-butanol + Toluene the γ_{ow} data as measured by pendant drop method agreed with the literature data (where another method was used (12)).

The pendant drop method was satisfactory for low γ_{ow} values, i.e. 0.02 mN/m. Typical data are given in Table III. In the systems where ultra-low γ_{ij} values have been reported by other methods (like spinning drop), the pendant drop needs further investigations before it can be applied, since this would require syringes with much smaller diameters (i.e. 10^{-3} mm). As regards the theoretical analyses, we cannot find any concern why pendant drop should have any limitations for such studies. (Same is valid for spinning drop method).

The presence of liquid-crystalline structures (25-28) at aque-

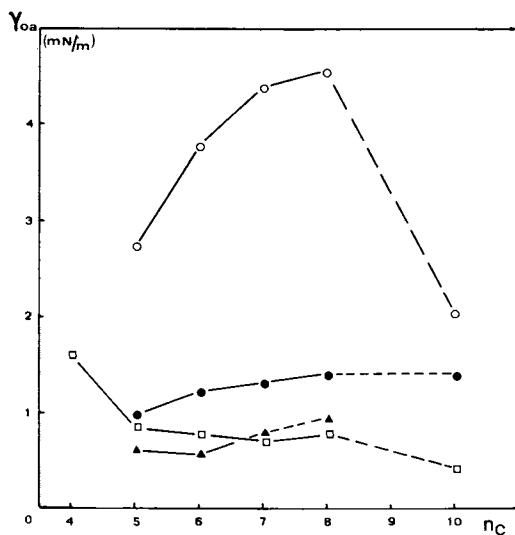


Figure 5: Variation of γ_{0a} of the systems:

Aqueous Phase: Surfactant; Oil Phase: n-alcohol;
CTAB, 20 g/L (○); NaDOC, 20 g/L (●); NaDDS, 10 g/L (□);
20 g/L (▲).

ous-oil (n-alcohol) was observed between (surfactant + H₂O) and n-decanol interfaces. The liquid-crystalline structures were found to be dependent on the magnitude of η_C in n-alcohol, with no dependence on the characteristics of the surfactant. In such systems the interfacial tensions measured are not valid, since the pendant drop theory is derived for liquid_i-liquid_j. The presence of liquid-crystalline phases at the interface would thus require modifications in the applications of pendant drop theory. This we will argue, is also the same if one uses other methods, such as the spinning drop.

In conclusion we will argue that if liquid-crystalline phases are indeed present at oil-aqueous phases, then the magnitudes of γ_{ij} reported by any method must be accepted with caution. This observation needs further analyses, which is the subject of research in the authors laboratory.

Table III. Interfacial Tension (γ_{ij}) Values by Pendant Drop Method: d_e , d_s , (1/H) and $\Delta\rho$ values for different interfaces (this study)

	tip dia- (mm)	factor of mag- nifica- tion	$\Delta\rho$ (kg/m ³)	d_e (mm)	d_s (mm)	1/H	γ_{ij} (mN/m)
NaDDS+H ₂ O+n-Butanol +Toluene (2.33 % NaCl)	0.20 0.45	21.05 20.18	153.0 153.0	0.369 0.555	0.244 0.458	1.666 0.5198	0.238 0.240
NaDDS+H ₂ O+n-Butanol +Toluene (4.76 % NaCl)	0.20	21.25	146.7	0.218	0.207	0.3583	0.0246
10 g/l SDS vs. n-Heptane	0.20 0.45	20.00 21.25	182.6 182.6	0.819 0.675	0.600 0.425	0.7120 1.063	0.854 0.868

Acknowledgments

Erling Stenby like's to thank the Danish Council for Scientific & Industrial Research (STVF) for a research grant. (Licentiatstip.).

Literature Cited

1. Adamson, A. W. "Physical Chemistry of Surfaces"; Interscience Publishers: New York, 3rd ed., 1976.
2. Jaycock, M. J.; Parfitt, G. D. "Chemistry of Interfaces"; John Wiley & Sons; New York, 1981.
3. Chatteraj, D. K.; Birdi, K. S. to be published.
4. Birdi, K. S.; Nikolov, A. J. Phys. Chem. 1979, **83**, 365.
5. Taber, J. J. Soc. Pet. Eng. J. March 1979, **3**; Trans., AIME, Vol. 246.

6. Foster, W. R. J. Pet. Tech. Feb. 1973, 205; Trans., AIME, Vol. 255.
7. Melrose, J. C.; Brandner, C. F. J. Cdn. Pet. Tech. 1974, 54.
8. Vayias, K. S.; Schechter, R. S.; Wade, W. H., in "adsorption at Interfaces"; ACS SYMPOSIUM SERIES No. 8, American Chemical Society: Washington, D.C., 1975, 234.
9. Manning, C. D. MS Thesis, University of Minnesota: Minneapolis, August 1976.
10. Puig, J. E.; Franses, E. I.; Davies, H. T.; Miller, W. G.; Scriven, L. E. Soc. Petr. Eng. J. April 1979, 71.
11. Bellocq, A. M.; Biais, J.; Clin, B.; Lalanne, P.; Lemanceau, B. J. Colloid Interface Sci. 1979, 70, 524.
12. Pouchelon, A.; Meunier, J.; Langevin, D.; Cazabat, A. M. J. Phys. Letts. 1980, 41, 239.
13. Ross, J. "Chemistry and Physics of Interfaces, II"; ACS Publications, Washington, D.C., 1971.
14. Fordham, S. Proc. Roy. Soc. (London) A, 1948, 194.
15. Bashforth, F.; Adams, J. C. "An Attempt to Test the Theories of Capillary Action"; University Press, Cambridge, England, 1983.
16. Stauffer, C. E. J. Phys. Chem. (1965) 1933, 69.
17. Arundel, P. A.; Bagnall, R. D. J. Phys. Chem. 1977, 81, 2077.
18. Bagnall, R. D.; Arundel, P. A. J. Phys. Chem. 1978, 82, 898.
19. Ambwani, D.; Fort, T. Surface Colloid Sci. 1979, 11, 93.
20. Laplace, P. S. "Mecanique Celeste", Supplement to the 10th Book, Duprat, Paris, 1806.
21. Andreas, J. M.; Hansen, E. A.; Tucker, W. B. J. Phys. Chem. 1938, 42, 1001.
22. Stegemeier, G. I.. Ph. D. Thesis, University of Texas, Austin, Texas, 1959.
23. Backlund, S.; Rundt, K.; Birdi, K. S.; Dalsager, S. J. Colloid Interface Sci. 1981, 79, 578.
24. Birdi, K. S. unpublished.
25. Frances, E. I.; Puig, J. E.; Talmon, Y.; Miller, W. G.; Scriven, L. E.; Davis, H. T. J. Phys. Chem. 1980, 84, 1547.
26. Ekwall, P.; Mandell, L.; Foutell, K. Mol. Cryst. Liquid Cryst. 1969, 8, 157.
27. Ekwall, P.; Danielsson, I.; Stenius, P. in "Surface Chemistry and Colloids"; Kerker, M., Ed.; MTP Intern. Rev. Sci., Phys. Chem. Ser. 1. Vol. 7, p.97, Butterworths, London, 1972.
28. Friberg, S., Ed. "Food Emulsions", Marcel Dekker Inc., New York, 1976.

RECEIVED January 10, 1984

Author Index

- Bell, A., 117
Birdi, K. S., 117,329
Bistline, Raymond G., Jr., 209
Chander, S., 311
Chang, David L., 129
Cheng, H. M., 89
Chiu, Y. C., 89
Dahanayake, M., 49
Damaszewski, Leona, 175
Flaim, Tony D., 107
Florence, Alexander T., 189
Friberg, Stig E., 107
Fuerstenau, D. W., 291,311
Gebhardt, J. E., 291
Han, Y. C., 89
Handa, T., 73
Hayakawa, Katumitu, 225
Holland, Paul M., 141
Kuwamura, Tsunehiko, 27
Kwak, Jan C. T., 225
Lin, J., 311
Linfield, Warner M., 209
Mackay, R. A., 175
Malovikova, A., 225
Middleton, R., 269
Nakagaki, M., 73
Parfitt, G. D., 311
Rosano, Henri L., 129
Rosen, Milton J., 49,61
Schwuger, M. J., 3
Somasundaran, P., 269
Stenby, E., 329
Tadros, Th. F., 153
Tucker, Ian G., 189
Viswanathan, K. V., 269
Walters, Kenneth A., 189
Wingrave, James A., 241
Zhu, Bu Yao, 61

Subject Index

- A
- Absorbance measurements, pyridinium ion with CN- in micro-emulsions, 177
- Absorption
 insulin
 discussion, 194-96
 effect of nonionic surfactants, 193t
 soil-water, modification by surfactants, 209-22
- Active charcoal, adsorption of surfactants, alkyl ether sulfates, 14t
- Activity
 at CMC, application, 81
 surfactant, various effects, 73-85
- N-Acyl α -amino acid POE monoesters, long, structural effects on properties, 35-46
- Acyl chain length, effect on binary phase diagram of G type nonionics, 42
- Adhesion, LAS detergency performance, 250f
- Adsorption
 alkyl ether sulfates on graphon, 13f
 effect
 POE chain length, 31t
 polymers, 291-309
- Adsorption--Continued
 hematite
 preadsorbed PAA, 296
 preadsorbed PAM, 302
 hydroxyapatite, 317-24
 interface, effect of inclusion of OE units in alkyl ether sulfates, 14
 rutile, 314-17
 SDS on hematite, 296
 standard free energies, betaine surfactant, 70
 surfactant
 effect of preadsorbed polymers, 291-309
 interactions of nonionic surfactants and biomembranes, 203
 on active charcoal, 14t
 thermodynamic parameters, zwitterionic surfactants, 56-58
 water-air interface, effect of OE units, 11-14
- Adsorption and electrokinetic effects of amino acids, solid-aqueous interface, 311-26
- Adsorption density, equilibrium
 PAA at various pH values, 299f
 PAA on hematite, 304f
 SDS with and without polymer, 298f,303f

Author Index

- Bell, A., 117
Birdi, K. S., 117,329
Bistline, Raymond G., Jr., 209
Chander, S., 311
Chang, David L., 129
Cheng, H. M., 89
Chiu, Y. C., 89
Dahanayake, M., 49
Damaszewski, Leona, 175
Flaim, Tony D., 107
Florence, Alexander T., 189
Friberg, Stig E., 107
Fuerstenau, D. W., 291,311
Gebhardt, J. E., 291
Han, Y. C., 89
Handa, T., 73
Hayakawa, Katumitu, 225
Holland, Paul M., 141
Kuwamura, Tsunehiko, 27
Kwak, Jan C. T., 225
Lin, J., 311
Linfield, Warner M., 209
Mackay, R. A., 175
Malovikova, A., 225
Middleton, R., 269
Nakagaki, M., 73
Parfitt, G. D., 311
Rosano, Henri L., 129
Rosen, Milton J., 49,61
Schwuger, M. J., 3
Somasundaran, P., 269
Stenby, E., 329
Tadros, Th. F., 153
Tucker, Ian G., 189
Viswanathan, K. V., 269
Walters, Kenneth A., 189
Wingrave, James A., 241
Zhu, Bu Yao, 61

Subject Index

- A
- Absorbance measurements, pyridinium ion with CN- in micro-emulsions, 177
- Absorption
- insulin
 - discussion, 194-96
 - effect of nonionic surfactants, 193t
 - soil-water, modification by surfactants, 209-22
- Active charcoal, adsorption of surfactants, alkyl ether sulfates, 14t
- Activity
- at CMC, application, 81
 - surfactant, various effects, 73-85
- N-Acyl α -amino acid POE monoesters, long, structural effects on properties, 35-46
- Acyl chain length, effect on binary phase diagram of G type nonionics, 42
- Adhesion, LAS detergency performance, 250f
- Adsorption
- alkyl ether sulfates on graphon, 13f
 - effect
 - POE chain length, 31t
 - polymers, 291-309
- Adsorption--Continued
- hematite
 - preadsorbed PAA, 296
 - preadsorbed PAM, 302
 - hydroxyapatite, 317-24
- interface, effect of inclusion of OE units in alkyl ether sulfates, 14
- rutile, 314-17
 - SDS on hematite, 296
 - standard free energies, betaine surfactant, 70
- surfactant
- effect of preadsorbed polymers, 291-309
 - interactions of nonionic surfactants and biomembranes, 203
 - on active charcoal, 14t
 - thermodynamic parameters, zwitterionic surfactants, 56-58
 - water-air interface, effect of OE units, 11-14
- Adsorption and electrokinetic effects of amino acids, solid-aqueous interface, 311-26
- Adsorption density, equilibrium
- PAA at various pH values, 299f
 - PAA on hematite, 304f
 - SDS with and without polymer, 298f,303f

- Adsorption effect, amino acids at solid-aqueous interfaces, 311-26
- Adsorption isotherm
alkyl sulfonate, 273f
alkylarylorthoxylene sulfonate, 280f
DDS on alumina, 272
glutamic acid
hydroxyapatite, 322f
lysine, and proline on rutile, 316f
- Adsorption model, disulfonate, 284f
- Aggregate size, surfactant, related to oil solubilization rate, 89-105
- Aggregate unit, microemulsions, effect of packing ratio, 161
- Aggregation, cationic surfactant binding to anionic polyelectrolyte, 238
- Aggregation behavior, fatty dicarboxylic acid hydrotrope, 120
- Aggregation number
micelle
ether sulfates, 11t
fatty dicarboxylic acid hydrotrope, 120,123f
SDS, 98-103
micelles at 25 °C, 98t
- Air-water interface, effect of OE units on adsorption, 11-14
- Alcohol, sulfated polyoxyethylenated, interfacial and performance properties, 3-24
- Alcohol chain length, nature and structure of microemulsions, 166f
- Alkyl addition, aromatic ring, effect on adsorption, 278
- Alkyl benzene sulfonate (LAS), with alkyl ether sulfates, 19-24
- Alkyl *N*-benzyl *N*-methylglycine, synthesis, 50-52
- N*-Alkyl betaines, number of carbon atoms vs. CMC, 75
- Alkyl chain length
effect in interaction of nonionic surfactants and biomembranes, 196f
effect on *n*-alkyl POE monoethers, 28-31
effect on crown ethers, 33
effect on interaction of nonionic surfactants and biomembranes, 202f
effect on thermodynamic parameters of micellization, 29f
- Alkyl ether, POE, interaction with biological membranes, 189-206
- Alkyl ether sulfates, interfacial properties, 3-24
- N*-Alkyl glycines, zwitterionic surfactants, 52
- Alkyl phosphoric acids, synthesis, 74
- n*-Alkyl POE monoethers, adsorption, micelle formation and thermodynamics, 28-31
- Alkyl sulfonate, adsorption isotherm, 273f
- Alkyl trimethylammonium bromide
application of surfactant activity, 83
CMA, 82
methylene free energy of transfer, 76
- Alkyl trimethylammonium chloride, CMA, 82
- Alkylarylorthoxylene sulfonate, adsorption isotherm, 280f
- Alkylpyridinium cations, binding by anionic polysaccharides, 225-38
- N*-Alkyltaurines, zwitterionic surfactants, 52
- Alumina, DDS on, adsorption isotherm, 272
- Amine groups, soil-water absorption, 210
- Amine oxide, LDAO-SDS interactions, 130,133
- Amino acid
adsorption and electrokinetic effects, 311-26
effect of insertion in POE monoesters, 35-36
- Amphiphilic molecule, conformation, 113
- Anionic and cationic surfactant mixing, 138
- Anionic nucleophile, pyridinium ion with CN⁻ in microemulsions, 185f
- Anionic polyelectrolyte, binding of cationic surfactants, 225-38
- Anionic polysaccharide, binding of alkylpyridinium cations, 225-38
- Anionic surfactant
effect of preadsorbed polymers on adsorption, 300
fatty dicarboxylic acid hydrotrope, 127
nature and structure of microemulsions, 169
oil solubilization, 98-103
solubilization of oleic acid, 99f,100f
solubilization of triolein, 102f
surfactant structure and adsorption, 282
various, wool soil removal, 16f
- Anisotropic aggregates, fatty dicarboxylic acid hydrotrope, 126
- Aqueous-solid interfaces, adsorption and electrokinetic effects of amino acids, 311-26

- Aryl addition, effect on surfactant adsorption, 272
- Aryl ethers, POE, interaction with biological membranes, 189-206
- B
- Benzene group, surfactant structure and adsorption, 278
- Betaines
effect of microenvironment, 61-70
synthesis and properties, 49-58
- Binary phase diagram
N-acyl α -amino acid POE
monoesters, 42
C₁₄GE₃-water system, 44f
- Binding, alkylpyridinium cations by anionic polysaccharides, 225-38
- Binding constant, surfactant-polyion binding, 236t
- Binding isotherm, cationic surfactant to anionic polyelectrolyte, 231
- Biological systems, interactions with nonionic surfactants, 189
- Branching
effect on solubilization, 170
effect on surfactant adsorption, 274
- Buffering action, LDAO-SDS interactions, 131
- Bulk phase concentration, betaine surfactant, 68-70
- Bulk properties, alkyl ether sulfates, 17
- C
- Calcium chloride
effect on surface properties of betaine surfactant, 65
LAS detergency performance, 265
- Calorimetry, isoperibol, nonideal mixed micelles, 145
- Carbon atoms, number
vs. CMC, ionic and nonionic surfactants, 75
vs. CMC and CMA, ionic and nonionic surfactants, 78t
effect on LDAO-SDS interactions, 139
effect on nature and structure of microemulsions, 163
vs. log CMA, ionic and nonionic surfactants, 82
- Carbon chain length, effect on LAS detergency performance, 257
- Carboxylic group, hydrotropic action, 114
- Cation
alkylpyridinium, binding by anionic polysaccharides, 225-38
betaine surfactant, 62,68
- Cationic detergent, fatty dicarboxylic acid hydrotrope, 127
- Cationic surfactant
binding to anionic polyelectrolytes, 225-38
effect on soil-water absorption, 210,218
mixing with anionic, 138
retention on soil, 220
- Cetyltrimethylammonium bromide (CTAB)
fatty dicarboxylic acid hydrotrope, 118
reaction of pyridinium ion with CN⁻, 177
- Chain length
alcohol, nature and structure of microemulsions, 166f
alkyl, effect in crown ethers, 33
cationic surfactant binding to anionic polyelectrolyte, 228,237
effect on n-alkyl POE monoethers, 28-31
effect on LDAO-SDS interactions, 139
effect on nature and structure of microemulsions, 162-70
effect on surfactant adsorption, 274
hydrocarbon, interactions of non-ionic surfactants and biomembranes, 200
hydrophilic, interactions of POE ethers with biomembranes, 190,191f
hydrophobic, effect on cationic surfactant binding to anionic polyelectrolyte, 235
nonionic surfactants and biomembranes, 196f
- Charcoal, active, adsorption of surfactants, 14t
- Charge density parameter, cationic surfactant binding to anionic polyelectrolyte, 231
- Charge neutralization, cationic surfactant binding to anionic polyelectrolyte, 238
- Charge production, microemulsions, 168
- Charge separation, nonideal mixed micelles, 146
- Chlorpromazine, interactions with biomembranes, 195
- Clay, surfactant effect on soil-water absorption, 219
- Cleaning action, alkyl ether sulfates, 14-17
- Cloth, LAS detergency performance, 242
- Cloud point
effect of α -amino acid insertion in POE monoesters, 35-46
effect of hydrophile structure, 34f

Cloud point--Continued

- effect of hydrophobe structure, 31-33
- effect of salt on N-alkyl monoaza crown ethers, 36f
- vs. OE units in nonionics, 40f
- Coadsorption of nonionics, surfactant structure and adsorption, 286
- Cohesive energy densities (CED), LAS detergency performance, 259
- Complexing agents, and alkyl ether sulfates, 15
- Concentration vs. surface tension, zwitterionic surfactants, 53,54f,63f,66f,67f
- Conductivity
 - nature and structure of microemulsions, 165-68
 - water-volume fraction curves, 166f,167f
- Conformation, dicarboxylic acid, hydrotropic action, 113
- Contact angle
 - effect of preadsorbed polymers on adsorption, 294
 - fiber-soil-bath system, 246
 - hematite
 - effect of PAA on SDS adsorption, 307f,308f
 - effect of preadsorbed polymers on adsorption, 305
 - surfactant effect on soil-water absorption, 215,222f
- Contiguous fibers and soil drop, cross-sectional view, 245f
- Corn germination, surfactant effect on soil-water absorption, 112
- Cosurfactant
 - adsorption contribution, microemulsions, 159
 - effect of nature and structure of microemulsions, 171
 - structure and chain length effect on microemulsions, 162-70
- Counter ion
 - association with micelle, 81
 - CMC, ionic and nonionic surfactants, 80 and CMC
 - log vs. log CMC, 83
- Critical micelle activity (CMA)
 - effect of methylene group, 74
 - vs. number of carbon atoms, ionic and nonionic surfactants, 78t
- Critical micelle concentration (CMC)
 - cationic surfactant binding to anionic polyelectrolyte, 228
 - effect of α -amino acid insertion, 37
 - effect of electrolytes, 64
 - effect of hydrophobe structure, 31-33

Critical micelle concentration (CMC)--

- Continued
- effect of methylene group, 74
- effect of OE units, alkyl ether sulfates, 8,14
- effect of pH, betaine surfactant, 64
- fatty dicarboxylic acid hydrotrope, 119
- interactions of nonionic surfactants and biomembranes, 200
- interfacial tension by pendant drop method, 334
- nonideal mixed micelles, 143,145,148f
- vs. number of carbon atoms, 78t
- phase equilibria, hydrotropic action, 111
- related to counter ion concentration, 80
- SDS, 93f
- zwitterionic surfactants, 55t
- Crown ethers, higher alkyl, synthesis and application, 33-35
- Cyanide, reaction with pyridinium ion in o/w microemulsions, 175-85
- Cyclization, one-step, oligoethylene glycol, 33

D

- Debye's equation, oil solubilization rate related to aggregate size, 91
- Debye-Huckel equation, ionic and nonionic surfactants, 82
- n-Decane, solubilization in nonionic surfactant, 90,97f
- Deformable interfaces, nature and structure of microemulsions, 169
- Degree of binding, cationic surfactant binding to anionic polyelectrolyte, 231
- Degree of dissociation, pyridinium ion with CN⁻ in microemulsions, 182t
- Dehydration, POE chain, alkyl ether sulfates, 8
- Delipidation, nonionic surfactants and biomembranes, 205
- Density, equilibrium adsorption
 - PAA at various pH values, 299f
 - PAA on hematite, 304f
 - SDS with and without polymer, 298f,303f
- De-oiling, effect on surfactant adsorption, 278
- Depression, Krafft point, alkyl ether sulfates, 6
- Desolvation, endothermic, zwitterionic surfactants, 55
- Destabilization, hydrotropic action, 114

- Detergency
 effect of OE units, 103
 LAS homologs, 241-68
- Detergent
 incorporation by fatty dicarboxylic acid hydrotrope, 120
 and water, with dicarboxylic acid, 112f
- Dicarboxylic acid, hydrotropic function, 107-14
- Dicarboxylic acid hydrotrope fatty aqueous solution
 properties, 117-27
 mixed-disc model, 126
- Diethylenetriamine (DETA)
 fatty-acid derivatives, 212
 reaction products
 infiltration properties, 217t
 physical properties, 216t
 soil-water absorption, 210,212
- Differential scanning calorimetry (DSC), *N*-acyl α -amino acid POE monoesters, 42
- Dishwashing
 alkyl ether sulfates, 23f
 LAS-alkyl ether sulfate mixtures, 21
- Disodium alkyl phosphate, CMA, 82
- Dissociation
 counterions of micelles, alkyl ether sulfates, 9
 dodecyl ether sulfate micelles, 10f
 pyridinium ion with CN⁻ in microemulsions, 182t
 surfactant molecules in microemulsions, 168
- Disulfonate
 adsorption model, 284f
 effect on surfactant adsorption, 282
- Docosyldimethylamine oxide, monolayer properties, 130
- Dodecanol ethoxylate, oil solubilization rate related to aggregate size, 90
- Dodecyl chain, effect on interactions of nonionic surfactants and biomembranes, 195
- Dodecyl ether sulfates, adsorption at the water-air interface, 11
- n*-Dodecyl ether sulfates, Krafft points, 7t
- Dodecyl ether sulfates, micelle dissociation, 10f
- Dodecyl polyglycol ethers, adsorption at air-water interface, 12
- Dodecylsulfonate (DDS) on alumina, adsorption isotherm, 272
- Double layer
 nature and structure of microemulsions, 159
- Double layer--Continued
 pyridinium ion with CN⁻ in microemulsions, 185f
- E
- Effective surface potential, pyridinium ion with CN⁻ in microemulsions, 179,182t
- Electrical conductivity, nature and structure of microemulsions, 162
- Electrical double layer, nature and structure of microemulsions, 160
- Electrical resistance, LDAO-SDS interactions, 131
- Electrokinetic and adsorption effects of amino acids, solid-aqueous interface, 311-26
- Electrokinetic behavior
 amino acids at solid-aqueous interfaces, 311-26
 hydroxyapatite, 317-24
 rutile, 314-17
- Electrokinetics, effect of preadsorbed polymers on adsorption, 294
- Electrolyte
 addition to ionic and nonionic surfactants, 81
 effect on alkyl ether sulfates, 18
 effect on betaine surfactant, 65-68
 surface tension vs. log concentration, zwitterionic surfactants, 66f,67f
- Electrophoretic mobility, effect of preadsorbed polymers on adsorption, 294-321
- Electrostatic interaction
 adsorption of amino acids, 317
 betaine surfactant, 68
 characteristic regions of adsorption, 272
 effect of preadsorbed polymers on adsorption, 300
 free energy of micelle formation, 79
- Endothermic desolvation, zwitterionic surfactants, 55
- Enthalpy of micellization, zwitterionic surfactants, 52
- Enthalpy of mixing, excess, nonideal mixed micelles, 143
- Entropy contribution, nature and structure of microemulsions, 159
- Entropy of micellization, zwitterionic surfactants, 52
- Entropy of mixing, nonideal mixed micelles, 149
- Equilibrium, isotropic liquid-liquid crystalline, 108-12
- Equilibrium adsorption density
 PAA at various pH values, 299f

American Chemical
 Society Library

1155 16th St. N. W.

Equilibrium adsorption density--

Continued

- PAA on hematite, 304f
- SDS with and without polymer, 298f,303f
- Ether, POE alkyl and aryl, interaction with biological membranes, 189-206
- Ether groups, reduction of Krafft point, 6
- Ether linkage, effect on surfactant adsorption, 282
- Ethoxylated alcohol, effect on surfactant adsorption, 287f,288f
- Ethoxylated surfactant, discussion, phase diagrams, 156
- Ethoxylation, nonideal mixed micelles, 146
- Ethylene oxide
 - effect on interactions of nonionic surfactants and biomembranes, 195
 - effect on surfactant adsorption, 282
- Excess enthalpy of mixing, nonideal mixed micelles, 143
- Excess entropy of mixing, nonideal mixed micelles, 149

F

- Fabric-soil morphology, LAS detergency performance, 242-48
- Fatty acid, soil-water absorption, 210
- Fatty acid DETA derivatives, soil-water absorption, 212
- Fatty dicarboxylic acid hydrotrope aqueous solution properties, 117-27
- mixed-disc model, 126
- Fiber-soil geometry, cross-sectional view, LAS detergency performance, 247f
- Fiber-water-soil contact angle, dependence of detergency, 247f
- Film bending, schematic representation, 158f
- Film pressure, LAS detergency performance, 253
- Flexible interfaces, nature and structure of microemulsions, 165,169
- Fluid characteristics, non-Newtonian, LDAO-SDS interactions, 133
- Fluidity, biomembrane, surfactants, 195
- Foam decay, LAS-alkyl ether sulfate mixtures, 21
- Foam volume, various detergent formulations, 15t
- Free energy of formation
 - micelle, ionic and nonionic surfactants, 73-85
 - microemulsions, 157

- Free energy of microemulsion, Overbeek theory, 159
- Free energy of mixing, binary mixture, 143
- Free energy of transfer, methylene group, ionic and nonionic surfactants, 76

G

- Gel prevention, hydrotropic action, 108-11
- Geometric model, LAS detergency performance, 246
- Geometry
 - microemulsions, 161,163
 - surfactant, effect on microemulsion formation, 170
- Germination, seed, effect of soil hydrophobe, 221,222f
- Girifalco-Good equation, LAS detergency performance, 252f,256
- Glass surface, wettability, LDAO-SDS interactions, 131
- Glutamic acid
 - and hydroxyapatite, 322-25
 - and rutile, 316-19
- Glycerine
 - effect on hydrophobicity, 213,218
 - soil-water absorption, 222f
- Glycerol trioleate, oil solubilization rate related to aggregate size, 90
- Graphon, adsorption of alkyl ether sulfates, 13f
- Group additive concept, LAS detergency performance, 259
- Guest molecules and host molecules, interaction, hydrotropic action, 113

H

- Halides, alkylpyridinium, surface tension, 229f
- Hardness, effect on LAS detergency performance, 254t
- Head group
 - ionic and nonionic surfactants, 81
 - surfactant, effect on cationic surfactant binding to anionic polyelectrolyte, 235
 - various, zwitterionic surfactants, 58t
- Heats of micellar mixing, nonideal mixed micelles, 145-47
- Hematite, effect of preadsorbed polymers on surfactant adsorption, 291-309
- Hemimicellization, characteristic regions of adsorption, 272

- Hemolysis, interactions of nonionic surfactants and biomembranes, 195,193t
- Hexadecylbenzene sulfonate, effect on surfactant adsorption, 274
- Hexaethyleneglycol alkyl ethers, number of carbon atoms vs. CMC, 75
- Hexylamine and water, isotropic liquid phase, 110f
- Homogeneous isotropic region, effect on microemulsion formation, 170
- Host molecules and guest molecules, interaction, hydrotropic action, 113
- Hydrated solid state, surfactant, and Krafft point, 4
- Hydration sheath, ionic and nonionic surfactants, 81
- Hydrocarbon, three phases, LAS detergency performance, 257
- Hydrocarbon chain length and Krafft point, 6
nonionic surfactants and biomembranes, 200
- Hydrochloric acid, viscosity variation, LDAO-SDS interactions, 131
- Hydrogen bonding
ionic and nonionic surfactants, 81
LDAO-SDS interactions, 133,138
- Hydrophile-lipophile balance (HLB), nonionic surfactants and biomembranes, 192,205
- Hydrophilic chain length
interactions of POE ethers with biomembranes, 190,191f
nonionic surfactants and biomembranes, 196f,202f
- Hydrophilic compounds, effect on soil-water absorption, 218
- Hydrophilic domain
betaine surfactant, 64
effect of preadsorbed polymers on adsorption, 305
effect on nature and structure of microemulsions, 161
interactions of nonionic surfactants and biomembranes, 200
LAS detergency performance, 258
microemulsions, 169,170
- Hydrophilic structure
effect on cloud point, 34f
zwitterionic surfactants, 57
- Hydrophobic chain length, effect on cationic surfactant binding to anionic polyelectrolyte, 235
- Hydrophobic domain
betaine surfactant, 70
effect on nature and structure of microemulsions, 161
- Hydrophobic domain--Continued
microemulsions, 169,170
- Hydrophobic interaction, free energy of micelle formation, 80
- Hydrophobic structure
discussion, POE nonionic surfactants, 31
effect on cloud point, 31-33
effect on soil-water absorption, 218
soil, effect on plant growth, 221,222f
- Hydrophobicity
diminished, alkyl ether sulfates, 8
effect of glycerine on soil-water absorption, 213,218
effect on nature and structure of microemulsions, 161
effect on surfactant adsorption, 274
ether sulfates, 9
surfactant structure and adsorption, 278
- Hydrotrope
definition, 126
fatty dicarboxylic acid, aqueous solution properties, 117-27
- Hydroxy group, LDAO, 138
- Hydroxyapatite, adsorption and electrokinetic behavior, 317-24
- I
- Infiltration
DETA reaction products, 217
discussion, soil-water absorption, 213
- Insulin absorption, nonionic surfactants and biomembranes, 193-96
- Interaction
electrostatic, betaine surfactant, 68
LDAO-SDS, discussion, 133-38
low density lipoprotein, model membranes, 205
surfactant-polymer, effect of preadsorbed polymers, 295
- Interaction parameter
binary surfactant mixtures, 144t
Girifalco-Good, LAS detergency performance, 248
- Interface
flexible, nature and structure of microemulsions, 169
solid-aqueous, adsorption and electrokinetic effects of amino acids, 311-26
- Interfacial free energy, microemulsion thermodynamic theory, 157
- Interfacial parameter, LAS detergency performance, 253,257

- Interfacial tension
 alkyl ether sulfates in mixtures, 19-24
 correlated to oil solubilization rate, 91
 effect on microemulsion formation, 170
 LAS detergency performance, 248,265
 LAS-SDS mixtures, 22f
 microemulsion mixed-film theory, 155
 pendant drop method, 329-40
 related to surfactant aggregate size, 89-105
 role of cosurfactant, 171
- Interlayer spacing
 effect of hydrotropic action, 114f
 influence of sodium oleate, 114
- Ion exchange (IE) model
 pseudophase, micellar systems, 175
 pyridinium ion with CN⁻ in microemulsions, 183f
- Ionic strength
 effect on cationic surfactant binding to anionic polyelectrolyte, 231
 effect on pyridinium ion with CN⁻ in microemulsions, 178
- Ionic surfactants, effect of structure, 73-85
- Isotherm, adsorption
 alkyl sulfonate, 273f
 alkylarylorthoxylene sulfonate, 280f
 DDS on alumina, 272
 dodecylsulfonate (DDS) on alumina, 272
 hydroxyapatite, 322f
- Isotropic liquid-liquid crystalline equilibrium, 108-12
- Isotropic liquid phase, water and hexylamine, 110f
- Isotropic region, effect on microemulsion formation, 170
- K
- Kinetics, pyridinium ion with CN⁻ in microemulsions, 177,178
- Krafft point
 addition of electrolytes, 334
 alkyl ether sulfates, 4-7
 effect of α -amino acid insertion in POE monoesters, 35-46
- L
- Lamellar liquid crystalline matrix, fatty dicarboxylic acid hydrotrope, 126
- Lamellar neat phase, alkyl ether sulfates, 17
- Lamellar structure, inhibition by hydrotropic action, 109f
- Lateral association, characteristic regions of adsorption, 272
- Lateral stress gradient theory, microemulsion, 156
- Lauryl chain, effect on interactions of nonionic surfactants and biomembranes, 203
- Law of mass action, ionic and nonionic surfactants, 75
- Light scattering technique interpretation, 91-94
 oil solubilization rate, 90
- Light transmittance, LDAO-SDS interactions, 131
- Linear fatty alcohol ethoxylate, fatty dicarboxylic acid hydrotrope, 118
- Linear sodium alkylbenzene sulfonate (LAS) homologs, detergency performance, 241-68
- Lipid bilayers, interactions of non-ionic surfactants and biomembranes, 203
- Lipophilicity
 effect on biological activity, 190
 effect on LAS detergency performance, 258
 membrane, and surfactants, 192
 surfactant, interactions with biomembrane, 195
- Lipoprotein interactions, low density, model membranes, 205
- Liquid crystalline-isotropic liquid equilibrium, 108-12
- Liquid crystalline phase
 N-acyl α -amino acid POE monoesters, 42
 LDAO-SDS interactions, 139
- Liquid crystalline structures, interfacial tension by pendant drop method, 338
- Long chain dimethylamine oxide (LDAO), interaction with SDS, 129-38
- Low density lipoprotein interactions, model membranes, 205
- Lysine
 and hydroxyapatite, 323f,326f
 and rutile, 316f,318f,320f
- M
- Magnesium chloride, LAS detergency performance, 265
- Mass action law, ionic micelle formation, 79
- Melting point
 alkyl ether sulfates, 7t
 effect of α -amino acid insertion in POE monoesters, 35-46

- Melting point--Continued
 interaction of nonionic surfactants and biomembranes, 202f
- Membrane, interactions with nonionic surfactants, 189-206
- Membrane osmometry, fatty dicarboxylic acid hydrotrope, 118,120
- Mesomorphous phases
 alkyl ether sulfates, 17
 fatty dicarboxylic acid hydrotrope, 126
- N-Methylbenzylamine, and betaine surfactant, 62
- Methylene group, effect on CMC, 74
- Micelle
 aggregation number, fatty dicarboxylic acid hydrotrope, 120,123f
 aggregation numbers, ether sulfates, 11t
 aqueous CTAB, reaction of pyridinium ion with CN⁻, 177
 dodecyl ether sulfate, dissociation, 10f
 effect of chain length variation in n-alkyl POE monoethers, 28-31
 effect of OE units in alkyl ether sulfates, 8
 formation, discussion, 74-76
 heats of mixing, nonideal mixed micelles, 147f
 monomer equilibrium, ionic and nonionic surfactants, 81
 properties related to solubilization rate, 89-105
 protonation, LDAO titration, 137
 SDS, aggregation number, 98t
 size related to oil solubilization rate, 91
 surfactant, and Kraft point, 4
- Micelle system
 microemulsion theory, 156
 pseudophase IE model, 175
- Micellization
 characteristic regions of adsorption, 272
 effect of pH, betaine surfactant, 64
 effect of POE chain length, 31t
 mixed, effect of surfactant structure on thermodynamics, 141-50
 nonionic surfactants, thermodynamic data, 38t
 thermodynamic parameters, 52-58
 as function of alkyl chain length, 29f
 zwitterionic surfactants, 58t
- Microemulsion
 formation theories, 153-71
 influence of surfactant structure and chain length, 153-71
- Microemulsion
 mixed film theory, 155
 oil-water, pyridinium ion with cyanide, 175
- Mineral oil soil, LAS detergency performance, 243f
- Mixing
 excess enthalpy, nonideal mixed micelles, 143
 excess entropy, nonideal mixed micelles, 149
 excess free energy, binary mixture, 143
- Model
 disulfonate adsorption, 284f
 microemulsion, 155
 pseudo-phase separation, nonideal mixed micellization, 142
 pseudophase IE, micellar systems, discussion, 175
 pyridinium ion with CN⁻ in microemulsions, 179
- Model membranes, surfactant in low density lipoprotein interactions, 205
- Molar absorptivities, betaines and sulfobetaines, 51
- Molar-attraction constant
 cohesive energy density determination, 264t
 LAS detergency performance, 259
- Molecular mechanism, hydrotropic action, 113
- Molecular structure, effect on LAS detergency performance, 258-63
- Molecular weight, effect on solubilization, 170
- Monoesters, long N-acyl α -amino acid POE, structural effects on properties, 35-46
- Monolayer properties
 docosyldimethylamine oxide, 130
 LDAO, 138
- Monomer contributions, nonideal mixed micelles, 147f
- Monomer-micelle equilibrium, ionic and nonionic surfactants, 81
- Monomer protonation, titration of LDAO, 137
- Monomeric equilibrium constant, LDAO-SDS interactions, 130
- Monosoap
 dicarboxylic acid, conformation at interface, 115f
 fatty dicarboxylic acid hydrotrope, 127
- N
- Nonideal behavior
 microemulsions, 159

Nonideal behavior--Continued

- sulfate surfactants, 146
- Nonionic surfactant
 - discussion, phase diagrams, 156
 - effect of structure, 73-85
 - fatty dicarboxylic acid
 - hydrotrope, 127
 - interactions with membranes and biological systems, 189-206
 - micellization, thermodynamic data, 38t
 - microemulsion formation, 170
 - POE, structural effects on properties, 27-46
 - solubilization
 - n*-decane, 97f
 - oil, 94-98
 - oleic acid, 95f
 - triolein, 96f
 - surfactant structure and adsorption, 282,286
- Non-Newtonian fluid characteristics, LDAO-SDS interactions, 133
- Nonyl phenyl ethers, interactions with biomembranes, 195
- Nuclear magnetic resonance (NMR), nature and structure of microemulsions, 162,168
- Nucleophile concentration, pyridinium ion with CN⁻ in microemulsions, 184

O

- Octyl phenyl ethers, interactions with biomembranes, 195
- Oil
 - effect on surfactant adsorption, 278
 - in microemulsions, effect on solubilization, 170
- Oil droplet, on substrate in water, 20f
- Oil solubilization rate, related to surfactant aggregate size, 89-105
- Oil-water microemulsion
 - discussion, 161
 - mixed film theory, 155
 - pyridinium ion with cyanide, 175-85
- Oily soil removal
 - alkyl ether sulfate mixtures, 19-24
 - hydrotropic action, 113
- Oleic acid
 - effect on soil-water absorption, 218
 - solubilization in anionic surfactant, 99f,100f
 - solubilization in nonionic surfactant, 95f
- Oligoethylene glycol
 - esters and various *N*-acylo-*α*-amino acids, 35-46

Oligoethylene glycol--Continued

- one-step cyclization, 33
- Olive oil-water, interfacial tension for LAS-SDS mixtures, 22f
- Organic ammonium ions, soil-water absorption, 210
- Oxyalkylene units, Krafft-point reduction, 6
- Oxyethylene (OE) unit
 - alkyl ether sulfates, 8-14
 - vs. cloud point, 40f
 - effect
 - alkyl ether sulfates, 17
 - n*-alkyl POE monoethers, 30
 - bulk properties, 17
 - crown ethers, 33
 - detergency, 103
 - interaction of nonionic surfactants and biomembranes, 202f
 - interfacial properties, 21
 - LAS-alkyl ether sulfate mixtures, 21
 - oil solubilization rate related to aggregate size, 94
 - fatty dicarboxylic acid
 - hydrotrope, 118
 - nature and structure of microemulsions, 171

P

- Packing ratio, microemulsions, various effects, 161
- Paraquat transport, through gastric mucosa, 191f
- Pectate, cationic surfactant binding to anionic polyelectrolyte, 234f,235t
- Pectinate, cationic surfactant binding to anionic polyelectrolyte, 234f,235t
- Pendant drop method, interfacial tension of aqueous surfactant, 329-40
- pH, effect
 - adsorption of amino acids, 318f,323f
 - betaine surfactant, 62-64
 - LDAO-SDS interactions, 130,133
 - nature and structure of microemulsions, 161
 - surface tension vs. log concentration, zwitterionic surfactants, 63f
- Phase, LAS detergency performance, 257
- Phase diagram
 - LDAO-SDS interactions systems, 123f,124f,125f
 - microemulsions, 164f
- Phase distribution, pyridinium ion with CN⁻ in microemulsions, 178-82

- Phase region, fatty dicarboxylic acid hydrotrope, 119
- Physicochemical properties, HLB as index, 192
- Plant growth, effect of soil hydrophobe, 214,221
- Polarizing microscopy, *N*-acyl α -amino acid POE monoesters, 42
- Polarographic data, pyridinium ion with CN^- in microemulsions, 178
- Polyacrylic acid (PAA)
chemical structure, 293f
effect of polymers on adsorption, 291-309
- Polyacrylic amide (PAM), effect of polymers on adsorption, 291-309
- Polyelectrolyte, anionic, binding of cationic surfactants, 225-38
- Polyglycol, hydration, alkyl ether sulfates, 11
- Polymer, preadsorbed, effect on surfactant adsorption, 291-309
- Polymer structure, cationic surfactant binding to anionic polyelectrolyte, 229f,235
- Polymer-surfactant interactions, effect of preadsorbed polymers on adsorption, 295
- Polyoxyethylenated alcohols, sulfated, interfacial and performance properties, 3-24
- Polyoxyethylene (POE)
alkyl and aryl ethers, interaction with biological membranes, 189-206
alkyl ether sulfates, partial dehydration, 8
nonionic surfactants, structural effects on properties, 27-46
- Polysaccharide, anionic, binding of alkylpyridinium cations, 225-38
- Polyuronide, cationic surfactant binding to anionic polyelectrolyte, 234f
- Potentiometry, cationic surfactant binding to anionic polyelectrolyte, 228
- Preadsorbed polymer, effect on surfactant adsorption, 291-309
- Precipitation, LDAO-SDS interactions, 133
- Pressure difference, interfacial tension by pendant drop method, 330
- Profile, pendant drop, 332f
- Proline, and rutile, 316f,318f,321f
- Protonation, LDAO-SDS interactions, 133,137
- Pseudophase ion exchange (IE) model, micellar systems, discussion, 175
- Pseudophase separation model, nonideal mixed micellization, 142
- Pyridinium ion, reaction with cyanide in o/w microemulsions, 175-85
- Q
- Quasi-thermodynamic analysis, LAS detergency performance, 261t
- Quaternary system
discussion, interfacial tension by pendant drop method, 333-35
interfacial tension by pendant drop method, 338
- R
- Rate constant, dependence, pyridinium ion with CN^- in microemulsions, 181f
- Reaction models, pyridinium ion with CN^- in microemulsions, 179
- Relative viscosity, LDAO-SDS interactions, 134f-136f
- Repellency, soil water, modification by surfactants, 209-22
- Retention on soil, cationic surfactant, 220
- Rollup mechanism, LAS detergency performance, 242
- Rutile, adsorption and electrokinetic behavior, 314-17
- S
- Salt
effect on cationic surfactant binding to anionic polyelectrolyte, 235
effect on cloud point in *N*-alkyl monoaza crown ethers, 36f
- Salt micelles, fatty dicarboxylic acid hydrotrope, 120
- Sandy soil, surfactant effect on soil-water absorption, 213-19
- Scanning electron micrograph (SEM), fabric, LAS detergency performance, 244f
- Secobarbital, absorption in goldfish, 191f
- Second-order reaction, pyridinium ion with CN^- in microemulsions, 178
- Seed germination, effect of soil hydrophobe, 221
- Self-diffusion coefficient, nature and structure of microemulsions, 168
- Separation model, pseudo-phase, non-ideal mixed micellization, 142
- Size, surfactant aggregate, related to oil solubilization rate, 89-105

- Sodium alkyl carboxylate
CMA, 82
methylene free energy of transfer, 76
- Sodium alkyl sulfate
CMA, 82
methylene free energy of transfer, 76
- Sodium alkylbenzene sulfonate, linear (LAS), detergency performance, 241-68
- Sodium chloride, effect on cationic surfactant binding to anionic polyelectrolyte, 231,4
- Sodium chloride, effect on Krafft point, 334
- Sodium chloride, effect on oil solubilization rate, 90
- Sodium chloride, effect on SDS aggregation number, 98-103
- Sodium chloride, effect on surface properties of betaine surfactant, 65
- Sodium chloride, effect on viscosity of surfactants, 18
- Sodium dodecyl sulfate (SDS)
CMA, 83
CMC, 93f
effect of preadsorbed polymers on adsorption, 291-309
interaction with LDAO, 129-38
micelle aggregation number, 98t
oil solubilization rate related to aggregate size, 90,92
properties, 92t
solubility, 5f
- Sodium dodecylbenzenesulfonate (SDBS), fatty dicarboxylic acid hydrotrope, 118
- Sodium oleate, influence on interlayer spacing, 114
- Sodium perfluorooctanoate, application of surfactant activity, 83
- Sodium tetradecyl diglycol ether sulfate, surface tension, 16f
- Sodium triphosphate, complexing, deterioration of soil removal, 15
- Soil, retention of cationic surfactant, 220
- Soil column test, surfactant effect on soil-water absorption, 213,218
- Soil drop between contiguous fibers, cross-sectional view, 245f
- Soil-fabric morphology, LAS detergency performance, 242-48
- Soil-fiber-water contact angle, dependence of detergency, 247f
- Soil hydrophobe, effect on plant growth, 221,222f
- Soil infiltration test, soil-water absorption, 213
- Soil removal
effect of Na triphosphate complexing, 15
wool, 16f
- Soil-water absorption, modification by surfactants, 209-22
- Solid-aqueous interface, adsorption and electrokinetic effects of amino acids, 311-326
- Solid state electrodes, cationic surfactant binding to anionic polyelectrolyte, 225-38
- Solubility
alkyl ether sulfates, 7t
sodium dodecyl sulfate, 5f
temperature dependence, 4
- Solubilization
effect of surfactant structure, 170
membrane, interactions with surfactants, 205
nature and structure of microemulsions, 156
schematic representation, 158f
- Solubilization rate, relationship to micellar properties, 89-105
- Solution properties, aqueous, fatty dicarboxylic acid hydrotrope, 117-27
- Soybean germination, surfactant effect on soil-water absorption, 214,222f
- Stability, microemulsion theories, 153-71
- Stability constants, amino acids, 313t
- Stern layer, pyridinium ion with CN⁻ in microemulsions, 184,185f
- Stokes radius, interactions of non-ionic surfactants and biomembranes, 205
- Straight-chain surfactants, effect of hydrotropic action, 109f
- Structure
effect on ionic and nonionic surfactants, 73-85
LDAO-SDS interactions, 121f
molecular effect on LAS detergency performance, 258-63
surfactant
effect on nature and structure of microemulsions, 162-70
effects on thermodynamics of mixed micellization, 141-50
- Structure-activity relationship, interaction of nonionic surfactants and biomembranes, 154,190
- Sulfated polyoxyethylenated alcohols, interfacial and performance properties, 3-24
- Sulfobetaines, synthesis and properties, 49-58
- Surface-active agents, fatty dicarboxylic acid hydrotrope, 119

- Surface-active crown ethers,
discussion, 33-35
- Surface activity, effect of OE units
in alkyl ether sulfates, 14
- Surface adsorption sites, effect of
preadsorbed polymers on
adsorption, 300
- Surface charge, hematite, effect of
preadsorbed polymers on
adsorption, 302
- Surface phase concentration, betaine
surfactant, 68-70
- Surface potential, effective,
pyridinium ion with CN⁻ in
microemulsions, 179, 182t
- Surface pressure vs. surfactant
concentration, biomembranes, 202f
- Surface properties
effect of chain length variation in
n-alkyl POE monoethers, 28-31
zwitterionic
surfactants, 49-58, 61-70
- Surface tension
betaines and sulfobetaines, 51
vs. concentration and zwitterionic
surfactants, 53, 54f, 63f, 66f, 67f
effect
hydrophobe structure in POE non-
ionic surfactants, 31-33
OE units in alkyl ether
sulfates, 8
preadsorbed polymers on
adsorption, 294
- LAS detergency performance, 265
- LDAO-SDS
interactions, 131, 133, 134f-136f
pyridinium surfactants, 228
SDS with and without polymer, 297f
sodium tetradecyl diglycol ether
sulfate, 16f
- Surface wettability, effect of pread-
sorbed polymers on adsorption, 305
- Surfactant
adsorption contribution,
microemulsions, 159
adsorption on active charcoal, alkyl
ether sulfates, 14t
aggregate size related to oil
solubilization rate, 89-105
with alkyl ether sulfates, 19
aqueous
interfacial tension by pendant
drop method, 329-40
three phases, LAS detergency
performance, 257
cationic
and anionic, mixing, 138
binding to anionic
polyelectrolytes, 225-38
effect
microemulsion formation, 153-71
- Surfactant--Continued
effect--Continued
microemulsions, 162-68
preadsorbed polymers on
adsorption, 291-309
structure, 73-85
thermodynamics of mixed
micellization, 141-48
modification of soil-water
absorption, 209-22
nonionic, interactions with mem-
branes and biological
systems, 189-206
nonionic POE, structural effects on
properties, 27-46
single, microemulsion
formation, 170-72
solubilization of various
oils, 89-105
structure related to adsorption, 270
structure related to
performance, 103
zwitterionic, surface
properties, 49-58, 61-70
- Surfactant head group, cationic sur-
factant binding to anionic
polyelectrolyte, 235
- Surfactant-polymer interactions,
effect of preadsorbed polymers on
adsorption, 295
- Surfactant-water systems, non-
Newtonian behavior, 139
- Synergistic interactions, surfactant
structure and adsorption, 286
- T
- Temperature
effect on microemulsion
formation, 157
effect on nature and structure of
microemulsions, 161
- Temperature dependence, CMC, n-acyl
POE monoethers, 38
- Temperature dependence, solubility, 4
of alkyl ether sulfates, 7t
- Tension, interfacial, low, effect on
microemulsion formation, 170
- Ternary system, interfacial tension by
pendant drop method, 334, 338
- Tertiary amine, synthesis, 50-52
- Theory
interfacial tension by pendant drop
method, 330-33
oil solubilization rate related to
aggregate size, 91
- Thermodynamic data, micellization of
nonionic surfactants, 38t
- Thermodynamic parameters
effect of chain length variation in
n-alkyl POE monoethers, 28-31

- Thermodynamic parameters--Continued
 micellization, 52-58
 as function of alkyl chain length, 29f
- Thermodynamic theories, nature and structure of microemulsions, 157-61
- Thermodynamics of mixed micellization, effects of surfactant structure, 141-50
- Three-phase equilibrium, surfactant, and Kraft point, 4
- Three-phase region, hydrotropic action, 112f
- Titration
 LDAO, discussion, 131,132f,137
 mixed CMC, nonideal mixed micelles, 146
- Transition, micelle shape, LDAO titration, 137
- Transparent domain, nature and structure of microemulsions, 163
- Transport rates, interactions of nonionic surfactants and biomembranes, 203
- Triethanolamine (TEA), fatty dicarboxylic acid hydrotrope, 118
- Trimethylammonium head group, effect on cationic surfactant binding to anionic polyelectrolyte, 235
- Triolein
 oil solubilization rate related to aggregate size, 91
 solubilization in anionic surfactant, 102f
 solubilization in nonionic surfactant, 96f
- Triple-phase line (TPL), LAS detergency performance, 242,247f
- Turbidity, oil solubilization rate, 90
- V
- Valency and Krafft point, 6
- Viscosity
 LDAO-SDS interactions, 131
 surfactants, effect of NaCl, 18
- W
- Water
 in microemulsions, effect on solubilization, 170
 oil droplet on substrate in, 20f
- Water-air interface, effect of OE units on adsorption, 11-14
- Water and detergent, with dicarboxylic acid, 112f
- Water and hexylamine, with dicarboxylic acid, 110f
- Water content, hydrotropic action, 108-11
- Water core, nature and structure of microemulsions, 169
- Water hardness, practical applications of alkyl ether sulfates, 14
- Water infiltration tests, surfactant effect on soil-water absorption, 219
- Water-oil microemulsion discussion, 161
 mixed film theory, 155
- Water-poor system
 fatty dicarboxylic acid hydrotrope, 126
 liquid crystalline phase, 111
- Water repellency, soil, modification by surfactants, 209-22
- Water-rich system
 fatty dicarboxylic acid hydrotrope, 126
 gelling, 111
- Water-soil-fiber contact angle, dependence of detergency, 247f
- Water volume-conductivity fraction curves, 166f,167f
- Wettability
 detergency, 248-51
 effect of chain length variation in *n*-alkyl POE monoethers, 28-31
 glass surface, LDAO-SDS interactions, 131
 surface, effect of preadsorbed polymers on adsorption, 305
- Wetting tension, discussion, alkyl ether sulfates in mixtures, 19-24
- Winsor system, LAS detergency performance, 259
- Wool, soil removal, 16f,24f
- X
- X-ray methods, conformation of fatty dicarboxylic acid hydrotrope, 126
- Xylene sulfonates, surfactant structure and adsorption, 278
- Z
- Zwitterion
N-alkyl betaines, temperature dependence of CMC, 38
 amino acids, effect on adsorption, 314
 betaine surfactant, 62,68
 effect of structure, 73-85
 surface properties, 49-58,61-70